M-Pos277

EFFECT OF INITIAL MUSCLE LENGTH ON INJURY INDUCED BY A SINGLE LENGTHENING CONTRACTION. ((KD Hunter and JA Faulkner)) Department of Physiology and Institute of Gerontology, Univ. of Michigan, Ann Arbor, MI 48109. (Spon. by T Coffin)

Single lengthening contractions injure muscle fibers mechanically, resulting in an immediate disruption in the ultrastructure of single sarcomeres and decreased force development (force deficit). For a maximally activated muscle with fibers at optimal length for force production (L_0), the most important factor in determining the magnitude of the injury produced after a lengthening contraction is the strain on the muscle. Our working hypothesis is that the critical variable that determines the magnitude of contraction-induced injury is the length to which the muscle is stretched rather than the displacement the muscle undergoes. We tested the hypothesis that regardless of the initial muscle length, the force deficit is not different when maximally activated muscles are stretched to the same final length. Mice were anesthetized and secured to a platform maintained at 37^0 C. The extensor digitorum longus muscle was attached to a servomotor. Each muscle was maximally activated and stretched at a velocity of 2 L_0/sec from an initial fiber length of either 90%, 100%, or 120% of L_0. Of fifteen muscles studied at each initial length, five were stretched to a final fiber length of 150% L_0, five to 160% L_0 and five to 170% L_0. Isometric force production was measured prior to and 2 minutes after the lengthening contraction. For each final length examined, muscles exposed to lengthening contractions starting at the longest initial fiber length (120% L_0) showed a smaller force deficit than those exposed to contractions which started at 100% L_0 (0.4% ± 1.3% vs. 8.4% ± 1.2% for final fiber length 150% L_0, 7.8% ± 2.3% vs. 19.7% ± 6.6% for 160% L_0, 30.7% ± 11.5% vs. 47.2% ± 3.9% for 170% L_0, mean ± 1 SEM). With fiber lengthening to 170% L_0, muscles with an initial fiber length of 90% L_0 had a smaller force deficit, 29.5% ± 1.6%, than those with an initial fiber length of 100% L_0, 47.2% ± 3.9%. We conclude that although final length is the single best predictor of the magnitude of contraction-induced injury (r^2 = 0.49), initial length and displacement are also important determinants. Supported by AG-06157.

M-Pos278

INCREASES IN LABILE FRACTIONS OF MYOFIBRILLAR PROTEINS IN CHRONICALLY STIMULATED SKELETAL MUSCLE. ((William O. Kline[1] and Peter J. Reiser[1,2])) [1]Exercise Science and [2]Oral Biology, The Ohio State University, Columbus, OH 43210.

We observe a marked decrease in the total amount of protein between adult rabbit tibialis anterior (TA) muscle that has been chronically and continuously stimulated electrically (10 Hz, 3 weeks) compared to control TA muscles when glycerinated (G) samples of both are examined with SDS-PAGE. We tested in the present study whether there is a greater loss of protein during glycerination in stimulated TA compared to control TA. Fresh (F) samples were dissected from stimulated and control muscles, macerated, weighed, placed in gel samplebuffer (8 M urea, 2 M thiourea, .05 M tris, .075 DTT, 3% SDS, pH 6.8), heated and frozen until run on gels. Bundles of fibers were prepared from strips adjacent to the fresh samples from control and stimulated muscles and stored in glycerinating solution at -20^{0}C for up to one week. The glycerinated samples were then macerated and prepared in the same manner as the fresh samples except they were blotted on filter paper to remove excess fluid prior to weighing. Densitometric scans of gels, on which G and F samples were run, reveal significant differences in the G/F band area ratios for several proteins (myosin heavy chain, actin, beta-tropomyosin) in stimulated, compared to control, TA. There is an ~50-70% labile fraction of each of these proteins, possibly not assembled into filaments, in fresh stimulated TA. This result can explain discrepancies among reports of altered protein expression during stimulation-induced transformation of muscle between studies based on whole, fresh muscle homogenates and those based on glycerinated samples. Supported by NIH Grant AR39652.

COMPUTER SIMULATIONS

(See also M-Pos313)

M-Pos279

ANALYTICAL SOLUTION OF REVERSIBLE THREE AND FOUR STEP REACTIONS. ((R. Rhoads, J.A. Watkins, C-Y. Li, and J. Glass)) Center for Excellence in Cancer Research, Treatment, and Education, Dept. of Medicine, LSUMC-S, Shreveport, LA, 71130.

The analytical solution of the three step reversible reaction given by A ↔ B ↔ C ↔ D has been a significant kinetic problem while the four step reaction, A ↔ B ↔ C ↔ D ↔ E has been considered to be analytically intractable. Using a symbolic logic algorithm, the algebra has been computed and expressions describing the relationships between intrinsic rate constants and eigen values (λ_r) as well as pre-exponential factors has been determined for the general and specific solutions of the form $A_i=\Sigma Q_r B_{ir} \exp(-\lambda_r t)$. The eigen values of the three step reaction were computed from the determinant $\lambda^4-a\lambda^3+b\lambda^2-c\lambda=0$ while λs for the four step reaction were determined from the determinant $x^4+px^2+qx+r=0$ which is obtained following the substitution of $\lambda=x+d/4$, and the constants a,b,c,d,p,q, and r are sums of products of the intrinsic rate constants (k_{ij}). The amplitude terms were determined, using the method of cofactors, from $Q_r=B_{ir}^{-1}C_i$, where B_{ir}^{-1} is the inverse matrix of B_{ir} and C_i is the matrix of initial conditions. In terms of the k_{ij}s, the observed rate constants and amplitudes are very complex and indicate the formidable nature of the problem when approached without the use of symbolic logic algorithms. Expressions describing the time dependence of the relative concentrations of reactants and products are particularly involved. The equations have been applied to several examples of physical-biochemical significance with satisfactory results. Similar manipulations to those routinely used for the two step reaction have been employed and are discussed. These expressions may provide a basis for more detailed kinetic analysis of complex biochemical reaction networks. Supported by NIH DK-37866

M-Pos280

TOWARDS PHASE TRANSFERABLE COMPUTATIONAL POTENTIAL FUNCTIONS: METHODOLOGY, BIOPHYSICAL IMPLICATIONS AND APPLICATION TO NITROGEN ((Peter C. Jordan[1,2], Paul J. van Maaren[1], Janez Mavri[1,3], David van der Spoel[1] and Herman J.C. Berendsen[1])) [1]Bioson Research Institute, Department of Biophysical Chemistry, University of Groningen, The Netherlands, [2]Department of Chemistry, Brandeis University, Waltham, MA 02254, USA, and [3]National Institute of Chemistry, P.O.B. 30, 61115 Ljubljana, Slovenia

We describe a generalizable approach to the development of phase transferable effective intermolecular potentials (reliable over wide regions of thermodynamic phase space) and discuss its implications for systems of biophysical interest (water, hydrocarbons, polypeptides). It is based on a polarizable shell model description of the isolated molecule and uses experimental data to establish the parameters. We describe a procedure that, using quantum calculations as a guide, permits very accurate modeling of not only a molecule's electrostatic field (i.e., a practical representation of the molecular charge distribution) but also its response to electrical and mechanical stress (polarization and deformation), and apply the method to nitrogen. The shells are surrogate electrons and purely intermolecular terms in our potential function reflect shell-shell interactions. They are determined from properties of low pressure, low temperature solid nitrogen (the cubic α phase). The resulting potential is phase transferable. It accounts for the second virial coefficient, the pressure induced phase transition between nitrogen's cubic and tetragonal phases, and a wide range of liquid properties (pair distribution function, heat of vaporization, self diffusion coefficient and dielectric constant).

M-Pos281

SIMULATING ENERGY FLOW IN BIOMOLECULES. ((Q. Wang*, C.F. Wong* and H. Rabitz^)) *Department of Physiology and Biophysics, Mount Sinai School of Medicine, NY, NY 10029 and ^Department of Chemistry, Princeton University, Princeton, NJ 08544.

By constructing a continuity equation of energy flow, we can utilize results from a molecular dynamics simulation to calculate the energy flux or flow in different parts of a biomolecule. A key objective of this work is to examine whether there are preferred pathways of energy flow in biomolecules and whether one can control or alter the pathways of energy flow in a biomolecule to change the function or activity of the biomolecule in a desired manner. The method was first tested on a cluster of 13 argon atoms. We demonstrated that it was possible to follow the pathways of energy flow after the velocity of an atom in the cluster was perturbed. We then applied the method to study the pathways of energy flow after the iron in the heme of a tuna ferrocytochrome c molecule was oxidized. We found that energy redistributed in an earthquake-like fashion after a cytochrome c molecule was oxidized. There was a hierarchy of time scales that the atoms in the surrounding of the heme group responded to the perturbation introduced to the heme. The time scales range from ~1 fs to ~40 fs.

M-Pos282

BINDING ENERGETICS: MODEL STUDY OF CYCLIC DIPEPTIDES. ((P. Brady, K. Sharp)) U. of Pennsylvania, Philadelphia, PA 19104.

During a bimolecular binding event, three translational and three rotational degrees of freedom are replaced by six internal modes of vibration. To accurately calculate binding energies from structures of complexes, these contributions must be determined. However, calculations of this nature are presently difficult for protein systems. We are using the gas to crystal and water to crystal transfer of cyclic dipeptides as a model for molecular association. We employ a variety of different methods to compute the contributions to binding: We use Finite-Difference Poisson-Boltzmann for the electrostatic contributions, Molecular Mechanics for the internal energies, a Surface Free Energy method to account for hydrophobic solvation, Quasiharmonic Analysis for intramolecular vibrations, and an Einstein Model for crystalline lattice vibrations. The calculations are compared to experimental enthalpies and free energies.

M-Pos283

APPLICATION OF "MD-ENGINE", AN ACCELERATOR FOR MOLECULAR DYNAMICS SIMULATIONS, TO BIOMOLECULAR SYSTEMS.
((Kunihiro Kitamura[1], Hiroh Miyagawa[1], Takashi Amisaki[2], Shinjiro Toyoda[3], Eiri Hashimoto[3], Hitoshi Ikeda[3], Nobuaki Miyakawa[3], and Akihiro Kusumi[4])) [1]Mol. Sci. Res. Ctr., Taisho Pharmaceutical, Omiya 330. [2]Dept. of Comp. & Info. Sci., Shimane Univ., Matsue 690. [3]Electronic Imaging & Devices Lab., Fuji Xerox, Atsugi 243. [4]Dept. Life Sci., Univ. of Tokyo, Tokyo 153.

MD-engine, a hardware accelerator we developed for molecular dynamics simulations, has been tested for its speed and precision using a program Amber 4.0. Basically, MD-engine is called from the main program when non-bonded forces are calculated. To test the speed, we used two systems: a Ras p21 protein immersed in water containing 11940 atoms and a phospholipid bilayer membrane with a periodic boundary condition containing 56 dimyristoylphosphatidylcholine and 1197 water molecules in a cell (6167 atoms). In the latter simulation, Coulombic interaction was calculated using the Ewald mode of the MD-engine. The MD-engine used contained 24 MODEL processors and interfaced with a SPARCstation 10 (90 MIPS). In the simulation of Ras, the MD-engine accelerated simulation by a factor over 100 as compared with the SPARCstation. In the simulation of the membrane, the MD-engine accelerated by a factor of 120, and it is 5 times faster than the simulation that employs an 8 Å cutoff on the SPARCstation. The accuracy of calculation was examined by microcanonical simulations of an NaCl molten salt consisting of 1000 atoms employing various calculation steps. Mean values and fluctuation of the total energy calculated as a function of the width of the time step behaved as predicted for the Verlet algorithm and were the same as those calculated with double precision on the SPARCstation.

M-Pos284

DEVELOPMENT OF "MD-ENGINE", A HARDWARE ACCELERATOR FOR MOLECULAR DYNAMICS SIMULATIONS.
((Shinjiro Toyoda[1], Takashi Amisaki[2], Eiri Hashimoto[1], Hitoshi Ikeda[1], Hiroh Miyagawa[3], Kunihiro Kitamura[3], Akihiro Kusumi[4], and Nobuaki Miyakawa[1])) [1]Electronic Imaging & Devices Lab., Fuji Xerox, Atsugi 243. [2]Dept. of Comp. & Info. Sci., Shimane Univ., Matsue 690. [3]Mol. Sci. Res. Ctr., Taisho Pharmaceutical, Omiya 330. [4]Dept. Life Sci., Univ. of Tokyo, Meguro-ku, Tokyo 153.

The use of molecular dynamics simulations (MDS) is severely limited by the availability of computational resources because MDS requires vast amounts of calculations. As the size of the system of interest increases, the number of non-bonded forces to be calculated increases as $O(N^2)$, where N is the number of atoms in the system. Cut-off of Coulombic interactions should be avoided because it causes various detrimental effects. Since over 99% of CPU time is used for calculating non-bonded forces in MDS involving over 10,000 atoms, the entire simulation would be accelerated if the time needed to calculate non-bonded forces is decreased. We produced a hardware accelerator, called "MD-engine", which is optimized for calculation of non-bonded forces. MD-engine is a parallel processor system which has 4-80 processors called MODEL in a chassis. The host computer sends coordinates, charges, and species of the atoms to the MD-engine and the MD-engine sends back forces to the host. MD-engine also calculates virials simultaneously with forces for calculation of pressure, accommodates periodic boundary conditions, and can be used for Ewald summation. The precision of MDS using MD-engine was the same as that calculated with double precision by a usual workstation. MDS of a system containing about 12,000 atoms using an MD-engine containing 24 MODELs was accelerated by a factor of more than 100 on a SPARCstation 10 (90 MIPS).

M-Pos285

PARTIAL MOLAR HEAT CAPACITIES OF POLAR AND NON-POLAR SOLUTES BY MOLECULAR DYNAMICS CALCULATION.
((S.R. Durell and A. Wallqvist)) Lab. of Math. Biol., NCI, NIH, Bethesda, MD 20892.

The thermodynamics of protein association and solvation of macromolecules is intimately connected with the properties of the aqueous solvent. One macroscopic manifestation of this is the relatively large partial molar heat capacities of alkanes and rare-gas atoms in water. To better understand this phenomenon, we have studied the thermodynamic and structural aspects of these systems with molecular dynamics simulations. Two main methods are explored for calculating the heat capacity of the model solutions: determining the fluctuation of the energy and the temperature dependence of the solvation enthalpy. These studies will also serve to test the ability of the commonly used, semi-classical water models and potentials to reproduce these subtle thermodynamic effects. Initial results indicate that the heat capacity of the solvent can be accurately calculated within the temperature range of at least 300-350°K. More interestingly, it is tentatively found that approximately 30% of the partial molar heat capacity of krypton is due to the temperature dependence of the solute-solvent interaction energy; the rest, of course, is due to changes in the solvent-solvent energy. Simulations will also be used to investigate the opposite effects that positive and negatively charged ions have on the heat capacity of the solution.

M-Pos286

PROTEIN POLAR GROUP OR POLAR SOLVENT DYNAMICS IN CHARGE TRANSFER REACTIONS
((V.B.P. Leite and J.N. Onuchic)) Department of Physics, University of California at San Diego, La Jolla, CA 92093-0350.

The dynamics of solvent polarization or polar groups in proteins plays a major role in the control of charge transfer in chemical or biological systems. The success of Marcus theory of accounting for the solvent effect via a single quadratic polarization coordinate can not be questioned. Onuchic and Wolynes have recently proposed a simple model showing how a very complex model with many dipole moments (or polar groups in proteins) can be reduced under the appropriate limits into the Marcus Model. The thermodynamics of this model has been discussed in the context of electron transfer reactions [1]. We will present a dynamical study of the same model. At high temperatures, the system exibits a diffusive dynamics, where a Born-Marcus model is recovered. At low temperatures, a glassy phase appears with a slow non self-averaging dynamics. At intermediate temperatures, we will discuss the concept of *diffusion pathways* and polarization dependence effects. The different regimes will be shown in a phase diagram as a function of characteristic parameters of the system. A discussion of how these different regimes affect the rate of charge transfer will be presented.

[1] J.N. Onuchic, P. Wolynes *J. Chem. Phys.* **98**,2218 (1993).

*Supported by NSF Grant # MCB-9316186 and by the Beckman Foundation. VBPL is partially supported by CNPq Brazilian agency.

M-Pos287

LARGE-SCALE MOLECULAR DYNAMICS SIMULATIONS OF PROTEINS IN AQUEOUS SOLUTION WITHOUT TRUNCATION OF LONG-RANGE FORCES.
((Francisco Figueirido, Gabriela S. Del Buono and Ronald M. Levy)) Department of Chemistry, Wright-Rieman Laboratories, Rutgers, The State University of New Jersey, Piscataway, NJ 08855-0939. (Spon. by N. Marky)

The correct treatment of the long-range electrostatic forces in molecular dynamics (MD) simulations of biological systems continues to be a subject of debate. The consideration of all interacting pairs takes time proportional to N^2, where N is the number of atoms in the system. Since this becomes unreasonably slow for typical simulations the preferred method is the use of a cutoff, with the corresponding truncation of the long-range forces. This truncation has strong effects on the structure and dynamics of the aqueous solvent surrounding the macromolecule. Moreover, all simulations that include biological macromolecules and explicit solvent are run under conditions that resemble extremely high concentrations, and no systematic study of the effect of the system size has been performed. To avoid this truncation and, at the same time, be able to study the size dependence, we have implemented the Fast Multipole Algorithm (FMA) of Greengard and Rokhlin as a subroutine of the MD program IMPACT. Our implementation is such that it can be run on a single workstation as well as on a heterogeneous network using PVM (Parallel Virtual Machine) or on the CM-5, a massively parallel machine. We have run a simulation of lysozyme (1980 atoms) in a cubic box of linear dimension 76 Å (14024 water molecules) and report here structural and energetic characteristics of this system. In particular, we have computed the distribution of electrostatic potentials at the titratable sites, which can be used to obtain free energies of ionization.

M-Pos288

BROWNIAN DYNAMICS SIMULATIONS OF AN α-HELIX IN SALT SOLUTIONS.
((W.-B. Yu*, C.F. Wong* and J. Zhang^)) *Department of Physiology and Biophysics, Mount Sinai School of Medicine, NY, NY 10029 and ^Department of Chemistry, New York University, NY, NY 10003.

Since it is difficult to include salt effects in molecular dynamics simulations of biomolecules, we have begun to carry out Brownian dynamics simulations to study biomolecules in salt solutions. An initial study focuses on the simulation of a 0.1 M solution of sodium chloride and a 13-residue polyalanine α-helix in a 0.1 M sodium chloride solution. By carrying out two series of simulations using two different cutoffs (20 Å and 40 Å) for the electrostatic interactions, we found that long-range interactions (>20 Å) were important in describing the structural and dynamical properties of the solutions. The ion-ion radial distribution functions obtained by using a 40 Å cutoff were close to those predicted by using the Debye-Hückel theory. The fluctuation of the collective dipole moment of the ions calculated with a 40 Å cutoff was found to be ~25% smaller than that obtained by using a 20 Å cutoff. This result suggests that the polarizability of an ionic solution would be overestimated if the electrostatic cutoff was not chosen large enough. We also found that the α-helix had little influence on the Na^+-Cl^- and Cl^--Cl^- radial distribution functions but had appreciable influence on the Na^+-Na^+ radial distribution function. The sodium ions were found to have a higher preference of staying close to the α-helix than the chloride ion. The simulations have so far been carried out to 300 ns. To improve the precisions of the simulation results, we plan to extend the simulations to the microsecond range. Results of changing salt concentrations will also be presented.

M-Pos289

SALT EFFECTS ON PEPTIDES: A COMPARISON OF MOLECULAR DYNAMICS SIMULATIONS. ((Gail E. Marlow and B. M. Pettitt)) Department of Chemistry, University of Houston, Houston, TX 77204-5641 and W. M. Keck Center for Computational Biology, Houston, TX. (Spon. by B. M. Pettitt)

It is well-known that the addition of salts to solutions of peptides and proteins can have pronounced effects on the structure, solubility and stability of these molecules. Qualitative experimental trends describing the effects of different anions and cations on proteins are expressed in the lyotropic or Hofmeister series. The exact underlying physical processes, however, are poorly understood. The effect of various salts on peptide conformation in solution has been studied using the molecular dynamics technique. The peptide of interest is the bis(penicillamine)enkephalin, a small zwitterionic pentapeptide of sequence Tyr-c[(D)Pen-Gly-Phe-(D)Pen], also known as DPDPE. Four independent simulations of DPDPE in explicit 1.0 M sodium chloride, sodium acetate, ammonium acetate and ammonium chloride solution have been performed. Differences in the behavior of the studied ions in solution and the subsequent changes in the properties of DPDPE are presented. Implications for a microscopic picture of the Hofmeister series are discussed.

M-Pos290

PROTEIN SUBSTATE IDENTIFICATION USING THE SINGULAR VALUE DECOMPOSITION. ((T.D. Romo, J.B. Clarage, †D.C. Sorensen, G.N. Phillips, Jr.)) Department of Biochemistry and Cell Biology, †Department of Computational and Applied Mathematics, Rice University, Houston, TX 77251

X-ray crystallography is able to provide high-resolution maps of the average structure of a protein, but this structure represents only a static conformation. The dynamical information of accessible substates and their transitions are lost. Time-averaged crystallographic refinement is an extension of molecular dynamics where the average structure is restrained to fit the observed X-ray data. With this methodology, an ensemble of structures consistent with both the dynamics force-fields and the observed data is generated that represent a range of conformations accessible to the protein in the crystalline state. One difficulty with time-averaged refinements is the plethora of generated conformations. It is possible to analyze this data manually watching movies of each residue, but this is not always feasible. The singular value decomposition or SVD is an important and popular matrix decomposition that can be used to analyze the ensemble of structures. The SVD constructs a basis set of vectors that describe the modes of atomic motion in the dynamics trajectory. What sets the SVD apart for the more traditional eigendecomposition analysis is that it includes temporal information. Combining the spatial and temporal information, the SVD is able to locate substates for any unit of the protein, such as a residue that swings between two distinct conformations. The SVD is also a convenient method for visualizing complex motions and understanding the sampling of the accessible configuration space for the protein in the dynamics trajectory.

This work supported by NIH, NLM, NSF, The W.M. Keck Center for Computational Biology, and the Robert A. Welch Foundation.

M-Pos291

PREDICTION OF pK_a'S FOR DIACID MOLECULES: AN EXPLICIT SOLVENT CALCULATION WITHOUT TRUNCATION OF ELECTROSTATIC INTERACTIONS. ((Gabriela S. Del Buono, Francisco Figueirido and Ronald M. Levy)) Department of Chemistry, Wright-Rieman Laboratories, Rutgers, The State University of New Jersey, Piscataway, NJ 08855-0939. (Spon. by R. M. Levy)

pK_a prediction of proteins in solution using explicit solvent still presents a challenge for theoreticians in the molecular computer simulation field. A major obstacle to accurate simulations of macromolecular systems concerns the treatment of long-range electrostatic forces. Often these forces are approximated by truncated Coulomb potentials. Such methods have been shown to yield unphysical behavior for some systems. The Ewald summation method has proven to be a viable alternative, yielding self-consistent results for the solvent dielectric response. Our objective is to test the accuracy of the Ewald method when applied to pK_a calculations of small molecules. Molecular dynamics simulations of various dicarboxilic acids in aqueous solution were performed using the Ewald method in order to calculate pK_a shifts. Free energy perturbation methods were used, and results were compared with those obtained using a Gaussian fluctuation analysis (linear response theory). The importance of testing the validity of linear response theory for these types of calculations lies in the simpler nature of the method, that helps ease the computational load.

M-Pos292

HYDROPHOBIC HYDRATION OF CARBOXILIC ACIDS

((I.Ortega Blake[1], ML San Román Zimbrón[2])) [1]Instituto de Física, UNAM, Laboratorio de Cuernavaca [2]Laboratorio de Ingeniería molecular UAEM Apdo. Postal 139-B, Cuernavaca, Mor, 62191, MEXICO.

Hydrophobicity is a rather important phenomenon that has gained due attenttion. However, the understanding of its molecular nature still elude us. With the purpose of providing some light on this point we have performed a Monte-Carlo simulation, for the hydration of propionic and valeric acids (as amphiphile models) at infinite dilution, in the temperature range of 285 K to 355 K. These studies are intended for:
a)Reproducing known anomalous behaviour, such as the non monotonous variation of solubility with temperature.
b) Gaining insight into the molecular picture through a dissection of the role that different phenomena playe in the microscopic behaviour.
We analyze the changes in the thermodynamical and structural properties around the polar and nonpolar elements in the acid vicinity i.e. internal energy, free energy and heat capacity. Also how the solute-water and water-water interactions around these moieties contribute to the above and look into the effect that adding intermolecular relaxation has in them. From this analysis we can concude that there is no solute water negative interaction, either between the molecules or the solute with liquid. Structure is noticeable around the head but not at the tail. An analysis of the results permit us to advance in the understanding of the hidrophobic effect at these molecules.

M-Pos293

LUMINAL HCO_3^- CONCENTRATION AND APICAL Cl^- CONDUCTANCE AFFECT HCO_3^- SECRETION AND pH_i IN A MATHEMATICAL MODEL OF PANCREATIC DUCT CELLS. ((*Y. Sohma, M.A. Gray, *Y. Imai and B.E. Argent)) Dept. Physiol. Sci., Univ. Med. Sch., Newcastle upon Tyne, NE2 4HH, U.K., and *Dept. Physiol., Osaka Med. Coll., Osaka, Japan.

Pancreatic duct cells secrete HCO_3^- ions via Cl^-/HCO_3^- exchangers which operate in parallel with apical CFTR Cl^- channels. We have now investigated how variations in luminal HCO_3^- concentration ($[HCO_3^-]_l$) and apical Cl^- conductance (gCl_a) affect HCO_3^- secretion (J_{HCO3}) and intracellular pH (pH_i) in rat pancreatic duct cells (see Table).

$[HCO_3^-]_l$ (mM)	gCl_a (fold-change)	pH_i	J_{HCO3} (nmol/min/cm²)
25	x1	7.21	19.4
25	x20	6.89	37.4
70	x1	7.52	9.2
70	x20	7.23	18.9

The computer simulation shows that when gCl_a is increased (x1 = basal and x20 = stimulated), pH_i falls, and there is an increase in J_{HCO3}. These data confirm that gCl_a is an important control point in HCO_3^- secretion and predict that changes in gCl_a will affect duct cell pH_i. Moreover, increasing $[HCO_3^-]_l$ from 25 to 75 mM increased pH_i and decreased J_{HCO3} at all levels of gCl_a. This suggests that cells facing a high luminal HCO_3^- concentration, as would be expected in stimulated ducts, will have a higher pH_i and a lower rate of HCO_3^- secretion. (Funded by the MRC and the CFT (U.K.)).

M-Pos294

ACCURATE PREDICTION OF ONE-ELECTRON REDUCTION POTENTIALS FOR BIOREDUCIBLE NITROHETEROARENES: A COMBINED QM/FEP APPROACH.

((T.C. Jenkins[1] and A.J. Beveridge[2])) [1]CRC Biomolecular Structure Unit, Sutton SM2 5NG, UK; [2]ANU, Canberra ACT 200, Australia. (Spon. by T.M. Dwyer)

A combined quantum mechanical (QM) Hartree-Fock and free energy perturbation (FEP) computational approach has been used to examine the 1-electron reduction of structurally related nitroarenes based on 5-membered heterocycles. Thermodynamic cycle analysis for pairs of compounds enables the prediction of redox potentials for these agents. Geometries for the parent molecules and their derived radical anions were optimised at the SCF and MP2 levels using a 6-31G* basis set, and zero-point corrections were determined for the gas-phase species. FEP simulations for mutation of ground-state molecules and radical anions were run using AMBER. Free energy data were accumulated during 42 or 105 ps, following (i) hydration, (ii) relaxation using MM, (iii) MD equilibration at 298 K and constant volume, and (iv) equilibration at 298 K and constant pressure (1 atm). Differences in electron affinity computed for pairs of nitrocompounds in this series compare favourably with E1 values determined using pulse radiolysis methods, and correctly predict the ranking order for redox activity. The application of this strategy to prediction of reliable E1 and E2 values for candidate bioreductive agents will be discussed.

M-Pos295

SIMULATED PROTON UPTAKE IN COMPLEX FORMATION BETWEEN CYTOCHROME C AND CYTOCHROME B_5

((K. A. Thomasson[1], S. H. Northrup[2], and M. M. Humbert[1])) [1]Chemistry Department Box 9024, University of North Dakota. Grand Forks, ND 58202-9024. [2]Chemistry Department Box 5055, Tennessee Technological University, Cookeville, TN 38505.

Brownian dynamic (BD) simulations have been used to predict a range of loosely docked precursor complexes of yeast usi-1-ferricytochrome c (cytc) with bovine ferrocytochrome b_5 (cytb5) as a prelude to electron transfer. The pH-dependent changes in proton binding that accompany complex formation between cytc and cytb5 have also been simulated using the BD predicted complexes and titration calculations applying the Tanford-Kirkwood method with the static-accessibility modification. The protonation state of each titratable amino acid residue on the proteins was determined allowing assignment of net charge for the proteins based on the protein environment, pH, ionic strength, and temperature. Proton uptake was determined based on the difference between the net charges of the complex and the net charges of the isolated proteins. Results agreed qualitatively experiment showing proton release at acidic pH's and proton uptake at basic pHs, but predictions consistently underestimated release. Both the isolated proteins and the BD complexes were then subjected to energy minimizations using 750 steps of Adopted Basis Newton Raphson with CHARMM 22 and applying distance constraints to retain the heme intact in the protein. This procedure yielded slightly more intimate complexes in which at least one of the close loose contacts became intimate enough to form a weak hydrogen bond. Repeating the proton uptake calculations for the minimized complexes yielded greatly improved results at basic pHs, but only slightly improved results at acidic pHs.

M-Pos296

ROLE OF ELECTROSTATIC STEERING IN DYNAMICS OF ACETYLCHOLINESTERASE CATALYSIS.

((J. Antosiewicz[1], S. Wlodek[1], J.A. McCammon[1,3] and M.K. Gilson[2])) [1]Dept. of Chemistry, University of Houston, Houston, TX 77204; [2]Center for Advanced Research in Biotechnology, Rockville, MD 20850; [3]Address after 1/1/95: Dept. of Chemistry and Biochemistry, and Dept. of Pharmacology, University of California at San Diego, La Jolla, CA 92093.

The finite-difference Poisson-Boltzmann method and Brownian dynamics simulations are used to evaluate influence of the electrostatic potential of acetylcholinesterase on the dynamics of its diffusional encounter with charged ligands. It is shown that, at physiological conditions, electrostatic steering of the ligand increases the rate constant of the enzyme-ligand encounter by more than one order of magnitude. It is also shown that referring to electrostatic interactions enables reasonable explanation for many puzzling experimental results obtained recently for variety of acetylcholinesterase mutants.

M-Pos297

THE EFFECT OF CALCIUM INFLUX ON INTRACELLULAR FREE CALCIUM RESPONSES IN ANTIGEN-STIMULATED RBL-2H3 CELLS: A COMPARISON OF EXPERIMENT AND THEORY.

((G. D. Smith, R. J. Lee, J. M. Oliver, J. Keizer)) Institute of Theoretical Dynamics, Section of Neurobiology, Physiology, and Behavior, and Biophysics Graduate Group, U.C. Davis, Davis, CA 95616; Dept. of Pathology and Cancer Research and Treatment Center, UNM.

We undertake a quantitative investigation of changes in cytosolic free calcium ($[Ca^{2+}]_i$) in antigen-stimulated rat basophilic leukemia (RBL)-2H3 cells that includes contributions of both Ca^{2+} stores release and Ca^{2+} influx from the medium. Following Keizer and De Young (1992), we develop a highly constrained mathematical model for $[Ca^{2+}]_i$ oscillations which includes a simple representation of plasma membrane (PM) fluxes. Using this model, we simulate protocols in which antigen concentration and Ca^{2+}_{ext} are manipulated while $[Ca^{2+}]_i$ responses are recorded, and we explicitly compare our calculations with experimental data. In Protocol A, cells are simulated in the presence of Ca^{2+}_{ext}; in Protocol B and Protocol C cells are stimulated in the absence of Ca^{2+}_{ext}. In Protocol C external Ca^{2+} is later reapplied. With a very simple characterization of a cell's time-dependent response to changing experimental conditions, we are able to reproduce the important features of all three protocols, the dose response of Protocol B, as well as thapsigargin and lag time results. We provide qualitative explanations for cell responses that are derived from our calculations.

M-Pos298

RE-ENTRANT ROTATING WAVES IN A NETWORK OF CARDIAC CELLULAR AUTOMATA.

((G. Bedfer)) Laboratoire des Cellules Cardiaques et Vasculaires, CNRS EP021, Faculté des Sciences, 37200 Tours, FRANCE. (Spon by C.O. Malécot)

I have developed a cellular automaton model of electrical conduction in the heart ventircule. Each model element can be in one out of four states : Resting (R), Action Potential (AP), Absolute or Relative Refractory Period (ARP, RRP). To take into account the nonlinearity of the electrical activity, the AP and RRP states were divided into 32 sub-states. Each automaton is connected by conductors (G_{gap}), representing gap-junction, to its nearest neighbors. During the R, ARP and RRP states, the membrane potential at the ijth automaton (V^{ij}) is derived by application of the Kirchoff's current law :

$$\frac{dV^{ij}}{dt} = \frac{-I_l + \left(S_{ij} - N_{ij}V_l^{ij}\right) \times G_{gap}}{Cm}$$

where I_l is the leak current, S_{ij} and N_{ij} the sum of the membrane potentials of the neighbors automata and their number and C_m the membrane capacitance. During the AP state, the potential is given by tabulated values obtained from the Beeler & Reuter Model (J.Physiol. **268**, 177-210). The rule of conduction is the following : an automaton in the R or RRP state depolarizes if its potential is greater than a threshold, else , after a delay, the automata goes into the next state. Applying a cross-field stimulation to the network, ($G_{gap} = 10^{-8}$ S), can induced Vortex re-entry (see Fig 1).

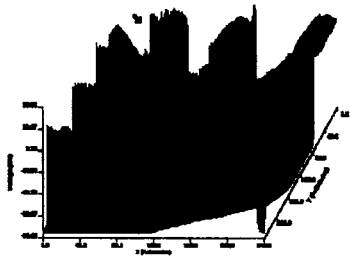

Figure 1 : Automata potentials after 2 s of simulation showing the begining of the 5th re-entry arrow)

M-Pos299

MAXIMUM LIKELIHOOD ESTIMATION OF KINETIC PARAMETERS FOR SINGLE CHANNELS FROM DWELL-TIME SEQUENCES.

((Feng Qin, Anthony Auerbach and Frederick Sachs)) Department of Biophysical Sciences, SUNY at Buffalo, Buffalo, NY 14214.

To alleviate the inherent limitations of histogram fitting techniques, Horn and Lange (*Biophys. J. 43:207*) introduced the use of a maximum likelihood approach to estimate single-channel kinetic parameters using every data point. Assuming no missed events, they maximized the probability of the observed sequence given the model. To improve computational speed, Ball and Sansom (*Proc. R. Soc. Lond. B236:385*) made use of the fact that there are many fewer dwell times than there are data points and presented a new likelihood function. However, their approach also required the assumption of no missed events.

We present here a more general approach for the kinetic analysis of channel gating based on a dwell-time sequence. There are four main improvements. 1) The algorithm has the explicit capability of dealing with multiple conductance levels and multiple channels. This is accomplished by modeling the overlapping of multiple channels as a composition Markov process following Horn and Lange. 2) To correct for missed events, an algorithm has been derived by generalizing the theory of Roux and Sauve (*Biophys. J. 48:149*) to the case of multiple conductance levels. 3) The optimization uses analytical derivatives of the likelihood function to improve speed and stability. The derivative is calculated from forward and backward recursions as utilized in the Baum-Welch reestimation formula for hidden Markov modeling. 4) We have included the capability of optimizing over data sets obtained with variable experimental conditions such as voltage, concentration, or force. Additionally, the program permits constraints on the parameters such as imposition of detailed balance.

Supported by NSF, ARO (DAAL0392G0014 to FS) and SUNYAB School of Medicine and Biomedical Sciences.

M-Pos300

QUATERNION CONTACT RIBBONS AND SURFACES: A NEW APPROACH FOR EVALUATING NON-LOCAL INTERACTIONS IN PROTEINS

((K. Albrecht†, J. Hart†, A. Shaw§ and A.K. Dunker§)) †Dept. of Electrical Engineering & Computer Science, and §Dept. of Biochemistry & Biophysics, Washington State University, Pullman, WA 99164

Protein folding involves contacts between amino acids that are well-separated along the amino acid sequence. Understanding such contacts is crucial for understanding protein structure and folding. Here we describe a procedure for inserting ribbons or surfaces that bisect the distances between main-chain atoms of interacting segments of secondary structure, followed by quaternion-based deformations of the ribbons or surfaces to display the zones of contact between the side chains. We have developed the algorithms so far for helix/helix quaternion contact ribbons; work is in progress for other contact ribbons and surfaces. For helix/helix contact analysis, we first identify the axes of the contacting helices. Next, a ribbon is constructed midway between the helix axes in contact zones using quaternions, which describe the orientation of each ribbon segment. Quaternions facilitate computer animation because of their simple interpolation of orientations. Using this property of easy interpolation, the contact ribbon is untwisted while preserving the various side chain/ribbon spatial relationships. Relative relationships between contacting side chains are largely preserved by this procedure, while reducing the clutter by simplifying the geometry and by removing nearby, but non-contacting side chains. Applying these methods to the membrane helices of the photoreaction center (1PRC), we find that knobs-into-holes packing (Crick, Acta Crystallogr. 6: 689-692 [1953]) is verified for several of the helix/helix pairs, as suggested previously for membrane protein helices in general (Dunker & Jones, Membrane Biochem. 2: 1-16 [1978]), but other categories of helix/helix contacts are also observed.

M-Pos301

EXTENSION OF THE HYDROPHOBIC ZIPPER MODEL OF PROTEIN FOLDING TO AN OFF-LATTICE PROTEIN REPRESENTATION

((Klaus M. Fiebig[†] and Ken A. Dill[‡])) [†]*Oxford Centre for Molecular Science, Oxford University, England; and* [‡]*Department of Pharmaceutical Chemistry, University of California, San Francisco.*

To model the early events of protein folding we recently have proposed the hydrophobic zippers (HZ) hypotheses [1,2] of protein collapse: spatially close hydrophobic (H) residues form contacts which act as constraints that bring other H-residues into proximity, which then form additional contacts and facilitate a cooperative assembly of the hydrophobic core of the protein. To study such a process we have modeled a protein as a copolymer of hydrophobic (H) and polar (P) residues. Here we present an extension to the present model in which the protein chain is no longer confined to the cubic lattice. Instead, the protein is represented by a chain of spherical residues which exhibit local bond and dihedral angle preferences. This model more accurately resembles the local bond geometry of the peptide chain. We analyze conformations generated by HZ process which were biased toward formation of native contacts. The importance of forming local and nonlocal native contacts is discussed.

[1] Fiebig, K. M., & Dill, K. A. (1993) *J. Chem. Phys. 94*, 3475–3487.
[2] Dill, K. A., Fiebig, K. M., & Chan, H. S. (1993) *Proc. Natl. Acad. Sci. USA 90*, 1942–1946.

M-Pos302

Actin Rotational Dynamics Studies by TPA and TAA

((Q. Zhang, E. Prochniewicz, and D. D. Thomas)) Dept. of Biochemistry, University of Minnesota Medical School, Minneapolis, MN 55455.

Both TPA (time-resolved phosphorescence anisotropy) and TAA (time-resolved absorption anisotropy) were used to study the rotational dynamics of F-actin labeled with ErIA (erythrosin iodoacetamide) at Cys 374. Data were analyzed in terms of three models: (1) rigid body diffusion about the filament axis, (2) twisting of a chain composed of finite rigid bodies connected to each other with twisting flexibility, and (3) twisting of the whole actin filament regarded as a continuous flexible rod. In a refinement of previous analyses, non-parallel emission and absorption dipoles were considered. The angle between the filament axis and the absorption transition moment was determined by TAA data to be $29\pm5°$. The angle between absorption and emission dipoles was determined by the anisotropy of PMMA-ErIA solid block. The simulation results show that the rigid body model can be ruled out, implying that intrafilament motions exists. We found that model (2) gives the best simulation and has a reasonable physical explanation.

M-Pos303

MOLECULAR DYNAMICS OF SPERM WHALE MYOGLOBIN

((B. K. Andrews, B. M. Pettitt[†], and G. N. Phillips Jr.))
Department of Biochemistry and Cell Biology
Rice University
[†]*Department of Chemistry and Biochemistry*
University of Houston

Ligand binding to myoglobin and hemoglobin has long been a paradigm for structure-function relationships in proteins. The chemical nature of water, the natural medium of biologically active molecules, plays a determinant role in protein structure, dynamics, and functionality. However, the computational cost of explicitly including water molecules in a molecular dynamics (MD) simulation has severely limited the number of computations that include fully-solvated proteins. Indeed, a great deal of MD research on hydrated systems has focused on simplifying models and indentifying what may be neglected while still obtaining satisfactory results. Advances in parallel computation are making biologically relevant calculations tractable without compromise. Here we report the results of a molecular dynamics simulation of hydrated sperm whale myoglobin using a parallelized version of CHARMM23.

This work supported by NLM, NSF, The W.M. Keck Center for Computational Biology, and The Center for Research on Parallel Computation

M-Pos304

MOLECULAR DYNAMICS STUDY OF THE EARLY INTERMEDIATES IN THE BACTERIORHODOPSIN PHOTOCYCLE.

((W. Humphrey, D. Xu, K. Schulten and M. Sheves)) Beckman Institute, UIUC, Urbana, IL 61801.

The early stages of the bacteriorhodopsin (bR) photocycle, including the J_{625}, K_{590}, and L_{550} intermediates, are studied by means of molecular dynamics simulations. These calculations use as a starting structure a model of bR based on earlier electron-microscopy studies and subsequent molecular dynamics refinement (Humphrey et al. (1994) **Biochemistry 33**, 3668-3678). To model the dependence of the dynamics on the protein initial conditions, 50 separate isomerization trials are done for each model, at both 300 K and 77 K, distinguished by different initial, random velocity distributions. From these trials are seen mainly four unique product structures: (1) 13-*cis* retinal, with the Schiff base hydrogen oriented toward Asp-96; (2) 13-*cis* retinal, highly twisted about the C_6-C_7 bond, with the Schiff base hydrogen oriented perpendicular to the membrane normal; (3) 13,14-*dicis* retinal; (4) all-*trans* retinal. Structural characteristics of these products are compared to experimentally observed spectral shifts and changes in HOOP mode intensities for the J and K states. These simulations suggest support for the possibility of multiple pathways in the initial photoisomerization process, only one of which, case (2), leads to an active photocycle. The distinct cases resulting from the different trials highlight the need for multiple samples to better illuminate the possible final protein configurations. From these trials, representative K_{590} structures are used to determine the L_{550} structure; simulated annealing is used to bridge the μs K_{590} to L_{550} transition time.

M-Pos305

Molecular Dynamics/Quantum Chemistry Study of Retinal Photoexcitation, Photoisomerization, and Dark Adaptation in Bacteriorhodopsin.

((I. Logunov and K. Schulten)) Beckman Institute, UIUC, Urbana, IL 61801.

A combination of molecular dynamics and quantum chemistry techniques have been employed to study the electronic structure and conformational potential surface of retinal in the binding site of bacteriorhodopsin (bR). Calculations have been performed for both the ground state (S0) and the first excited singlet (S1) state. The structure of bR has been previously refined by means of molecular dynamics simulations (Humphrey et al. (1994), Biochemistry 33, 3668:3678). The CASSCF(6,9)/6-31G level of ab initio calculations (within Gaussian92) has been used for the treatment of both the ground and the excited state of retinal. Charges of all atoms in the protein are explicitly included in the electronic Hamiltonian of retinal. A crucial admixture (more than 50%) of high excitations is observed for the electronic structures of S0 and S1. The weights of particular electronic configurations are strongly dependent on retinal's conformation and modification of amino residues in the binding pocket of bR. The energy differences between the S1 and S0 states in the native form, in the low and high pH forms, and for various mutants of bR consistently reproduce a strong opsin shift observed for these pigments. However, the level of ab initio calculations and/or fine details of the retinal binding site are not accurate enough to reproduce the experimentally observed absorption maxima. Modelling the photoisomerization of the shortened retinal analog is consistent with the experimentally measured lifetimes of the excited state in different pigments. Simulation of the dark adaptation process supports the notion that it occurs via co-rotation around the 13-14 and the 15-N bonds, and is catalyzed by the reduction of negative charge in the vicinity of the Schiff base.

M-Pos306

INTERACTION OF AN AMPHIPHILIC PEPTIDE WITH A PHOSPHOLIPID BILAYER SURFACE BY MOLECULAR DYNAMICS SIMULATION STUDY.

((P. Huang and G. H. Loew)) Molecular Research Institute, 845 Page Mill Rd., Palo Alto, CA 94304.

Corticotropin-releasing factor (CRF) is the principal neuroregulator of adrenocorticotropic hormone (ACTH) secretion. Previous experiments have demonstrated that CRF binds avidly to the surface of single egg phosphatidylcholine vesicles and its amphiphilic secondary structure might play an important role in the function. In this study, the interaction of human CRF13-41 with the surface of a DOPC bilayer was investigated by MD simulation to understand the role of the membrane surface in the formation of the amphiphilic α helix as well as to determine the effects of the peptide on the lipid bilayer. The model used included 60 DOPC molecules, 1 helical peptide on the bilayer surface, and explicit waters of solvation in the lipid headgroup regions, together with periodic boundary conditions in three dimensions. The MD simulation was carried out for 510 ps. In addition, CRF13-41, initially in a helical form, was simulated *in vacuo* as a control. The results indicate that while it was completely unstable *in vacuo*, the peptide helical form was generally maintained on the bilayer surface, but with distortions near the terminal ends. The peptide was confined to the bilayer headgroup/water region. The amphiphilicity of the peptide matches that of the bilayer headgroup environment in that the hydrophilic side chains are all locating at the surface exposed to water and the hydrophobic surface packs with that of the bilayer hydrocarbon core. These results support the hypothesis that the amphiphilic environment of membrane surface is important in the induction of amphiphilic helical secondary structure. Two major effects of the peptide on lipids were also found: the first CH_2 segment in the lipid chains was significantly disordered and the lipid headgroup distribution was broadened towards the water region.

M-Pos307

REPRESENTING PHOSPHOLIPIDS AS TWO CONNECTED CHAINS IN A LATTICE: A MONTE CARLO SIMULATION STUDY.((R. Jerala†, P.F.F. Almeida, and R.L. Biltonen)) Univ.Virginia, Dept.Parmacology, Charlottesville, VA 22908. †On leave from IJS, Ljubljana, Slovenia. (spon. by P.F.F. Almeida).

In lipid bilayers the acyl chains occupy the sites of a triangular lattice in the crystal state; this is also the case in the gel, and probably in the liquid-crystalline state. In a phospholipid molecule two acyl chains are covalently connected. In published Monte Carlo (MC) simulations of phospholipid bilayers the acyl chains have been treated as independent units on a triangular lattice, or else the phospholipids themselves were positioned on the lattice sites. In the present work we have addressed the question of the effect of acyl chain connectedness on the simulation of the macroscopic observables in these lipid systems, such as the excess heat capacity function, cluster size, and percolation probabilities. In order to allow for the sampling of the configurational space in these simulations, it was necessary to introduce, besides the usual Glauber step, a new type of step that consists of the concerted movement of two adjacent phospholipid molecules. The only free parameter in the simulation, the liquid-gel interaction free energy, was fixed by the maximum of the experimental excess heat capacity function. Both simulations of coupled and independent acyl chains produced very similar heat capacity profiles as a function of temperature, in good agreement with the experimental data. The main differences occurred in the number and size of clusters.(Supported by NIH and NSF, R.J. partially supported by MZT.)

M-Pos308

TWO DIMENSIONAL COMPUTER SIMULATION OF BILAYER MEMBRANE ((A. Chanturiya)) LTPB/NICHD - NIH Bethesda, MD 20892.

Since the fusion of two lipid bilayers involves thousands of lipid molecules, computer modelling of this phenomenon can be extremely complicated. An attempt is made to develop a simplified model of lipid bilayers and to evaluate the possibility of using this system for studying membrane fusion. The model developed operates in a two dimensional environment instead of three dimensional reality. Five to six hundred lipid molecules are represented by rod-like structures and forces between them were limited to attraction/repulsion between heads and tails. After each cycle of calculations, a randomly chosen molecule moves towards the position of energy minimum. Thermal fluctuations are introduced in a form of random movement of individual molecules when they are in the state of energy minimum. With a certain set of parameters it was possible to obtain a behavior of these "lipids" similar to what is known for lipid molecules in water solution: *i.e.*, 1. formation of micelle-like structures from initially random distribution; 2. relatively stable linear or circular bilayer structures ("planar membranes" and "liposomes"). When two "bilayers" were placed close enough to interact, some reorganization of they structure in the area of contact was observed but they did not fuse spontaneously.

M-Pos309

DIFFUSION INFLUENCED BINARY REACTIVE PROCESSES IN MEMBRANES: A MONTE CARLO STUDY. ((S.Bergling)) Institute of Theoretical Dynamics, UC Davis, Davis CA 95616. bergling a itd.ucdavis.edu

Simple random walk simulations on triangular lattices were performed in order to obtain a basic quantitative understanding of the kinetics of diffusion influenced binary reactive processes of membrane associated peptides or proteins within the two dimensionality of lipid bilayers. The results are compared with various formal approximate steady state approaches such as presented by Keizer (Acc.Chem.Res.,18:235-241,1985) in the context of statistical nonequilibrium thermodynamics or by Hardt (Biophys.Chem.,10:239-243,1979), based on the well known work of Adam and Delbrück. For diffusion controlled binary reactions of identical particles, nice agreement with the numerically simulated values is found in the low concentration limit for both Hardt's and Keizer's approach. For the latter a fluctuating steady state particle source has to be considered. The dependence of the steady state rate coefficient on system size is investigated, and the results are compared to the work of Swartz and Peacock-Lopez (J.Chem.Phys.95(4):2727-2731,1991). An application to a dimerization reaction on vesicles of typical experimental dimensions is given.

M-Pos310

THEORETICAL DESCRIPTIONS OF BACTERIAL MIGRATION IN POROUS MEDIA ((Kevin Duffy, Roseanne Ford and Peter Cummings)) Department of Chemical Engineering, Thornton Hall, and the Biophysics Program, University of Virginia, Charlottesville, VA 22903-2442. (Spon. by S. Frasier-Cadoret)

An understanding of bacterial migration in porous media is important in developing strategies for the bioremediation of hazardous waste in the environment. Our laboratory has quantified bacterial migration in porous media through experiment and cellular level simulations that incorporate parameters based on a fundamental description of the microscopic motion of bacteria. The present work concerns theoretical methodologies which provide effective bounds on experimental measures of bacterial migration.

Bacteria migrate using a series of straight line segments interrupted up changes in direction. This behavior is referred to as random motility and resembles a three-dimensional random walk similar to Brownian motion in molecular diffusion.

By analogy to diffusion theory, random motility within a sandy aquifer is expected to occur in the transition between the bulk diffusion and the Knudsen diffusion regimes because the bacterial mean free path is of the same order as the magnitude of the mean pore diameter. A harmonic average of the effective diffusivities in the ordinary and Knudsen limits provides an approximation for effective diffusion in porous media (Tomadakis *et al.*, 1993, *AIChE J*, 39, 397-412). Here an adaptation of this approximation to incorporate bacteria-surface effects is shown to predict the random motility of *Pseudomonas putida* in porous media by comparison to simulations and experiments.

M-Pos311

A Mathematical Model of the Isolated Guinea-Pig Ventricular Myocyte. **((G.C.L. Bett)) Department of Physiology, Charing Cross & Westminster Medical School, London W6 8RF. ((Spon. by I.P. Mulligan))**

The wealth of data concerning cardiac myocytes (especially details of cellular components) is vast, and growing rapidly as technological advances allow more intricate experiments to be performed. The challenge is to integrate these data into a physiological model of the whole cell which is capable of explaining and predicting cellular behaviour. A mathematical model of an isolated guinea-pig ventricular myocyte was constructed, based on available electrophysiological data and an existing model (Noble *et al.*, 1992, Ann. N.Y. Acad. Sci. 639: 334-353) from the *OXSOFT HEART* computer program. The internal structure of the model cell was completely redesigned, to allow a more physiological representation of the ionic concentrations and, in particular, enable a more faithful reconstruction of the characteristics of intracellular calcium cycling. The model cell and surrounding space is divided into a minimum number of compartments: two cytosolic areas (one between the junctional sarcoplasmic reticulum (SR) and the T-tubules, the other representing the rest of the cytosol); three sarcoplasmic reticular sections (junctional, network, and corbular); and three extracellular regions (the T-tubules, a space just-extracellular, and the bulk solution). The calcium release channels of the SR were entirely remodelled, as the revised cell structure allowed a more physiological representation of calcium release from the intracellular calcium store. The guinea-pig model correctly reproduces the main features of excitation-contraction coupling, and is now ready for rigorous examination of its capabilities.

M-Pos312

ANALYSIS OF LIGAND BINDING TO HEME PROTEINS USING A FLUCTUATING PATH DESCRIPTION ((A.R.Panchenko, J.Wang, G.U.Nienhaus, P.G.Wolynes)) Department of Physics, School of Chemical Sciences, University of Illinois, Champaign-Urbana, IL 61801 (Sponsored by P.G.Debrunner)

Protein motions affect the course of reactions such as the binding of ligands to heme proteins. Understanding of protein reaction mechanisms requires knowledge of the coupling of conformational and relaxational coordinates. The rate coefficients of this processes can be taken as a function of some stochastic environmental variable. Reaction kinetics in systems exhibiting stretched exponential relaxation, such as heme proteins, have been described using a path integral formalism. The model accurately reproduces the kinetics of geminate process of CO binding to myoglobin between 160K and 200K measured by Steinbach P.J., Ansari A., Berendzen J. et al . (Biochemistry, 1991 (30), 3988-4001). Estimated values of activation enthalpy for relaxation process and of preexponential factor in Arrhenius law agree with ones obtained directly from experimental data and molecular dynamics computation.

M-Pos313 *(See Computer Simulations posters)*

SHAPES OF CAVITIES AND INTERFACIAL REGIONS IN PROTEINS **((Pamidighantam V. Sudhakar, Jie Liang, Herbert Edelsbrunner, Shankar Subramaniam)) Dept. of Physiology and Biophysics, Center for Biophysics and Computational Biology, Beckman Institute for Advanced Science and Technology, National Center for Supercomputing Applications, and Dept. of Computer Science, University of Illinois, Urbana, IL 61801**

Precise measurements of cavities inside proteins and buried interacting regions in protein-protein complexes are important for understanding protein structure and molecular recognition. A method to accurately locate intra-protein cavities and pockets and accurately measure their metric properties is now available. It is based on the general idea of the combinatorial duality between the weighted Voronoi dissection of the space filling model and the corresponding weighted Delaunay triangulation. 3D alpha-shape algorithms and data structures newly developed in combinatorial computational geometry are used to compute cavities in proteins and geometry of contact regions in protein-protein complexes. Cavities in myoglobin are shown to correlate with xenon-binding sites and those in other proteins are shown to contain water molecules. The area of buried surface in the interface regions of protein-protein complexes and the volumes of cavities that are encompassed in the contact region are measured. A docking algorithm based on the alpha shape method is being developed [supported through funds from the National Science Foundation].

M-Pos314

PERIPHERAL SUBSTITUENT AND FE LIGATION AND SPIN STATE DEPENDENCE OF MODE SELECTIVE VIBRATIONAL ENERGY REDISTRIBUTION IN MODEL FE PORPHYRINS. ((C. M. Cheatum[1], M. R. Ondrias[1], M. C. Simpson[1,2])). [1]University of New Mexico, Department of Chemistry, Albuquerque, NM 87131. 2Current Address: Sandia National Laboratories, Fuel Sciences Div., Albuquerque, NM 87185

Vibrational energy redistribution may be important in regulating the function of hemes and related macrocycles. Transient resonance Raman experiments have previously revealed a non-Boltzmann vibrational energy distribution among heme normal modes in deoxyhemoglobin that is not present in cytochrome c. Several iron porphyrin model compounds have been probed with 10 nanosecond excitation pulses. Flux-dependent anti-Stokes peak positions, Stokes and anti-Stokes linewidths, and anti-Stokes:Stokes area ratios are found for some modes (ν_4) but not others (ν_7). The studies indicate that specific heme-protein interactions cannot be entirely responsible for this mode-selective behavior. However, results from six-coordinate, low-spin iron model porphyrins suggest that the protein may affect energy redistribution in some systems. The dependence of this mode-selective vibrational energy redistribution/relaxation upon porphyrin peripheral substitutents and ligation and spin states of the central iron is explored in order to find correlation with biological systems.

This research was funded by the National Institutes of Health (GM33330) and a D.O.E. Distinguished Postdoctoral Fellowship (MCS). M. C. Simpson was previously M. C. Schneebeck.

M-Pos315

X-RAY DIFFRACTION AND RESONANCE RAMAN SPECTROSCOPY REVEAL A PLANAR CONFORMATION FOR NICKEL PORPHINE IN SOLUTION AND IN THE CRYSTAL. ((W. Jentzen,[1] M. C. Simpson,[1] X. Song,[1,2] I. Turoska-Tyrk,[3] W. R. Scheidt,[3] J. A. Shelnutt[1,2])) [1] *Fuel Science Department, Sandia National Laboratories, Albuquerque, NM 87185-0710,* [2] *Department of Chemistry, University of New Mexico, Albuquerque, NM 87131,* [3] *Department of Chemistry, University of Notre Dame, Notre Dame, Indiana 46556.*

It is widely known that nickel porphyrins like nickel octaethylporphyrin exist in solution in planar and nonplanar conformers. The corresponding resonance Raman (RR) spectra for these two structures are different; and the nonplanar conformer is thought to result from the short metal-nitrogen distance for nickel(II) and the steric crowding at the periphery. Nickel porphine (NiP), with only hydrogen atoms as peripheral substituents, reduces the peripheral steric interactions and thus would be expected to be planar. To check this issue we measured the RR spectra of NiP in solution and in the crystalline form and obtained the X-ray structure. The RR spectra in both phases exhibit no significant deviations in frequencies and band shapes. The X-ray structure of NiP shows a planar macrocycle in a small lateral shift dimer configuration. Therefore, the similarity of the Raman spectra in solution and in the crystal indicate that NiP exists only in a planar conformation in solution. (Supported by U. S. DOE Contract DE-AC04-94AC85000 and Associated Western Universities Fellowships (WJ and XS).)

M-Pos316

O_2 AND CO_2 REDUCTION USING BIOMIMETICALLY DESIGNED METALLOPORPHYRIN CATALYSTS. ((T. Klitsner[1], G.N. Ryba[1], J.D. Hobbs[1], C.J. Medforth[2], K.M. Smith[2], M. Berkey[3] and J.A. Shelnutt[1,3])) [1]*Fuel Science Department, Sandia National Laboratories, Albuquerque, NM 87185-0710,* [2]*University of California, Davis, CA 95616,* [3]*University of New Mexico, Albuquerque, NM 87131.*

The reduction of O_2 and CO_2 are processes with obvious biological importance for both plants and animals. These processes also have a wide range of potential industrial applications. For example, catalytic O_2 reduction is important for such things as fuel cells and batteries, and catalytic CO_2 reduction has potential uses for the reduction of greenhouse gases and the production of fuels and chemical feedstocks. Where possible, we study the physical and chemical structure of the appropriate enzymes and using Computer-Aided Molecular Design (CAMD) methods attempt to incorporate similar features into highly-substituted metalloporphyrin macrocyclic complexes. These designed catalysts are then synthesized, characterized by resonance Raman spectroscopy and other experimental techniques, and tested for electro-catalytic activity. Using gas diffusion electrodes impregnated with metalloporphyrin catalysts, we have shown catalytic activity for O_2 reduction approaching that of precious metal catalysts (Pt) in fuel cell tests. This is true for both alkaline and acid electrolytes. Reduction takes place via a two-step, 2-electron reduction process. Present design efforts are focusing on designing catalysts for single-step 4-electron reduction to H_2O under similar conditions. For CO_2 reduction, we observe conversions of up to 5 percent (CO_2 to CO) in the CO_2 stream, using a setup similar to that used for the O_2 experiments. This occurs for electrodes impregnated with cobalt tetraphenylporphyrin (CoTPP) as well as cobalt dodecaphenylporphyrin (CoDPP) even at rather low loading using both 1.0 M KOH as well as 0.5 M $NaHCO_3$ electrolytes. Cells using bare electrodes (no catalyst) produce no CO even at sizable overpotentials. (Supported by U S DOE Contract DE-AC04-94AL85000).

M-Pos317

PLANAR AND NONPLANAR CONFORMATIONS OF NICKEL TETRAARYLPORPHYRIN COEXIST IN SOLUTION AND THE EFFECT OF DNA-BINDING ON PLANARITY. ((W. Jentzen,[1] E. Unger,[2] R. Schweitzer-Stenner,[2] W. Dreybrodt,[2] S. K. Subbarao,[1,3] T. Mahmud,[1,3] J. D. Hobbs,[1] J. A. Shelnutt[1,3])) [1]*Fuel Science Department, Sandia National Laboratories, Albuquerque, NM 87185-0710,* [2]*Institute of Exzperimental Physics, University of Bremen, 28359 Bremen, Germany,* [3]*Department of Chemistry, University of New Mexico, Albuquerque, NM 87131.*

We have measured the resonance Raman (RR) spectra of nickel tetraphenylporphyrin (NiTPP) in CS_2 solution for temperatures of 170 and 300 K. The band shapes of ν_2 and ν_8 are clearly asymmetric and can be decomposed into two sublines and are attributed to different conformers. The widths of the sublines differ by nearly a factor of two and their areas are temperature dependent. Their intensity ratios reveal, via the van't Hoff equation, an enthalpic difference of (1.8 ± 0.5) kJ/mol. The broad sublines result from the more stable conformer. They are at lower frequency for ν_2 and at higher frequency for ν_8. From the relative subline positions of ν_2 we infer that the broad sublines belong to the nonplanar, more stable conformation, whereas the narrow sublines correspond to the planar, less stable conformation. This is confirmed by comparison with the RR spectra of NiTPP in the crystalline form and CuTPP in solution. The crystal form of NiTPP is nonplanar as indicated by reported the short nickel-nitrogen distance (1.928 Å). CuTPP shows single Raman lines for ν_2 and ν_8 which suggests that only one planar conformation exists. Further, a comparison of the RR spectra of the 4-coordinate, nickel(II) tetra(N-methylpyridyl)porphyrin in DNA and in aqueous solution indicates that DNA-bound porphyrin is entirely planar. (Supported by U. S. DOE Contract DE-AC04-94AC85000 and AWU Fellowships (WJ and JDH).)

M-Pos318

Ligand Photolysis and Recombination of Fe(II) Protoporphyrin IX Complexes in Dimethylsulphoxide ((R. W. Larsen [1],E. W. Findsen[2], and R. E. Nalliah[2])) [1] Department of Chemistry, University of Hawaii at Manoa, Honolulu, HI 96822. [2] Department of Chemistry, University of Toledo, Toledo, OH 43606.

Steady-state and transient absorption spectroscopies have been employed to investigate ligand photolysis and recombination associated with (dimethylsulphoxide)$_2$ Fe(II) protoporphyrin IX [(DMSO)$_2$Fe(II)PPIX], (imidazole)$_2$Fe(II) protoporphyrin IX [(Imid)$_2$Fe(II)PPIX], and (2-methyl imidazole) (dimethylsulphoxide)Fe(II) protoporphyrin IX [(2-MeIm)(DMSO)Fe(II)PPIX] complexes in neat DMSO. Photo-excitation of the (DMSO)$_2$Fe(II)PPIX complexes results in the formation of a transient species consistent with a five-coordinate, high-spin heme iron. This species decays with a first order rate constant of (2.13 ±0.04) x10^6 s^{-1}. In contrast, photolysis of the (2-MeIm)(DMSO)Fe(II)PPIX complex results in the formation of a transient species that decays with biphasic kinetics. The fast phase of the decay was found to be dependent on the concentration of 2-MeIm exhibiting a second order rate constant of (7.9 ±0.5)x10^6 M^{-1}s^{-1}.The slow kinetic phase displays first order kinetics with a rate constant of (4.6 ±0.6)x10^{4}s^{-1}. These results will be discussed in the context of organic oxygen based ligand binding to heme proteins.

M-Pos319

ANALYSIS OF HEMOGLOBIN KINETICS USING TWO-STATE ALLOSTERIC MODELS. ((E. R. Henry, C. M. Jones, J. Hofrichter and W. A. Eaton)) Laboratory of Chemical Physics, NIDDK, NIH, Bethesda, MD 20892.

We have analyzed the carbon monoxide rebinding and conformational relaxation kinetics of hemoglobin measured by Jones, et al. (*Biochemistry* 31, 6692 (1992)) in photodissociation experiments at different degrees of photolysis. The kinetics are complex, exhibiting non-exponential geminate rebinding, non-exponential tertiary conformational relaxation, and multiphasic bimolecular ligand rebinding resulting from quaternary conformational changes. We are exploring the possibility that the kinetics can be explained by a class of two-state allosteric models incorporating both tertiary conformational relaxation and geminate ligand rebinding. These models require that deoxy protein subunits within the R quaternary structure exist in two possible tertiary states, an unstable transient species initially populated by ligand dissociation, and the stable equilibrium species. They further require that each tertiary species exist in three possible ligation states--ligand bound to the heme, ligand unbound but within the protein, and ligand free in the solvent. The simplest such model, which consists of 75 microscopic states, treats α and β subunits as identical. This model fits the ligand rebinding data almost perfectly (residuals <1%) and gives a good fit to the much smaller amplitude conformational relaxation data (residuals <10%). We are currently exploring whether the conformational relaxation kinetics are better described using more complicated models which introduce α-β subunit inequivalence and some intra-dimer cooperativity in the T state.

M-Pos320

THE HEME-GLOBIN LINKAGE: A COMPARISON OF ASSOCIATION RATES ((D. Balwinski, S. Song, J. Wenk, and M.D. Chávez)) Blood Research Detachment, Walter Reed Army Institute of Research, Washington, D.C. 20307.

Heme affinity is vitally important in the field of hemoglobin-based blood substitutes. Heme loss is especially undesirable in cell-free hemoglobin solutions since oxidation sensitive membranes such as endothelial cells become exposed directly to free heme. Using stopped-flow rapid scanning optical spectroscopy, the association of heme with a variety of apoglobins has been studied. Complete spectra can be collected in seven seconds with millisecond resolution. A comparison of horse heart myoglobin (Mb), hemoglobin A$_0$ (HbA), and hemoglobin cross-linked between α subunits with 3,5-(dibromosalicyl)fumarate ($\alpha\alpha$Hb) reveals progressively greater association rates for these apoproteins (Mb > HbA > $\alpha\alpha$Hb). Heme exchange experiments have shown that the amount of dissociation proceeds as HbA > $\alpha\alpha$Hb > Mb. Mb has a higher affinity for heme than Hb; hence, Mb has the higher association rate and lower dissociation rate. However, cross-linked $\alpha\alpha$Hb has both lower association and dissociation rates than HbA. This suggests that the cross-linking of hemoglobin may restrict globin motion, thus both rates are lowered by inhibiting heme access to the hemepocket. Other metalloporphyrins have also been investigated to fully understand the driving force of the heme-globin linkage. The exchange of nickel for iron does not affect the association rate, whereas the use of both nickel and iron mesoporphryin identically lowers the overall association rate by a factor of three.

M-Pos321

NANOSECOND CD AND ORD SPECTROSCOPY: APPLICATION TO THE QUATERNARY STRUCTURE TRANSITION IN HEMOGLOBIN. ((R.A. Goldbeck, D.B. Shapiro, D. Che, R.M. Esquerra, S.C. Björling, S.J. Paquette, S.J. Milder, and D.S. Kliger)) Department of Chemistry and Biochemistry, University of California, Santa Cruz, CA 95064.

We present novel, quasi-null optical techniques for measuring circular dichroism and optical rotatory dispersion that provide high signal sensitivity and fast time resolution, and apply these methods to ns chiroptical studies of hemoglobin structural dynamics after photodissociation of the carbonmonoxy complex. We find that the near-UV time-resolved CD (TRCD) of the aromatic residues Trp β37 and Tyr α42 indicates that the $\alpha_1\beta_2$ interface responds within several hundred nanoseconds to photolysis events at the heme by shifting from an R towards a T-like interface. The appearance of T-like character at the $\alpha_1\beta_2$ interface preceding the appearance of equilibrated T-state deoxyHb by tens of microseconds indicates that the transmission of tertiary structural forces to the dimer interface triggers a stepwise R→T transition. In a comparison of the TRCD and time-resolved ORD (TRORD) techniques, we find that the wider dispersion of ORD bands means that TRORD measurements can extend the time resolution of chiral spectroscopy beyond the signal to noise limitations of TRCD to provide new structure/function information in biological molecules, as demonstrated here for the Soret band of hemoglobin. In particular, we envision that ns TRORD may offer signal to noise advantages over CD for the fast monitoring of secondary structure changes in protein folding.

M-Pos322

DYNAMICS OF HUMAN HEMOGLOBIN IN POLY(ETHYLENE) GLYCOL-WATER SOLUTIONS: EFFECT OF SOLVENT ON THE KINETICS OF THE ALLOSTERIC TRANSITION. ((S.J. Paquette, R.A. Goldbeck, D.B. Shapiro and D.S. Kliger)) Department of Chemistry and Biochemistry, University of California at Santa Cruz, Santa Cruz, CA 95064.

Photodynamics were monitored for carbon(monoxy) human hemoglobin in the presence of various concentrations of the co-solute, poly(ethylene)glycol (PEG), in both the Soret (400–470 nm) and near-UV (250–335 nm) spectral regions with nanosecond flash photolysis. Singular value decomposition and global fitting produced amplitudes and lifetimes for six exponential processes. Variation of the PEG concentration from 0% to 40% (w/w) perturbs the allosteric kinetics, as evidenced by an increased lifetime for the $R_0 \rightarrow T_0$ quaternary transition, as well as an additional submicrosecond process, and a concomitant attenuation in amplitude for the diffusional T + CO millisecond rebinding step. Control experiments demonstrate that the effect of PEG is not due to pH or viscosity changes, suggesting that the influence of PEG on protein subunit motion during the hemoglobin R → T transition can be attributed to changes in the solution osmotic strength.

M-Pos323

ASSEMBLY OF THE GIGANTIC EARTHWORM HEMOGLOBIN: STOICHIOMETRY AND HEME CONTENT. ((H. Zhu, D.W. Ownby, K. Linse, Q. Xie and A.F. Riggs)) Dept. of Zoology, University of Texas, Austin, TX 78712.

The extracellular hemoglobin of the earthworm, *Lumbricus terrestris*, has four major O_2-binding chains *a*, *b*, and *c* (forming a disulfide-linked trimer) and *d* ("monomer"). Additional non-heme "linker" chains L1, L2 and L3 are required for assembly of the ~200 polypeptide hemoglobin. Both the stoichiometry and heme content have been controversial. Densitometry of Coomassie Blue-stained SDS gels by Vinogradov and colleagues suggested that linkers comprised one-third of the total mass, whereas the 220nm absorption peaks in the reverse phase HLPC gave 16.3% linkers (Ownby, *et al. J. Biol. Chem. 268*, 13539-13547, 1993). SDS capillary electrophoresis monitored at 214 nm avoids the use of Coomassie Blue and provided results identical with those obtained by HPLC. Analysis of size-exclusion chromatograms at pH 9 together with HPLC show that the linkers lack heme. The heme content, calculated from the stoichiometry and the known masses of linkers and heme-binding chains, is found to be 2.9%. Heme loss can account for lower values. (Supported by NIH Grant GM-35847).

M-Pos324

EFFECT OF Cl^- ON THE ENTHALPHY OF THE INTERMEDIATES OF OXYGENATION OF HUMAN AND BOVINE HEMOGLOBINS.

M. Karavitis, M.T. Sanna & C. Fronticelli
Dept. Biochem. U. Maryland Medical S. Baltimore, MD.

The temperature dependence of oxygen binding of HbA and HbBv has been measured in 50 mM glycine at pH 9.0, in the absence of Cl^- and in the presence of 16 and 8 mM Cl^- for HbA and HbBv, respectively. Global analysis was used to recover the thermodynamic parameters. For HbA, in the absence of Cl^-, the overall enthalphy of oxygenation calculated from the van't Hoff plot is ΔH=-22.5 kcal/heme. At 25 °C the n value is 1.5 and the heat released upon oxygen binding is similar at each step of oxygenation. In the presence of 16 mM Cl^-, the overall enthalphy of oxygenation is ΔH=-16 kcal/heme with a value of n=2.2. The sequential release of heat of oxygenation becomes non-linear and the enthalphy of oxygenation acquires a positive value at the third step of oxygenation. For HbBv, in the absence and in the presence of Cl^-, van't Hoff plots showed a similar enthalphy of oxygenation of -8.0 kcal/heme. In both conditions the value of n is 2.2, and the enthalphy of oxygenation becomes positive upon the binding of the second and third molecule of oxygen. These data suggest differences in the molecular mechanism of oxygen affinity modulation in HbA and HbBv.

Supported by PO1-HL-48517

M-Pos325

KINETICS ASSOCIATED WITH CARBON MONOXIDE REBINDING TO HEMOGLOBIN S AND C FOLLOWING LIGAND PHOTOLYSIS

((D.B. Shapiro, S. J. Paquette, R.M. Esquerra, E. Ghelichkhani, R.A. Goldbeck, R.E. Hirsch*, N. Mohandas✈, and D.S. Kliger)) University of California, Santa Cruz, CA; *Albert Einstein College of Medicine, Bronx, NY; ✈Lawrence Berkeley Laboratory, Berkeley, CA.

The kinetics associated with ligand rebinding to hemoglobin S and C in the tetramer and polymerized (HbS) and crystallized (HbC) forms have been studied with nanosecond resolution using laser photolysis techniques, including a novel ellipsometric technique that measures linear dichroism. Previous studies have shown that the kinetics of second-order ligand rebinding to tetrameric HbS and hemoglobin A (HbA) are identical. In addition to comparing these kinetics of rebinding in tetrameric forms of HbS, HbC and HbA, the nanosecond resolution in the present work allows comparison of the fast kinetics involved in tertiary and quaternary relaxations after ligand photolysis. Absorption spectra were measured between 10 ns and 200 ms after excitation and analyzed using singular value decomposition (SVD) and global analysis to determine kinetic lifetimes. The results show that, in the tetramer form, HbS and HbC exhibit the same kinetics associated with CO recombination as HbA, verifying the expectation that these β6 mutations do not significantly perturb the functional dynamics of the allosteric core. Time resolved linear dichroism has been measured using a new ellipsometric technique developed to study kinetics associated with ligand rebinding to aggregated forms, polymerized HbS and crystals of HbC. These measurements, together with time resolved absorption measurements that monitor the parallel rebinding of CO to aggregated and non-aggregated forms, have been used to characterize ligand rebinding to the aggregated forms.

M-Pos326

GEMINATE REBINDING KINETICS OF MYOGLOBIN IN A ROOM-TEMPERATURE GLASS.

((S.J. Hagen, J. Hofrichter, and W.A. Eaton)) Laboratory of Chemical Physics, NIDDK, NIH, Bethesda, MD 20892-0520.

Below the glycerol/water glass transition (~185 K), myoglobin exhibits distributed geminate rebinding kinetics as a result of "frozen" conformational substates (Austin *et al., Biochemistry* **14**, 5355 (1975)). As the temperature is increased through the solvent glass transition, the apparent rate of geminate rebinding *decreases*. This slowing has been attributed to a protein relaxation that impedes CO rebinding at high T, but that is itself prevented at low T by energetic barriers to conformational change (Steinbach *et al., Biochemistry* **30**, 3988 (1991)). Using time-resolved spectroscopy with nanosecond lasers, we have studied ligand rebinding in sperm whale MbCO embedded in a glass at room temperature. Over a wide temperature range T = 105–297 K, the kinetics of rebinding are well-characterized by the same inhomogeneous distribution $g(H_{BA})$ of enthalpy barriers H_{BA}, and changes in the shape of the Soret difference spectrum during rebinding can be explained by "kinetic hole burning." That is, at sufficiently high viscosity the multiexponential "low temperature" rebinding of MbCO can be observed at all T, as predicted by Ansari *et al.* (*Science* **256**, 1796 (1992)). Moreover, the average geminate rate predicted from the observed rate distribution is more than 100 times larger than the geminate rate in the completely relaxed protein in aqueous solution (Ansari *et al., Biochemistry* **33**, 5128 (1994)). Thus we have shown that high solvent viscosity prevents both interconversion of conformational substates and functionally important relaxation in the interior of the protein, independent of T.

M-Pos327

A SIMPLE KINETIC METHOD TO PROBE QUATERNARY STRUCTURE IN Hb REVEALS DIFFERENCES AMONG OXY-LIKE DERIVATIVES AND PARTIALLY LIGATED Hbs

((A. Tsuneshige and T. Yonetani)) Department of Biochemistry & Biophysics. University of Pennsylvania, PA 19104-6089.

The reactivity of the -SH groups of βCys93 of hemoglobin (Hb) with 4,4'-dithiopyridine (4-PDS) can be used to monitor conformational changes in Hb [1-3]. As the βCys93 residues are located in the β1-β2 cleft, the accessibility /reactivity of their -SH groups is sensitively influenced by structural changes in the β1-β2 interface and thus the reactivity to 4-PDS is a convenient probe for quaternary structure changes in Hb. The rate of reaction of the -SH groups with 4-PDS increases about an order of magnitude in oxyHb over deoxyHb.

We investigated the reactivity of these -SH groups for several Hb derivatives known to be "oxy-like" and also for partially and fully substituted metal Hbs over a wide pH range and found that: (1) the reaction is pH dependent; (2) there are subtle but consistent differences among oxyHbA, cyanmetHbA, and carbonmonoxyHbA: oxyHbA exhibited the highest kinetic constant, and carbonmonoxyHbA, the lowest at any pH studied; (3) metal-substituted Hbs, such as Ni- or ZnHb, showed a kinetic behavior similar to that of deoxyHbA; (4) α-substituted metal hybrid Hbs showed a kinetic behavior that ranged from that of deoxy at low pH values to that of oxy at high pH values; and (5) β-substituted metal hybrid Hbs exhibited a strikingly high kinetic constant over the entire pH range studied.

Supported by Research Grants, HL 14508 and GM 48130.

[1] Grasetti, D.R. and Murray J.F. (1967) *Arch. Biochem. Biophys.* **119**, 41-49; [2] Ampulski, R.S., Ayers, V.E., and Morell, S.A. (1969) *Anal. Biochem.* **32**, 163-169; [3] Imai, K., Hamilton, H.B., Miyaji, T., and Shibata, S. (1972) *Biochemistry* **11**, 114-121

M-Pos328

ZINC-IRON HYBRID HEMOGLOBINS: MODELS FOR INTERMEDIATE SPECIES OF LIGATION

((A. Tsuneshige[1], Y. Zhou[2], and T. Yonetani[1])) [1]Dept. of Biochemistry & Biophysics, University of Pennsylvania, PA 19104-6089, and [2]Dept. of Biol. Sci. & Biotech., Tsinghua Univ., Beijing, People's Republic of China.

Artificial hemoglobins (Hb), in which Fe(II) protoporphyrins IX are substituted with (metallo)porphyrins such as Zn(II)-, Mg(II)-, Cu(II)protoporphyrin IX, or metal-free protoporphyrin IX, are known to assume deoxy-like T-quaternary structure. Thus, these (metallo)protoporphyrins mimic unligated (or deoxy) protohemes in Hb. We have prepared two types of symmetric Zn-Fe hybrid Hbs, namely, $\alpha(Zn)_2\beta(Fe)_2$ and $\alpha(Fe)_2\beta(Zn)_2$, and measured their oxygen binding and tetramer-dimer dissociation properties in order to characterize intermediately ligated states of Hb.

Compared with native HbA, these Zn-Fe hybrids exhibit reduced oxygen affinity and similar Bohr effect. However, the oxygen affinity of $\alpha(Zn)_2\beta(Fe)_2$ is slightly higher than that of $\alpha(Fe)_2\beta(Zn)_2$, indicating subunit inequivalence. Their cooperativity increases with pH. The increases in oxygen affinity at the first and second oxygen-binding steps are controlled primarily by pH. Major changes in oxygen-binding characteristics occur around pH 7.4. Comparison of these observations with those of Ni-Fe [1] and protoporphyrin-Fe [2] hybrid Hbs leads to the conclusion that the axial coordination of the metal ion with the proximal histidine in the α subunits plays a key role in maintaining normal oxygen binding characteristics in Hb. The tetramer-dimer dissociation properties of these Zn-Fe hybrids are qualitatively similar to those of HbA.

Supported by Research Grants, HL14508 and GM48130.

[1] Shibayama, N., Morimoto, H. & Miyazaki, G. (1986) *J. Mol. Biol.* **192**, 323-329; [2] Fujii, M., Hori, H., Miyazaki, G., Morimoto, H., and Yonetani, T. (1993) *J. Biol. Chem.* **268**, 15386-15393

M-Pos329

DIMER-TETRAMER ASSEMBLY KINETICS OF ASYMMETRIC DOUBLY LIGATED CYANOMET HEMOGLOBIN

Yingwen Huang & Gary K. Ackers. Dept. of Biochemistry and Molecular Biophysics, Washington University School of Medicine, St. Louis, MO 63110

Tetrameric human hemoglobin (Hb) consist of two identical $\alpha\beta$ dimers which assemble into either quaternary structure T (tense or deoxy) or R (relaxed or oxy). Switching between T and R structure upon ligand binding follows the Symmetric Rule mechanism (Ackers, et al., (1992) *Science* 255, 54-63). To investigate structural features of partially ligated cyanomet Hb, we have used dimer-tetramer assembly kinetics. Kinetic analysis of dimer-tetramer assembly of species [21] ($\alpha_{CN\text{-}met}\beta_{CN\text{-}met}$•$\alpha\beta$) suggests that a slow structural rearrangement ($k=2\times10^{-5}\ s^{-1}$) in the interface occurs during species [21] formation. On the other hand, assembly of species [22] ($\alpha_{CN\text{-}met}\beta$•$\alpha\beta_{CN\text{-}met}$) is fast (within seconds), indicating that the $\alpha_1\beta_2$ interface of this species is different from that of species [21]. The slow structural rearrangement of the $\alpha_1\beta_2$ interface in forming species [21] is consistent with symmetry rule behavior: tertiary constraint is created upon initial ligation of one dimer within the tetramer and released in the T-R switch upon ligating the other dimer across the interface. These results provide support for assigning species [21] and [22] to quaternary T and R, respectively. Quantitative analysis of the slow kinetics of species [21] formation discovered in this study also provides necessary information for further investigation of structural feature in this species. Supported by NIH and NSF.

M-Pos330

RECOMBINATION KINETICS OF REPHOTODISSOCIATED COHbA. ((M. Yang*, J. Wang and J. Friedman)),Albert Einstein College of Medicine, Bronx, NY. Three distinct phases are observed for ligand recombination subsequent to photodissociation of COHbA with a nanosecond laser pulse at ambient temperatures. A geminate phase persists from tens to hundreds of nanoseconds. Slower microsecond and millisecond recombinations have been attributed to solvent derived recombination to the R and T structures respectively. A two pulse protocol was used to determine the recombination properties of transient populations created by photodissociating partially recombined populations of photodissociated COHbA. In this protocol an initial 6 ns photolysis pulse completely photodissociates the sample. At a variable delay a second pulse rephotolyzes the sample. The recombination kinetics of the rephotolyzed fraction is compared to those generated from the single pulse excitation. In aqueous buffer the geminate phase of both populations are identical within 60 ns of the initial photodissociative event, indicative of the protein being homogeneous on this time scale with respect to the distribution of potential energy barriers controlling bond formation. In contrast, at 95% glycerol the sample becomes thermally averaged between 60 and 500 ns. In aqueous buffer the rephotolyzed population shows an increase in the fraction of molecules undergoing T state recombination for all delays between 60 ns and 25 μseconds. The rephotolyzed population created between 60 ns and ~ 1 μs subsequent to the initial photolysis, shows an increased rate in the rebinding kinetics for the phase associated with R state recombination. Since these kinetics are associated with a population that had undergone partial recombination prior to photolysis, the enhanced kinetics may be due to an increase in the fraction of molecules in the R2 quaternary state. The R2 quaternary state is thought to be a high ligand affinity transition state structure between R and T that may be associated with triliganded HbA.

M-Pos331

NMR SPECTROSCOPY, PRIMARY SEQUENCES AND STRUCTURAL MODELS OF GLYCERA DIBRANCHIATA MONOMER HEMOGLOBIN COMPONENTS II, III & IV. ((Gail Davis, Scott Studham, Sacha Place, Steve Alam, Charles G. Edmonds and James D. Satterlee)) Department of Chemistry, Washington State University, Pullman, WA 99164-4630

The three purified monomer hemoglobins from *Glycera dibranchiata*, Components II, III & IV, have been sequenced, characterized and studied by proton NMR spectroscopy. The results show some disagreement with published data. In order to correlate NMR results structural models of these three hemoglobins were created by homology modelling based upon a published crystal structure of a related monomer hemoglobin.

supported by NIH Grant GM 47645 and NSF Grant DMB 9018982

M-Pos332

EVIDENCE THAT WATER PLAYS A SIGNIFICANT ROLE IN STABILIZING THE TERTIARY STRUCTURE IN HbI, A COOPERATIVE DIMERIC CLAM HEMOGLOBIN FROM SCAPHARCA INAEQUIVALVIS ((J.Huang, S.Huang, E. Peterson, J. Friedman*, AECOM; W. Royer, Jr.)), Univ. of Mass. Med Center, Worcester, MA.; A. Boffi and E. Chianconi, Univ."La Sapienza" Rome

X-ray crystallographic studies indicate that water plays a role in stabilizing the interface between the two myoglobin like subunits that comprise the HbI dimer [J. Mol. Biol. 235 657, 1994]. The interface for the deoxy form of the dimer contains a greater number of ordered waters than does the ligand bound form. The deoxy and ligand bound forms have distinctly different tertiary structures that are thought to be responsible for the cooperative ligand binding properties of this hemoglobin. Based on the difference in the number of interfacial ordered waters in the two structures, it is hypothosized that substantial changes in the osmolarity of the solution of HbI could alter the stability of the interface and thereby lead to a change in tertiary or quaternary structure. Using resonance Raman and near IR absorption to characterize the structure of native HbI, we find evidence that increasing the osmolarity destabilizes the deoxy structure. Time resolved and cw Raman studies on both native and mutant forms of HbI are being pursued to determine the communication pathway that couples the waters to several key elements of the tertiary structure. Comparisons with HbA and Mb will be presented.

M-Pos333

KINETICS OF THE OXIDATIVE REACTIONS IN HEMOGLOBIN-LIPID VESICLE MIXTURES ((Merita Dias, Sharron K. Jenkins and L. W.-M. Fung)) Department of Chemistry, Loyola University of Chicago, Chicago, IL, 60626.

The conversion of oxyhemoglobin to methemoglobin results in the production of oxygen radicals, initially as superoxide anion with the subsequent generation of other reactive oxygen radicals, causing membrane damage and further hemoglobin oxidation/denaturation. Many studies have shown that lipid peroxidation products promote hemoglobin oxidation/denaturation. Our previous studies showed that bovine phosphatidylserine (BPS) lipid vesicles, in the absence of lipid peroxidation products, enhance hemoglobin oxidation in buffers with physiological pH and ionic strength values. We have now continued our oxidation studies in buffers of different pH and ionic strength. Pseudo-first order rate constants for the initial disappearance of oxygenated normal and abnormal hemoglobin were compared. Our previous studies also showed that, during the process of hemoglobin oxidation, heme was partitioned into the lipid phase. We have now studied the kinetics of the heme destruction and lipid peroxidation in hemoglobin - BPS vesicle mixtures with and without EDTA. We have also monitored the release of free iron in hemoglobin-BPS vesicle mixtures incubated at 37°C as a function of time. The availability of free iron and heme has been suggested to promote peroxidation processes. A detailed study of the kinetics of the individual oxidative reactions may provide a better understanding of the enhanced hemoglobin oxidation/denaturation and the role of iron/heme in oxidative damages such as lipid peroxidation and membrane rigidity. (Supported by NIH, American Heart Association of Metropolitan Chicago and Loyola University of Chicago.)

M-Pos334

HEMOGLOBINS AND RED CELLS OF THE BRITTLE STAR, *HEMIPHOLIS ELONGATA* (Say). ((C. Bonaventura[1], A.M. Beardsley[2], J.M. Colacino[2], and R.D. Stevens[3])) Duke University Marine Lab, Beaufort, NC[1], Clemson University, Clemson, SC[2], and Duke University, Durham, NC[3].

Hemipholis is normally found buried in anoxic sediment with two arms extended into the water column. Hemoglobin-containing blood cells in the water vascular system appear to play an important role in oxygen transport into the buried parts of the animal. The unusual enucleate red cells are of varied sizes and have been observed to divide into smaller cells or fuse with one another. Chromatography of red cell hemolysates separates three major hemoglobin components containing single types of chains with molecular weights of 16,080, 16,118 and 16,143 daltons as determined by electrospray ionization mass spectrometry. Thus, the system does not contain the α and ß chain types typically found in vertebrate hemoglobin. The hemoglobins are unlike typical vertebrate hemoglobins in that homopolymers show significant cooperativity. P_{50} of the hemoglobin in single intact cells was measured by microspectrophotometry and was 11.1±1.2mmHg (pH8, 20°C, buffered sea water). The hemoglobin present in highest concentration is the component whose subunit molecular weight is 16,118. When isolated from other components it has a P_{50} of 6.07 and n_{50} of 1.83, showing it to be a cooperative homopolymer. P_{50} of the hemolysate under the same conditions was 11.0 mmHg. At pH 7, the hemolysate P_{50} was 8.8mmHg, indicating a possible reverse Bohr shift. Supported in part by NIH Center Grant ESO-1908 to C.B. and the North Carolina Biotechnology Center.

M-Pos335

MEASUREMENT OF THE CONCENTRATION DEPENDENCE OF SICKLE HEMOGLOBIN NUCLEATION RATES BY STOCHASTIC FLUCTUATIONS ((Zhiqi Cao and Frank A. Ferrone)), Department of Physics and Atmospheric Science, *Drexel University*, Philadelphia, PA 19104

Sickle hemoglobin polymerizes by homogeneous and heterogeneous nucleation. Homogeneous nucleation is a molecular process which is fundamentally stochastic, and the fluctuations in time of nucleation have been used to determine the rate of nucleation. [1,2] We have developed a method in which a laser beam is broken into an array of small spots which are focussed on a COHbS sample and can be interrogated simultaneously to study fluctuations on timescales which are intractable if done in sequence. We have thus measured the concentration dependence (apparent reaction order = 47) and temperature dependence (activation energy = 60-80 kcal/mol) of the homogeneous nucleation rate. Previous determinations of the homogeneous nucleation rate[3], by measuring and parametrizing kinetic progress curves, yield an apparent reaction order of 41 for the same range of concentrations, in reasonable agreement with the present value.

1. J Hofrichter (1986) J. Mol. Biol. 189 553-571
2. A Szabo (1988) J. Mol. Biol. 199 539-544.
3. F. A. Ferrone, J. Hofrichter & W. A. Eaton (1985), J. Mol. Biol. 183 611-631

M-Pos336

UPDATING THE DOUBLE NUCLEATION MODEL FOR SICKLE HEMOGLOBIN POLYMERIZATION

((Frank A. Ferrone)) Department of Physics and Atmospheric Science, *Drexel University*, Philadelphia, PA 19104

The double nucleation mechanism[1] proposed in 1980 that polymerization of sickle hemoglobin occurs by homogeneous nucleation (from monomers alone), and heterogeneous nucleation (onto pre-existing polymers). Observations of this process by DIC microscopy confirm that two such pathways do occur[2]; observation of the concentration dependence of homogeneous nucleation confirms that it is a nucleation process. These new methodologies provide direct experimental input into the parametrization of the model. Monomer diffusion, which was not included in the original model, is now seen to be extensive[3], and must be accounted for. Attempts to update the mechanism in this way will be presented. Finally, the mechanism will be examined to determine with what success it can model polymerization in physiologically important partially-saturated solutions.

1.Ferrone, Hofrichter, Sunshine, & Eaton, (1990) Biophys. J., 32, 361-380
2 Samuel, Solomon, & Briehl (1990) Nature 345 833-835
3 Cho & Ferrone, 1992) Biophys. J. 62 205-214

M-Pos337

DESIGN OF MUTANT HEMOGLOBINS BY MOLECULAR DYNAMICS SIMULATION

((H.-W. Kim*, T.-J. Shen*, D. P. Sun*, N. T. Ho*, M. Zou*, M. Madrid+, and C. Ho*.))
*Dept of Biol. Sci., Carnegie Mellon University and +Pittsburgh Supercomputing Center, 4400 Fifth Avenue, Pittsburgh, PA 15213

We have used molecular dynamics simulations successfully to design compensatory amino-acid substitutions in an abnormal Hb which restores its allosteric properties. In particular, for Hb Kempsey (β99Asp→Asn), which has a high oxygen affinity and exhibits essentially no cooperativity in binding oxygen, computer simulations indicate that a new hydrogen bond involving β99Asn can be induced by replacing α42Tyr by a strong hydrogen-bond acceptor such as Asp. This double-mutant recombinant hemoglobin, r Hb (β99Asp→Asn, α42Tyr→Asp), or mutant of Hb Kempsey was produced using our *E. coli* expression plasmid, pHE2, by site-directed mutagenesis. The oxygen affinity of this r Hb, while still high, is significantly lower than that of Hb Kempsey, and very substantial cooperativity has been restored. This results demonstrate that the functional defects of Hb Kempsey can be compensated by the amino-acid replacement of tyrosine by asparate at the α42 position in the $\alpha_1\beta_2$ subunit interface. The change in the free energy of cooperativity resulting from the mutations could be indirectly obtained from the thermodynamic cycle. By using a thermodynamic integration method, the contributions of specific interactions to the free energy change of cooperativity are evaluated. This work is supported by NIH grants HL-24525 and Grant RR-06009 to the Pittsburgh Supercomputing Center, and NSF grants DMB920024p.

M-Pos338

PROTON NMR STUDIES OF NATIVE AND RECOMBINANT GLYCERA DIBRANCHIATA MONOMER METHEMOGLOBIN COMPONENT IV.

((Steve L. Alam, David Dutton and James D. Satterlee)) Department of Chemistry, Washington State University, Pullman, WA 99164-4630.

Part I: Proton NMR spectroscopy in the guise of standard one- and two-dimensional experiments, suitably tailored for paramagnetic molecules, has been used to completely assign the heme proton resonances of the low-spin, cyanide-ligated monomer Component IV methemoglobin. The efficiency of this is compared to confirmatory studies on the recombinant perdeuterated low-spin, cyanide-ligated monomer Component IV. The results also allow tentative assignments to be made for several heme-pocket amino acids. Part II: Proton NMR is used to characterize mutant monomer Component IV in order to evaluate the effect of point mutations at primary sequence position 41, a potentially unrecognized site of heme contact.

supported by NIH Grant GM 47645

M-Pos339

ARTEMIA HEMOGLOBIN LIGAND BINDING KINETICS.

((Y. Gu and L. J. Parkhurst)) Dept. Chemistry, Univ. of Nebraska, Lincoln, NE 68588

Hemoglobin from Artemia, the brine shrimp, consists of two polypeptide chains, each with nine hemes. HbI is α_2 whereas HbII is $\alpha\beta$. At pH 7.5, 20°C, HbII is co-operative (Hill No. = 2.7) and high affinity in oxygen binding (median oxygen activity = 8.7μM.) but low affinity with respect to CO binding. To first order, the properties of the Hb can be described by a two state allosteric model, but with an average rate of binding to the R state that is only twice that to the T state. In the nsec time regime, geminate recombination could be observed for oxygen, but not for CO. The R→T conformational rate is four orders of magnitude slower than for human Hb, ca. 3.5 sec^{-1} at pH 7, 20° C. From laser photolysis measurements, the R/T cross-over point for CO association appears to be between $Hb(CO)_{17}$ and $Hb(CO)_{16}$. From oxygen pulse studies, the cross-over for oxygen must be much earlier in the ligation process. The two binding domains probed by azide binding differ in ligand affinity by factors of 20 and 30 for HbI and HbII, respectively, showing that the heterogeneity derives from site differences within a given chain. The dimer to monomer dissociation constant is 0.24μM, and the protein dissociates to monomer upon ligand binding within about one second when the hemoglobin is 5μM in heme. All of the CO, oxygen, and azide binding and dissociation reactions were fitted well by a biphasic model. Grant support: NIH DK 36288.

M-Pos340

FACTORS CONTROLLING CYANIDE BINDING TO MYOGLOBIN

((Y. Dou, S.J. Smerdon, A.J. Wilkinson, J.S. Olson, and M. Ikeda-Saito)) Physiol./Biophys., Case Western Reserve Univ., Cleveland, OH 44106, Chem., Univ. of York, York, U.K., and Biochem./Cell Biol., Rice Univ. Houston, TX. 77251

Cyanide dissociation rate constants were determined for 31 sperm whale, pig, and human recombinant ferric Mb with mutations at position 29, 46, 64 and 68. In contrast to the association rate constants which varies up to 1000 times, the cyanide dissociation rate constants, k_{CN}, changes less than 40 times upon the mutations: cyanide affinity of ferric Mb is primarily controlled by the association rate constant. Size of residues at position 64 and 68 affects less than 10 times on k_{CN}. Introducing a negative electrostatic field next to the bounded cyanide results in an increase of k_{CN} for 10~20 fold, indicating the significant role of the electrostatic field on k_{CN}. Hydrogen bonding between the residue at position 64 and cyanide stabilizes cyanide form. Replacement of Phe^{46} by Val, Leu and Ile causes disorder in position of distal histidine, and increases k_{CN} by 2~5 fold thus lowers cyanide affinity.

Supported by NIH GM51588, GM35649, and HL47020, SERC GR/H 68864

M-Pos341

STRUCTURAL STUDIES OF D-HELIX MUTANTS OF SPERM WHALE MYOGLOBIN

((Michael B. Berry, Timothy Whitaker, Emai L. Ho, George N. Phillips, Jr., and John S. Olson))
W. M. Keck Center for Computational Biology and Department of Biochemistry and Cell Biology
Rice University, Houston, Texas 77251-1892

Several mutants of the D-helix region of sperm whale myoglobin are in the process of being investigated by X-ray crystallography. $Mb^{\Delta 51\text{-}55}$, a deletion mutant of residues 51-55 (the D-helix), crystallizes in space group $P2_12_12_1$, and the crystals diffract to 2.0 Å resolution. A second mutant, Mb^{alam}, has residues 51-54 of the D-helix replaced by alanines. Crystals of Mb^{alam} are in space group $P6_522$, and also diffract to 2.0 Å resolution. Molecular replacement has been used to solve both $Mb^{\Delta 51\text{-}55}$ and Mb^{alam}. A third mutant, Mb^{alaD}, in which residues 51-55 of the D-helix have been replaced by alanines, is in the initial stage of crystallization. The impact of these mutations on the structure, their effects on crystallization, and the biological relevance of the D-helix both towards the function and stability of the protein are discussed.

M-Pos342

MOLECULAR DYNAMICS SIMULATIONS OF V68A, I107V, and V68A-I107V MYOGLOBIN MUTANTS. ((M.L. Carlson, R. Regan, and Q.H. Gibson)) Section of Biochemistry, Molecular and Cell Biology, Cornell University, Ithaca, NY 14853 (Spon. by Q.H. Gibson)

Qualitative differences in the experimental picosecond recombination curves for NO in myoglobin following flash photolysis are represented well by simulations of ligand diffusion without involving chemical bonding (Gibson et al.,1992). Simulations of the V68A, I107V, and V68A-I107V mutants of sperm whale Mb show markedly different ligand-iron collision tallies than wild-type. The differences in the collisions for various mutants are not easily related to the changes in the inter-atomic space volume that accompanies residue substitution. I107V, the mutant having the least impact on that volume, differs as much or more with wild-type as the others. Detailed inspection of the distal pocket reveals that modest thermal motions redistribute the inter-atomic space volume to create, deform, and relocate ligand-accessible cavities, which constitute only a few percent of that volume. The existence, position, and connectivity of these spaces, which fluctuate on a sub-picosecond time scale, determine ligand access to the heme iron. Positions 68 and 107 are of particular interest since they appear to gate the passage of ligands from the cavity adjacent to the iron to another cavity, over the B pyrrole's vinyl group. This more remote cavity, which is common to nearly all the sperm whale Mb mutants and can be found in Hb's and other Mb's, is the only other one visited by ligands during these 50ps simulations.

M-Pos343

THE ROLE OF AND INTERACTION BETWEEN ARG45 AND HIS64 IN SPERM WHALE MYOGLOBIN. ((F. Yang, T. Li, J.S. Olson, and G.N. Phillips)) Dept. of Biochemistry and Cell Biology, Rice University, Houston, TX 77251.

In sperm whale myoglobin (Mb), Arg45 is part of a hydrogen bonding lattice formed with the heme-6-propionate, Asp60(E3), and His64(E7). This lattice seems to inhibit rotation of His64 and hence access to the distal pocket. The positively charged side-chain of Arg45 may also reduce the pKa of His64 keeping it unprotonated and in the "down" conformation. Replacing Arg45 with Glu should disrupt the interactions at the heme periphery and increase the pKa of His64. We have studied the kinetics of CO and O_2 binding, the crystal structures, and the IR spectra of the Glu45 mutant as a function of pH. Below pH 6, the Glu45 mutant shows a greater rate of CO association than that of native Mb. However, the CO dissociation rate constant for the mutant is also greater, and as a result, K_{CO} for the mutant at pH 4 is the same as that for the native protein. The O_2 association and dissociation rate constants of both native and Glu45 Mb increase with decreasing pH. Over the pH range from 7 to 4.5, K_{O2} is constant for Glu45 Mb while that for native Mb decreases ~40%. In the crystal structures of Glu45 MbCO, His64 is in the "up" conformation at pH 4 and rotates more freely at pH 5 than in native MbCO. At pH 4.5, the IR spectrum for Glu45 MbCO shows roughly a single A_0 band whereas that for native MbCO shows A_0 and $A_{1,2}$ bands with the intensity ratio of 1:0.9, indicating the enhancement of the pH affect by the mutation resulting probably from the change of pKa and conformation of His64.

Supported by NIH grants AR40252, GM 35649, HL47020, the Robert A. Welch Foundation, and the W.M. Keck Center for Computational Biology

M-Pos344

TIME-RESOLVED X-RAY ABSORPTION SPECTROSCOPY : NOVEL METHOD APPLIED TO EXAMINING THE STRUCTURE OF THE MYOGLOBIN-CO PHOTOPRODUCT

((M.R. Chance, A. Xie, L.M. Miller, E.M. Scheuring, Y. Hai, Y. Lu)), *Department of Physiology and Biophysics, Albert Einstein College of Medicine, Bronx, NY.*

X-ray absorption spectroscopy (XAS) is an excellent tool to study the structure of metalloproteins as it gives very accurate distance information around the metal center and can be applied to solution phase. With the advent of time-resolved pump-probe XAS (TRXAS), we are able to detect dynamic changes of metal centers as the reaction of interest proceeds and structurally describe short-lived intermediates in cases where other spectroscopies can only give indirect structural information. We have further developed our data acquisition system to provide x-ray edge data on microsecond timescales and EXAFS data on millisecond timescales. We have applied these methods, as well as improvements in x-ray beam focus geometry for XAS, to observing the relaxation of myoglobin subsequent to photolysis at a range of temperatures. The structures observed at liquid helium temperatures and above the glass transition (where relaxation of the heme iron comes into play) are compared to crystallographic data to contrast the strengths and limitations of the two methods, as well as to show the utilization of state-of the art *ab initio* XAS calculations based on structural coordinates.

This work is supported by NIH grants HL-45892 and RR-01633 and NSF grant BIR-9303830.

M-Pos345

STRUCTURAL AND ELECTRONIC FACTORS WHICH INFLUENCE OXYGEN AFFINITIES: A SPECTROSCOPIC COMPARISON OF FERROUS AND COBALTOUS MYOGLOBIN

((L.M. Miller and M.R. Chance)) *Department of Physiology and Biophysics, Albert Einstein College of Medicine, Bronx, NY, 10461.*

The role of iron in oxygen binding and release in myoglobin has been studied by addressing structural and electronic factors that result in similar rates of oxygen association (k_{on}) and different rates of oxygen dissociation (k_{off}) for ferrous (FeMb) and cobaltous (CoMb) myoglobin. Comparable values of k_{on} imply similar barriers to oxygen binding, which in turn, are correlated to low temperature quantum yields of photolysis. Through optical spectroscopy, we have found that the quantum yields of photolysis for $CoMbO_2$ (0.55 ± 0.05) and $FeMbO_2$ (0.50 ± 0.05) at 10 K are the same. Structurally, the barrier to oxygen binding is influenced by the metal displacement from the heme plane of the oxy and/or deoxy species. The x-ray absorption near edge spectra of CoMb and FeMb reveal similar metal-heme displacements for the deoxy, oxy, and low temperature photoproduct states of CoMb and FeMb. Lower values of k_{off} for $FeMbO_2$ versus $CoMbO_2$ imply different barriers to oxygen release. Electronically, x-ray edge positions of CoMb and FeMb indicate that, upon oxygenation, more electron density is transferred to the oxygen ligand from iron than from cobalt. This difference is reflected in a weaker Co-O bond when compared to Fe-O. Using photolyzed/unphotolyzed FTIR difference spectra of $CoMbO_2$ and $FeMbO_2$, we find the dioxygen stretching frequency, $\nu(O=O)$, to be higher in $CoMbO_2$ (~1135 cm^{-1}) than $FeMbO_2$ (~1125 cm^{-1}). The implication of a stronger dioxygen bond in $CoMbO_2$ is likely a reflection of the weaker Co-O bond, and also may be evidence of a weaker hydrogen bond between oxygen and the distal histidine. This work is supported by NIH grant HL-45892.

M-Pos346

pH-DEPENDENT SPECTROSCOPIC AND KINETIC CHANGES IN CO-LIGATED SPERM WHALE MYOGLOBIN ((Joachim D. Müller*, Ellen Y.T. Chien, Chester D. Eng, Stephen G. Sligar & G. Ulrich Nienhaus)) Department of Physics, Biophysics, Biochemistry & Chemistry, University of Illinois at Urbana-Champaign, IL 61801, and *Technische Universität München, Germany.
(Sponsored by H. Frauenfelder)

Site-directed mutagenesis of sperm whale myoglobin was used to study the role of titratable side groups close to the active site at room temperature. Spectroscopic and kinetic measurements of the mutants combined with a systematic variation of the pH allow by direct comparison with the native protein the assignment of processes and pK's to individual amino acids. This study concentrates mainly on two histidine replacements, the proximal mutant H97F and the distal mutant H64V. The absorption changes in the α-band can be modeled using a Henderson-Hasselbalch equation assuming a distinct pK for each histidine. The same model can be used to describe the pH-dependent on-rate of the ligand CO rebinding after flash photolysis. In contrast to the two distinct titrations in the α-band, the titration of the distal histidine is sufficient to describe the pH-dependent binding kinetics of the wildtype. (Supported by NIH PHS 2 R01 GM18051 and GM31756).

M-Pos347

PRESSURE AND TEMPERATURE EFFECTS ON THE RAMAN SPECTRUM OF LIGAND BOUND AND PHOTODISSOCIATED MYOGLOBIN. ((A. Schulte, S. Buchter, C. Williams)) Department of Physics and Center for Research and Education in Optics and Lasers, University of Central Florida, Orlando, FL 32817.

The frequency doubled output (425 - 442 nm) of a tuneable cw Ti:sapphire laser is employed to excite the resonance Raman spectrum of (horse) myoglobin in different oxidation states. We present measurements of the temperature (100 to 300 K) and pressure (0.1 to 180 MPa) dependence of the Raman bands of oxy, carbonmonoxy, deoxy and photodissociated myoglobin in aqueous solution. Differences in shifts of vibrational frequencies with temperature and pressure are discussed with respect to thermal expansion and conformational changes. We explore pressure effects on the Fe-C-O and Fe-O-O bending frequencies to probe the arrangement of conformational substates.

* Supported by NSF, Grant No. MCB-9305711.

M-Pos348

RECOMBINATION OF DIOXYGEN TO HORSE-HEART MYOGLOBIN ((K. Chu, H. Frauenfelder, B. McMahon and G. U. Nienhaus)) Department of Physics, University of Illinois, 1110 W. Green St., Urbana, IL 61801.

The physiological role of myoglobin is oxygen storage. We seek to understand the control mechanism for O_2 recombination to myoglobin (Mb) and the differences between the rebinding of O_2 and the more commonly studied ligand, CO.

We use near-infrared FTIR, nanosecond flash photolysis and time-resolved optical multichannel analyser (OMA) techniques to probe the rebinding of O_2 to horse-heart Mb. Temperature-derivative spectroscopy measurements of ν_{III}, the near-infrared charge transfer band of the $hMbO_2$ photoproduct, reveal a low-barrier fast-rebinding process which is absent in measurements with CO as a ligand. Flash photolysis results are presented in terms of a distribution of rebinding enthalpies (at temperatures from 60 - 150K). At T > 170K, the kinetics suggest a sequential rebinding model with discrete states. Lifetimes for the relaxing populations are calculated using the Maximum Entropy method (MEM).

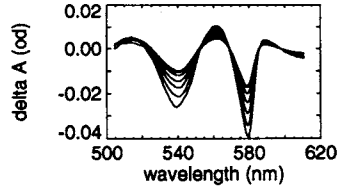

Difference spectra of the rebinding reaction $Mb + O_2 \rightarrow MbO_2$ in the α-β region. (T=70K)

(Supported by NIH PHS 2 RO1 GM 18051.)

M-Pos349

The near infrared absorption band III and the $\nu_{Fe\text{-}His}$ Raman band probe the same conformational substates of deoxymyoglobin.

H. Gilch[1], R. Schweitzer-Stenner[1], W. Dreybrodt[1], M. Leone[2], A. Cupane[2] and L. Cordone[2]
[1]Institut für Experimentelle Physik, Universität Bremen, D-28334 Bremen
[2] Instituto di Fisica and INFM-GNSM, University of Palermo, Italy.

The near infrared band III of deoxymyoglobin was measured as a function of temperature between 10 and 300 K.This band can be decomposed into two Gaussian subbands 165 cm^{-1} apart. The ratio of their absorption cross sections exhibits a van't Hoff behaviour between 150 and 300 K, bends over in a region between 150 and 80 K and remains constant at lower temperatures. It parallels quantitatively the temperature dependence of the sublines underlying the Raman band resulting from the Fe-N_ε (His F8) stretching mode. This observation provides strong evidence that the frequency positions of the band III subbands and the $\nu_{Fe\text{-}His}$ sublines are governed by the same coordinates. Probable candidates are the Fe^{2+} displacement out of the heme plane and the tilt angle of the Fe-N_ε bond. Moreover the frequency positions and halfwidths of the band III subbands also depend on temperature. This is rationalized in terms of a model which assumes a coupling between the electronic transition and a bath of low frequency modes. Our data indicate that these modes are harmonic below 130 K, but become anharmonic above this temperature. This onset of anharmonic motions is interpreted as resulting from protein substates interconversion which affect the prostethic group via heme protein coupling.

M-Pos350

THE HYDRATION DEPENDENCE OF ANHARMONIC MOTIONS IN MYOGLOBIN. ((Peter J. Steinbach and Bernard R. Brooks)) DCRT, NIH, Bethesda, MD 20892

Novel 150-ps molecular dynamics (MD) simulations of carboxymyoglobin (MbCO) have been performed during which dihedral transitions were prohibited by large energy barriers. Dynamics was simulated for: *i)* dehydrated MbCO at eleven temperatures from 100 to 400 K, *ii)* MbCO hydrated by 350 water molecules at ten temperatures from 100 to 325 K, and *iii)* MbCO solvated by 3830 waters at 300 K. Starting conformations for the low-temperature simulations were obtained by quenched MD simulations, cooling from 300 to 100 K over 1 ns (1).

Conventional MD simulations have correlated the anharmonic motion at temperatures above 220 K measured by neutron scattering to the number of dihedral angles that undergo transitions (2). In the absence of dihedral transitions, dehydrated MbCO exhibited only motions that are very nearly harmonic at all temperatures up to 400 K. In contrast, hydrated MbCO underwent both harmonic and highly anharmonic fluctuations. Upon elimination of dihedral transitions, mean-square fluctuation at 300 K was reduced by only 28% and 10% for hydrated and solvated MbCO, respectively. The effect of hydration on main chain fluctuation at 300 K was remarkably insensitive to torsional interconversion. Thus, the simulations suggest that hydration enhances the dynamical transition near 220 K by facilitating collective anharmonic motions that do not require dihedral transitions.

1. P.J. Steinbach and B.R. Brooks, *Chem. Phys. Letters 226* (1994) 447.
2. P.J. Steinbach and B.R. Brooks, *Proc. Natl. Acad. Sci. USA 90* (1993) 9135.

M-Pos351

ELECTRON-NUCLEAR COUPLING TO THE PORPHYRIN NITROGENS IN FERROUS NITROSYL COMPLEXES OF MYOGLOBIN ((H. Caroline Lee[1], and Jack Peisach[1,2])) Depts. of [1]Molecular Pharmacology, [2]Physiology & Biophysics, Albert Einstein College of Medicine, Bronx, NY 10461.

Electron spin echo envelope modulation (ESEEM) spectroscopy was applied to the ferrous nitrosyl complex of native (PP), mesoheme (MP)- and deuteroheme (DP)-substituted myoglobin (Mb) in order to measure electron-nuclear coupling to the porphyrin nitrogens. Nuclear quadrupole coupling parameters are similar for all three proteins, while the hyperfine coupling constant decreases slightly from MPFeNOMb > PPFeNO-Mb > DPFeNOMb. Spectra of all three proteins could be simulated using an angle of ≈60° between the z axis of the g and porphyrin ^{14}N nuclear quadrupole tensors. This predicts that the Fe-NO bond is tilted ≈30° from the heme normal, assuming the same assignment of the g tensor orientation as in PPFeNOMb based on a single crystal EPR study and for the porphyrin ^{14}N nuclear quadrupole tensor of four-coordinate metalloporphyrins based on a single crystal ENDOR study (figure). A similar Fe-NO tilt angle for PPFeNOMb was obtained from a single crystal EPR study and X-ray crystal structure. This work demonstrates the potential applicability of ESEEM spectroscopy to evaluate the Fe-NO bond geometry of hemoproteins.

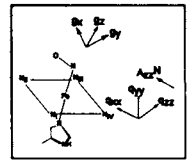

M-Pos352

AN ELECTRON SPIN ECHO ENVELOPE MODULATION (ESEEM) STUDY OF UNLIGATED AND PARTIALLY-LIGATED Fe-Co HYBRID HEMOGLOBINS ((H. Caroline Lee[1], Antonio Tsuneshige[2], Takashi Yonetani[2] and Jack Peisach[1,3])) [1]Molecular Pharmacology, [3]Physiology & Biophyics, Albert Einstein College of Medicine, Bronx, NY 10461; [2]Biochemistry & Biophysics, University of Pennsylvania, Philadelphia, PA 19104.

ESEEM spectra and their analysis by computer simulation were obtained for the deoxyCo-substituted subunits of four Fe-Co hybrid hemoglobins (Hbs): deoxy(αCoβFe)$_2$, deoxy(αFeβCo)$_2$, and the di-ligated (αdeoxyCoβFeCO)$_2$ and (αFeCOβdeoxyCo)$_2$. From comparison with model compounds, ESEEM components arising from the proximal imidazole N_δ were assigned. These were found to differ for the αCo subunits of an unligated Hb as compared to a di-ligated Hb, while the ESEEM of the proximal N_δ in the βCo subunits was invariant with the ligation state of the protein. All deoxyCo subunits show similar ^{14}N nuclear quadrupole coupling parameters while the nuclear hyperfine coupling constant for the α subunits in an unligated Hb is reduced by ≈ 0.15 MHz as compared to the others. The relative orientation of the ^{14}N nuclear quadrupole and g tensors is different in the deoxyCo β and α subunits. Based on magnetic tensor relationships, a discussion of the relative orientation of the proximal imidazole with respect to the porphyrin plane in the various deoxyCo subunits is presented.

M-Pos353

CIS EFFECTS OF PORPHYRIN SUBSTITUENTS ON ELECTRON-NUCLEAR COUPLING TO THE PROXIMAL IMIDAZOLE IN OXY COBALT-SUBSTITUTED MYOGLOBINS ((H. Caroline Lee[1], and Jack Peisach[1,2])) Depts. of [1]Molecular Pharmacology, [2]Physiology & Biophysics, Albert Einstein College of Medicine, Bronx, NY 10461.

Application of electron spin echo envelope modulation (ESEEM) spectroscopy to oxy cobalt-substituted globins measures nuclear hyperfine and quadrupole coupling to the N_ε of the proximal imidazole. We have previously demonstrated that these couplings decrease with an increase in the ionicity of the Co-O_2 bond leading to an increase in O_2 affinity. Independent O_2-binding studies of iron porphyrin-substituted globins have suggested that O_2 affinity increases with the pK_3 of the metal-free porphyrin[1]. To investigate the relationship between the pK_3 of the porphyrin nitrogens and the ionicity of the axial Co-O_2 bond in Co-substituted globins, ESEEM spectroscopy was applied to several Co porphyrin-substituted horse myoglobins (Mbs), including those with mesoporphyrin, deuteroporphyrin and protoporphyrin. We found that electron-nuclear coupling to the proximal N_ε decreases with an increase in the pK_3 of the porphyrin, indicating an increase in ionicity of the Co-O_2 bond. This predicts an increase in O_2 affinity for the substituted Co globins in a way analogous to the substituted Fe globins.

[1](a) Sono & Asakura (1975) *J. Biol.Chem. 250*, 5227; (b) Seybert et al. (1977) *J. Biol. Chem. 252*, 4225.

M-Pos354

pH-DEPENDENCE OF THE LOW-TEMPERATURE QUANTUM YIELDS OF PHOTOLYSIS IN OXY MYOGLOBIN: STRUCTURAL AND PHYSIOLOGICAL IMPLICATIONS

((D. Durst, L. M. Miller, M. Patel and M. R. Chance)) *Department of Physiology and Biophysics, Albert Einstein College of Medicine, Bronx, NY, 10461.*

The physiological rate of oxygen association in myoglobin (k_{on}) reflects the overall barrier to oxygen binding, which in turn, is correlated to low temperature quantum yields of photolysis, i.e. higher observable photoproduct yields indicate higher barriers to oxygen rebinding. Thus, the contribution of the distal side hydrogen bond to the overall barrier to oxygen binding in myoglobin has been investigated through a study of the pH dependence of MbO_2 photoproduct yields. Below ~pH 5, the hydrogen bond between the oxygen ligand and the distal histidine is broken due to protonation of the distal histidylimidazole -- which results in motion of the distal histidine away from the oxygen ligand. Through optical spectroscopy, we have found that the 10 K photoproduct yields decrease at low pH for MbO_2 (pH 7: 0.50±0.05; pH 5: 0.20±0.05) and cobalt-substituted MbO_2 (pH 7: 0.55±0.05; pH 4: 0.20±0.05), suggesting that the overall barrier to oxygen binding is lower when the hydrogen bond to the distal histidine is broken. This result is supported by higher k_{on} values for myoglobin mutants which lack a distal side hydrogen bond to the oxygen ligand. For the mutant $Mb(H64Q)O_2$, where the hydrogen bond to the distal glutamine does not titrate with pH, the photoproduct yield is constant (0.50±0.05) from pH 5 to pH 9. Additionally, the pH versus quantum yield "titration curve" for ferrous MbO_2 has a higher pK than that of cobaltous MbO_2, indicating that protonation of the distal histidylimidazole is easier in ferrous MbO_2. This result may be evidence for different hydrogen bond strengths in ferrous versus cobaltous MbO_2. This work is supported by NIH grant HL-45892.

M-Pos355

ACID-INDUCED TRANSFORMATIONS OF HEME POCKET IN MYOGLOBIN DERIVATIVES. ((V. Palaniappan and D. F. Bocian)) Department of Chemistry, University of California, Riverside, CA 92521. (Spon. by D. A. Johnson)

A stable equilibrium intermediate heme pocket structure in the acid-induced unfolding pathway of deoxymyoglobin has been identified and characterized. pH-dependent optical absorption and resonance Raman (RR) studies indicate that this intermediate exists in the 3.5-4.5 pH range. The Soret maximum for this intermediate is observed at ~426 nm which is different from that observed for either the native (~435 nm; pH 4.4-7.6 range) or the unfolded (~383 nm; pH 2.6-3.5 range) forms. The absorption and RR data indicate that the structure of the heme pocket in the intermediate form is distinctly different from that of native or unfolded forms. As is the case with the unfolded form, the intermediate form lacks the proximal iron-histidine bond which covalently links the prosthetic heme to the protein. The histidine ligand in the intermediate form is replaced by a relatively strongly bound, exchangeable water molecule. This water ligand appears to be absent in the unfolded form. The absence of the iron-histidine bond in the intermediate indicates a local structural perturbation of the heme pocket and may signal a more global perturbation of the protein. The properties of the intermediate strongly suggest that this form corresponds to the molten globule intermediate observed in the acid-induced unfolding/refolding pathways of apomyoglobin.

M-Pos356

ELECTRONIC TRANSITIONS OF METMYOGLOBIN. ((M.L. Carlson and A.S. Brill)) Biophysics Program, University of Virginia, Charlottesville, VA 22901. (Sponsored by J. Ellena)

The absorption spectrum of horse skeletal aquo-metmyoglobin between 14,500 and 46000 cm^{-1} is well represented by 19 Gaussian bands. The same pattern of bands, with parameters allowed to vary, simulates closely related spectra produced by temperature change, methanol complexation, and species sequence differences. While the profile of a general high-spin spectrum can be approximated with only 13 bands, reproduction of all the structure observed in difference spectra requires 19. Additional bands (beyond 19) reduce the structure present in residuals of the absolute spectra, but the unifying pattern of bands shared among the spectra is lost. The spectrum of the fluoride complex, recognizably high-spin, differs substantially from that of the aquo complex; it too can be represented by the same pattern of bands, albeit with different parameter values. (For the F^- complex an additional visible band, which does not disrupt the pattern, is warranted.) Temperature difference spectra are consistent with a spectroscopic sum rule for the heme and aromatic acid transitions taken together.

M-Pos357

MEDIATION OF Co-C BOND CLEAVAGE BY COBALAMIN DEPENDENT ENZYMES.

((E. M. Scheuring and M. R. Chance)) *Department of Physiology and Biophysics, Albert Einstein College of Medicine, Bronx, N.Y., 10461.*

Cobalamin dependent enzymes participate in a number of carbon skeleton rearrangement reactions as well as methylation reactions essential to all mammals. The key step in all of these reactions is the breakage of the Co-C bond. We have been intensively studying different forms of the free cobalamins and also the enzyme bound complexes by X-ray absorption spectroscopy (XAS) to answer the question how the enzyme accelerates the Co-C bond cleavage. The 5,6-dimethylbenzimidazole group (DMB or "base"), connected to the Co atom on the opposite side of the Co-C bond, has a significant role modulating the Co-C bond cleavage. The "base-on"/base-off" configuration has a proven effect on favoring homolytic versus heterolytic cleavage. An interesting hypothesis concerns the possible replacement of the DMB ligand with ligand from the enzyme. This is not the case for the cobalamin transport protein cobalophilin (Frisbie, S. M. and Chance, M. R. *Biochemistry*, **1993**, *32*, 13886). We have collected XAS data on different cobalamin dependent enzymes and analyzed them in combination with *ab initio* X-ray Absorption Fine Structure (XAFS) calculations using FEFF 6. For the FEFF calculations we modified the crystallographic structure of the free cobalamin cofactor to simulate the possible changes of the cofactor structure upon binding to enzymes, and compared these results with the experimental data. This work is supported by NRICGP/CSRS/USDA Program in Human Nutrients #91-6180-6798.

M-Pos358

SPECTROSCOPIC CHARACTERIZATION OF HORSE CYTOCHROME *C* IN NEAT DIMETHYL SULFOXIDE. ((B.S. Wicks; E.W. Findsen)) Department of Chemistry, Bowman-Oddy Laboratories, University of Toledo, Toledo, Ohio 43606.

We report the results of spectroscopic characterization of horse cytochrome *c*, lyophilized from a HEPES Buffer solution and dissolved in neat DMSO. Analysis using absorption and resonance Raman spectroscopies suggest that the protein conformation adopted in the organic solvent is similar to that observed for unfolded intermediate II, in the unfolding scheme proposed by Drew and Dickerson. The cyt. *c* can be reduced with sodium dithionite. The absorption studies indicate that the axial methionine ligand is lost, and CO binding studies to the ferrous species prove that one axial ligation site, presumably that of the axial methionine, is open and accessible to bind CO. Resonance Raman spectra of the equilibrium species indicate that with the unfolding of the protein, the heme pocket relaxes, allowing the heme to become more planar. Preliminary results of low temperature ESR studies of the ferric complex will also be presented.

Drew, H.R. and Dickerson, R.E. (1978) J. Biol. Chem. *253*, 8420.

M-Pos359

REFINEMENT AND ELECTROSTATIC ANALYSIS OF THE SOLUTION STRUCTURES OF FERRO- AND FERRICYTOCHROME C. ((Phoebe X. Qi§, Marilyn. R. Gunner†, Arieh Warshel‡, A. Joshua Wand§)) §Department of Biochemistry, University of Illinois at Urbana-Champaign, Urbana, IL 61801. †Department of Physics, City College of New York, New York, NY 10031. ‡Department of Chemistry, University of Southern California, Los Angeles, CA 90089

High resolution solution structures of ferro- and ferricytochrome c have been determined using a combination of multidimensional-1H NMR techniques and hybridized distance geometry-simulated annealing calculations. A family of 44 individually refined structures was obtained for each redox state. The all-residue rmsd about the average structure for ferrocytochrome c is 0.32 ± 0.07 Å for the backbone N, Cα and C' atoms and 0.85 ± 0.05 Å for all heavy atoms while 0.34 ± 0.04 Å and 0.93 ± 0.05 Å for the ferri-form. Examination of long lived structural waters in both redox states reveal potentially significant redox dependent structural changes. The orientation of the electron spin *g*-tensor was determined and the resulting pseudo-contact shifts were used to independently confirm observed structural differences. In an attempt to address the accuracy and the precision of the determined structures, electrostatic and midpoint potential calculations across the two families of structures were performed. Specific electrostatic interactions such as heme propionic acids and heme ligands that were previously considered to modulate the midpoint potentials were examined. Finally, heme solvent reorganization energy calculations were undertaken to provide a fundamental understanding of the electron-transfer process.

This work is supported by grant GM35940 from NIH.

M-Pos360

THE STRUCTURE OF Zn-SUBSTITUTED CYTOCHROME *c* EXAMINED BY OPTICAL AND NMR SPECTROSCOPY.
((H. Anni, J.M. Vanderkooi and L. Mayne))
University of Pennsylvania, Department of Biochemistry & Biophysics, Philadelphia, PA 19104-6089.

The prosthetic group, heme, in cytochrome *c* (cyt *c*) has a structural role; it is required for maintaining the protein globular structure. Even under denaturing conditions, the heme iron couples to the protein through two axial ligands. On the basis of studies with Zn-porphyrin model compounds, it was expected that reconstitution of cyt *c* with Zn would produce a Zn-protein with a single nitrogenous (His) ligand and an altered overall conformation. Our proton NMR (1D, 2D: COSY, TOCSY, NOESY) and optical studies (absorption, fluorescence and phosphorescence emission, phosphorescence lifetimes) show that Zn-cyt *c* preserves a native-like structure. This is mainly accomplished by the protein matrix that constrains the Zn-porphyrin into a hexa-coordinated geometry, with an enlarged porphyrin core to accommodate the bigger Zn metal. Both His-18 and Met-80 remain as axial ligands to Zn-porphyrin, though with weaker bonding. The thioether links of the porphyrin to the protein via Cys-14 and Cys-17 are also in place. Other amino acids in the vicinity of the porphyrin, like Phe82, have not changed positions. Furthermore, the amino acids in the protein-protein interface between cyt *c* and its redox protein partners are likewise unaffected by the change of the central metal in porphyrin.

(Supported by NIH P01-GM48130, University of Pennsylvania Research Foundation and Internatl. Human Frontier of Science Program RE-331/93)

M-Pos361

Effect of Porphyrin Electronic Environment upon Electron Transfer Characteristics in Anionic Porphyrin-Cytochrome *c* Complexes ((D. H. Omdal and R. W. Larsen))[1] Dept. of Chemistry, University of Hawaii at Manoa, Honolulu HI, 96822.

In this study we investigate the role of protein environment on the electron transfer rates of free-base uroporphyrin and 4-carboxyphenyl porphyrin complex with bovine cytochrome *c*. Electronic interactions between the porphyrin and the protein are investigated using steady-state optical absorption, second derivative absorption, near UV circular dichroism, and fluorescence spectroscopies. These data demonstrate that, although both porphyrins presumably bind to a similar site on the protein the extent of electronic perturbations to the porphyrin macrocycle are quite distinct between the two porphyrins. We also demonstrate that the electron transfer rates between porphyrin triplet state and the heme group of the cytochrome vary considerably depending upon the nature of the porphyrin. These results suggest a role for the docking domain between the porphyrin and the protein in modulating electron transfer rates.

M-Pos362

COMPLETE HEME PROTON NMR ASSIGNMENTS OF NATIVE YEAST ISO-1 FERRICYTOCHROME C AND TUNA FERRICYTOCHROME C USING ONLY STANDARD ONE-DIMENSIONAL AND TWO-DIMENSIONAL PROTON NMR SPECTROSCOPY. ((Steven F. Sukits & James D. Satterlee))
Department of Chemistry, Washington State University, Pullman, WA 99164-4630

Although fairly small proteins, the molecular paramagnetism of ferricytochromes *c* complicate making proton hyperfine resonance assignments. However, by wise application of standard one- and two-dimensional NMR experiments it is possible to arrive at a highly probable, self-consistent, complete set of heme hyperfine resonance assignments. This, in turn, leads to proton assignments of several additional amino acids near to the paramagnetic center, which in turn can lead to elucidation of the orientation of the molecular magnetic axis system.

supported by NIH grant GM 45986

M-Pos363

PROTON NMR SPECTROSCOPY COMPARISON OF LIFETIMES FOR CYTOCHROME C PEROXIDASE COMPLEXES WITH FERRICYTOCHROMES C. ((Qian Yi & James D. Satterlee)) Department of Chemistry, Washington State University, Pullman, WA 99164-4630

Under conditions of equilibrium chemical exchange in 1:2 mixtures of yeast cytochrome *c* peroxidase (CcP) with ferricytochromes *c* from three species (yeast iso-1, horse and tuna), NMR spectroscopy provides evidence that there are quantitative differences in the lifetimes of the 1:1 CcP/ferricytochrome *c* complexes. At low salt concentrations and 20 °C, variable temperature proton NMR studies reveal that the lifetimes of the 1:1 CcP/horse ferricytochrome *c* complex and the 1:1 CcP/tuna ferricytochrome *c* complex are less 1.76 (± 0.24) msec and probably in the μsec range.

supported by NIH grant GM 45986

M-Pos364

ACID-SENSITIVITY OF RAPID CYTOCHROME *C* OXIDASE: REGULATION BY BOUNDARY PHOSPHOLIPID. ((G. Rai, J.A. Tayh, and G.M. Baker)) Northern Illinois University, Department of Chemistry, DeKalb, IL 60115 .

Resistant or sensitive behavior, following an acid jump, has been characterized in rapid cytochrome *c* oxidase isolated from bovine heart and *Paracoccus denitrificans*. Resistant cases were associated with a monophasic 2 - 3 nm blue shift in the Soret maximum (λ_{max}) that was complete within the first few seconds. No further optical change was observed. Sensitive cases showed a biphasic 4 - 7 nm shift in λ_{max} that required 2 - 3 hours for equilibration. At the end of this period, there was > 60 % conversion to the slow form (detected by cyanide). Resistant cases showed only rapid to intermediate conversion. Acid-resistant samples were also resistant to formate. Resistance or sensitivity was statistically correlated with the bound phosphorus content of the enzyme. The 99.9 % confidence interval estimate of all sensitive preparations examined was 2.6 to 3.7 P_i / heme A. Resistant populations had interval estimates above or below this range. In addition, acid-sensitivity was blocked by adding phospholipid to solubilized enzyme. Membrane-bound preparations of the bovine enzyme were invariably resistant to an acid jump or formate. Sensitivity to acid or formate was not inducible in solubilized preparations of the bacterial enzyme. Our model suggests that changes in boundary phospholipid can alter proton accessibility to the a_3-Cu_B site in bovine heart enzyme, but not in the bacterial enzyme.

M-Pos365

FAR-RED RESONANCE RAMAN STUDY OF COPPER *A* IN SUBUNIT 2 OF CYTOCHROME *c* OXIDASE ((Stacie E. Wallace-Williams*, J. Sanders-Loehr§, S. De Vries‡, and William H. Woodruff*)) *CST-4, Mail Stop C345, Los Alamos National Laboratory, Los Alamos NM 87545; § Oregon Graduate Inststute, Beaverton OR; ‡ University of Leiden, The Netherlands.

The structure of Copper *A* (CuA), the proximate electron acceptor from cytochrome *c* in in cytochrome *c* oxidases (CcO), is an unresolved issue in respiratory bioenergetics. Elemental analysis, EPR, and MCD results have suggested that CuA is a coupled two-copper center analogous to that inferred in N_2O reductase, contrary to the earlier belief that CuA is a single-Cu site. More recent EXAFS evidence may suggest the existence in CuA of an actual Cu-Cu bond approximately 2.4 Å in length. The latter scenario, if correct, should be evident as a Cu-Cu stretching vibration observable by resonance Raman spectroscopy (RR). We have employed RR with Cu isotopic substitution on a genetically modified, solubilized form of CcO subunit 2 (wherein CuA resides) to examine these issues. To probe CuA we exploit resonance with its unique far-red (700-900 nm) electronic transitions, using titanium-doped sapphire laser excitation which is tunable over this wavelength range. The far-red excited RR spectra, and their dependence on excitation wavelength and $^{63-56}Cu$ isotopic substitution, are reported. The significance of these results as regards the structural environment of CuA are discussed.

M-Pos366

INFRARED SPECTROSCOPIC STUDIES OF NITRIC OXIDE BINDING BY CYTOCHROME c OXIDASE AT LOW-TEMPERATURE. ((Stacie E. Wallace-Williams, Douglas D. Lemon, Skip Williams, and William H. Woodruff)) Los Alamos National Laboratroy, Los Alamos, NM 87545.

It has been suggested, based on CO photodissociation and rebinding studies, that Cu_B plays a crucial role in the binding of exogenous ligands to the binuclear site of heme-copper oxidases. After photolysis at low temperatures two peaks identified as Cu_B-CO have been observed at 2062 and 2043 cm^{-1}. These experiments as well as numerous investigations at room temperature indicate that Cu_B may be a waystation for CO ligation to the binuclear site. Investigations of other ligand systems having varying properties regarding spin, charge, and steric bulk are needed to elucidate the important details of the gateway to the active site of this enzyme super-family. Here, these low-temperature IR studies have been extended to the ligand, NO, which may more closely mimic the O_2 ligand. In these studies NO is photolyzed from the $Fe^{2+}{}_{a3}$ by a 532 nm pulse from an Nd:YAG laser at temperatures between 9 and 200 Kelvin. At very low temperatures rebinding is very slow, essentially trapping the enzyme in the unliganded form. At higher temperatures the rebinding can be monitored. The results of these studies will be presented including low-temperature static FTIR difference spectra of the liganded vs. unliganded enzyme, time-dependent rebinding studies of NO to $Fe^{2+}{}_{a3}$, and the activation energy for NO rebinding. In addition, NO binding studies with the oxidized enzyme will also be presented.

M-Pos367

STUDIES OF REVERSIBLE INHIBITORS OF CYTOCHROME P450*cam*. ((Dan Harris and Gilda Loew)), Molecular Research Institute, 845 Page Mill Rd., Palo Alto, CA 94304

The relative binding free energies of several reversible inhibitors of cytochrome P450 are predicted employing free energy simulation methods applied to the enzyme-inhibitor complexes as well as the solvated inhibitor systems. In several cases examined, the simulation predictions made are based on known inhibitor crystal starting structures for both endpoints of the enzyme-inhibitor free energy simulation, thus providing some validation of sampling adequacy. It is shown that the desolvation free energy component is a dominant factor in determining the relative order of inhibition for most cases studied. Exceptions are discussed in detail. The magnitude of the desolvation free energy derived from free energy simulations is verified by additionally employing Poisson Boltzman (continuum electrostatic) and AMSOL semiempircal predictions of this quantity.

M-Pos368

HOMOLOGY MODELING OF THE THREE DIMENSIONAL STRUCTURE OF THE HUMAN P4501A1 ENZYME. ((Y-T. Chang and G. H. Loew)) Molecular Research Institute, 845 Page Mill Road, Palo Alto, CA 94304.

The P450 isozymes are a family of ubiquitous enzymes responsible for the biotransformation of various groups of compounds. The substrate specificity of each enzyme is not determined by its sequence alone, but more importantly, by its architecture in the binding site. Therefore, the understanding of the function and activity of each P450 isozyme requires the knowledge of its detailed three dimensional structure. However, experimental determination of 3D structures was very difficult especially for membrane bound proteins. The only three P450 isozymes with solved structures are P450cam, P450terp, and P450bm3. The availability of the P450bm3 structure provides a unique opportunity to obtain the structures of some mammilian P450s with higher accuracy since P450bm3 resembles more closely eukaryotic P450s in sequence and functional properties than it does other bacterial P450s such as P450cam. In this study, we attempted to build the 3D structure of human P4501A1 enzyme with the homology modeling technique based on the knowledge of P450cam, P450terp, and more importantly, P450bm3.

M-Pos369

CRYSTALLOGRAPHIC STUDIES ON CROSSLINKED HEMOGLOBINS ((E. J. Fernandez and K. W. Olsen)) Dept. of Chemistry, Loyola Univ., 6525 N. Sheridan, Chicago, IL 60626

X-ray diffraction data were collected on two chemically crosslinked hemoglobins. The first was crosslinked between the two Lys-α99 (α99XLHbA) with bis(3,5 dibromosalicyl) fumarate (DBSF). Crystals were grown under high salt, deoxy conditions. The structure was solved by difference Fourier methods and refined to an R-factor of 17.6%. There were no major displacements from native deoxy HbA. The only residues affected, besides the Lys-α99s, were the two Glu-β101s and Arg-β104s. Like the Lys-α99, these residues into the central cavity. The second crosslink was put between the Lys-β82 (β82XLHbA) using DBSF. Crosslinking was done under oxy conditions. Crystals were grown under deoxy conditions from PEG-6000 ($P2_1$, a=65.3, b=96.0, c=101.5 and β=101.5°, 2 tetramers per asymmetric unit). The structure was solved by molecular replacement using X-PLOR. The R-factor was 17.2%. While the structure remained largely similar to deoxy HbA, there were portions that had moved towards the liganded oxy HbA. There were also parts of β82XLHbA that were unlike both the deoxy and the oxy HbA structures and these were explained to be a consequence of the crosslink between the β-chains.

M-Pos370

Continuum Electrostatic Calculation of Hemoglobin Protonation ((P. Beroza, and D. Case))
The Scripps Research Institute, La Jolla, CA 92037

Using a continuum electrostatic model, we calculated the titration curves of amino acids in hemoglobin for the R (oxygen bound) and T (no oxygen bound) states. Preliminary results indicate that several histidine residues have higher pK's in the T state than in the R state. This causes a proton uptake in the R → T state transition, in agreement with experiments,[1] although the proton uptake is over-estimated.

The calculations are based on a finite-difference solution to the linearized Poisson-Boltzmann equation; thus, ionic strength effects were included through Debye-Hückel theory. Chloride ions, which also bind to hemoglobin in the R → T state transition, were not included explicitly in the calculation. The results suggest that conformational changes resulting from the transition may be sufficient to account for increased protonation in the T state. The effect of chloride binding on the energetics of the R and T states will also be investigated.

1. Rollema, et al., J. Biol. Chem. 250,1333-1339 (1975).

M-Pos371

MULTI-VARIABLE APPROACH TO THE DESIGN OF CROSSLINKED HEMOGLOBINS ((K.W. Olsen, Q. Zhang, H. Huang, E. J. Fernandez, Y. Zheng and K. Sujatha)), Dept. of Chemistry, Loyola Univ., 6525 N. Sheridan Rd., Chicago, IL 60626.

Computer-aided molecular design is being used to propose new crosslinking reagents for human hemoglobin. In this design process, molecular dynamics calculations have been used to assess the flexibility of both the reagent and the reaction site on the protein. Double crosslinking, in which the same reagent is under two different conditions, and multi-linking, in which a reagent that reacts at more than two sites in used, offer the possibility of greater control over the stability and function of a hemoglobin-based blood substitute. A more interesting double crosslinked hemoglobin has fumarate crosslinks between both the α99 lysines and the β82 lysines. The T_s is 20°C, which is 4°C greater than the singly crosslinked species. The oxygen affinity and cooperativity are similar to that of α99XLHb but unaffected by inositol hexaphosphate (IHP). The autoxidation is slower than that of α99XLHb. Tetralinkers based on a benzophenone nucleus can be designed to greatly lower the oxygen affinity. X-ray crystal structures of some of the crosslinked hemoglobins are being determined.

M-Pos372

CRYSTALLOGRAPHIC INVESTIGATIONS OF ERYTHROCRUORIN FROM *LUMBRICUS TERRESTRIS* ((Kristen Strand and William E. Royer, Jr.)) Program in Molecular Medicine and Dept. of Biochemistry and Molecular Biology, University of Massachusetts Medical Center, Worcester, MA 01605 (spon. by F.R. Smith)

Lumbricus hemoglobin is an extracellular respiratory protein complex located in the hemolymph of the common earthworm, where it functions to exchange O_2 and CO_2 in the tissues. We are investigating the crystal structure of this molecule in order to learn the mechanism for the self-limited assembly of a cooperative complex from more than 200 polypeptide chains. Self-rotation calculations reveal molecular D_6 symmetry with a molecular dyad coincident with the crystallographic dyad along the **a** axis and the molecular 6-fold axis tilted 15° from the **c** axis. The position of the molecular center is approximately at 1/4**a** as indicated by packing considerations and inspection of the intensities of the l=2n versus l=2n+1 low angle reflections in the h0l plane. To solve the phase problem , we are using model based refinement techniques. Initial phases were derived from a 3D reconstruction from cryo-electron microscopy (M.Schatz and M. vanHeel) and combined with x-ray intensities. These phases were improved by multiple cycles of 6-fold averaging followed by phase extension extending from 35 Å to 5.5 Å yielding electron density maps with interesting features. Currently efforts are focused on improving and interpreting these maps. (Supported by NIH and AHA)

PHOTOSYNTHESIS

M-Pos373

STABILIZATION AND RECONSTITUTION OF OXYGEN-EVOLVING PHOTOSYSTEM II REACTION CENTER. ((J. Parkash and A.M. Saxena)) Biology Department, Brookhaven National Laboratory, Upton, NY 11973.

Photosystem II (PS II) particles were prepared from thermophillic cyanobacterium *Phormidium laminosum* by following the procedure of Bendall et al. 1988 (see Methods in Enzymology, 167, 272-280) with the exception that after sucrose density gradient centrifugation the PS II particles were not subjected to ultrafilteration for concentration. These PS II particles were then reconstituted with DOPC (dioleyl phosphatidylcholine) by sonication and dialysed against buffers in absence or presence of 25% (v/v) glycerol. After dialysis the PS II particles were either ultracentrifuged or passed through Sephadex G-50 column first and then ultracentrifuged. The PS II particles thus obtained were then incubated in dark at 4^0C and the oxygen evolving activities of the samples were determined every 24 hours for upto 96 hours. The results obtained indicate that (i) in control PS II particles the oxygen evolving activity remained almost constant even after 96 hours of incubation with or without glycerol, (ii) the reconstituion of PS II particles with DOPC increased the oxygen evolving activity as well as helped in further stabilization of PS II complex and (iii) passage through Sephadex G-50 column was less effective as compared to direct ultracentrifugation in maintaining the oxygen evolving activity for extended period of time. These observations will be presented and discussed in the light of damaging effect of ultrafilteration and stabilizing effect of DOPC on the maintenance of PS II structure and function.

M-Pos374

REGULATION OF PHOTOSYSTEM II THROUGH THE MANGANESE-STABILIZING PROTEIN DURING NITROGEN FIXATION CYCLES IN CYANOTHECE SP. ATCC 51142. ((P.C. Meunier, M.S. Colon, and L.A. Sherman)) Department of Biological Sciences, Purdue University, West Lafayette, IN 47907

Cyanothece sp. ATCC 51142 is a cyanobacterium that alternates N_2-fixation and photosynthesis in cycles that display the phenotypic behavior of circadian rhythms. We report on the occurrence of reversible and very fast photoactivations and deactivations of manganese under physiological conditions. At certain times during the cycle, the oxygen production capacity can be increased or decreased by more than an order of magnitude in a few minutes. This behavior is phenomenologically similar to that of the *psbO* deletion mutant of *Synechocystis* sp. PCC 6803, thus suggesting that the extrinsic proteins of Photosystem II may be regulated in *Cyanothece*. Furthermore, our data suggest that *Cyanothece* modulates the 'ratcheting' mechanism that normally stabilizes the S_1 and S_0 states. As a result, the super-reduced S-states, S_{-1} and S_{-2}, may be present in large quantities. If allowed to proceed further, the deactivation process results in non-functional manganese centers or, possibly, the release of manganese. Under these conditions, the quantities of super-reduced S-states undergo cyclic behavior, as do the probabilities of backward transitions, misses and single-hits. We describe the kinetics of the reactivation process by using the new probability of reactivation, "ε", where reactivated centers enter the S_{-2} state. Thus, we suggest that the *psbO* protein is an important regulatory site for Photosystem II in cyanobacteria. Supported by DOE grant DE-FG02-89ER14028 and USDA grant 93-37306-9238.

M-Pos375

ACETATE-TREATED PHOTOSYSTEM II LIMITED TO TWO TURNOVERS BY AN ELECTRON-ACCEPTING HERBICIDE DOES NOT YIELD THE S3 EPR SIGNAL. ((Veronika A. Szalai and Gary W. Brudvig)) Department of Chemistry, Yale University, New Haven, CT 06511.

A 230-Gauss wide "S3" EPR signal is induced in acetate-treated Photosystem II (PSII) by 30 seconds of illumination at 277K followed by freezing under illumination to 77K [MacLachlin & Nugent (1993) *Biochemistry* **32**, 9772-9780]. This signal has been interpreted to arise from an S_2X^+ species where X^+ is an amino acid radical. We have produced the S_3 state in high yield by using an electron-accepting herbicide (phenylnitroxylphenyldimethylurea) which binds to the Q_B site [Bocarsly & Brudvig (1992) *J. Am. Chem. Soc.* **114**, 9762-9767]. When the S_3 state is generated by this method in acetate-treated PSII, the "S3" EPR signal is not observed. By EPR spectroscopy, we have monitored the parallel oxidation of the oxygen-evolving complex (OEC), reduction of the nitroxide radical of the electron-accepting herbicide, and the reduction of Q_A^- to insure that PSII has been limited to two turnovers. In acetate-treated PSII without an electron-accepting herbicide, both the FeQ_A^- and the S3 EPR signals exhibit biphasic decay kinetics at 250K. The fast decay phase of the S3 EPR signal (k_{fast} = 1.0 ± 0.2 min^{-1}) at 250K does not match that found for the FeQ_A^- EPR signal (k_{fast} = 0.18 ± 0.05 min^{-1}). Based on these results, we offer several interpretations of the origin of the S3 signal. The S3 signal could be derived from a higher oxidation state of the OEC than S_3. By using a redox-active herbicide to limit the donor side to two turnovers, pathways to higher oxidation states have been blocked. Another interpretation is that the S3 signal may not originate from the OEC, but from an acceptor-side species. Supported by the National Institutes of Health.

M-Pos376

A DIFFERENCE INFRARED STUDY OF HYDROGEN BONDING TO THE Z•TYROSYL RADICAL OF PHOTOSYSTEM II ((M.T. Bernard[1], G.M. MacDonald[1], A.P. Nguyen[2], R.J. Debus[2], and B.A. Barry[1])) [1]Department of Biochemistry, University of Minnesota, St. Paul, MN 55108; [2]Department of Biochemistry, University of California, Riverside, CA 92521

Photosystem II, the photosynthetic water oxidizing complex, contains two well characterized redox active tyrosines, D and Z. D forms a stable radical of unknown function. Z is an electron carrier between the primary chlorophyll donor and the manganese catalytic site. The vibrational difference spectra associated with the oxidation of tyrosines Z and D have been obtained through the use of infrared spectroscopy {MacDonald et al. (1994) *Proc. Natl. Acad. Sci. USA* **90**, 11024}. Here, we examine the effect of deuterium exchange on these vibrational difference spectra. While the putative C-O vibration of stable tyrosine radical D• downshifts in ^2H_2O, the putative C-O vibration of tyrosine radical Z• does not. This result is consistent with the existence of a hydrogen bond to the phenol oxygen of the D• radical; we conclude that a hydrogen bond is not formed to the Z• radical. In an effort to identify the amino acid residue that is the proton acceptor for Z, we have performed global ^{15}N labeling. While significant ^{15}N shifts are observed in the vibrational difference spectrum, substitution of a glutamine for a histidine that is predicted to lie in the environment of tyrosine Z has little or no effect on the difference infrared spectrum. There is also no significant change in the yield or lineshape of the Z• EPR signal under continuous illumination in this mutant. Our results are inconsistent with the possibility that this residue, histidine 190 of the D1 polypeptide, acts as the sole proton acceptor for tyrosine Z. Supported by NIH GM 43496 (R.J.D.) and GM 43273 (B.A.B.).

M-Pos377

ELECTRONIC STRUCTURE DETERMINATION OF THE PRIMARY DONOR IN PSI BY USING MULTIFREQUENCY PULSED-EPR

((Michelle Mac, Xiao-song Tang, Bruce A. Diner, John McCracken and Gerald T. Babcock)) Department of Chemistry, Michigan State University, E. Lansing, MI 48824 and Central Research and Development Department, Experimental Station, P.O. Box 80173, E.I. DuPont de Nemours and Company, Wilmington, DE 19880.

Photosynthesis in higher plants and cyanobacteria is accomplished by the interplay of two photosystems. Photosystem I (PSI), through a series of electron transfer reactions, catalyzes the reduction of $NADP^+$ to NADPH. The primary electron donor in PSI (P_{700}) is thought to be either a monomer or dimer of chlorophyll *a* molecules. The electronic structure of the $P_{700}^{+\bullet}$ is still controversial, although analogies to the primary donor in bacteria have been suggested. In bacteria, the primary donor has been shown to be a dimer of bacteriochlorophyll. Magnetic resonance studies have shown that the unpaired spin in the cation radical is delocalized asymmetrically over both halves of the dimer. Analysis of the unpaired spin density distribution leads to the suggestion that the unpaired electron resides in an a_{1u} molecular orbital. The electronic structure of the cation radical from PSI has been probed by using the pulsed-EPR method of electron spin echo envelope modulation (ESEEM). Preliminary results indicate a different unpaired spin density distribution for $P_{700}^{+\bullet}$. The consequences of this difference will be discussed.

M-Pos378

THE REDOXPOTENTIALS OF THE B-CYTOCHROMES OF THE CHLOROPLASTS BF-COMPLEX INCLUDING INTERACTION.

((C. Wagner and D. Walz)) Biozentrum Univ. Basel, CH-4056 Basel, Switzerland. (Spon. by R. Caplan)

The bf-complex in the membrane of chloroplast thylakoids contains four redox centres and two of them, viz. cytochrome b_L and cytochrome b_H, have the absorbance peak at the same wavelength. Thus it is impossible to distinguish between reduced cytochrome b_L and cytochrome b_H and the titration curve cannot be separated. Whether or not one includes the interaction between the b-cytochromes, different interpretations of the measured curve are possible, as already pointed out by Malmström (1974).

We present a model where the interaction is represented as repelling potential caused by a reduced cytochrome b (L or H). It affects the redox reaction between the plastoquinol and the other cytochrome b. The interaction was estimated by a valence bond approach for the electron transfer reaction where the reduced cytochrome b can be considered as an additional charge of the protein.

M-Pos379

TYR_D TO $TYR_D°$ TRANSITION STUDIED IN PHOTOSYSTEM II BY FTIR SPECTROSCOPY.

R. Hienerwadel, A. Boussac, J. Breton, W. Mäntele*, and C. Berthomieu
CEA-Saclay, SBE, 91191 Gif-sur-Yvette Cedex, France; *Inst. für Physik. und Theor. Chemie, Uni. Erlangen-Nürnberg, Egerlandst. 3, 91058 Erlangen, Germany.

The $Tyr_D°$ radical is normally stable in photosystem II. Conditions were found, where it decays in the dark, even in the presence of ferricyanide added to reoxidize Q_A^-. These conditions allowed a light-induced FTIR spectrum to be recorded, where only vibrational changes due to the Tyr_D to $Tyr_D°$ transition contribute. This was controlled by EPR in the same conditions and a $TyrD°$ decay in around 5 min was measured. The assignment of the Tyr and $Tyr°$ IR modes will be discussed by comparison with radical-minus-neutral UV-induced FTIR spectra obtained with Tyr and phenol (PhOH) model compounds in various conditions[1]. Analogies are found with the PhO°/PhOH spectrum obtained at pH 8. This is an experimental evidence that Tyr_D is protonated. The ν(CO) mode appears at 1252 cm^{-1} for Tyr_D and at 1504 cm^{-1} in the radical. The modification upon radical formation of the other Tyr modes identified at 1479, 1397, 1371, and 1350 cm^{-1} will be discussed as well as the contributions of His side-chain.

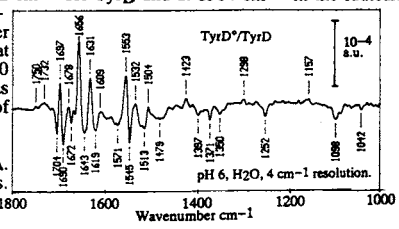

1. C. Berthomieu, and A. Boussac (1994) J. Phys. Chem. submitted.

M-Pos380

LIGHT-INDUCED FTIR DIFFERENCE SPECTROSCOPY OF THE Q_A AND Q_B VIBRATIONS IN BACTERIAL REACTION CENTERS RECONSTITUTED WITH SITE SPECIFIC LABELED QUINONES

J. Breton, C. Boullais, J.-R. Burie, C. Mioskowski, and E. Nabedryk
DBCM, CEA-Saclay, 91191 Gif-sur-Yvette Cedex, France

Photoreduction of the quinone electron acceptors Q_A and Q_B in bacterial RCs has been characterized by FTIR difference spectroscopy[1]. The vibrations of each individual quinone carbonyl were discriminated against protein absorbance changes by using RCs reconstituted with ubiquinones selectively ^{13}C-labeled on either one of the two carbonyls. In *Rb. sphaeroides*, the two carbonyls of Q_A appear decidedly unequivalent with the C_1=O (proximal to the isoprenoid chain) at 1660 cm^{-1} essentially free from interaction with the protein and the C_4=O (proximal to the methyl group) at 1601 cm^{-1} extensively downshifted compared to *in vitro*, probably due to a strong interaction with His M219[2]. These results contrast with the conclusions derived from (i) X-ray crystallography of the RCs, indicating the stronger hydrogen bond at C_1 and (ii) ^{13}C-MAS NMR, suggesting no hydrogen bond at either C_1 or C_4. FTIR study of a chainless symmetrical ubiquinone in the Q_A site further shows that the chain is not responsible for the unequivalent binding of the carbonyls[3].

In both *Rb. sphaeroides* and *Rp. viridis*, the two carbonyls of Q_B (at 1640 cm^{-1}) are equivalent, showing moderate bonding interactions with the protein. Further isotope effects on Q_B^-/Q_B FTIR spectra of RCs reconstituted with ubiquinone labeled either on the two carbonyl oxygens or on all the carbon atoms show that the conformation of Q_B in the protein site as well as its bonding interactions are very similar in *Rp. viridis* and *Rb. sphaeroides*.

(1) Breton et al., 1994a, *Biochemistry* 33, 4953-4964; (2) 1994b, *ibid.*, in press; (3) 1994c, *ibid.* in press.

M-Pos381

FTIR SPECTROSCOPY OF HETERODIMER MUTANTS OF *RB. SPHAEROIDES*: THE EFFECT OF ADDITIONAL MUTATIONS.

((E. Nabedryk and J. Breton)) SBE/DBCM, CEA-Saclay, 91191 Gif-sur-Yvette Cedex, France; ((M. Kuhn, A. Fetsch, C. Schulz and W. Lubitz)) Max-Volmer-Institut, Techn. Univ. Berlin, D-10623, Berlin, Germany.

Light-induced $P^+Q_A^-/PQ_A$ FTIR difference spectra of *Rb. sphaeroides* chromatophores have been obtained at 100K for several heterodimer mutants. In addition to the His M202 to Leu substitution, a second mutation was designed in order to introduce or to delete a potential hydrogen (H) donor group, either near the 9-keto (Leu L131 or Leu M160 changed to His) or the 2a-acetyl (His L168 to Phe or Phe M197 to His) carbonyl of P. In the single-site mutant HL(M202), the signal at 1697 cm^{-1} is assigned to the 9-keto C=O (free from interaction with the protein) of P_L which gives rise to a split signal at 1722-1712 cm^{-1} in the P_L^+ state, in agreement with FTIR data from *Rb. capsulatus* (1). For all the new heterodimer mutants, the 9-keto C=O of P_L is observed at 1698 ± 3 cm^{-1}, implying that it is not involved in a H-bond in the neutral state of P. In LH(L131)+HL(M202), the 1722-cm^{-1} peak is downshifted to 1707 cm^{-1}, while in LH(M160)+HL(M202) the 1712-cm^{-1} peak disappears and a new peak is observed at 1691 cm^{-1}. These changes possibly reflect H-bonding of the 9-keto C=O in the P+ state. A small band at 1618 cm^{-1} in wild-type, previously assigned to the 2a-acetyl C=O of P_L bound to His L168, is present in HL(M202) but absent in HF(L168)+HL(M202), suggesting that the H-bond is lost in this particular mutant. Furthermore, the five heterodimer mutants display neither the Newband at 2600 cm^{-1} nor the bands at ≈1550, 1480 and 1296 cm^{-1}, characteristic of the BChl homodimer state of P+ in wild-type RC. These FTIR data demonstrate that all these mutants are indeed heterodimeric. (1) Nabedryk E. et al., (1992) *Biochemistry* 31, 10852-10858.

M-Pos382

SITE-DIRECTED MUTAGENESIS OF RB. SPHAEROIDES REACTION CENTERS TO EXPLORE REPLACEMENT OF A AND B BRANCH MONOMER BACTERIOCHLOROPHYLLS WITH BACTERIOPHEOPHYTINS.

((T.K. Turanchik, D.M. Gallo, J.C. Williams, A.K. Taguchi, N.W. Woodbury)) Center for the Study of Early Events in Photosynthesis and the Department of Chemistry and Biochemistry, Arizona State University, Tempe, AZ 85287-1604.

Two mutants were designed to replace the A-branch and B-branch monomer bacteriochorophylls (Bchl) with bacteriopheophytins (Bpheo) in the photosynthetic reaction center (RC) of *Rhodobacter sphaeroides*. The A branch mutant was constructed by oligonucleotide-mediated mutagenesis of His L153 to Leu and the B branch mutant was created by the equivalent His M182 to Leu alteration. Analogous mutants have been constructed in *Rb. capsulatus*. (Bylina et al., (1990) Biochem. **29**, 6203) and RCs isolated from the B-side mutant His M180 to Leu have shown that the Bchl B-side monomer is replaced by Bpheo (Gallo et al., unpublished results). The monomer Bchl to Bpheo mutations have been created in *Rb. sphaeroides* for two reasons: 1) RC isolation in this species is usually facile and 2) the crystal structure of the RC has been determined (Chang et al., 1986; Allen et al., 1986). In addition to pigment extraction and HPLC analyses for Bchl:Bpheo ratios, the mutant RCs will be characterized using visible and near IR absorption spectroscopy, fluorescence quenching, and subpicosecond transient absorption spectroscopy.

M-Pos383

EPR/ENDOR ON THE PRIMARY ELECTRON DONOR OF HETERODIMER-HYDROGEN BOND REACTION CENTER MUTANTS.

((M. Huber[#,1], D. Davis[&] and C.C. Schenck[&])) [#]Institute of Organic Chemistry, FU Berlin 14195, Berlin, Takustr. 3. 14195 Berlin, FRG and [&]Department of Biochemistry, Colorado State University, Fort Collins, CO 80523 (Spon. by A. Dong)

Site directed mutagenesis has proven to be a powerful tool for determining factors influencing the electronic structure of the special pair (D) of two bacteriochlorophylls (BChl) in the photosynthetic reaction center protein. Thus far, two main approaches have been taken. In one approach, changes have been made in hydrogen bonding between D and the surrounding protein, resulting in changes in the redox potential of D and a small redistribution of spin density over the two BChls of D^+[1]. Changing hydrogen bonds could change the spin density either through effects on the energies of the relevant basis states and/or through effects on coupling between the BChls of D. Thus, it is not clear from these results how the changes in redox potential were mediated. In another approach, heterodimer mutants have been created in which one of the BChl molecules of D is replaced by a bacteriopheophytin. This results in a strongly asymmetric electronic state of D^+, in which the unpaired electron is essentially localized on the BChl, D_L [2]. Thus in the heterodimer mutants, a change in hydrogen bonding might not affect electron localization on D_L, and the EPR/ENDOR signal could reflect electronic effects of hydrogen bonds more directly. Therefore, we have combined these approaches by constructing heterodimer mutants in which potential hydrogen bonding residues are introduced (or removed). First EPR/ENDOR results on these mutants reveal small, but significant changes in electronic structure which are consistent with the changes in hydrogen bonding. [1] J.Rautter, et al. in: The Photosynthetic Bacterial Reaction Center II, J. Breton, A. Vermeglio (eds.), Plenum Press, New York (1992), p. 99ff [2] M. Huber, et al. in: Reaction Centers of Photosynthetic Bacteria, M.-E. Michel-Beyerle (ed.), Springer Verlag, Berlin (1990), p. 219ff.

M-Pos384

RESONANCE RAMAN STUDIES OF GENETICALLY MODIFIED BACTERIAL REACTION CENTERS.

((V. Palaniappan,[1] C. C. Schenck[2] and D. F. Bocian[1])) [1]Dept. of Chemistry, University of California, Riverside, CA 92521. [2]Dept. of Biochemistry, Colorado State University, Fort Collins, CO 80523.

A detailed resonance Raman (RR) study of mutant reaction centers (RCs) from *Rhodobacter (Rb.) sphaeroides 2.3.1* and *Rb. capsulatus* was conducted in order to assess the effects of mutations on the structures of RC pigments. The mutations involved residues near the special pair, P or the primary acceptor bacteriopheophytin, BPh_L. RR spectra of both the quinone-reduced and P-oxidized RCs were acquired by using a number of excitation wavelengths. The results indicate that (i) in the case of wild-type RCs the macrocycle of P_M is structurally more distorted than that of P_L. (ii) In H(M200)L RCs, $BPh_M(P)$ is less distorted relative to the other two BPhs. (iii) Comparison of data for wild-type and E(L104)L RCs indicates that factors other than hydrogen-bonding perturb the environment of BPh_L. One such factor might be the local dielectric constant (ε) near BPh_L *vs.* BPh_M. The RR data suggest that ε near BPh_L is higher than that of BPh_M which could facilitate anion formation on BPh_L. For both wild-type and mutant RCs, oxidation of P selectively perturbs the environment of BPh_L. This is manifested as an increase in ε near BPh_L, which could further stabilize BPh_L^- anion.

Acknowledgment: We thank Drs. D. C. Youvan and E. J. Bylina for RCs from *Rb. capsulatus*.

M-Pos385

HIGHER-ORDER STARK SPECTROSCOPY OF MUTANT REACTION CENTERS FROM *RB. SPHAEROIDES*.

((Laura J. Moore, Huilin Zhou, Kaiqin Lao, Steven G. Boxer)) Chemistry Department, Stanford University, Stanford CA 94305-5080

Higher-order Stark spectra have been measured in frozen glasses at 77 and 1.5K on the Q_Y bands of *Rb. sphaeroides* reaction center (RC) mutants: heterodimer ((M)H202L), in which one of the bacteriochlorophylls of the special pair is a bacteriopheophytin; and two mutants in which the hydrogen bonds to the acetyl group of the special pair dimer are symmetrized, (L)H168F and (M)F197H. Evaluation of the lineshape of the higher -order Stark spectra (with respect to the relative contributions from derivatives of the absorption spectrum) gives insight into the electro-optic properties of these RCs. The dimer band of these mutants all have different Stark lineshapes than that of wild type. The shapes of the 2ω and 4ω Stark spectra of the heterodimer mutant indicate that a large difference dipole ($\Delta\mu$) dominates the Stark spectrum. The hydrogen bond mutants display less significant change in the lineshape, but the derivative contributions still differ from that of wild type. This suggests that the contributions to the Stark lineshape from $\Delta\mu$ and the polarizability ($\Delta\alpha$) are altered by these perturbations of the dimer.

M-Pos386

OSCILLATIONS IN THE SPONTANEOUS FLUORESCENCE FROM PHOTOSYNTHETIC REACTION CENTERS.

((R. J. Stanley and S. G. Boxer)) Department of Chemistry, Stanford University, Stanford, California 94305-5080

The spontaneous fluorescence from the special pair primary electron donor in bacterial photosynthetic reaction centers has been measured at low temperature using fluorescence upconversion following excitation of the special pair with 80 fs pulses from a modelocked Ti:sapphire laser. Oscillations are observed during the first few ps of the decay (see figure 1). The frequency of the oscillations and the detection wavelength dependence of their intensity are similar to results obtained by Vos et al.,*Biochemistry*, 33, 6750-6757 (1994) using stimulated emission. This demonstrates that the oscillations are associated with the excited state of the special pair, not with stimulated Raman scattering. Vibrational coherence persists on the time scale of electron transfer. Possible relationships between these results and other observables is discussed.

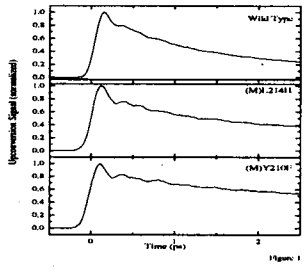

M-Pos387

STRUCTURAL CHANGES FOLLOW CHARGE SEPARATION IN BACTERIAL REACTION CENTERS

((P. Brzezinski and L-E. Andréasson)) Dept. Biochemistry & Biophysics, Göteborg University, Medicinareg. 9C, S-413 90 GÖTEBORG.

Reaction centers (RCs) from *Rb. sphaeroides* were treated with trypsin in the dark and under illumination (in the charge-separated state) to probe for light-induced structural changes (1,2). As evidenced from gel electrophoresis, optical spectra, electron-transfer kinetics and measurements of voltage changes in RCs oriented in lipid layers, tryptic treatment in the dark and during illumination resulted in different effects. The time constant of $P^+Q_A^- \rightarrow PQ_A$ increased during trypsination in the dark in RCs with the native ubiquinone in the Q_A site, whereas it decreased with anthraquinone. This indicates that trypsination affects charges close to the Q_A site. Trypsination resulted also in inhibition of the Q_A^- to Q_B electron transfer. Tryptic digestion during illumination resulted in a marked strengthening and acceleration of the effects seen already during dark treatment. The reduction kinetics of P^+ by cyt. c_2^{2+} was not affected by trypsin treatment in the dark, but in RCs trypsinated in light the binding affinity was enhanced by a factor of two. Measurements of light-induced voltage changes in RCs showed that only the acceptor side was degraded by trypsin in the dark. In addition, trypsination from the acceptor side impaired a voltage change previously ascribed to light-induced structural changes (2). In RCs treated from the donor side this voltage change was not affected. In conclusion, structural changes follow charge separation in bacterial RCs. The function of these light-induced structural changes may be to stabilize charge separation and facilitate forward electron transfer. (1) Kleinfeld et al. (1984) *Biochemistry* **23**, 5780. (2) Brzezinski et al. (1992) in *The Photosynthetic Bacterial Reaction Center II*, eds. J. Breton & A. Vermeglio (Plenum Press), 321.

M-Pos388

PREDICTION OF pKa VALUES FOR RESIDUES NEAR THE QUINONE BINDING SITES IN THE PHOTOSYNTHETIC REACTION CENTER OF RB. SPHAEROIDES.

((C. J. Gibas, C. A.Wraight, S. Subramaniam)) University of Illinois at Urbana-Champaign, Urbana, IL 61801.

The presence of several charged amino acid residues near the secondary quinone binding site in the bacterial photosynthetic reaction centers (RCs) is known to be required for protein function. These residues are thought to participate in the pathway of proton conduction from the aqueous phase to the protein interior. Experimental evidence shows that removal or alteration of some of these residues significantly changes the pH dependence of RC function. In this work, we have calculated pKas for ionizable residues near the quinone binding site by iterative solution of the finite-difference Poisson-Boltzmann equation. The photosynthetic reaction center contains 172 titratable residues, and without some approximation the number of ionization states to be described would become extremely large. We approach this problem using a method of clustering titratable sites and using finer grid spacings for short range interactions (Antosiewicz et al 1994). Mapping the states of protonation of key residues near the quinone-binding site has provided a conceptual model for proton conduction. [supported by GAANN graduate research fellowship and USDA].

M-Pos389

SITE-DIRECTED MUTAGENESIS OF THE H-SUBUNIT RESIDUE GLU^{H173} OF THE PHOTOSYNTHETIC REACTION CENTER FROM *RHODOBACTER SPHAEROIDES*. ((E. Takahashi and C.A. Wraight)) Department of Plant Biology, University of Illinois, Urbana, IL 61801.

The secondary quinone, Q_B, of the photosynthetic reaction center of *Rhodobacter sphaeroides* is surrounded by amino acid residues of the L-subunit and, very likely, some water molecules. The effects of site-directed mutagenesis upon reaction center turnover and quinone function have implicated several L-subunit residues in proton delivery to Q_B. Amongst these, Asp^{L213} is crucial for delivery of the first proton, coupled to transfer of the second electron, while Glu^{L212}, possibly together with Asp^{L213}, is required for delivery of the second proton, following the second electron transfer. Glu^{L212} and Asp^{L213} represent an inner shell of residues involved in proton transfer to Q_B.

We report here the effects of mutation of Glu^{H173}, a residue in the second shell around Q_B. Glu^{H173} was targeted for site-directed mutagenesis because it is located in a cluster of interacting residues near Q_B, and centered on Asp^{L213}, and including Asp^{L210} and Arg^{L217}. This is the first report of a site-directed mutation of the H-subunit, for which a site-directed mutagenesis and expression system has been developed.

Previous reports on mutations of Asp^{L210} and Arg^{L217} indicated only mild perturbations of Q_B function, but mutation of Glu^{H173} to glutamine (mutant H173EQ) seriously perturbed both the first and the second electron transfer events. The kinetics of both electron transfers were greatly retarded, as also observed previously for the Asp^{L213} → Asn mutant (L213DN), but the proton-linked, one electron redox equilibrium, $Q_A^-Q_B \leftrightarrow Q_AQ_B^-$, was diminished, in contrast to the L213DN mutant. These major disruptions of events coupled to proton delivery to Q_B are largely reversed by the addition of azide (N_3^-), as previously observed in the Asp^{L213} and Glu^{L212} mutants. The results support a major role for electrostatic interactions between charged groups in "potentiating" proton transfer function, by raising the pK of a functional proton carrier. The pK shifts induced by Asp^{L213} and Glu^{H173} are estimated to be +5 and +2 units, respectively. Candidates for the functional proton carrier include Ser^{L223} and water.

M-Pos390

MECHANISMS OF ELECTRON TRANSFER AND CONFORMATIONAL RELAXATION STUDIED BY MEASURING ET KINETICS OF PHOTOSYNTHETIC REACTION CENTER IN DARK AND LIGHT ADAPTED CONFORMATIONS. ((B. McMahon, T. Gross, C. Wraight*, G.U. Nienhaus)) Depts. of Physics and *Plant Biology, University of Illinois at Urbana, Urbana, IL 61801.

We investigate the conformational changes coupled to electron transfer in *Rhd. Sph.* by cryogenic trapping of both the ground state and the charge separated state. For each trapped protein conformation, physical parameters such as ΔG, the reorganization energy, the relative importance of long range and short range interactions, the electronic matrix element, the effect of thermal expansion and the size of static distributions of these parameters are deduced by fitting the non-exponential $Q_a \rightarrow P$ kinetics to the spin boson model for temperatures between 4K and 160K. Above the solvent glass transition temperature (175K), we observe the trapped charge separated conformation relax to the ground state conformation. At slightly higher temperatures, we observe recombination ocurring while the protein is still adapting to the charge separated conformation.

M-Pos391

MEASUREMENT OF DIRECT CHARGE RECOMBINATION FROM $D^+Q_AQ_B^-$ TO DQ_AQ_B IN BACTERIAL REACTION CENTERS FROM *RB. SPHAEROIDES* CONTAINING LOW POTENTIAL QUINONE IN THE Q_A -SITE.* ((A. Labahn[1], J. M. Bruce[2], M.Y. Okamura[1] and G.Feher[1])) [1]Phys. Dept., Univ. of Calif., San Diego, La Jolla, CA 92093. [2]Chem. Dept., Univ. of Manchester, Manchester M139PL, UK.

The charge recombination from $D^+Q_AQ_B^-$ to DQ_AQ_B in native RCs proceeds via the intermediate state $D^+Q_AQ_B$ (1). To observe direct recombination we increased the energy gap between the states $D^+Q_AQ_B$ and $D^+Q_AQ_B^-$ by 95, 110 and 120 meV by replacing the endogenous primary ubiquinone (Q_{10}) with various lower potential quinones, 2,3,5 trimethyl 1,4-naphthoquinone (TMNQ), 2-chloro 9,10-antraquinone (CLAQ) and 2,3,6,7 tetramethyl 1,4-naphthoquinone (TEMNQ), respectively, while retaining the native ubiquinone in the Q_B site. The observed recombination rates from Q_B^- in these "hybrid" RCs were found to be slower than in native RCs and the same for all the three low potential quinones indicating direct charge recombination (see Fig.). The data were fit using Marcus theory with a reorganization energy (λ_{BD} = 1.28 eV) in good agreement with the result for mutant RCs in which Asp(L213) was replaced by Asn (2). (1) D. Kleinfeld, M.Y. Okamura and G. Feher (1984) Biochim. Biophys. Acta 766, 126. (2) A. Labahn, M. L. Paddock, P. H. McPherson, M.Y. Okamura and G. Feher (1994) J. Phys. Chem. 98, 3417.

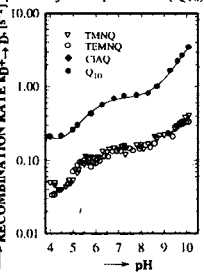

*Supported by NSF, NIH, NATO/DAAD and Deutsche Forschungsgemeinschaft

M-Pos392

FAR-UV TIME-RESOLVED CIRCULAR DICHROISM STUDIES *of* PHYTOCHROME ((Befei X. Chen*, Veniamin Lapko†, James W. Lewis*, Pill-Soon Song† & David S. Kliger*)) *Dept of Chemistry & Biochemistry, U. of California, Santa Cruz, CA 95064. †Dept of Chemistry & Institute for Cellular & Molecular Photobiology, U. of Nebraska, Lincoln, NE 68588.

This is a tale of a plant photoreceptor. It's phytochrome we study with our fine OMA detector. It's a molecule essential for a plant's well being, without which there would be no flowers, no greening.

Inactive (Pr) and active (Pfr) are its two favorite states. Which wavelengths of light determines its fate? A zap with 667 nm sends it far red. A zap with 730 nm sends it red instead.

The activation rxn - many studies, much info. Five species detected, some faster, some slow. From TRCD studies the species that are slow are the ones that make the helicity grow.

Thé reverse rxn is the story we want to relate. TROD says not five, not more, only two intermediates. But that's not it, the most bizarre result of all is the behaviour of the helix at the N-terminal.

How should it be? - Pr's CD signal to be exact. Conventional CD says less - look it up, it's a fact. With far-UV TRCD studies which way did it go? First more, then less, what a strange little show! What ho? A larger signal? Our heads need a rest. Working in the dark puts your sanity to the test. We'll repeat it, repeat it, as scientists always say. If it's not real, then really, it should go away.

This work is supported by NIH Grants GM-35158 (DSK) & GM-36956 (PSS).

BILAYERS: X-RAY, NEUTRON, AND ELECTRON PROBES

M-Pos393

STRUCTURE CHARACTERIZATION OF CYTOCHROME c ADSORBED AT AN AQUEOUS-METAL SURFACE/MEMBRANE INTERFACE WITH X-RAY STANDING WAVES ((S. Kirchner[a], J. Wang[a], Z. Yin[a], M. Caffrey[a], C.J.A. Wallace[b] and I. Clark-Lewis[c])) [a]Chemistry, The Ohio State Univ., Columbus, OH 43210, [b]Biochemistry, Dalhousie Univ., Halifax, Nova Scotia, Canada B3H4H7 and [c]Biomedical Research Center, Univ. of British Columbia, Vancouver, B.C., Canada V6T1W5.

X-ray standing waves (XSW) have been used to study the topology of cytochrome c, electrostatically bound to a negatively charged model membrane and adsorbed at a metal surface while bathed in a buffer solution. The protein was labeled with two XSW-sensitive atoms, selenium and bromine, at two distinct locations in the structure to facilitate protein structure, orientation and distribution determination. The protein was allowed to adsorb to a pure silver substrate and to a silver substrate covered with a negatively charged self-assembled monolayer of thiolundecanoic acid. In each case, measurements were made as a function of protein and buffer salt concentration. The data for both systems show that the protein distributes between an adsorbed monolayer and a homogenous bulk solution. A diffuse double layer near the surface, as is typical for ions at a charged surface, was not observed. Instead, the distribution of the protein at the solid-liquid interface can be described with a simple Helmholtz model, in agreement with theoretical estimates. The structure and orientation of the surface-bound cytochrome c *in aqua* are quite in contrast to that observed with cytochrome c prepared dry at a solid substrate/air interface (Wang *et al., J. Mol. Biol.* 237: 1-4, 1994). These measurements show that the composition of the aqueous medium next to the interface, as well as the nature of the interface itself, play an important role in governing the structure and orientation of surface adsorbed cytochrome c.

Supported by NIH DK 45295.

M-Pos394

REVERSIBILITY OF ION DISTRIBUTION AT A CHARGED MEMBRANE/AQUEOUS INTERFACE: DIRECT PROFILING USING X-RAY STANDING WAVES ((J. Wang[a], M. Caffrey[a], M.J. Bedzyk[b] and T. Penner[c])) [a]Chemistry Dept., The Ohio State University, Columbus, OH 43210, [b]Materials Science and Engineering Dept., Northwestern University, Evanston, IL 14853, [c]Corporate Research Laboratories, Eastman Kodak Co., Rochester, NY 14650.

We have conducted a direct test of thermodynamic reversibility of ion binding at a membrane/aqueous interface using variable period x-ray standing waves generated above a gold mirror. The interface consists of a negatively charged and polymerized phospholipid monolayer bathed in a dilute zinc chloride solution. Zinc ion distribution in the diffuse double layer was monitored as the *p*H of the aqueous medium was titrated from a value of 5.8 to a low of 2.0 and back again to *p*H 5.8. Upon lowering *p*H from 5.8 to 2.0, the decay length of the zinc ion distribution decreased from 21 Å to 8 Å and the surface concentration of bound zinc dropped from 150 mM to 20 mM. Recovery of the *p*H 5.8 distribution profile was essentially complete upon back titration from *p*H 2.0 to *p*H 5.8. These results attest to the reversibility of ion distribution at a charged membrane interface upon adjusting *p*H of the bathing electrolyte solution.

Supported by NIH DK36849 and DK45295

M-Pos395

CHAIN MELTING PHASE TRANSITION KINETICS AND MECHANISM IN MODEL MEMBRANES MONITORED BY TIME-RESOLVED X-RAY DIFFRACTION ((A. Cheng, M. Caffrey)) Chemistry Dept., The Ohio State University, Columbus, OH 43210.

Synchrotron-based time-resolved x-ray diffraction was used to monitor both low- and wide-angle diffraction changes during a partial lamellar liquid crystal (L_α) / lamellar gel (L_β) mesophase transition in fully hydrated lipid multilamellar vesicles in response to small pressure oscillations of different frequencies. The sinusoidal pressure oscillation amplitude was small enough to elicit a linear response. The response amplitude and phase shift are both presented. The fractional phase conversion response spectra for the two structure changes are very similar, indicating that the chain order/disorder transition correlates well with the lamellar repeat spacing change. The data are consistent with a transition best described by the Kolmogorov-Avrami kinetic model (Ye *et al., Biophys. J.* 60:1002-7, 1991) having an effective dimensionality close to unity (0.78 ± 0.05 and 0.9 ± 0.1 for the low- and wide-angle data, respectively) and a structural relaxation time of 13 ± 2 and 10 ± 3 s for the low- and wide-angle data, respectively. The results have been interpreted in the context of a layer-by-layer transition mechanism for the L_α/L_β phase transition.

Supported by NIH DK36849

M-Pos396

EFFECT OF PYRROLIDINE ON DIPALMITOYLPHOSPHATIDYLCHOLINE DISPERSIONS. ((J. M. Collins)) Physics Department, Marquette University, Milwaukee, WI 53233-2214

Pyrrolidine is a lachrymatory colorless liquid found in tobacco and carrot leaves. It is miscible in water and soluble in alcohol and has the following structure:

We are examining the effect of pyrrolidine on aqueous dispersions of dipalmitoylphosphatidylcholine (DPPC) in the temperature range of -20°C to +60°C, with aqueous concentrations between 0% and 80%; and pyrrolidine concentrations from 1 mM to 1 M. The pyrrolidine structure is naturally disruptive to bilayer packing and complicates the DPPC phase formation by being miscible in both the lipid layer and the external aqueous environment. We report on preliminary studies on pyrrolidine/DPPC/water mixtures using both polarizing light microscopy for phase transition behavior and static x-ray diffraction for phase structure parameters.

M-Pos397

A NEW LAMELLAR GEL PHASE INDUCED BY DISACCHARIDES IN SATURATED PHOSPHATIDYLETHANOLAMINES. ((B. Tenchov*, M. Rappolt# and G. Rapp#)) *Inst. of Biophysics. Bulg. Acad. Sci., 1113 Sofia, Bulgaria; #EMBL c/o DESY, Notkestr. 85, 22603 Hamburg, Germany.

By simultaneous small- and wide-angle X-ray diffraction a new lamellar gel phase (L_β*) was found at low temperatures in dihexadecylphosphatidylethanolamine (DHPE) and dipalmitoylphosphatidylethanolamine (DPPE) dispersions in sucrose and trehalose solutions. It forms via a cooperative, two-state phase transition upon cooling of the common lamellar gel phase of these lipids. The transformation between L_β and L_β* is readily reversible with a hysteresis of several degrees. In 2.4 M sucrose solution it takes place at about 10°C below the chain melting transition. A corresponding low-enthalpy transition, which appears only after low-temperature incubation, has been recorded by DSC in the heating direction. The transition temperature between L_β* and L_β phases drops by more than 30 degrees with decrease of sucrose concentration from 2.4 M to 1 M. The low-temperature lamellar gel phase is very well correlated. It is characterized by a repeat spacing by 0.8-1 nm larger than that of the common gel phase and a single symmetric wide-angle peak at $(0.42\text{nm})^{-1}$. It has been detected in 1, 1.25, 1.5 and 2.4 M solutions of sucrose, but not in 0.5 M of sucrose. We assume that the formation of the new gel phase is due to reorganization of the head-group layer of the PEs.

M-Pos398

THE SWELLING OF PHOSPHOLIPID MEMBRANES IN EXCESS WATER - A TIME-RESOLVED X-RAY DIFFRACTION STUDY. ((B. Klösgen*, G. Rapp#, M. Rappolt#, J. Thimmel*)) *FU Berlin, FB Physik, Inst. f. Exp. Physik, Arnimallee 14, D-14195 Berlin; #EMBL c/o DESY, Notkestr. 85, D-22603 Hamburg. (Spon. by Ch. Betzel)

The process of water uptake in systems of phospholipids in water (lipid/water = 5% w/w) has been monitored by time-resolved X-ray diffraction from the almost unhydrated state to the complete decomposition of multilamellar order. The small- and wide-angle diffraction patterns were recorded simultaneously with high spatial resolution. DMPC, DPPC, DOPC and POPC were investigated, thus covering a whole range of lipids with different physical properties. Especially, the swelling behaviour of DPPC at the transition temperature (41°C) from the gel to the liquid crystalline state has been observed in a temperature controlled experiment. From the moment of first water contact multilamellar stacks are seen to develop for all lipids under investigation. The respective Bragg peaks increase in intensity during ordering and move towards smaller scattering angles indicating that the repeat distance increases on swelling. The width of the initially sharp Bragg peaks increases drastically at a longer time scale indicating that the stacks are decomposed by a peeling off process. Most likely unilamellar vesicles coexist with a disperse phase of lipids.

M-Pos399

EVIDENCE FOR HEADGROUP SUPER-LATTICE IN SUBGEL PHASE DPPC BILAYERS. ((J. Katsaras and V.A. Raghunathan)) AECL Research, Chalk River, Ontario, K0J 1J0, Canada and CRPP-CNRS, Pessac, France. (Spon. by K.R. Jeffrey)

Using a combination of x-ray diffraction data from oriented films and multilamellar liposomes of 1,2-dipalmitoyl-sn-glycero-3-phosphatidylcholine (DPPC), we have established the formation of a 2D headgroup super-lattice having twice the area of the hydrocarbon chain lattice in the subgel phase. The proposed super-lattice is consistent with all of the x-ray diffraction data on the subgel phase of DPPC available in the literature. It is also found that the lipid molecules are positionally correlated across a single bilayer but not with those in adjacent bilayers.

M-Pos400

Lipid extracts from membranes of *Acholeplasma laidlawii* grown with different fatty acids have a nearly constant spontaneous curvature

F. Österberg[1], L.Rilfors[2], Å.Wieslander[2], G.Lindblom[2],S. M. Gruner[1]

[1]Department of Physics, Joseph Henry Laboratories Princeton University,Princeton, NJ 08544[2]Department of Physical Chemistry and Department of Biochemistry,University of Umeå, Umeå, 90187,Sweden (Spons by S.M.Gruner)

X-ray diffraction methods were used to explore the variation in the spontaneous curvature of lipid extracts from *Acholeplasma laidlawii* strain A-EF22 grown with different mixtures of palmitic acid and oleic acid. It was shown that the cells respond to the different growing conditions by altering the polar head group compositions in order to keep the phase transition between lamellar and nonlamellar structures within a narrow temperature range. This has been interpreted to mean that the membrane lipids are adjusted toward an optimal packing [Lindblom et al., Biochemistry 25, (1986) 7502]. Here it is shown that for these extracts, the membrane curvature is kept within a narrow range (58-73 Å), compared to the range in curvatures exhibited by pure lipids extracts from the membrane (17-123 Å). These observations support the hypothesis [Gruner, J. Phys. Chem., 93(1989) 7562] that the spontaneous curvature is a functionally important membrane parameter which is regulated by the organism and is likely to be one of the constraints controlling the lipid composition of the bilayer.

M-Pos401

METASTABILITY OF LAMELLAR AND INVERTED HEXAGONAL PHASES IN DIPHYTANOYL PHOSPHOLIPIDS ((T. Harroun, K. He,W. Heller, S.J. Ludtke,and H.W. Huang)) Rice University, Houston, TX 77251-1892.

A different type of phospholipid system is used to study the lamellar-inverted hexagonal phase transition. Diphytanoyl-phosphocholine, which overwhelmingly prefers the lamellar state, is mixed with Diphytanoyl-phosphoethanolamine, which alone is always found in the inverted hexagonal phase. We use X-ray diffraction to measure the structural parameters of this mixed system. We have seen that the same sample composition can be prepared to be stable in either phase. This indicates that at least one phase is a metastable state, and a high potential barrier exists between the two phases. For one preparation, at all ratios by weight, the phase was hexagonal, and the unit cell length d varied continuously with the PE/PC ratio. For another preparation, the sample was never seen to leave the lamellar phase, despite taking the sample through extremes of temperature and hydration. No coexistence of phases was detected.

M-Pos402

X-RAY SCATTERING STUDIES OF THE ANOMALOUS SWELLING OF DMPC NEAR THE CHAIN MELTING TRANSITION. ((R. Zhang, R. M. Suter, W. Sun, S. Tristram-Nagle, R. Headrick (CHESS) and J. F. Nagle)) Carnegie Mellon University, Pittsburgh, PA 15213.

The anomalous increase in the lamellar D spacing as the temperature is lowered to the chain melting transition temperature T_M has recently been interpreted as an increase in the water spacing D_W due to increased Helfrich bilayer undulation forces (Honger et al., Phys. Rev. Lett. 72, 3911 (1994)). This requires an increase of at least a factor of two in the Caille scattering parameter η that characterizes the long tails in the scattering peaks. We have obtained high resolution ($\pm 0.002^o$) scattering data that fully resolves the shape of the h=1 and h=2 lamellar peaks. Our quantitative theory (Zhang et al., Phys. Rev. E in press) fits these shapes very well and obtains corrected form factors. Our data show no increase in η with decreasing temperature nor can the form factors fit on a single continuous transform, so it is necessary to consider a different model. We propose that it is the bilayer thickness D_B that primarily increases, consistent with theories that predict accelerated straightening of the hydrocarbon chains as T_M is approached. The increased sensitivity of D_B to temperature near a phase transition is another example of how lipid bilayers can be modulated to accommodate preferentially different integral membrane proteins. This research was made possible by NIH grant GM44976 and CHESS project #619.

M-Pos403

NEUTRON REFLECTIVITY STUDIES OF SUPPORTED SINGLE LIPID BILAYERS IN WATER

((B. W. Koenig+, K. Gawrisch++, S. Krueger+++, W. Orts+++, C. F. Majkrzak+++, and N. Berk+++))
+NHLBI, ++ NIAAA, NIH, Bethesda, MD 20892; +++NIST, Reactor Radiation Division, Gaithersburg, MD 20899

Neutron reflectivity has been used to characterize the structure of single lipid bilayers adsorbed to a planar silicon surface from aqueous solution. We used a novel experimental setup which decreases incoherent background scattering by more than one order of magnitude. Reflected neutron intensities could be measured for momentum transfers up to 0.3 $Å^{-1}$. Data were fit using scattering length density profiles composed of 1) histogram functions based on the theoretical lipid composition and 2) randomly-generated smooth functions represented by parametric B-splines. The measurements show a SiO_2 layer, a water layer between SiO_2 and lipid, and a single lipid bilayer. Chain-protonated and -deuterated DSPC and DPPC bilayers were investigated in D_2O and a mixture of D_2O and H_2O which matches the scattering density of silicon. The method detects the angstrom-scale thickness changes of the lipid bilayer as a function of the phase state of the lipid and of the hydrocarbon chain length. The measured values agree with trends seen in bulk samples.
(B.W.K. acknowledges financial support by a grant from the German Academic Exchange Service)

M-Pos404

MACRO-RIPPLE PHASE FORMATION IN BILAYERS COMPOSED OF GALACTOSYLCERAMIDE AND PHOSPHATIDYLCHOLINE ((R. E. Brown, W. H. Anderson, and V. S. Kulkarni)) The Hormel Institute, Univ. of Minnesota, Austin, MN 55912.

As determined by freeze fracture electron microscopy, increasing levels of bovine brain galactosylceramide (GalCer) altered the surface structure of 1-palmitoyl-2-oleoyl-phosphatidylcholine (POPC) bilayers by inducing a striking "macro-ripple" phase in the larger, multilamellar lipid vesicles at GalCer mole fractions between 0.4 and 0.8. The term "macro-ripple" phase was used to distinguish it from the $P_{\beta'}$ ripple phase observed in saturated, symmetric-chain length PCs. Whereas the $P_{\beta'}$ ripple phase displays two types of corrugations, one with a wavelength of 12 to 15 nm and the other with a wavelength of 25 to 35 nm, the "macro-ripple" phase occurring in GalCer/POPC dispersions is of one type with a wavelength of 100 to 110 nm. Also, in contrast to the extended linear arrays of adjacent ripples observed in the $P_{\beta'}$ ripple phase, the "macro-ripple" phase in GalCer/POPC dispersions is interrupted frequently by packing defects resulting from double dislocations and various disclinations and thus, appears to be continuously twisting and turning. Control experiments verified that the macro-ripple phase is not an artifact of incomplete lipid mixing or demixing during preparation, or "slow" freezing. The macro-ripple phase is always observed in mixtures that are fully annealed by incubation above the main thermal transition of both POPC and bovine brain GalCer prior to rapid freezing. If the GalCer mixed with POPC contained only nonhydroxy acyl chains (NFA-GalCer) or only 2-hydroxy acyl chains (HFA-GalCer), then the macro-ripple phase is rarely seen. (Support: USPHS Grant GM-45928 and the Hormel Foundation).

BILAYERS/STEROL INTERACTIONS

M-Pos405

PHYSICOCHEMICAL CHARACTERIZATION BY ^2H NMR OF MODEL LIPID DIGESTIVE MIXTURES CONTAINING PHYSIOLOGICAL LEVELS OF CHOLESTEROL. ((P.W. Westerman, R. Jacquet and B. Quinn)) Department of Biochemistry, Northeastern Ohio Universities College of Medicine, Rootstown, OH 44272 and Liquid Crystal Institute, Kent State University, Kent, OH 44242.

The phase properties of aqueous dispersions of mixtures containing 4 mol % cholesterol and varying ratios of mixed intestinal lipids (MIL; myristic acid/monomyristin/dimyristoylphosphatidylcholine) to mixed bile salts (MBS) have been characterized by ^2H NMR. The composition of micellar and multilamellar vesicular (MLV) phases have been determined using as a probe a terminal deuteriomethyl group, chemically incorporated into each of the several lipid components. As the relative amount of MBS in the mixture increases, fatty acid and monoglyceride are selectively removed from the MLVs, which progressively increase in cholesterol and lecithin content. ^2H relaxation times (T_1 and T_2) of 2,2-[$^2H_2$]-myristic acid and glycoholic[2,2-$^2H_2$]glycine have been measured for the micellar phase in the same mixtures. Differences between T_1 and T_2 values have been utilized to estimate particle size assuming either a spherical of ellipsoidal shape. As the relative amount of MBS in the mixture increases, the diameter of the mixed micelles remains in the range 31 to 39 Å until simple MBS micelles become the predominant species whereupon particle size decreases to approximately 18 Å diameter. (Supported by the American Heart Association, Ohio Affiliate)

M-Pos406

CHOLESTEROL INDUCES ORDERED MICRODOMAINS IN MEMBRANES. ((T. Parasassi, A.M. Giusti, D.M. Jameson* and E. Gratton**)) Istituto di Medicina Sperimentale, CNR, Roma; *Univ. of Hawaii at Manoa, Biochemistry & Biophysics, Honolulu 96822; **Laboratory for Fluorescence Dynamics, Dept. of Physics, Univ. of Illinois at U-C, Urbana, Il 61801.

Formation of ordered molecular microdomains in phospholipid vesicles at different cholesterol concentrations were studied using the Generalized Polarization function (GP) of LAURDAN fluorescence. By constructing a surface plot of the emission (or excitation) GP as a function of cholesterol mol% with respect to total phospholipid content, particular concentrations were identified, producing discontinuities of the GP surface. The changes in the fluorescent properties of LAURDAN have been interpreted as due to ordered lipid structure which inhibit water penetration in the membrane and affect LAURDAN GP. Those structures only occur in a very narrow range of cholesterol concentration. To further characterize these ordered molecular structures, oxygen quenching experiments were also performed. The diffusion of oxygen in gel-phase membranes is facilitated by the presence of packing defects introduced by the addition of cholesterol. However, oxygen quenching measurements showed that, at cholesterol concentrations at which ordered molecular structures are formed, oxygen diffusion is reduced. This observation points out that the diffusion properties of the membrane are modified in a discontinuous way at specific cholesterol concentration. (Supported by CNR and by NIH grant RR03155)

M-Pos407

EVIDENCE FOR REGULAR DISTRIBUTIONS OF CHOLESTEROL IN LIPID BILAYERS

((Daxin Tang, B. Wieb Van Der Meer and S.-Y. Simon Chen)) Department of Physics and Astronomy, Western Kentucky University, Bowling Green, KY 42101.

Cholesterol/dimyristoylphosphatidylcholine multilamellar vesicles were studied by steady-state fluorescence using diphenylhexatriene as a probe. A series of dips were found in the plot of fluorescence intensity versus cholesterol concentration at certain specific cholesterol concentrations. This observation indicates that cholesterol molecules are regularly distributed on an hexagonal super-lattice in the acyl chain matrix of the phospholipids at critical cholesterol concentrations. These concentrations can be predicted by an equation or a mathematical series, except the one at 33 mol%. These dips of fluorescence intensity are temperature dependent. The excellent agreement between experimental data and calculated values as well as similar previous findings of dips in the excimer over monomer fluorescence in Pyrenephosphatidylcholine/phospholipid mixtures confirm our conclusion about lateral organizations of cholesterol and acyl lipid chains in cholesterol/phospholipid multilamellar vesicles. The relation between this regular distribution of cholesterol and the phase diagram of cholesterol/dimyristoylphosphatidylcholine mixtures is discussed. This work is supported by the National Science Foundation EPSCoR program (EHR-9108764).

M-Pos408

IS CHOLESTEROL AN Na^+ PLUG IN MEMBRANES? ARE PLANT STEROLS, *ISO- ANTEISO* LIPIDS, AND SQUALENE, H^+ PLUGS?

((Thomas H. Haines))Dept. of Chem.& CUNY Med. School, City College, NY 10031.

The role of sterols, including cholesterol, is unknown. Fluidity cannot explain their absence in prokaryotes, intracellular membranes and their ubiquity in eukaryote plasma membranes. Based on the Haines-Liebovitch-Trauble model for water transport, a random walk calculation shows that (see Haines, T.H., FEBS Lett. 346,115-22 (1993)) the lateral diffusion of phospholipids and water permeability are linked processes in bilayers. Thus each water molecule is isolated within the hydrocarbon domain during its transport. The model suggests the rate of water transport is independent of the chainlength of the lipid. This has been demonstrated for a series of PC's with from C_{12} to C_{24} chains. If each water molecule were H-bonded to a water molecule on an adjacent chain the water transport model suggests that proton leakage may occur via a "proton wire", as proposed by H. Morowitz and J.F. Nagle, **in each monolayer**. Connecting these wires would require water in the bilayer center. **Cholesterol has been found to inhibit** water transport, H^+ leakage and **Na^+ leakage**. H^+ leakage, according to this model (which correlates with natural membrane lipid composition), is inhibited by lipid branches in the center of the bilayer (plant sterols in plants, yeast and fungi; *iso- anteiso*-lipids in acidophiles and alkaliphiles), or hydrocarbon in the center of the bilayer (squalene in alkaliphiles, dolichol in lysosomes). Examination of the literature shows that wherever an Na^+,K^+ gradient occurs, cholesterol is found in the plasma membrane; wherever an H^+,K^+, gradient occurs, branched sterols are found. It is thus suggested that these sterols reduce Na^+ and H^+, leakage respectively, **saving the cell substantial ATP energy!**

M-Pos409

EFFECT OF STEROL SIDE CHAIN STRUCTURE ON THE THERMOTROPIC PHASE BEHAVIOR OF SOPC AND DPPC BILAYERS

((T.P.W. McMullen[1], C. Vilcheze[2], R.N. McElhaney[1] and R. Bittman[2])) [1]Dept. of Biochemistry, University of Alberta, Edmonton, Alberta, Canada T6G 2H7 and the [2]Dept. of Chemistry and Biochemistry, Queens College of the City University of New York, Flushing, N.Y., U.S.A. 11367.

Using high-sensitivity differential scanning calorimetry, we have examined the effect of a series of cholesterol C17 side chain analogues varying in length and conformation on both DPPC and SOPC bilayers. In both SOPC and DPPC bilayers the progressive decrease in main phase transition enthalpy towards 0 by 50 mol% sterol requires a sterol side-chain at least 3 carbons in length. However in the case of SOPC, sterols with side chains longer than the isooctyl chain of cholesterol show partial gel-state immiscibility. DPPC/sterol and SOPC/sterol main chain melting phase transitions also clearly exhibit multicomponent behavior indicative of sterol-rich and sterol-poor lipid domains. These domains demonstrate different sterol dependent T_m shifts depending on the degree of hydrophobic mismatch between the sterol and host phospholipid molecules and thus differ for DPPC and SOPC. In addition the apparent stoichiometry of DPPC/sterol and SOPC/sterol interactions varies with changes in side chain structure. These results, as well as with recent parallel studies using FTIR and cholesterol oxidase, illustrate the importance of the cholesterol side chain in sterol-phospholipid interactions. (Supported by the Medical Research Council of Canada and the Alberta Heritage Foundation for Medical Research.)

M-Pos410

THE EFFECT OF CHOLESTEROL ON THE THERMOTROPIC BEHAVIOR OF PHOSPHOLIPID BILAYERS VARYING IN HEADGROUP STRUCTURE AS WELL AS ACYL CHAIN LENGTH AND SATURATION: A SYSTEMATIC COMPARISON.

((T.P.W. McMullen and R.N. McElhaney)) Dept. of Biochemistry, University of Alberta, Edmonton, Alberta, Canada, T6G 2H7.

To understand how variations in phospholipid structure alter phospholipid/cholesterol interactions, we have systematically characterized the thermotropic phase behavior of cholesterol- containing phosphatidylethanolamine, (PE), phosphatidylserine, (PS), phosphatidylglycerol (PG), and phosphatidic acid (PA) bilayers with both saturated and unsaturated hydrocarbon chains of various lengths. We have also used Fourier transform infrared spectroscopy and ^{31}P-NMR to study changes in phospholipid headgroup and acyl chain conformation. Cholesterol incorporation into PS, PG, PE, and PA decreases the host bilayer main chain-melting transition enthalpy, to an extent which varies significantly with headgroup and acyl chain length. In fact, gel-state immiscibility of cholesterol is common in each of these phospholipids with chain lengths greater than 16:0 carbons, and at 20:0 carbons cholesterol exhibits liquid-crystalline immiscibility in PE, PG, and PS bilayers. In all cases cholesterol-poor and cholesterol-rich lipid domains are present in which the enthalpy, T_m, and cooperativity are governed by either, or both, hydrophobic mismatch and polar headgroup charge. The presence of a double bond in one or both of the acyl chains also dramatically alters the effect of cholesterol on the host phospholipid bilayer. Our results clearly demonstrate that cholesterol-phospholipid interactions are sensitive to both headgroup and acyl chain structure.

M-Pos411

INTERFACIAL COMPRESSIBILITY CHANGES INDUCED BY CHOLESTEROL'S INTERACTIONS WITH SPHINGOMYELINS AND PHOSPHATIDYLCHOLINES

((J. M. Smaby, H. L. Brockman, and R. E. Brown)) The Hormel Institute, Univ. of Minnesota, Austin, MN 55912.

Cholesterol's apparent molecular area condensations of different sphingomyelins (SMs) and phosphatidylcholines (PCs) are very similar as long as the phospholipids are in the same phase state (prior to cholesterol addition) and hydrocarbon structural differences are minimized [Smaby, J. M., Brockman, H. L., & Brown, R. E. (1994) *Biochemistry* 33, 9135-9142]. For PCs, this means that one acyl chain must be long and capable of assuming an extended conformation (e.g. palmitate or myristate) so that the resulting configuration is similar to the long-chain base of SM. Interestingly, under such conditions, the structural requirements of PC's *sn*-2 chain are mitigated and have little effect on the observed apparent molecular area condensation induced by equimolar cholesterol. To evaluate further the contributions of the ceramide and diacylglycerol regions of SM and PC in modulating their interactions with cholesterol (Chol), we investigated the interfacial compressibility of Chol-SM and Chol-PC mixed monolayers at 24°C. In contrast to the condensation results described above, we found the interfacial compressibility changes induced by cholesterol in various SMs and PCs' with saturated *sn*-1 chains to be very sensitive to SM's acyl and PC's *sn*-2 chain structure. However, little difference was observed in the compressibilities of SM-Chol and PC-Chol mixed monolayers when SM's acyl and PC's *sn*-2 acyl chains were the same. (Supported by USPHS Grants GM-45928, HL- 49180, and the Hormel Foundation)

M-Pos412

COMPARISON OF PHOSPHATIDYLCHOLINES CONTAINING ONE OR TWO DOCOSAHEXAENOIC ACID CHAINS ON PROPERTIES OF PHOSPHOLIPID MONOLAYERS AND BILAYERS.

((W. Stillwell, M. Zerouga, and L.J. Jenski)) Department of Biology, Indiana University - Purdue University at Indianapolis, Indianapolis, IN 46202-5132

Docosahexaenoic acid (DHA) is the longest and most unsaturated of the omega-3 fatty acids found in membranes. Although a number of membrane properties have been demonstrated to be affected by the presence of this fatty acid, its mode of action has yet to be clearly elucidated. Prior reports on biological membranes have not distinguished the effect of mono-docosahexaenoyl phospholipids from those caused by phospholipids containing docosahexaenoic acid in both chains. This report compares properties of monolayers and bilayers composed of either 1-stearoyl-2-oleoyl-*sn*-glycero-3-phosphocholine or 1,2 docosahexaenoyl-sn-glycero-3-phosphocholine. When compared to the mono-DHA phosphatidylcholine (PC), the di-DHA PC: occupies a much larger area/molecule, supports a more fluid, and permeable bilayer, and is less peroxidazable. Monolayers made from either phospholipid are not condensable by cholesterol. Perhaps many of the membrane properties linked to the presence of DHA may be the result of phospholipids which have lost their normal positional selectivity and have incorporated DHA into both positions.

M-Pos413

SQUALAMINE INDUCES LEAKAGE OF TRAPPED CARBOXYFLUORESCEIN FROM NEGATIVELY CHARGED LIPID VESICLES. ((S.R. Jones*, A.E. Shinnar#, W. Kinney#, T. Williams#, and B.S. Selinsky*)) *Department of Chemistry, Villanova University, Villanova, PA 19085, and #Magainin Pharmaceuticals, Inc., Plymouth Meeting, PA 19462.

The recent discovery of squalamine from shark tissue establishes sulfated aminosterols as a new class of antibiotics[1]. Squalamine exhibits broad spectrum antimicrobial activity, similar to that observed for many classes of peptide antibiotics. As part of our effort to elucidate squalamine's mechanism of action, we were interested in determining if it causes membrane permeabilization of membranes, as observed with magainin peptides. To test this hypothesis, we have prepared large unilamellar vesicles (LUVs) from both anionic and zwitterionic phospholipids containing encapsulated carboxyfluorescein (CF) as a marker for membrane integrity. We find that squalamine does induce leakage of CF from anionic LUVs, as monitored kinetically by the increase in CF fluorescence. The rate of leakage is dependent upon the molar ratio of squalamine to phospholipid, and exhibits apparent cooperativity similar to that observed with magainins. Future studies will focus on determining the selectivity of squalamine for different classes of lipid headgroups.

[1] Moore, K.S., Wehrli, S., Roder, H., Rogers, M., Forrest, J.N. Jr., McCrimmon, D., and Zasloff, M. (1993) *Proc. Nat. Acad. Sci. USA* 90: 1354-1358.

M-Pos414

THE SYNTHESIS AND CHARACTERIZATION OF ANTIBIOTIC ANALOGS OF SQUALAMINE. ((Steven R. Jones)) Chemistry Department, Villanova University, Villanova, PA 19085.

In recent years, the quest for new classes of naturally occurring antibiotics has led to the discovery of squalamine[1,2]. This unusual sulfated aminosterol displays a broad spectrum of antimicrobial activity against both gram-negative and gram-positive bacteria, as well as antifungal activity[1]. Since squalamine might provide important insights into new strategies for antiinfective compounds, we have undertaken efforts aimed at elucidating the mechanism of action of squalamine. Using squalamine as a reference, we are studying physical chemical properties of synthetic analogs as a means of understanding the structure-function relationships of the aminosterol class of membrane active compounds. Among the properties of these amphiphilic sterols that we have examined are: a) their propensity to aggregate in aqueous solution, and b) their ability to induce leakage of carboxyfluorescein from large unilamellar vesicles of varying lipid compositions. The underlying goal of this work is to develop a rational approach for designing squalamine-like compounds exhibiting greater potency and selectivity.

[1] Moore, K.S., Wehrli, S.L., Roder, H., Rogers, M., Forrest, J.N.Jr., McCrimmon, D., and Zasloff, M. (1993) *Proc. Nat. Acad. Sci. USA* 90: 1354-1358.
[2] Wehrli, S.L., Moore, K.S., Roder, H., Durell, S., and Zasloff, M. (1993) *Steroids* **58**: 370-378.

TRANS-BILAYER FLUX

M-Pos415

ELECTROCHEMICAL IMPEDANCE SPECTROSCOPY OF HUMAN SKIN *IN VIVO*. *((Yogeshvar N. Kalia, Norris G. Turner & Richard H. Guy)). Departments of Pharmacy and Pharmaceutical Chemistry, University of California at San Francisco. San Francisco. CA 94143-0446.*

The enhanced transport of molecules across human skin by iontophoresis is well established. However, the mechanism of enhancement remains in question, in particular, the nature of the effect of the iontophoretic current on the electrical impedance properties of skin. Traditionally, these have been modeled by using a capacitor and a resistor in parallel. The limited applicability of this model is evidenced by its prediction, in the complex plane impedance plot, of a semi-circle whose center lies on the resistance axis. In contrast, skin tissue exhibits an impedance locus with a depressed center. More accurate models of biological membranes, including skin, have incorporated a constant phase element (CPE) into the equivalent circuit. Previous studies investigating the impedance properties of human skin have used either cadaver skin or excised full-thickness tissue obtained during surgery. However, can avascular and metabolically compromised skin tissue provide accurate information? To overcome this dilemma, we have performed an *in vivo* human skin study where impedance spectra were recorded, over a frequency range of 1Hz to 100kHz, in the passive state - before application of an iontophoretic current, during current flow and in the post-iontophoretic state. Spectra taken immediately after passage of an iontophoretic current (0.1mA/cm^2 for 15 minutes) show a 20-fold reduction in skin impedance. As the recovery time is increased, the impedance shows a corresponding increase: after 30 minutes it has attained approximately 20% of its passive value. Any structural reorganization induced by application of the iontophoretic current has already begun to be reversed. We have used these data as a basis for designing an equivalent circuit for human skin *in vivo*.

M-Pos416

SURFACTANT INDUCED SEALING OF PORATED CELL MEMBRANE. ((T.R. Gowrishankar and R.C. Lee)) The University of Chicago, IL 60637.

Loss of cell membrane integrity due to structural disruptions in membranes is a common pathway of tissue injury in such events as high-voltage electrical shock or exposure to membrane permeabilizing agents. Increased membrane permeability and decrease in metabolic activity are direct consequences of this effect. Estimation of membrane integrity is essential for cell survival in such cases. The use of poloxamer class of non-ionic triblock copolymers (P1107 and P188) in restoring membrane integrity and function following membrane damage was studied. Methods: Isolated cells from rat flexor digitorum brevis muscle were stained with 0.1 μM calcein-AM (membrane permeability studies) or 0.1 μM rhodamine 123 (metabolic energy assays) and imaged at 37°C using real-time confocal microscopy. Cells were either subjected to 200V/1Amp 4-msec pulses or exposed to sodium dodecyl sulphate (SDS) to cause membrane damage. Changes in cellular fluorescence intensity was used as an indicator of changes in membrane permeability or cellular metabolic energy. Results: In both cases of SDS and electric shock induced membrane damage, P1107 and P188 at concentrations of 0.1 mM restored the membrane permeability close to pre-injury levels ($p<0.01$). Metabolic energy was restored to approximately 60% of its normal value following treatment with P188. These results indicate that the poloxamer class of non-ionic surfactants are potent inducers of membrane sealing and hold promise as therapy for cell membrane injuries.

M-Pos417

PERMEATION OF WATER, GLYCEROL AND UREA ACROSS PHOSPHOLIPID BILAYERS. ((S. Paula, A.N. Van Hoek*, A.G. Volkov, T.H. Haines** and D.W. Deamer)) Department of Chemistry and Biochemistry, University of California, Santa Cruz, CA, 95064. *Cardiovascular Research Institute, University of California, San Francisco, CA, 94143. ** Department of Chemistry, CUNY, New York, NY, 10031.

The permeation process by which small neutral molecules such as water cross membranes is generally believed to occur by a partitioning-diffusion mechanism. This model treats the membrane as a thin slab of hydrophobic matter embedded in an aqueous environment. In order to cross the membrane, the permeating particle must dissolve in the hydrophobic region, diffuse across, and leave by re-dissolving into the aqueous phase. If the membrane thickness and the diffusion and partition coefficients of the permeating species are known, the permeability coefficient can be calculated. To obtain the partition coefficient, hydrophobic energies and specific interactions of neutral molecules with their solvent are taken into account. According to the partitioning-diffusion mechanism, the permeability should exhibit a modest dependence on the thickness of the membrane. This model was tested by measuring osmotically driven water, urea, and glycerol fluxes across phosphatidylcholine bilayers prepared as liposomes. In a stopped-flow apparatus, the time course of light scattered by vesicles was used to follow volume changes upon dilution into hypertonic solutions. To vary the thickness of the membranes, phosphatidylcholines with fatty acid chain lengths ranging from fourteen to twenty-four carbon atoms were used. The results support a partition-diffusion mechanism for water and small neutral molecules. They are not consistent with mechanisms suggesting that permeation of these molecules occurs through transient defects within the bilayer. Supported by NASA NAGW-1119.

M-Pos418

PASSIVE ION PERMEATION OF LIPID BILAYERS: PARTITIONING OR TRANSIENT AQUEOUS PORES? ((A.G. Volkov, S. Paula and D.W. Deamer)) Department of Chemistry, University of California, Santa Cruz, CA 95064, USA

The Gibbs free energy of ion permeation of lipid bilayers can be calculated as a sum of all electrostatic and solvophobic contributions. The electrostatic term dominates permeation of smaller ions, but the solvophobic effect becomes significant for larger ions to the extent that the Gibbs free energy can be negative for ions larger than 0.45 nm diameter. Partitioning models are consistent with some features of ionic permeation, particularly if solvophobic energy is taken into account. We show here that ionic permeability is extremely sensitive to ionic radius, changing by 50 orders of magnitude as ionic radius is varied from 0.1 to 0.5 nm. Despite this sensitivity, calulations of permeability can be carried out for typical monovalent cations and provide reasonable estimates, but only for hydrated species. An alternative hypothesis is that fluctuations in bilayer structure produce transient hydrated defects which permit ionic solutes to bypass the electrostatic energy barrier. The two alternative hypotheses - partitioning versus transient pores - can be tested by measuring ionic permeation through bilayers of varying thickness. If the partition model is correct, a substantial barrier to ionic flux should occur as soon as a stable bilayer is produced, even with relatively short-chain lipids, and permeability will not vary significantly with bilayer thickness. The transient pore model predicts that ionic permeability will increase as a logarithmic function of bilayer thickness. Experimental observations for both potassium and proton permeability are consistent with the transient pore mechanism for shorter chain lipids, but trend toward the theoretical line for partitioning models for longer chain lipids. Both mechanisms may play a role for typical hydrated monovalent ions, depending on lipid chain length, but proton flux still has unexplained anomalies.

M-Pos419

MELITTIN-INDUCED LEAKAGE FROM VESICLES CAN BE CONTROLLED BY LIPID BILAYER PROPERTIES. ((M. Lafleur and T. Benachir)) Département de chimie, Université de Montréal, Montréal, Québec, H3C 3J7.

Melittin, an amphipathic helical peptide, is known to induce leakage from lipid vesicles and biological membranes. Our work reveals that it is possible to control melittin-induced leakage by modifying the physico-chemical properties of a lipid membrane. First, this can be achieved by changing its lipid composition. The presence of cholesterol or of negatively charged lipids in a phosphatidylcholine bilayer inhibits calcein leakage induced by melittin. The stiffening effect of cholesterol on the lipid acyl chains reduces the affinity of melittin for the membrane and, as a consequence, the leakage induced by the peptide. Alternatively, the presence of negatively charged lipids increases the affinity of melittin (which is positively charged) for the membrane. However, the electrostatic interactions appear to anchor the peptide at the interface and prevent the formation of leaks. Second, the leakage induced by melittin increases when a Na^+ osmotic gradient is applied across the membrane (high concentration inside), likely due to structural defects in the bilayer. Our results reveal that both lipid composition and transmembrane osmotic gradient can control melittin activity.

M-Pos420

RECOMBINANT IRK1 CHANNEL SHOWS INWARD RECTIFICATION IN THE ABSENCE OF INTRACELLULAR Mg^{2+}. ((A.Aleksandrov, B.Velimirovic, D.E.Clapham)) Dept. Pharmacology, Mayo Foundation, Rochester, MN,55905.

The inwardly rectifying IRK1 channel was reconstituted in lipid bilayers to study its single channel properties under simultaneous control of internal and external solutions. Membrane vesicles were isolated from *Xenopus* oocytes that had been injected with mRNA coding for IRK1 channels and incorporated into preformed lipid bilayers. Orientation of single channels in bilayers was determined by rectification of the I-V relation. Single channel conductance in the inward direction was 26 pS in symmetrical 200 mM K^+ and varied with the square root of external K^+ concentration. The channel was blocked by mM Cs^+ and Ba^{2+}. In the mM range of intracellular Mg^{2+}, IRK1 channels rectified strongly in the open state in addition to displaying gating-dependent rectification. In the absence of intracellular Mg^{2+} the open state of recombinant IRK1 channels still showed weak inward rectification. We propose that an additional fast gating process rectifies the open channel and that this fast gating process is enhanced by Mg^{2+} but is not due to Mg^{2+} alone.

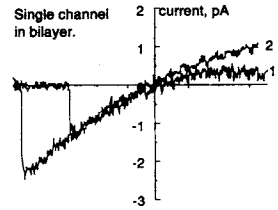

M-Pos421

PHOTOCONTROL OVER ELECTRICAL PROPERTIES OF PLANAR BILAYER LIPID MEMBRANES CONTAINING AZOBENZENE CHROMOPHORES.
((H. Yamaguchi, N. Ikeda and H. Nakanishi)) Adv. Res. Lab., R&D Center, Toshiba Co., Saiwai-ku, Kawasaki 210, JAPAN

Azobenzene(AZ) is a well-known photochromic compound, which undergoes cis-trans photoisomerization similar to retinal in rhodopsin. We have been studying a photocontrol over electrical properties of artificial bilayer lipid membranes(BLMs) containing azobenzene chromophores as a model of visual light processing. In this study the formation process and the photoresponse of bilayers including AZ were investigated using simultaneous multi-observation method, in which spectroscopic, electrical, and microscopic measurements were combined. The rapid and reversible changes in the electrical properties of the membrane were observed when irradiated with light. These changes were found to be completely synchronous with photoisomerization of AZ, which clearly demonstrated that structural changes in AZ upon irradiation by light induced changes in electrical properties of BLMs. To investigate the mechanism of the induction, specific capacitance and conductance of BLMs were elucidated as a function of AZ content in BLMs, structure of hydrophilic part of AZ derivatives, and ion species in solution. These experimental results will be discussed in terms of changes in membrane structure around AZ.

M-Pos422

Evidence That Aggregates of the Fullerene, C_{70}, Are Responsible for the Large Conductance of Negative Charge Across a Lipid Bilayer
S. Niu & D. Mauzerall, The Rockefeller University, New York, NY10021

We have found that the fullerenes are very efficient carriers of negative charge across a lipid bilayer whether the charge is generated by light absorbed in a porphyrin sensitizer or by the fullerene itself (Hwang & Mauzerall, *Nature*, 361, 138,**1993**). The powerful electron donor dithionite causes a current in the dark. The photovoltage observed in the asymmetric system: buffer, 100mM $S_2O_4^{2-}$| C_{70}| buffer, ~ 3mV, has a rise time of ~ 15 ns. It remains as fast but doubles in amplitude when acceptors such as anthraquinone-2-sulphonate (0.1 mM) or methyl viologen (10 mM) are present on the trans side (Hwang, Niu, & Maurerall, *ECS Fullerene Symp. Proc.* 94-24, 845, **1994**). The stronger acceptor ferricyanide (10 mM) causes a 15 fold increase in the photovoltage. The ferricyanide itself only causes a small photovoltage (~ 0.5 mV) with a long half rise time of 30 µs. These photovoltages live at least as long as the RC time of the measurement setup, ~ 5 ms. These observation are strong evidence for electronic conduction across the bilayer by the fullerene. Earlier measurements indicated an "S" shaped response of photovoltage with increasing C_{70} concentration in the lipid bilayer forming solution suggesting aggregation of C_{70}, but the variation between membranes prevented drawing a strong conclusion. By plotting the ratio of the photovoltage for the system $S_2O_4^{2-}$| C_{70}| $Fe(CN)_6^{3-}$ to that of the $S_2O_4^{2-}$| C_{70}| buffer system, we see the ratio only increases from 2 to 4 between 0.05 and 0.4 mM C_{70}, but jumps to 15±3 between 0.5 and 0.8 mM C_{70}. There is independent evidence that C_{70} aggregates at higher concentrations in poor solvents (Sun & Bunker, *Nature*, 365, 398, **1993**). We conclude that aggregates of C_{70} are responsible for the large, fast photoeffects in the lipid bilayer. This work was supported by NIH grant GM-25693.

NUCLEIC ACIDS

M-Pos423

HIGH RESOLUTION STRUCTURE OF A BACTERIOPHAGE T4 RNA HAIRPIN. ((Suman R. Mirmira and Ignacio Tinoco, Jr.)) Department of Chemistry, University of California and Structural Biology Division, Lawrence Berkeley Laboratory, Berkeley, CA 94720.

Bacteriophage T4 DNA polymerase behaves as an autogenous regulator by binding to the ribosome binding site of its mRNA, thereby preventing its own translation. A hairpin with a stem-loop structure is crucial for polymerase binding. Selection experiments in which the loop nucleotides were randomized, (Tuerk et al, *Science* **249**, 505-510) showed that two hairpins bound the polymerase with equal affinity. One was the wild-type hairpin and the other differed from the wild-type at four positions (see figure). Here, we present the high resolution structure of the wild-type hairpin as determined by NMR experiments. A single major conformation was observed. Strong imino-imino NOE cross peaks confirmed the formation of the U-G base pair at the stem-loop junction. Although no imino peak is seen for the A6-U11 pair, data from other 2-D NMR experiments indicate that the A5-C12 and A6-U11 pairs stack on the stem. Hence, the two hairpins have similar 3D structures (see figure), even though their proposed secondary structures are different. This could explain their equal affinity for the DNA polymerase.

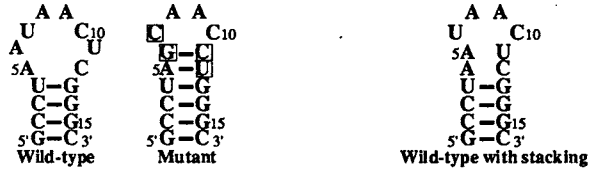

M-Pos424

STABILITY OF AN RNA TETRALOOP IN A RANGE OF SOLUTION CONDITIONS. ((J. Duhamel, J. Kanyo and P. Lu)) Department of Chemistry, University of Pennsylvania, Philadelphia, PA 19104.

The RNA sequence, r(CUUCGG), is exceptionally common in ribosomal RNAs and in the intercistronic regions of messenger RNAs. Furthermore, this motif forms a hairpin (tetraloop) with greater than expected thermal stability.

A specific version of the tetraloop, the oligonucleotide r(GGACUUCGGUCC) has been observed to adopt a hairpin conformation (tetraloop) by NMR (Cheong, C., et al. (1990) *Nature*, **346**, 680-682) and a double helical conformation by X-ray diffraction (Holbrook, S.R., et al (1991) *Nature*, **353**, 579-581). In order to understand this apparent conflict, we monitored the secondary structure of this RNA dodecamer as the solution composition was changed stepwise from the solution NMR experimental conditions (10 mM sodium phosphate, 0.01 mM EDTA, pH 6.5) to those used for crystallization (100mM sodium citrate, 50 mM Tris, pH 8.5, 2.5 mM $MgCl_2$, 12-32% polyethylene glycol 400).

A calculation of the dodecamer strand concentration in the crystal (180 mM) prompted the investigation of a tethered species in an effort to increase the local relative single strand concentration of the RNA sequence. The tethered RNA remains as two independent hairpins. We repeated our series of observations with a DNA analog of this sequence, since it is known to also adopt a loop structure in solution, but without remarkable thermal stability. Again we find that even the DNA analog yields two independent hairpin loops. These experiments, which used time-resolved Fluorescence Depolarization and Fluorine Nuclear magnetic Resonance, show that the RNA tetraloop, as well as its less stable DNA analog, maintains a single-strand hairpin conformation in solution. Crystal packing, in addition to solvent changes and high RNA concentrations, is required to obtain the double helix.

Supported by funds from NASA and U.S. ARO.

M-Pos425

$tRNA^{phe}$ ROTATIONAL TIME AND KERR CONSTANT CALCULATIONS
((Kerwin Ng and Don Eden)) Dept. of Chemistry and Biochemistry, San Francisco State University, San Francisco, CA 94132

A Mg^{++} induced conformation change in yeast $tRNA^{phe}$ has been observed in optical Kerr effect (OKE) experiments. In the presence of 0.5 mM Mg^{++}, tRNA has shorter rotational time constants (τ) and lower volume specific Kerr constant (K_{sp}) than the Mg^{++} free sample. K_{sp} and hydrodynamic calculations have been performed to aid in the interpretation of the results. Starting with the X-ray crystallographic data, the angle between the amino acceptor stem and the anticodon stem was changed to simulate potential bending due to Mg^{++}. K_{sp} is calculated from the polarizability tensor of the bases and includes the dipole-dipole interactions acting through the surroundings with dielectric constant (ϵ). When ϵ is 2, the unaltered model has K_{sp} of $2.2\times10^{-20}m^2/V^2$, and when ϵ is infinite, the K_{sp} is $6.0\times10^{-20}m^2/V^2$. The minimum K_{sp} occurs when the unaltered bending angle is increased by 5°. Calculations showed that K_{sp} increases by about 35% when the angle is changed in either direction by 15° from the minimum K_{sp} position for ϵ of 2. The Kerr constant change is less sensitive to the bending angle as ϵ increases. Hydrodynamic calculations are performed by replacing each base with a 6Å bead to obtain τ. The longest τ component of the unaltered molecule is 44 nS. τ decreased and increased by 2.5% when the angle is decreased and increased by 15°, respectively. These calculations suggest that K_{sp} is more sensitive to this tertiary structure change of tRNA than τ, but K_{sp} alone cannot determine the sign of the angle change.

M-Pos426

EFFECTS OF FLANKING SEQUENCES AND LONG RANGE INTERACTIONS ON OVERALL DNA STRUCTURE.
((M. Dlakic and R.E. Harrington)) Department of Biochemistry, School of Medicine, University of Nevada Reno, Reno, NV 89557-0014 USA

The concept of sequence-dependent DNA structure, proposed more than a decade ago, establishes that primary DNA structure provides not only genetic information, but serves also as a source of structural information important in regulation of gene expression, transcription, replication and DNA packaging within the nucleus. Defining the rules to describe the space trajectory of DNA based on its primary sequence has therefore been a major objective of structural biologists. Rules developed to date have included only nearest neighbor interactions between adjacent base pairs, thus neglecting the possible influence of non-adjacent base pairs and ionic environment. It is likely that DNA structural parameters must be defined at least at the level of tri- or tetranucleotides to account for sequence cooperativity. In an attempt to resolve this question, we have done cyclization, DNase I and hydroxyl radical cutting on repetitive DNA sequences with sequence motifs of interest located differently with respect to one another. Our results strongly suggest that sequence parameters at levels larger than dinucleotide, as well as certain long range interactions between specific sequences and specific ion effects, must be considered in future models for DNA structure prediction, and provide an initial basis for appropriately refined structural models.

M-Pos427

MOLECULAR DYNAMICS SIMULATION OF PLASMID MODELS INCORPORATING CURVED REGIONS AND ANISOTROPIC BENDING
((D. Sprous, R. K.-Z.- Tan & S.C. Harvey)) Dept. Biochemistry & Mol. Gen. • Univ. Alabama at Birmingham • 1918 Univ. Blvd. • Birmingham, AL 35294-0005

We recently completed a study of a variety of plasmid models over the size range of 140 bp to 1260 bp. We utilized a low resolution computer model with basepair resolution. Molecular dynamics was used to produce ensembles at 300 K and to investigate intramolecular motions. The plasmid models varied by their sequence. Branching occurs at the 1260mer plasmid size. We also observed that curves organize plasmid structures for up to 150 bp on both flanks of the curved insert. Even the most mildly curve bearing sequence was seen to inhibit slither motions. The plasmid ensemble average properties at 300 K were seen to be quite distinct from properties of structures arrived at by minimization protocols.

M-Pos428

AN ATTEMPT TO MEASURE THE DYNAMIC PERSISTENCE LENGTH OF DNA.
((B. S. Fujimoto and J. M. Schurr)) Department of Chemistry, BG-10, University of Washington, Seattle, WA 98195

Estimates of the dynamic persistence length (P_d) of DNA yield significantly larger results (1500–2400 Å) than are obtained for the static persistence length (450–500 Å) for DNAs measured under similar ionic conditions. We attempt to estimate P_d by measuring the time resolved fluorescence polarization anisotropy (FPA) of ethidium intercalated into a series of DNAs of differing length. These DNAs are 83% GC and have a pseudo-random sequence. We assume that (1) the actual hydrodynamic radius (R_H) is independent of the DNA length, and (2) the minimum energy conformation of the DNA is straight. Analysis of simulated FPA data show that the apparent R_H is independent of the DNA length only if the correct value of P_d is assumed in the data analysis. However, our FPA measurements indicate that the apparent R_H increases with length for any assumed value of P_d. This may be evidence that assumption (2) is violated, that on the time scale of the experiment the DNA does not relax to a straight minimum energy conformation, but instead exhibits a distribution of long-lived curved conformations. Such curvature will reduce the diffusion coefficient for rotation about the long axis of DNA, resulting in a larger apparent R_H. These data provide strong evidence for the existence of long lived bends in these DNAs, but has not yet enabled us to estimate P_d. For longer DNAs, the appropriate R_H appears to be 11 to 12 Å, rather that the $\sim$ 10 Å measured for very short DNA fragments where R_H is not significantly influenced by permanent bends.

M-Pos429

ANALYSIS OF LOCAL HELIX BENDING IN CRYSTAL STRUCTURES OF DNA OLIGONUCLEOTIDES
((M.A. Young, G. Ravishanker, D.L. Beveridge and H.M. Berman†)). Chemistry Department, Wesleyan Univeristy, Middletown, CT 06459. †Chemistry Department, Rutgers University, New Brunswick, NJ 08903.

Sequence-dependent bending of the helical axes in 121 oligonucleotide duplex crystal structures resident in the Nucleic Acid Database (NDB) have been analyzed and compared using "bending dials", a computer graphics tool. Our analysis includes structures of both A and B forms of DNA, and considers both uncomplexed forms of the double helix as well as those bound to drugs and proteins. The patterns in bending preferences in the crystal structures are analyzed by base pair step and emerging trends are noted. Analysis of the 66 B-form structures in the NDB indicates that uniform trends within all pyrimidine-purine and purine-pyrimidine steps are not necessarily observed, but are found particularly at CG and GC steps of dodecamers. The results support the idea that AA steps are relatively straight, and that larger roll bends occur at the junctions of these A-tracts with their flanking sequences. The data on 16 available crystal structures of protein-DNA complexes indicate that the majority of the DNA bends induced via protein binding are sharp localized kinks. The analysis of the 30 available A-form DNA structures indicates that these structures are also bent, and show a definitive preference for bending into the deep major groove over the shallow minor groove.

M-Pos430

AN EXTENDED NUCLEIC ACID MODELING TOOL-NAMOT2.
((E.S. Carter and C.-S. Tung)) Theoretical Biology and Biophysics(T-10), Theoretical Division,Los Alamos National Laboratory, Los Alamos, NM. 87545.

The ability to alter nucleic acid structure while maintaining base pairing is crucial to the building and manipulating of these molecules. Using a set of reduced coordinates developed in our laboratory enables modeling of these structures while maintaining proper pairing. These reduced parameters have recently been extended to include the description of unusual nucleic acid structures. A program has been developed to allow users to model nucleic acids using these coordinates. A set of modifiable external libraries for base, unit, helix, sugar, and phosphate enables users to build their own customized environment. A set of graphic routines and a specifier language allows visualization within the program. The program is written in C/Xlib. Since Motif and XView interfaces exist, the program is portable to most UNIX workstations.

M-Pos431

COMPARISON OF STRUCTURES OF D(CGCAAAAATGCG) OBTAINED FROM X-RAY CRYSTALLOGRAPHY, NUCLEAR MAGNETIC RESONANCE, AND MOLECULAR DYNAMICS SIMULATION ((M.A. Young, S. Kumar, I. Goljer, J. Srinivasan, P.H. Bolton, and D.L. Beveridge)) Wesleyan University Department of Chemistry, Middletown, CT 06459.

The B-DNA oligonucleotide d(CGCAAAAATGCG) contains a stretch of five sequential adenine residues, a structural feature implicated in sequence specific DNA bending. A detailed description of this sequence dependent DNA bending that is consistent with all available data has not yet been determined. Structures for the B-DNA oligonucleotide of interest have been determined both from NMR proton-proton distances incorporated into restrained molecular dynamics (MD), and independently from trajectories of unrestrained MD. The results from the restrained and unrestrained MD are compared with each other, as well as with the two crystallographic structures for the sequence published by DiGabriele, et al. in 1989. Our comparison emphasizes three areas, the analysis of the helicoidal properties of the DNA, the detailed description of the bending of the DNA helical axis, and the analysis of the structures of the major and minor grooves. Additionally, simulated 2-D NOE spectra have been generated from each of the structures, and these are compared with the experimental spectra.

M-Pos432

LIGHT SCATTERING STUDIES OF SUPERCOILED AND SINGLE-STRAND-NICKED PLASMIDS. ((D.M. Fishman*, G.D. Patterson†, W.R. McClure††)) *Department of Physics, †Department of Chemistry, and ††Department of Biological Sciences, Carnegie Mellon University, Pittsburgh, PA 15213

Static and dynamic light scattering measurements were made of solutions of pGem1a plasmids (3730 base-pairs) in the supercoiled and nicked forms. The static structure factor and the spectrum of decay modes in the autocorrelation function were examined in order to determine the salient differences between the behavior of supercoiled DNA and nicked DNA. The DNA was dissolved in TE buffer at pH 8 with 0.1 M added NaCl, which minimized the charge-related interactions. The concentrations ranged from 10.5 μg/ml to 76 μg/ml. These concentrations are within the dilute regime. Homodyne intensity autocorrelation functions were collected for both DNAs at angles corresponding to $0.01\ nm^{-1} < q < 0.03\ nm^{-1}$. At the smallest scattering vectors the probe size was comparable to the longest intramolecular distance, while at the largest scattering vectors the probe size was smaller than the persistence length of the DNA. Static structure factors for nicked and supercoiled DNA superpose when scaled by the radius of gyration. The contribution to the correlation function from the internal dynamics of the DNA was seen to result in a strictly bimodal decay function. The q-dependence of the contribution to the scattered light from internal modes and the low-angle limiting values of the internal mode rate were monitored. The internal mode behavior reflected the difference between the nicked DNA and the supercoiled DNA dynamics. The supercoiled DNA behavior seen here suggests that conformational dynamics play a larger role in DNA behavior than is suggested by the notion of a branched interwinding structure.

M-Pos433

ORIGIN OF THE TEMPERATURE DEPENDENCE OF THE SUPERCOILING FREE ENERGY ((Jeffrey J. Delrow, Patrick J. Heath, John A. Gebe, Bryant S. Fujimoto, and J. Michael Schurr)) Department of Chemistry, University of Washington, BG-10, Seattle, WA 98195

Monte Carlo simulations were employed to estimate the twist-energy parameter (E_T), which governs the supercoiling free energy, for a 1515 bp circular DNA over the temperature range from 7 to 85 °C. Simulations using temperature-independent elasticity parameters gave E_T values virtually independent of temperature, irrespective of whether hard-cylinder or screen Coulomb methods were used to model DNA self-interactions. We found, however, using time-resolved fluorescence polarization anisotropy (FPA), that for a 1876 bp restriction fragment from pBR322 the twisting elasticity parameter (torsion constant) has a strong, reversible temperature dependence. Average torsion constant values ($<\alpha>$) varied linearly from 5.63 to 2.80 x 10^{-12} erg over the temperature range from 7 to 59 °C. In addition, circular dichroism measurements performed on this fragment displayed a 20 percent increase in θ_{273} over this same temperature range. Similar results were also observed for $<\alpha>$ of supercoiled pUC8 DNA (2717 bp) over a much smaller temperature range (20 to 40 °C). Incorporating the measured temperature-dependent $<\alpha>$ for the 1876 bp fragment into our Monte Carlo simulations yielded E_T values with a temperature-dependence $dE_T/dT = -14.2$ from 7 to 85 °C. This is comparable to the experimental value reported for pBR322, namely $dE_T/dT = -15.6$.

M-Pos434

KINETICS OF HELIX FORMATION AT HIGH PRESSURE ((RB Macgregor* & MC Lin)) Faculty of Pharmacy, University of Toronto, Toronto, Ontario M5S 2S2

We have presented data on the influence of hydrostatic pressure on the thermal stability of double and triple stranded DNA. Briefly, the double and triple stranded forms are stabilized by pressure and the stabilization increases linearly with the logarithm of the salt concentration. The pressure-induced shifts in the helix-coil transition temperature were used to calculate the molar volume change (ΔV_t). In our studies we have found that ΔV_t depends on the sequence and base composition of the DNA, the radius of the counter ion, the number of strands involved, the charge of the DNA and the length of the oligonucleotide.

We are now studying the effect of pressure on the kinetics of the helix-coil transition. We observe the kinetics the transition by measuring the hysteresis between the UV thermal denaturation and renaturation curves at different pressures. At given heating and cooling rates, the size of the hysteresis is determined by the rate of the process, a larger hysteresis is evidence of a slower process. We have measured the denaturation/renaturation hysteresis of the double stranded oligonucleotide, $dA_{19}dT_{19}$, in 50 m*M* NaCl. We found that the hysteresis increased from 1 °C at 0.1 MPa to 3 °C at 200 MPa. Thus, hydrostatic pressure slows the transition. Assuming a single step reaction, and standard Arrhenius behaviour, this change in the hysteresis corresponds to a 14-fold reduction in the rate at 200 MPa, or an activation volume of approx. +35 mL mol^{-1}. Decreasing the salt concentration reduces the affect of pressure on the kinetics of the transition.

M-Pos435

VIBRATIONAL ANALYSIS OF DIETHYL PHOSPHATE: A MODEL FOR THE DNA PHOSPHODIESTER GROUP. ((Yifu Guan and George J. Thomas, Jr.)) Division of Cell Biology and Biophysics, School of Biological Sciences, University of Missouri, Kansas City, MO 64110.

In order to develop a molecular force field for the DNA phosphodiester group and to improve understanding of the conformational dependence of its vibrational spectrum, we have carried out a detailed normal mode analysis of the diethyl phosphate anion, $(CH_3CH_2O)_2PO_2^-$ (DEP), which serves as a model compound representing the nucleic acid sugar-phosphate moiety. New experimental data, including Raman depolarization ratios and complete vibrational spectra of five isotopic derivatives (^1H, ^2H, ^{13}C) of DEP, resolve previously problematic spectral assignments. *Ab initio* calculations were also performed on the geometry-optimized *trans-gauche-gauche-trans* conformation of the DEP isotopomers. The *ab initio* results are in good agreement with the experimental data. The experimental and calculated results have been combined to develop a consistent generalized valence force field (GVFF) for normal modes of the C-C-O-P-O-C-C network and its hydrogenic substituents. This molecular GVFF is being adapted to other conformers of DEP to examine the conformational dependence of the vibrational spectrum. The results are expected to advance understanding of Raman bands in spectra of DNA which serve as indicators of backbone conformation. [Supported by NIH Grant AI18758.]

M-Pos436

NUCLEAR OVERHAUSER EFFECT-DERIVED INTERPROTON DISTANCES INDICATE MINOR SUGAR CONFORMERS IN A DNA DUPLEX. ((N.B. Ulyanov and T.L. James)) UCSF, San Francisco, CA 94143-0446.

A restrained Monte Carlo (rMC) method was used to study the solution structure for the DNA decamer CATTTGCATC:GATGCAAATG. The average conformation of this decamer has been previously obtained by restrained molecular dynamics (rMD) with 2D NOE-derived interpoton distance restraints (DR) and torsion angle restraints (TR) derived from the deoxyribose vicinal proton coupling constants; this structure belongs to the B-family of forms, with C1'-exo and C2'-endo sugar puckers for pyrimidine and purine residues, respectively [Weisz, Shafer, Egan & James, Biochemistry 33:354, 1994]. A significantly more irregular conformation, however, was obtained by rMC calculations using DR but no TR, with most of the pyrimidine residues having O1'-endo or C4'-exo sugar puckers. Detailed analysis showed that H6/H8-H3' DR were responsible for the appearance of unusual sugar puckers. Indeed, rMC refinement against the subset of DR that excluded H6/H8-H3' distances resulted in a conformation very similar to the rMD-refined structure. These results can be explained by a C2'-endo/C3'endo conformational equilibrium for the DNA decamer. While coupling constants are averaged in a linear manner in the case of conformational equilibrium, NOE intensities are strongly biased towards shorter distances. Consequently, experimental TR are determined largely by the major C2'-endo conformers, while the minor C3'-endo conformers with short H6/H8-H3' distances strongly affect the corresponding DR derived from NOE. A comparison with other sequences studied allowed us to suggest that the described phenomenon is common for short DNA duplexes in solution.

M-Pos437

MOLECULAR DYNAMICS SIMULATION OF A-TRACT DNA d(CGCAAATTTGCG)$_2$ IN AQUEOUS SOLUTION

((K.J. McConnell, G. Ravishankar, D.L. Beveridge)) Wesleyan University, Biophysics Program, Middletown, CT 06459

In our current study we look at how A tracts effect the fine structure of DNA through the use of Molecular Dynamics. Oligo DNA sequences with A tracts have been observed in gel migration studies to have greater propensity to bend over any other sequence. Crystallographic data of the sequence d(CGCAAATTTGCG)$_2$ describes two different fine structures of the A-tract. Rich and co-workers (*Proc. Natl. Acad. Sci.* 84, 8385-8389 (1987)) describes a network of triple centered or bifurcated hydrogen bonds as well as a narrow minor groove in the A-tract. The other crystal structure of Neidle and coworkers (*J. Mol. Biol.* 226, 1161-1173 (1992)) describes the A-tract as having high propeller twist with only one possible bifurcated hydrogen bond and a ribbon of water distinct from the "spine of hydration" in the minor groove.
The simulation was carried out using a modified version of the GROMOS 86 force field called Wesdyn on the Cray C90 super computer. The system was setup using a hexagonal prism cell under periodic boundary conditions containing ~3000 water molecules to provide a 12Å shell of water around the edge of the DNA. The simulation is compared to crystallographic data including hydration of the minor groove and bending analysis of each of the base steps. The current simulation will also be compared to other A-tract DNA simulation performed in this lab.

M-Pos438

A-DNA HEXANUCLEOTIDES PACK IN A NEW CRYSTAL LATTICE ((B. H. M. Mooers)) Dept. of Biochemistry and Biophysics, Oregon State University, Corvallis, OR 97331

The first four members of a new class of A-DNA crystal strucutres, the A-DNA hexanucleotides, have been crystallized in our lab in the space group C222$_1$ (Mooers et al., submitted). This lattice has not been observed before in crystals of any other A-DNA oligonucleotides. The hexanucleotides (or hexamers) retain the A-DNA packing motif in which the terminal base pairs pack in the minor grooves of symmetry mates. Hexamers in this new lattice surround oval cavities as in previous A-DNA crystals (Figure A). However, the hexamers form planar sheets rather than spiraling in an infinite right-handed helix as in the A-DNA tetramer and octamer crystal structures. The sheets of hexamers stack in layers along the b-axis of the unit cell (Figure B). Water molecules link these sheets by hydrogen bonding to DNA molecules in adjacent sheets. The stability of this new crystal environment is studied by using crystal packing geometry and calculating molecular packing energies.

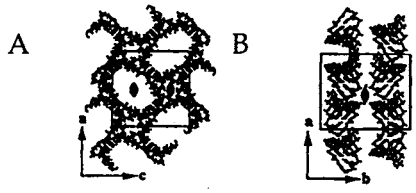

M-Pos439

INCLINATION OF BASES IN Z' FORM DNA IN SOLUTION ((C.Krittanai and W.C. Johnson, Jr.)) Department of Biochemistry and Biophysics, Oregon State University, Corvallis, OR 97331

The Z'-form of synthetic poly(dG-me^{5}dC):poly(dG-me^{5}dC) is prepared from the B-form in a high concentration of ethanol, and studied by flow linear dichroism (FLD). The optical density and linear dichroism data are analyzed by a multiple variable algorithm, yielding the inclinations of the bases, and the axis around which the bases incline. This is compared with Z-form DNA.

M-Pos440

THERMODYNAMIC STUDIES ON Z-FORMING AND B-Z JUNCTION FORMING DNA OLIGOMERS. ((Stephen P. Marotta, Ebenezer O. Otokiti & Richard D. Sheardy)) Department of Chemistry, Seton Hall University, South Orange, NJ 07079.

A series of DNA oligomers with the general sequence **XX**-(5meC-G)$_4$ and (5meC-G)$_4$-**XX** (where **X** = A, T, G or C) have been synthesized to investigate the effect of 5' or 3' two base overhangs on the free energies of duplex formation relative to (5meC-G)$_4$ in both B and Z conformations. Analyses of the thermally induced denaturations of these oligomers in 3.0 M NaCl indicated a linear relationship between T_m^{-1} vs ln C_T over a 50-fold range of DNA concentrations. At [NaCl] less than 200 mM, we observe an equilibrium between duplex and hairpin forms which depends upon both the [DNA] and the nature of the overhang. At all NaCl concentrations the presence of an overhang results in a stabilizing effect with the 5'-overhang showing a greater degree of stabilization relative to the 3'-overhang. We have also investigated the thermodynamic stabilities of B-Z junction forming DNA oligomers of general sequence (5meC-G)$_4$-**GXYG**-ACTG (where **X** and **Y** represent all permutations of pyrimidine bases). Thermal denaturation studies were carried out in one of two fashions: at constant [DNA] and variable [NaCl] or at constant [NaCl] and variable [DNA]. The results indicate that these oligomers behave in a manner similar to other B-Z junction forming DNA oligomers [Sheardy et al, *Biochemistry* **33**, 1385 (1994)].
Acknowledgment is made to the Donors of the Petroleum Research Fund, administered by the American Chemical Society for support of this research.

M-Pos441

DETECTION OF DYNAMIC EFFECTS ASSOCIATED WITH A PLASMID B-Z TRANSITION AND WITH ECOR1 BINDING. ((R.S. Keyes, O.K. Strobel, and A.M. Bobst)) Department of Chemistry, University of Cincinnati, Cincinnati, OH 45221.

The ability to effectively monitor nucleic acid dynamics has become increasingly important to understanding conformational transitions and protein-nucleic acid interactions relevant to biological function. The development of an interpretive framework for analyzing changes in the internal and global dynamics of spin-labeled nucleic acids [1] has provided a powerful tool for studying these motions. The analysis is based upon the model-free approach of Lipari and Szabo [2]. Two lines of research will be presented: I) The EPR spectrum of an eleven-atom tethered spin label enzymatically incorporated into the plasmid pRDZ8 undergoes a distinct line shape change upon transition from the B to the Z form. The conformational change and associated dynamics are consistent with earlier studies on linear polymers [3]. II) A complex consisting of the EcoR1 protein site-specifically bound to a DNA 26mer provides a model system for studying possible conformational changes that occur upon protein binding. EPR has been applied to this complex spin labeled in three different positions adjacent to the binding site. The spectral line shapes are distinct for each of these complexes. A dynamics analysis distinguishes between spectral effects due to a change in the hydrodynamic shape of the complex and those resulting from conformational variations.

1. Keyes, R.S., & Bobst, A.M., submitted for publication.
2. Lipari, G., & Szabo, A. (1982) *J. Am. Chem. Soc. 104*, 4546.
3. Strobel, O.K., Keyes, R.S., & Bobst, A.M. (1990) *Biochemistry 29*, 8522.

M-Pos442

MOLECULAR STRUCTURES OF DNA AND RNA TRIPLE HELICES. (G. Raghunathan[1], R.L. Jernigan[1], H.T. Miles[2] and V. Sasisekharan[2]) Laboratory of Mathematical Biology, NCI and Laboratory of Molecular Biology, NIDDK, NIH, Bethesda, MD 20892

Detailed molecular structures of DNA and RNA triple helices containing two pyrimidines and one purine are proposed. The structures are consistent with recent infrared spectral and X-ray diffraction studies. In these structures, the three chains are symmetry related, have identical backbone conformations and standard torsion angles and are stereochemically satisfactory. In the DNA triple helix, a pseudodyad relates the Watson-Crick purine and pyrimidine strands, a dyad relates the two pyrimidine strands and, a pseudorotational symmetry relates the Hoogsteen paired purine and pyrimidine strands. The structure and conformation of this triple helix are similar to the double helical B-form DNA and it has sugar puckers in the C2'-endo region. Stereochemically satisfactory RNA triple helices containing sugars in the C3'-endo region are constructed using a rotational screw symmetry and appropriate tilt of the bases. In the proposed RNA triple helix, the Hoogsteen paired purine and pyrimidine strands are related by a screw symmetry, while still preserving the pseudodyad between the Watson-Crick paired purine and pyrimidine strands and, the dyad between the two pyrimidine strands. The proposed DNA and RNA structures with the new symmetry elements do not have the disallowed short inter chain nonbonded distances present in the earlier models proposed by Arnott and coworkers.

M-Pos443

DEOXYRIBONUCLEOTIDE TRIPLEXES FORMATION OF 5'-A-(G-A-)$_2$G with 5'-d-T-(C-T-)$_2$C-(T-)$_4$C-(T-C-)$_2$T, 5'-d-T-(^{m}C-T-)$_2$^{m}C-(T-)$_4$C-(T-C-)$_2$T, 5'-d-T-(C-T-)$_2$C-(T-)$_4$^{m}C-(T-^{m}C-)$_2$T,or 5'-d-T-(^{m}C-T-)$_2$^{m}C-(T-)$_4$^{m}C-(T-^{m}C-)$_2$T. A TRIPLEX WITH THREE T·A·T & THREE C$^+$·G·C BASES TRIADS

((L.-S. Kan[a], L. M. Tsay[a], S. B. Lin[b], H. T. Tsay[a,c], and H. H. Chen[c]))
[a]Institute of Chemistry, Academia Sinica; [b]Graduate Institute of Medical Technology, National Taiwan University; and [c]Institute of Applied Chemistry, Culture University, Taipei, Taiwan.

The UV mixing titration, gel electrophoresis, and CD measure-ments indicate that oligomers with a basic sequence of 5'-d-T-(C-T-)$_2$C-(T-)$_4$C-(T-C-)$_2$T form a hairpin type triplex with the target 5'-A-(G-A-)$_2$G. The stability, measured UV melting temperatures, were studied in aqueous solution as functions of ^{m}C (5-methylcytidine) replacement of C, pH (4 to 7), and salt concentration (up to 1 M). The order of stability is 5'-A-(G-A-)$_2$G + 5'-d-T-(C-T-)$_2$C-(T-)$_4$C-(T-C-)$_2$T < 5'-A-(G-A-)$_2$G + 5'-d-T-(^{m}C-T-)$_2$^{m}C-(T-)$_4$C-(T-C-)$_2$T = 5'-A-(G-A-)$_2$G + 5'-d-T-(C-T-)$_2$C-(T-)$_4$^{m}C-(T-^{m}C-)$_2$T > 5'-A-(G-A-)$_2$G + 5'-d-T-(^{m}C-T-)$_2$^{m}C-(T-)$_4$^{m}C-(T-^{m}C-)$_2$T at pH 4.5. These results indicate that (a) a stable triplex is formed with three T·A·T and three C$^+$·G·C base triads and (b) ^{m}C is more effect than C to stablize the triplex formation in acidic condition. In addition, the stable triplex can also be formed in the same system by replacing one C$^+$·G·C base triad to C C C as using 5'-A-G-A-C-A-G for the target. Thus, this provides a simple system for studying usual base triads including analog.

(Supported by National Science Council of ROC grant # NSC84-2113-M-001-013)

M-Pos444

STRUCTURAL PROPERTIES OF THE K$^+$-[d($G_3T_4G_3$)]$_2$ QUADRUPLEX AND SEQUENTIAL SYN-SYN DEOXYGUANOSINES.

((G.D. Strahan, M.A.Keniry and R.H. Shafer)) Univ. of Calif., S.F., San Francisco, CA 94143-0446.

Two dimensional ^{1}H-^{1}H and ^{1}H-^{31}P NMR studies and molecular dynamics (MD) calculations with energy component analysis were performed on the hairpin quadruplex formed by d($G_3T_4G_3$) in a KCl solution. Experimental evidence indicates a unique arrangement of the sequential deoxyguanosine conformations, in which the deoxyguanosines do not strictly alternate between syn and anti glycosidic bond angles along the individual strands as they do in other hairpin quadruplex species. Thus, the following sequences were found (S = syn, A = anti):

5'-G1$_S$G2$_S$G3$_A$T4$_A$T5$_A$T6$_A$T7$_A$G8$_S$G9$_A$G10$_A$-3'
5'-G11$_S$G12$_S$G13$_A$T14$_A$T15$_A$T16$_A$T17$_A$G18$_S$G19$_A$G20$_A$-3'

Energy component analysis of models resulting from unrestrained MD indicates that for guanines, the sequential syn-syn/anti-anti and syn-anti quartet stacking energies are nearly identical, whereas the unobserved anti-syn quartet stack is highly destabilizing to the over-all structure and is energetically less favorable by ~4 kcal/mol. Although coordinated cations were not included in these calculations, the lower stability of the anti-syn stack is sufficient to account for its absence in our experimentally determined structure. Not included in this calculation were the effects of internally coordinated cations and the thymine loops upon the arrangement and stability of the quartets. We note, however, that all hairpin-loop quadruplex structures solved to date have the purine preceding the first thymine of the loop in the anti conformation, and the guanine immediately after the loop in the syn conformation. Possible reasons for this are presented.

Interestingly, this sequential relationship does not imply or require either the diagonal- or edge-looped quadruplex form, and each form has similar potential energy.

M-Pos445

SOLUTION STRUCTURE OF AN IMMOBILE HOLLIDAY JUNCTION BY 2D ^{1}H NMR

((Siobhan M. Miick and Walter J. Chazin))
The Scripps Research Institute, Department of Molecular Biology, 10666 North Torrey Pines Road, La Jolla, CA 92037

The Holliday junctions (HJs) is a transient DNA structure formed during the course of genetic recombination when two homologous duplex DNA are brought together, aligned and exchange strands. The structure of the HJ intermediate appears to play a central role in determining the outcome of the recombination event. An inherent property of HJs is branch migration within the regions of homology. To facilitate biophysical and structural studies, we study 32-bp immobile HJs, where the sequences of the four DNA strands form one unique four-arm model junction in which branch migration is not possible. A 1mM solution of J1 was prepared from four 16-mer DNA oligos titrated by ^{1}H NMR to a 1:1:1:1 equimolar ratio. Using ^{1}H NMR spectroscopy, complete assignments have been made of the labile and nonlabile protons. The ratio of the two crossover isomers isomers of these junctions was measured by a site specific ^{15}N label incorporated into one thymine at the crossover. To generate input constraints for structure calculations, NOE build-up curves were measured from NOESY spectra with three different mixing times. It was evident immediately that a differential build-up of the sequential and intra-residue internuclear vectors is present, indicating anisotropic motion. thus, our analysis of the NOE data must include a specific motion model and special techniques for ensemble integration of overlapped peaks and conversion to distance constraints. The structure will be refined by restrained MD making extensive use of relaxation matrix methods. Six unique long range distance constraints and corresponding distance distributions available from time resolved FRET will be implemented as a symmetrical potential in the AMBER forcefield. The goal of the calculations is to understand the local geometry at the crossover and establish a correlation between crossover sequence preference rules and propensity for recombination.

M-Pos446

CONFORMATIONAL ANALYSIS OF THREE-ARM AND FOUR-ARM DNA JUNCTIONS USING ENERGY TRANSFER.

((D. P. Millar and M. Yang)) Department of Molecular Biology, The Scripps Research Institute, La Jolla, CA 92037.

DNA junctions occur as intermediates in various cellular processes involving rearrangement of DNA, including homologous genetic recombination and DNA replication. Enzymes that resolve branched DNA species may recognize the global conformation of the junction. We have used fluorescence energy transfer methods to analyze the conformation of a series of three-arm and four-arm DNA junctions formed from synthetic oligonucleotides. Donor (D) and acceptor (A) dyes were attached to the junction arms in various pairwise combinations. Since DNA junctions have considerable conformational flexibility, we analyzed the fluorescence decay of the donor using a distance distribution model. The recovered D-A distance distributions not only reveal the average distance between each pair of arms, but also the range of distances that exists between each pair. This has provided information about the global conformation of the junctions and their intrinsic flexibility. Four-arm junctions form X-shape structures comprised of two stacking domains, with considerable flexibility between domains. We have examined a series of related four-arm junctions with different base sequences at the junction, to elucidate the stacking preferences of junction bases and to assess their effects on the geometry and flexibility of the junction. Three-arm junctions form extended structures with less dispersion in the interarm distances than observed in four-arm junctions. The addition of unpaired bases at the branch alters the global conformation of the three-arm junction and enhances its flexibility. We have compared the effects of various unpaired bases on the flexibility of three-arm junctions.

Supported by NSF grant MCB-9317369.

M-Pos447

FLUORESCENCE QUENCHING STUDIES OF ETHIDIUM BROMIDE BOUND TO IMMOBILE THREE ARM JUNCTIONS

((Luis I. Hernandez, Min Zhong, Scott H. Courtney, and Neville R. Kallenbach))
Department of Chemistry, New York University, New York NY 10003

The structural and dynamic properties of branched DNA states are of interest in connection with the mechanisms of recombination, repair and mutagenesis. We have reported that the dye ethidium bromide (EB) interacts selectively at the branch point of three and four arm junctions, and that such specific interactions give rise to a 12 to 14 ns lifetime in addition to the 22 to 25 ns lifetime of ethidium bound to duplex DNA. This faster lifetime can be identified with EB bound near open structures in DNA, including certain mis-matches, unpaired regions, and even ends, as well asbranched structures. To further characterize states that give rise to the faster lifetime, we have carried out fluorescence quenching studies in three arm junctions with and without mis-matches. The quenching constant is dependent on EB:DNA ratio and construct. Binding near the branch site can be differentiated from binding near the ends of the branched constructs by its affinity and quencher accessibility using steady state and time correlated fluorescence measurements.

Supported by grants CA24101 fron National Cancer Institute, NIH and 9011268 from NSF.

M-Pos448

DIRECT DETERMINATION OF DNA HANDEDNESS IN SOLUTION BY FLUORESCENCE RESONANCE ENERGY TRANSFER.

((Elizabeth A. Jares-Erijman and Thomas Jovin)) Dept. of Mol. Biol., Max Planck Inst. for Biophys. Chem. P.O. Box 2841. D-37018 Göttingen. F.R.G.

Fluorescence Resonance Energy Transfer (FRET) has been previously used to provide information on helical parameters such as the rise and twist of a helix. However this technique alone cannot in general provide information on helical handedness. The problem is being addressed using a novel approach based on the construction of a molecule consisting of two segments, one of which has a known handedness. The molecules are covalently labeled at one end with a donor and at the other with an acceptor. By moving the position of the junction while maintaining constant the total length of the helix, the efficiency of energy transfer becomes primarily a function of the relative handedness of both segments. When both segments have equal handedness one obtains a monotonic function of FRET with the junction position. In contrast, a periodic function is obtained when both segments have opposite handedness. The method is being validated with a group of oligonucleotides containing a d(m^5C-G)$_n$ segment labeled at the end with fluorescein and a second parallel-stranded d(A·T)$_m$ segment labeled with the cyanine dye Cy3. A B-Z junction is created between the two segments by inducing a B-Z transition in the d(m^5C-G)$_n$ segment with $NaClO_4$ (3.4 M) and Mg^{2+} (150 mM). The concentration range required was investigated by CD and absorbance measurements (Abs 295/260). The junction was moved by decreasing the number of bases in one segment and increasing it in the other, while maintaining constant the total length of the molecule. Constant values of FRET were obtained for the group of oligonucleotides in which the d(m^5C-G)$_n$ segment was in the B conformation. The values changed dramatically by induction of the B-Z Transition.

M-Pos449

INTERACTION OF BIS-ETHIDIUM TO THE STEM AND LOOP SITES OF DNA HAIRPINS ((Dionisios Rentzeperis, Miriam Medero and Luis A. Marky)) Department of Chemistry, New York University, New York, New York 10003.

We used a combination of isothermal titration calorimetry (ITC) and spectroscopic techniques to thermodynamically characterize the interaction of bisethidium to short DNA hairpins with sequences: d(GCGCT$_5$GCGC) and d(CGCGT$_5$CGCG). Deconvolution of the ITC isotherms indicates the following: i) complex stoichiometries of three ligands per hairpin, corresponding to a high affinity site in the stem ($K_b \sim 10^7$) that accommodate one bisethidium molecule, and a lower affinity site ($K_b \sim 10^6$) in the loop that accommodates two bisethidium molecules: and ii) binding of bisethidium results in enthalpy driven reactions, ΔH_b's of -13.1 kcal/mol and -12.1 kcal/mol for the stem and loop sites, respectively. Comparison to the thermodynamic profiles of ethidium and of propidium binding reveals that the bisethidium binding to the stem site of each hairpin has a more favorable free energy terms of -1.4 kcal/mol and more favorable enthalpy of -4.2 kcal/mol. These suggest that only one phenanthridine ring of bisethidium intercalates in the stem, while the second planar ring is weakly associated with the surface of DNA. The K_b's for bisethidium binding to the loop sites are about two orders of magnitude larger than the monointercalators, and correspond to more favorable free energy (-2.0 kcal/mol) and enthalpy (-2 to -4 kcal/mol) contributions. Overall, the magnitude of K_b for each ligand, and for each site, is in qualitative agreement with the electrostatic contribution from the actual number of positive charges of the ligand. The increased favorable enthalpic contributions of bisethidium are consistent with larger hydrophobic contributions, while the increase in unfavorable entropic contributions are consistent with the higher ordering of the ligand to the stem and loop sites. Supported by grant GM-42223 from the National Institute of Health.

M-Pos450

DNA CLEAVAGE KINETICS OF THE ENEDIYNE ANTICANCER DRUG C-1027. (C. Kirk,* J. Goodisman,* T. Beerman† and J.C. Dabrowiak*) *Department of Chemistry, CST 1-014, Syracuse University, Syracuse, New York, 13244-4100, †Roswell Park Cancer Institute, Elm & Carlton Streets, Buffalo, New York, 14263.

In order to identify the molecular basis for the extreme toxicity of the anticancer drug C-1027, which contains an enediyne chromophore, we studied the ability of the drug to cleave purified and intracellular SV40 DNA. BSC-1 cells infected with the SV40 virus were treated with various concentrations of drug for 2 hours at 37°C. After lysis the DNA forms were separated by agarose gel electrophoresis and the amount of DNA in each form quantitated by microdensitometric scanning of photographic negatives of the gel. Rate constants for single- and double-strand cleavage of purified SV40 DNA were 2.2 and 1.2 x10^5 M^{-1} min^{-1}. The antibiotic cleaves DNA inside the cell at a rate much greater than its rate of cleavage of extracellular DNA. Moreover, determination of the number of single and double strand breaks revealed that the drug produces more double strand breaks on intracellular DNA than on its extracellular counterpart. The study suggests that the high toxicity of C-1027 is probably related to both active uptake of the drug chromophore into cells and the ability of the agent to produce double strand breaks which are difficult to repair.

M-Pos451

HIGH RESOLUTION SOLUTION STRUCTURE OF THE ANTITUMOR AGENT DUOCARMYCIN SA COMPLEXED WITH DUPLEX DNA. ((P.S. Eis, J.A. Smith, J.M. Rydzewski, D.L. Boger, and W.J. Chazin)) The Scripps Research Institute, Department of Molecular Biology, 10666 North Torrey Pines Road, La Jolla, CA 92037.

The duocarmycins are a promising new class of antitumor antibiotics. Duocarmycins exhibit potent cytotoxicity via site-specific binding in the minor groove of DNA and subsequent alkylation at N_3 of adenine residues. We have surveyed the reactivity of duocarmycin SA (DSA) with several short (9-12mers) DNA duplexes, and have identified an 11mer duplex (GACTAATTGAC:GTCAATTAGTC) which produces a single product with a 95% yield. A large scale reaction was performed with DSA and the GAC:GTC 11mer, the DSA-GTC covalently bonded strand was isolated using HPLC, and an NMR sample was prepared by titrating DSA-GTC with the GAC strand. Complete ^{1}H NMR resonance assignments have been made using 2Q, TOCSY, NOESY, and natural abundance ^{13}C-^{1}H HSQC spectra. Distance constraints from NOESY spectra and dihedral angle constraints from a PE-COSY spectrum were utilized as input constraints for the structure calculations. This included fifty drug-DNA distance constraints. Initially, the DNA constraints alone were imposed on an ensemble of forty randomized duplex DNA structures, then forty duocarmycin conformations were generated using the drug only constraints. Arbitrary drug and DNA starting structures were docked, and the complexes fully refined using restrained molecular dynamics.

[Supported by a postdoctoral fellowship to P.S.E (NIH F32 CA61720-02) and grants DHP-123A and FRA-436 from the American Cancer Society.]

M-Pos452

SOLUTION STRUCTURE OF THE COMPLEX FORMED BY ANTITUMOR AGENT (+)-CC-1065 AND A DNA DODECAMER USING DISTANCE RESTRAINTS FROM RELAX MATRIX ANALYSIS OF 2D NOE SPECTRA AND RESTRAINED MOLECULAR DYNAMICS [[Y.-C. Yuan, L. H. Hurley, and T. L. James]] UCSF, San Francisco, CA 94143-0446

High resolution, sequence-dependent structural features of a complex between a potent antitumor agent, (+)-CC-1065 ($C_{37}H_{33}N_7O_8$, m.t.=703 g), and a non-self-complementary DNA 12-mer duplex [d(GGCGGAGTTA*GG).d(CCTAACTCCGCC)] (asterisk denotes the drug covalent modification site) has been investigated by using one- and two-dimensional proton and phosphorus NMR spectroscopy techniques and restrained molecular dynamics computer simulations. The assignments of the nonexchangable proton resonances (except some of the H5' and H5" protons due to severe resonance overlap), phosphorus resonances and the exchangeable resonances (except amino protons of adenosine and guanosine) of this DNA-drug complex have been made. More than 658 high quality interproton distance restraints with lower and upper bounds, derived from two-dimensional nuclear Overhauser effect (2D NOE) spectra in D_2O and H_2O, have been obtained from the iterative complete relaxation matrix program MARDIGRAS. Several pronounced conformational changes on DNA were observed upon adduct formation by comparing the chemical shifts and MARDIGRAS distances with the free 12-mer duplex from ^{1}H and ^{31}P NMR data. The dynamic structures of DNA 12-mer duplexes and their drug complexes for (+)-CC-1065 can be calculated by NOE-derived interproton distance restrained molecular dynamics calculations In aqueous solution, the (+)-CC-1065-12-mer duplex adduct maintains an overall B- form DNA structure, and the orientation of the bases is in the anti conformation throughout. (+)-CC-1065 binds snugly within the minor groove of DNA, overlapping from 6A to 11G on the covalently modified strand and from 15T to 21C on the noncovalently modified strand. The major distortion on DNA is localized at the 10A and 9T step of the covalently modified strand and at the 18C and 19T step of the noncovalently modified strand. Following the covalent bonding with (+)-CC-1065, the 12-mer duplex displays a compression of the minor groove at the 8T to 9T step and widening on both sides. The unusual structure features, such as DNA bending and transient kinks, can be examined by comparing the experimental 2D NOE spectrum with the theoretical spectrum of the resulting structure. Overall, these results provide additional support for the proposed sequence-dependent catalytic activation and conformational flexibility proposed to be important as the molecular basis for the sequence recognition of DNA for alkylation of (+)-CC-1065.

M-Pos453

STABILITY OF MODIFIED NUCLEIC ACID DUPLEXES: ANTISENSE MODELS. ((L. Ratmeyer, S. Gryaznov[1], K. Fearon[1], D. Lloyd[1], J.-K. Chen[1], L. Christensen[1], A. Raible[1], S. Yao, G. Zon[1] and W.D. Wilson)) Dept. of Chem., Georgia State Univ., Atlanta, GA 30303; [1]Lynx Therapeutics Inc., Hayward, CA 94545.

Antisense oligonucleotides promise high target sequence specificity with low host toxicity and are currently in clinical trials. Phosphorothioates and phosphoramidates are particularly promising therapeutic agents because of improved nuclease resistance and membrane permeability. We have investigated the effects of these modifications on the stability of antisense-sense complexes having either RNA or DNA sense strands. Phosphoramidates form remarkably stable duplexes with A-form type conformations. Antisense strands having nucleotide deletions and substitutions may be present as impurities in oligonucleotide products synthesized by automated oligonucleotide synthesizers. The stability of antisense-sense complexes containing base bulges and base pair mismatches that result from such impurities have been studied with phosphorothioate oligonucleotides currently in clinical trials.

M-Pos454

A NUCLEAR MAGNETIC RESONANCE INVESTIGATION OF THE EFFECT OF AMMONIA UPON DNA STRUCTURE AND DYNAMICS. ((Ewa J. Folta-Stogniew and I. M. Russu)), Department of Molecular Biology and Biochemistry, Wesleyan University, Middletown, CT 06459

NMR spectroscopy has been used to investigate the effect of ammonia on the structure and dynamics of the self-complementary dodecamer 5'-[d(CGCAGATCTGCG)]$_2$-3'. 2D NOESY and DQF-COSY data were collected at five ammonia concentrations ranging from 0.002 to 1M . Changes in chemical shift were observed for protons in the central part of the dodecamer. The largest shifts were 0.1 ppm and were observed for the sugar H1' and H4' proton resonances of the Cytosine in the eighth position. The volumes of NOESY cross-peaks were measured and scaled against volumes of Cytosine H5/H6 cross-peaks. Changes in the volumes of cross-peaks between base and sugar protons were observed for the central part of the dodecamer. They corresponded to variations in inter-proton distances of less than 15%. DQF-COSY experiments showed no significant changes in the coupling constants of sugar protons upon increasing ammonia concentration. All these results indicate that ammonia does not affect significantly the overall solution conformation of the dodecamer. However, we have observed that proton relaxation rates (i.e., transverse, longitudinal and cross-relaxation rates) increased by about 50% upon changing ammonia concentration from 0.002M to 1M. The observed changes were similar for all resonances suggesting that they originate from changes in the overall correlation time of the dodecamer. The implication of these results for structural studies and for measurements of base-pair opening in DNA will be discussed. (Supported by grant 88-17589 from the NSF)

M-Pos455

Polarization, Counterion Condensation, and Excluded Volume Effects in DNA. ((U. Mohanty and Y. Zhao)) Eugene F. Merkert Chemistry Center, Department of Chemistry, Boston College, Chestnut Hill, Massachusetts 02167, USA.

The polarization of counterions bound to short DNA fragments in low and high electric field strengths is described by the use of density functional theory of inhomogeneous systems. For low fields one finds that the polarizability p is $(Zq)^2 \rho_o \beta L^3/ (12[1 - L \rho_o \int (\lambda'-\lambda_o)\{dc(\lambda-\lambda')/d\lambda\}_{\lambda=\lambda_o} d\lambda'])$, where Z and L are the valence and the length of the polyion respectively, q is the proton charge, $\beta = 1/k_BT$, T is the temperature, k_B is the Boltzmann constant, $\lambda = x/L$, x_o is a reference point such that the inhomogeneous counterion density at x_o is equal to ρ_o - the density in the absence of an electric field, and c(x) is the direct correlation function of the homogeneous counterion phase. A dynamical generalization is proposed which incorporates the fact that in high fields the counterions conduct. We show that in a "dressed" polyelectrolyte formalism, the adsorption excess per monomer, obtained by an analytical solution of the cylindrical Poisson-Boltzmann equation, is identical to fraction of counterions condensed in Manning's counterion condensation model.# An intimate connection is found between counterion condensation and Kosterlitz-Thouless transitions. Finally, we obtain the second virial coefficient* in the counterion condensation framework and compare with experiments on DNA .

in collaboration with Barry W. Ninham

* in collaboration with Gerald S. Manning

M-Pos456

EFFECT OF MG^{2+} AND SUPERHELIX DENSITY ON THE CONFORMATIONS OF CIRCULAR DNAS. EXPERIMENTS AND MONTE CARLO SIMULATIONS. ((J. A. Gebe, P. J. Heath, J. J. Delrow, and J. M. Schurr)) Department of Chemistry BG -10, University of Washington, Seattle, WA 98195

The activity of chicken red cell Topo I on supercoiled p30δ DNA in 0.1 M NaCl increases dramatically upon addition of 5 mM Mg^{2+}. Is this due to some marked change in DNA tertiary structure induced by Mg^{2+}? The translational diffusion coefficient (D) and static structure factor (S(K)) of circular p30δ DNA (4752 bp) were measured at different superhelix densities in 0.1 M NaCl and in 0.1 M NaCl plus 5 mM Mg^{2+}. Addition of 5 mM Mg^{2+} causes a slight increase in D and a slight decrease in radius of gyration (R_G) at native superhelix density, and the magnitude of this effect declines with decreasing superhelix density. Monte Carlo simulations using the torsion constant measured for p30δ by fluorescence polarization anisotropy (FPA) and hard cylinder diameters appropriate for the ionic conditions yield D and S(K) values (and supercoiling free energies) in good absolute agreement with the measured values at the different superhelix densities in 0.1 M NaCl and in 0.1 M NaCl plus 5 mM Mg^{2+}. These molecules do **not** exhibit the highly extended structures with contiguous strands seen in cryoelectron microscopy studies. A comparison of the effects of using hard cylinder interactions versus screened coulomb interactions in the simulations is carried out for a 1000 bp DNA. For such short supercoiled DNAs, the end-loops act to extend the molecule somewhat, but again, the strands are not contiguous in 0.1 M NaCl plus 5 mM Mg^{2+}.

M-Pos457

THE ROLE OF DIVALENT CATIONS IN THE EXCISION OF DEOXYNUCLEOTIDES FROM DNA BY THE 3'-5' EXONUCLEASE OF THE BACTERIOPHAGE T4 DNA POLYMERASE: A Stopped Flow kinetic and Time Resolved Fluorescence Study. ((M. R. Otto[1], L. B. Bloom[2], R. Eritja[3], L. J. Reha-Krantz[4], M. F. Goodman[2], J. M. Beechem[1])) [1]Vanderbilt Univ., Nashville, TN, [2]USC, Los Angeles, CA, [3]CID-CSIC, Barcelona, Spain, [4]Univ. of Alberta, Alberta, Canada.

We are interested in the structural, kinetic and dynamics effects of divalent cations on the exonuclease site of DNA polymerases. Changes in fluorescent properties of the nucleotide 2-aminopurine (P) located at the primer terminus within the binary T4 polymerase-DNA complex were used to study binding and kinetics. A 17/30mer primer/template (see figure) which is "doubly" non-hydrolyzable (asterisks represent residues with phosphorothioate linkages) were necessary for these binding studies. As far as we can determine, these are the first cation binding titrations ever performed on a full DNA polymerase/DNA complex. Binding isotherms resolved two classes of sites with high ($K_d \approx 2\mu M$) and low ($K_d \approx$ 2mM) affinity. Exonuclease deficient (exo^-) mutants of the T4 polymerase exhibit reduced affinity for both classes of sites(see figure). Time-resolved studies of *wt* and exo^- polymerase DNA complexes suggest that populating the low affinity sites with Mg^{2+} results in a loosening of the binding "grip" of the exonuclease site for the DNA. Biphasic Hill plots of pre-steady state kinetic data show that the low and high affinity sites have different Mg^{2+} cooperativity values.

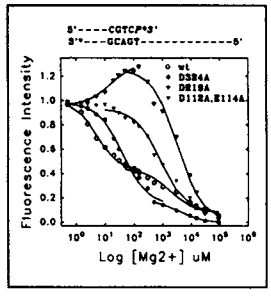

M-Pos458

A NOVEL CATIONIC AMPHIPHILE FOR TRANSFECTION OF MAMMALIAN CELLS. **((J.M. Ruysschaert; A. El Ouahabi; R. Fuks; M. Vandenbranden and P. Di Stefano)) ULB-CP206/2, B-1050 Brussels, Belgium**

We describe here a new cationic amphiphile, N-t-butyl-N'-tetradecyl-3-tetradecylaminopropionamidine (diC_{14}-amidine), which interacts with plasmid DNA and generates hydrophobic stable complexes resistant against DNase I. In partition experiments between two non-miscible phases, DNA was transferred into an organic phase upon complex formation with diC_{14}-amidine-containing vesicles. Finally, vesicles made of a diC_{14}-amidine and phosphatidylethanolamine (PE) (1:1, mol:mol) mixture or pure diC_{14}-amidine were efficient in mediating transfection of adherent (CHO) and suspension (K562) cell lines, using the chloramphenicol acetyltransferase (CAT) gene as reporter (1).
The presence of 10% foetal calf serum in culture medium does not preclude the transfection process. This advantage, along with the poor in vivo toxicity of diC_{14}-amidine (mice were apparently healthy after intravenous injection of up to 200 µg of DNA/diC_{14}- amidine complex) could make it a valuable delivery system for in vivo transfections and gene therapy.

(1) (J.M. Ruysschaert, A. El Ouahabi, V. Willeaume, G. Huez, R. Fuks, M. Vandenbranden and P. Di Stefano, Bioch. Biophys. Res. Comm. (in press)).

M-Pos459

APPLICATIONS OF MAGNETIC SEPARATIONS OF DNA AND ANTIGEN–ANTIBODY COMPLEXES IN VARIOUS MEDIA *Hao Yu* Operational Technologies Corporation, San Antonio, TX. *John G. Bruno* USAF/AL, Crew Systems Directorate at the Edgewood Research, Development, and Engineering Center, Aberdeen Proving Ground, MD.

Biotinylated biomaterials were reacted with streptavidin coated magnetic beads followed by exposure to a magnetic field to achieve rapid and specific separation even in complex media. Both nucleic acids and soluble proteins in solution may be separated by this technique. Many applications have been exploited for separating DNA, proteins and particles based on this principle. Small quantities of DNA and RNA can be amplified by the polymerase chain reaction (PCR) using biotin end labeled capture primers and ruthenium trisbipyridal Ru(bpy) end labeled reporter primers, which are incorporated in the specific ds-DNA. This enables direct capture, detection and quantitative determination of PCR product by use of magnetic separation and an electrochemiluminescence (ECL) assay. For determination of bacterial antigens (spores) in different types of media, a sandwich immunoassay was employed with biotinylated capture antibody and Ru(bpy) labeled reporter antibody. Antigen-antibody-magnetic bead complexes were separated from media, captured on an electrode overlying a magnet and analyzed by the ECL assay. ECL involves a redox reaction between Ru(bpy) and tripropylamine (TPA) in an electric field. This reaction results in photon emission at 620 nm when Ru(bpy) relaxes from an excited state. The number of emitted photons is directly proportional to the amount of Ru(bpy) labeled DNA or antibodies present. By using probe-based magnetic separation in conjunction with PCR and ECL techniques, DNA from the bacterum *Alteromonas JD6.5* and *HIV* were detected to 5 pg. Results were comparable with, but more sensitive than those obtained by gel electrophoresis. In sandwich immunomagnetic assays, *Bacillus anthracis* (nonpathogenic Sterne strain) spores were separated and detected as low as 100 spores by magnetic separation and ECL approaches, respectively. Immunomagnetic separation technique coupled with PCR and ECL technologies has shown great potential for separation, detection and quantitation of toxins, viruses, infectious bacteria, pesticides, drugs, explosive materials and other hapten-like agtigens in the food industry, clinical diagnostic and environmental monitoring arenas.

M-Pos460

DEVELOPMENT OF A TEMPERATURE SCANNING ULTRASONIC VELOCIMETER FOR STUDYING BIOPOLYMER TRANSITIONS
((A.P.Sarvazyan*, K.J.Breslauer, T.V.Chalikian and A.Fila)) Dept. of Chemistry, Rutgers Univ., New Brunswick, NJ, 08903. *Perm. address: Inst. of Theoretical and Exper. Biophys., Russian Acad. of Sciences, Pushchino, Russia.

Temperature induced conformational transitions in biopolymers are accompanied by significant changes in compressibility and, consequently, can be detected by speed of sound measurements. We will describe an experimental setup for acoustical studies of transitions in biopolymers and will provide some representative data from studies on proteins and nucleic acids. Differential ultrasonic resonator cells connected to a HP4195A network analyzer represent the essential components of the experimental setup. This arrangement allows one to measure with a very high precision the amplitude- and phase-frequency characteristics of a resonance peak formed by the standing acoustic wave in a liquid sample. The data from the network analyzer are transferred to an IBM PC compatible computer for analysis and processing. Two different types of ultrasonic resonators are used for the temperature scanning measurements: plain acoustical standing wave resonators operating in the frequency range from 4 to 90 MHz, with a chamber volume of 0.8 ml; and micro-volume cylindrical standing wave resonators with a chamber volume of 10 µl, with resonances in the range from 4 to 8 MHz. The temperature of the plain standing wave resonators is controlled by a Neslab Bath/Circulator, while the temperature of the micro-volume resonators is controlled by Peltier elements. The complementary features of acoustical versus calorimetric data for the study of thermally induced transitions in nucleic acids, lipids, and proteins will be discussed.

M-Pos461

DIASTOLIC MEMBRANE CURRENTS IN PURKINJE AND SINUS NODE MYOCYTES ((*M. Vassalle, H. Yu, Y. Liu, C. Tromba, and I.S. Cohen)) Dept. of Physiol. and Biophys. HSC, SUNY at Stony Brook NY 11794 and + HSC, SUNY at Brooklyn NY 11203.

We studied membrane currents at negative potentials (< -40 mV) in canine Purkinje and rabbit SA node myocytes. In both tissues, hyperpolarization resulted in a slow increase in net inward current, but with different properties.

In Purkinje myocytes held at -50 mV the threshold for this current was -62 mV (n=23) in 5.4 mM K-Tyrode. Its reversal potential was -84 mV (n=25). The slope conductance declined during this current relaxation. Reduction of $[K]_o$ to 2.7 mM shifted the apparent reversal with E_K. Increasing $[K]_o$ to 10.8 mM virtually eliminated this current. In the presence of 4 mM Ba no time dependent current was observed positive to about -88 mV (n=9). The current negative to -88 mV did not reverse at more negative potentials, increased in magnitude with increasing $[K]_o$, and the slope conductance increased during the current relaxation. Both the current observed in normal Tyrode (i_{sd}) and that in Ba-Tyrode (i_f) were blocked by 2 mM Cs.

In preliminary experiments in rabbit SA node myocytes held at -35 mV, a slow time dependent current was elicited at potentials as positive as -55 mV. This current did not reverse as negative as -105 mV and the slope conductance increased during the current relaxation (as expected for i_f). Both current and slope conductance increases were blocked by 2 mM Cs.

In summary, a slow time dependent decline of K conductance is present on step hyperpolarization to diastolic potentials in Purkinje myocytes, but appears absent in the SA node myocytes. I_f is present at more negative potentials in Purkinje myocytes.

Supported by NIH grants HL20558, HL28958, and HL27038.

M-Pos462

HYPERPOLARIZATION-ACTIVATED INWARD CURRENT IN CULTURED PACEMAKER CELLS FROM RABBIT S-A NODE. ((Z.W. Liu, A.R. Zou and R.D. Nathan)) Dept. of Physiology, Texas Tech University HSC, Lubbock, TX 79430.

The hyperpolarization-activated inward current (i_h, i_f) can be modulated by intracellular Ca^{2+} (*J. Physiol.* 409:121-141, 1989). In the present study, we utilized the perforated-patch technique to prevent alteration of $[Ca^{2+}]_i$ by the patch pipette. Pacemaker cells were studied after 1 - 3 days in culture. The pipette contained nystatin (300 μg/ml) in the following solution (mM): 55 KCl, 75 K_2SO_4, 7 $MgCl_2$, 10 glucose, and 10 HEPES. The Tyrode solution contained (mM): 130 NaCl, 5.4 KCl, 1.8 $CaCl_2$, 0.6 $MgCl_2$, 0.6 NaH_2PO_4, 16 $NaHCO_3$, and 5.5 dextrose. In some experiments, pipette K^+ was replaced by Cs^+, and 1 mM Ba^{2+}, 1 mM Ni^{2+}, 5 μM nifedipine, 4 mM 4-aminopyridine and 10 μM TTX were added to the Tyrode solution to block interfering currents. In this solution, the instantaneous I-V had a slope of 11.3 ± 1.2 nS (mean ± SEM, n = 10) and reversed direction at -24.9 ± 1.2 mV (n = 10). Inward current tails following 5-s voltage steps were fit by a Boltzmann equation with a half-activation potential and a slope factor, -83.0 ± 2.1 mV and 7.5 ± 0.4 mV, respectively (n = 17). Values obtained at more negative holding potentials and in *normal* Tyrode solution were not significantly different. At the end of 300-ms voltage steps, which better approximate diastole, i_h was negligible at -50 mV in 20/20 cells, but was measurable at -60 mV in 14/20 cells (-5 ± 1 pA) and at -70 mV in 19/20 cells (-36 ± 6 pA). At -70 mV, activation of i_h was fit by the sum of two exponentials having time constants, 0.57 ± 0.09 s and 2.85 ± 0.35 s (n = 19). The results suggest that, at potentials negative to -50 mV, i_h could contribute to the generation of diastolic depolarization. Supported by the Texas ARP (010674-039) and the NIH (HL 48836).

M-Pos463

SUPPRESSION AND INITIATION OF PACEMAKER ACTIVITY IN THE SINO-ATRIAL NODE PERFUSED IN HIGH $[K]_o$. ((E.M. Kim, Y. Choy and M. Vassalle)) SUNY, HSC at Brooklyn, NY 11203. (Spon. D. Erlij)

The hypothesis that the decay of I_K causes diastolic depolarization (DD) was tested in the intact SA node depolarized in high $[K]_o$ (8-12 mM) by using Cs (20 mM) which suppresses I_{Kdd} and I_f but not I_K. Also, the oscillations near the threshold for the action potential (AP) upstroke ("Th-V_{os}") in the initiation of spontaneous discharge were studied. As $[K]_o$ is progressively increased, subsidiary pacemaker cells depolarize, DD becomes shallow and U-shaped, and the APs become triangular. Eventually, the SA node stops, but, after driven APs, DD is still present and abruptly stops at a potential more negative than subsequently; when DD slowly decays, Th-V_{os} appear; if Th-V_{os} miss the threshold, they gradually decrease in size. Th-V_{os} may precede and follow slow spontaneous beats. In high $[K]_o$, Cs (20 mM) allows Th-V_{os} to attain the threshold and induces spontaneous activity; in spontaneous preparations, Cs accelerates the rate. Ni (40 μM) does not suppress the SA node discharge and actually may accelerate it; nifedipine (2 μM) and TTX stop spontaneous discharge. The action of nifedipine is counteracted to some extent by high $[Ca]_o$. In Tyrode solution, nifedipine slows, but does not stop the SA node. In zero $[Ca]_o$, there are no Th-V_{os}. The results suggest the possibility that DD is not caused by I_f either in subsidiary pacemakers (where DD is suppressed by high $[K]_o$) or in dominant pacemakers (where 20 mM Cs actually induces activity): in the latter, DD may be due to a decay of I_K (not blocked by Cs). Initiation of activity is due to increasing Th-V_{os}. I_{CaT} may not play a role in DD of dominant pacemaker cells, but the induction of quiescence by nifedipine and TTX suggests a role of both Ca and Na in excitation under these conditions. (Supported by NIH grant HL 27038).

M-Pos464

BLOCK OF K_{ATP} CHANNELS BY ACETATE IN VENTRICULAR MYOCYTES IS NOT SOLELY RELATED TO CHANGES IN INTRACELLULAR pH. ((R.G. WEBSTER, L.H. CLAPP, W.A. COETZEE)) Cardiovascular Research, UMDS, St Thomas' Hospital, London, SE1 7EH, UK.

Acetate has been shown to inhibit current through K_{ATP} channels in ventricular myocytes. The aim of this study was to examine whether this inhibition is related to changes in intracellular pH (pH_i). Guinea-pig ventricular myocytes were voltage-clamped (holding potential was -40mV), and pH_i measured using the fluorescent dye Carboxy-SNARF-1. DNP (100 μM) activated the K_{ATP} channel current from 0.73 ± 0.07 to 4.09 ± 0.52 nA (mean ± SEM, n=10) and caused a decrease in pH_i from 7.53 ± 0.05 to 7.15 ± 0.06 ($p<0.05$). Application of acetate (10 mM) inhibited the DNP-induced current by 49% to 1.99 ± 0.52 nA ($p<0.05$, n=10) and further acidified the cell to 6.87 ± 0.10 ($p<0.05$). The time to half maximal effect ($t_{1/2}$) for these decreases were 43.7 ± 6.6 and 10.3 ± 2.9 s, respectively ($p<0.05$). In the maintained presence of DNP and acetate, when extracellular pH was lowered from 7.4 to 6.6, the pH_i was further acidified in all 10 cells. However, the current was reactivated in only 7 of the 10 cells, with similar $t_{1/2}$ (24.7 ± 10.1 and 23.8 ± 9.7 s, respectively). This study shows that acetate causes changes in K_{ATP} channel current and pH_i that are temporally dissociated, suggesting the inhibitory role of acetate may not be solely related to changes in pH_i.

Supported by British Heart Foundation.

M-Pos465

THIOL-GROUP MODIFICATION OF OUTWARD PLATEAU CURRENTS IN RAT VENTRICULAR MYOCYTES. ((T.Y. Nakamura, M.J. Shattock and W.A. Coetzee)) Cardiovascular Research, Rayne Inst, London, SE1 7EH, UK

The transient outward current (I_{to}) determines the refractory period and hence the likelihood for arrhythmias during ischemia. Thiol (-SH) group modification occurs during ischemia; therefore, we investigated how the membrane impermeable SH-group modifying agent, p-chloromercuri-phenylsulphonic acid (pCMPS) affects I_{to}. Enzymatically isolated rat myocytes were voltage-clamped in the whole-cell configuration (20-22°C). I_{to} was elicited by 160 ms voltage steps (at 0.2 Hz) from a -80 mV to potentials between -30 and +60 mV. In time-matched controls, peak and steady-state currents were respectively 17.4±2.4 and 7.4±0.9 pA/pF (at +60 mV; n=3) after 10 min. Extracellular pCMPS (50 μM) increased the steady-state current in a time- and concentration dependent manner (from 6.7±2.3 to 9.3±1.0 pA/pF at +60mV over 10 min; n=12, $p<0.05$) whereas no change in peak current occurred (20.1±10.5 v.s. 21.0±6.2 pA/pF at +60mV over 10 min). This was reversible with DTT (3 mM). DTT alone did not influence peak- or steady-state currents. Intracellular dialysis with pCMPS also increased steady-state current (in a concentration dependent manner). Within ~1 min after break-in the steady-state current was 7.9±3.1 in control cells (+60 mV, n=3) and 9.1±1.8 pA/pF in cells dialysed with pCMPS (50 μM, n=6). Inactivation time-constants were increased by dialysis with pCMPS (34.6±4.6 ms in control, n=4; 44.5±8.4 ms with pCMPS, n=6; $p<0.05$) but not with pCMPS in the bath. In conclusion, thiol-group modification (as may occur in ischemia) affects outward plateau currents and may therefore contribute to changes in action potential, refractory period and arrhythmias.

M-Pos466

EFECTS OF DISOPYRAMIDE ON CARDIAC TRANSIENT OUTWARD CURRENT. OPEN CHANNEL BLOCK AND INACTIVATED CHANNEL UNBLOCK. ((J.Sánchez-Chapula and D.Snyders)). CUIB, Universidad de Colima, Apdo.Postal 199,28000,Colima, Col. México and Vanderbilt University, Nashville TN.

The effects of disopyramide (diso) on the transient outward current (I_{to1}) was studied in isolated rat ventricular myocytes using whole cell patch clamp techniques. Diso (10-1000 μM) reduced peak I_{to1} and accelerated the rate of apparent inactivation of the current. The latter suggested time-dependent open channel block. Recovery from inactivation at -80 mV was monoexponential in control (τ 33±7), but biexponential with diso (τ_1 35±13, τ_2 7157±1490, 100 μM) indicating slow recovery from block. Induction of block was assessed using a twin pulse protocol with steps +50 mV. As the duration of the conditioning pulse was increased from 1 to 50 ms, block increased as measured from the reduction of peak current during the fixed test pulse. Further prolongation resulted in relief of block, which was virtually complete with 1s conditioning pulse. Taken together, the results suggest that diso acts as a fast open channel blocker of rat I_{to1}, but competes with the inactivation process resulting in inactivated channel unblock, a mechanism supported by mathematical modelling of the drug-channel interaction.

M-Pos467

4-AMINOPYRIDINE ACTIVATES A POTASSIUM CURRENT BY ACTIVATION OF A MUSCARINIC RECEPTOR. ((R.Navarro-Polanco and J. Sánchez-Chapula)) CUIB. Universidad de Colima, Apdo. Postal 199, Colima, Col., México.(Spon. by M. Huerta)

4-aminopyridine (4-AP) is a known blocker of different potassium currents. In the present work, we found that 4-AP produced a shortening in action potential duration (APD) in cat atrial myocytes. Using the whole cell configuration of the patch clamp technique, we studied the effect of 4-AP (0.3 - 3 mM) on membrane currents of cat atrial myocytes. We found in atrial myocytes that 4-AP in addition to block the transient outward current present in these cells, induced a time- and voltage-dependent outward current. This current seems to be mainly carried by potassium. The time and voltage dependencies of this current were different from the delayed rectifier current present in these cells. This effect of 4-AP was blocked by the muscarinic antagonist atropine. In the continuous presence of atropina (100nM), 4-AP produced in atrial myocytes a lengthening of APD and a block of the transient outward and delayed rectifier currents. These results suggest that 4-AP can interact with colinergic receptors in cat atrial cells and induce a time- and voltage-dependent outward current.

M-Pos468

PROPRANOLOL BLOCKS THE RAPID COMPONENT OF THE DELAYED RECTIFIER (I_{Kr}) IN GUINEA PIG VENTRICULAR MYOCYTES. ((Neviana Nenova and Craig W. Clarkson)) Department of Pharmacology, Tulane University School of Medicine, New Orleans, LA

Propranolol, a class II antiarrhythmic agent, has been reported to cause prolongation of the QT interval in man (Milne et al. *Br Heart J*, 43:1-6, 1980). To investigate possible mechanisms for this effect we defined the effects of propranolol on the time-dependent potassium current (I_K) and inward rectifier (I_{K1}) in isolated guinea pig ventricular myocytes at 36°C using the whole-cell voltage clamp technique. I_K tail currents were evoked by hyperpolarization to -40 mV following a 1 sec depolarizing prepulse to a potential between -30 and +70 mV. The relationship between tail current amplitude and prepulse voltage could be well-fit by a Boltzmann relationship with a maximum asymptote achieved near +10 mV. Exposure to 3, 10 and 30 μM (DL) propranolol reduced the maximal tail current amplitude by 54±16% (n=5), 60±3% (n=6), and 81±4% (n=4), respectively. The estimated IC_{50} for block of tail current was 4.3 μM. Examination of the effect of propranolol on time-dependent I_K evoked during depolarizing pulses indicated that propranolol blocks a rapidly activating, inwardly rectifying current with characteristics identical to those defined for E-4031 sensitive I_K (I_{Kr}). In contrast to its inhibitory effects on I_{Kr}, 3, 10 and 30 μM propranolol produced no significant effect on steady-state I_{K1} defined using 1 sec pulses to potentials between -40 and -100 mV. These results indicate that high concentrations of propranolol may selectively block I_{Kr}.

M-Pos469

INHIBITORY EFFECT OF ω-3 FATTY ACIDS ON TRANSIENT OUTWARD K^+ CURRENT. ((K. Bogdanov, H. Spurgeon, A. Leaf, and E. Lakatta)) GRC, NIA, NIH, Baltimore, MD 21224, and Mass. Gen. Hospital, Boston, MA 02114 (Spon. by M.C. Capogrossi)

An infusion of ω-3 fatty acids (FA) can prevent ventricular fibrillation in dogs (PNAS, 91:4427,1994). To identify potential mechanisms of this antiarrhythmic action, we studied the effects of docosahexaenoic acid (DHA) on K^+ currents in rat and dog ventricular myocytes. While DHA (5-50 μM) has no effect on the inward or delayed rectifier currents, it accelerates the inactivation of the transient outward current (I_{to}) and decreases its amplitude (left, lower; 200 ms steps from -70 to 60 mV, rat cell). The same concentrations of arachidonic acid (AA), belonging to ω-6 class of FA, transiently (< 3 min) decrease I_{to} in about 20% of cells; however, the final action of AA in all cells was to increase I_{to}-(right, upper). Eicosatetraynoic acid, a nonmetabolized analog of AA, monotonically inhibits I_{to}. This suggests that the effect on I_{to} of AA and its metabolites may differ. Neither DHA nor AA changed I_{to} in the presence of 4-aminopyridine. Similar effects of DHA and AA were observed in dog cells. The blockade of I_{to} by DHA and augmentation of I_{to} by AA may underlie their effects on cardiac rhythm.

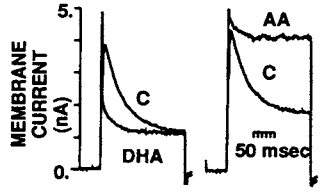

M-Pos470

EVIDENCE FOR DEVELOPMENTAL CHANGES IN THE TRANSIENT OUTWARD CURRENT IN HUMAN ATRIAL MYOCYTES ((William J. Crumb Jr., John D. Pigott, and Craig W. Clarkson)) Depts. of Pharmacology and Surgery, Tulane Univ. School of Medicine, New Orleans Louisiana

Previous studies indicate that there are significant age-related changes in the human atrial action potential, however the ionic basis for these changes remains poorly understood. In this study we used the whole-cell voltage clamp technique to define the properties of K currents at room temperature in atrial myocytes isolated from the hearts of 17 young (ages 1 day - 10 months) and 8 adult (11 - 68 years) patients. Application of depolarizing pulses positive to -20 mV typically induced a transient outward current (I_{to}) that rapidly decayed to a steady-state level of ~ half-peak amplitude during an 800 msec pulse. When comparing the currents in cells from young vs. adult hearts, we found evidence for marked age-related changes in the transient outward current including: **1)** the presence of I_{to} in only 67% of the cells isolated from young hearts versus 100% of the cells isolated from adult hearts, **2)** an almost 2 fold larger current density of I_{to} in adult (8.07 ± 0.54 pA/pF, n=14) vs. young cells (3.94 ± 0.35 pA/pF, n=9), and **3)** a two-fold slower kinetics of recovery from inactivation of I_{to} (V_{rec} = -40mV) in young (τ = 293.5 ± 39.9 ms, n=8) vs. adult myocytes (τ = 137.9 ± 11.9 ms, n=8). In contrast, there were no age-related changes found in the current density of either the steady-state current or I_{K1}. These results indicate that there are significant channel-specific changes which occur with age in the human atria.

M-Pos471

ALTERATIONS OF I_{to}, BUT NOT I_{Ks} AND I_{K1}, IN EPICARDIAL MYOCYTES FROM DOGS WITH INHERITED VENTRICULAR ECTOPY ((L.C. Freeman[1], L.M. Pacioretty[3], N.S. Moise[4], R.S. Kass[2], R.F. Gilmour Jr.[3])). Dept. of Anatomy & Physiology[1], Kansas State Univ., Manhattan KS 66506, Dept. of Physiology, Univ. of Rochester[2], Rochester, NY 14642, Depts. of Physiology[3] & Clinical Sciences[4], Cornell Univ., Ithaca NY 14853

We have established a colony of German shepherd dogs (*JACC* 1994;24:233) with inherited bradycardia-dependent ventricular ectopy. Because early after-depolarization-induced triggered activity is a likely mechanism for the ectopy, we determined if repolarizing K^+ currents are altered in these dogs. The inward rectifier I_{K1}, slow delayed rectifier I_{Ks}, and transient outward current I_{to} were recorded with whole cell patch clamp from epicardial myocytes obtained from animals that either did (+A) or did not (-A) exhibit ectopy. There were no significant differences between +A and -A in the density of I_{K1}, measured at -90 mV, $[K^+]_o$ = 4.0 mM (-8.4 + 0.7 pA/pF, n=43 vs. -9.2 + 1.3 pA/pF, n=16), or I_{Ks}, measured in the presence of 5 μM E4031, $[K^+]_o$ = 0 mM, as either time-dependent current after a 3 s test pulse to +60 mV, (0.9 + 0.2, n=26 vs 0.7 + 0.1 pA/pF, n=14) or tail current after return to -40 mV holding potential (0.4 + 0.1 vs 0.3 + 0.04 pA/pF). In contrast, peak I_{to}, measured at +40 mV, $[K^+]_o$ = 4.0 mM, was significantly reduced from 9.3 + 0.7 pA/pF (n=35) to 4.8 + 0.6 pA/pF (n=51) in -A vs +A. The τ for I_{to} decay was significantly greater in -A than in +A (32.7 + 1.3 vs 28.8 + 0.8), whereas the τ for recovery from inactivation were similar in both groups. Boltzmann analysis of the voltage-dependence of steady-state inactivation showed no differences in the slope factor, but a shift in $V_{1/2}$ from -36.1 mV in -A to -29.9 mV in +A (n=23 and 32). Reduction in I_{to} is consistent with development of arrhythmias related to action potential prolongation. Observed changes in τ inactivation and steady-state availability are not sufficient to explain a 50% reduction in peak current. The data suggest that a disease-related change in I_{to} expression may contribute to repolarization abnormalities and facilitate the development of arrhythmias in this model.

M-Pos472

THE CARDIAC L-TYPE CALCIUM CHANNEL IS MODULATED BY LEAD. ((J. Bernal, S. Ruvalcaba, J.-H. Lee and E. Perez-Reyes.)) Instituto. de Salud de Aguascalientes; Centro Biomédico, Univ. Aut. de Aguascalientes, Mex. and Physiology Dept. Loyola Univ. Medical Center, Maywood Il., USA.

OBJECTIVE: Evaluate the effects of lead (Pb^{2+}) and 2-3-Dimercapto-1-propanesulfonic acid (DMPS) on the ionic permeability of the cloned L-type cardiac calcium channels expressed in Xenopus laevis oocytes.

METHODS: The cRNA of the alpha-1 subunit of the cardiac L-type calcium channel was injected into Xenopus oocytes. For some experiments, a beta subunit (B2 or B4) was also co-injected. The inward currents from injected oocytes were elicited by depolarizing pulses when cells were clamped in the two microelectrode voltage clamp configuration using Ba^{2+} as a charge carrier. All other currents such as K^+, Cl^- or Na^+ currents were avoided. Compounds of interest were applied in the bath superfusion.

RESULTS: It was found that Pb^{2+} at concentrations in the range of 0.1-100 uM decreased the magnitude of the inward barium current through the calcium channels, in 28-95%. Such reduction was reversible at low Pb^{2+} concentrations. When cells were exposed to lead (at conc. of 1-100 uM), DMPS, a putative chelating agent for heavy metals, reverted the effects initially produced by lead.

M-Pos473

EXTRACELLULAR SITE OF ACTION OF PHENYLALKYLAMINES ON L-TYPE CALCIUM CURRENT IN RAT VENTRICULAR MYOCYTES.
((H. Nawrath and J.W. Wegener)) Department of Pharmacology, University of Mainz, D-55101 Mainz, Federal Republic of Germany.

The effects of the phenylalkylamines verapamil, gallopamil, and devapamil on L-type calcium currents (I_{Ca}) were studied in ventricular myocytes from rat hearts using the whole-cell patch-clamp technique. In particular, the question was addressed, whether the pharmacological binding sites for these drugs were located at the inner and/or at the outer surface of the cell membrane. Therefore, tertiary verapamil, gallopamil, and devapamil and their corresponding quaternary derivatives were applied either from the outside or the inside of the cell membrane. Extracellular application of verapamil, gallopamil and devapamil (each at 3 µmol/L) reduced I_{Ca} to 16.1 ± 8.6%, 11 ± 8.9%, and 9.3 ± 6% of control, respectively (means ± SD, n=3 each). Intracellular application of the same substances, via the patch pipette filled with 30 µmol/L of either verapamil, gallopamil, or devapamil, failed to depress I_{Ca}. The quaternary derivatives of the phenylalkylamines (30 µmol/L) were ineffective both when applied extracellularly or intracellularly. It is suggested that phenylalkylamines block I_{Ca} in their uncharged form by acting on a binding site of the calcium channel molecule located at the outer surface of the cell membrane.

M-Pos474

SERA FROM ANTI-Ro/La POSITIVE MOTHERS INHIBIT CARDIAC CALCIUM CURRENT.
((M. Boutjdir, B. Huang, Z.H. Zhang, C. Tseng*, N. El-Sherif, and J.P Buyon*)) Cardiology Division, SUNY, Health Science Center, VAMC at Brooklyn, N.Y, 11209 and *Hospital of Joint Diseases, NY, NY, 10003.

Maternal auto-antibodies to Ro and/or La are strongly associated with brady-arrhythmias in neonatal lupus syndrome; predominantly 3rd degree heart block (HB) but lesser degrees have been observed. It has been suggested that HB may be due to antibodies mediated reduction of L-type Ca current (I_{Ca}). We tested different sera from anti-Ro and/or anti-La positive mothers whose children have in-utero diagnosed HB, on whole-cell I_{Ca} using adult rat and guinea-pig ventricular myocytes. Serum from normal donors (with infant without HB) showed no effect on I_{Ca} at all voltages tested. Interestingly, serum from anti-Ro/anti-La negative mother whose infant yet had a HB, only slightly reduced I_{Ca} (9.8% at 0 mV). However, superfusion of cells with serum containing 0.5-1.0 mg/ml of anti-Ro & anti-La or anti-Ro alone reduced I_{Ca} in a reversible manner at all voltages. Sera containing both anti-Ro/anti-La had greater effect on I_{Ca} (58.9% inhibition) than anti-Ro (23.8%) or anti-La alone (15.9%).

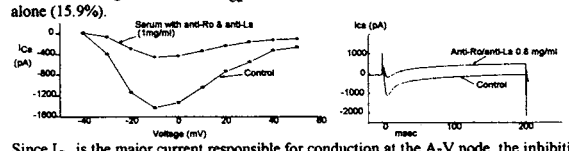

Since I_{Ca} is the major current responsible for conduction at the A-V node, the inhibition of I_{Ca} by serum containing both anti-Ro and anti-La antibodies may contribute to the pathogenesis of conduction abnormalities in neonatal Lupus. In addition, non-auto immune associated congenital HB may have another mechanism for conduction disturbances.

M-Pos475

L-TYPE CALCIUM CURRENT DENSITY IN DOCA-SALT HYPERTROPHIED RAT VENTRICULAR MYOCYTES.
((A. Momtaz, E. Coraboeuf, J.J. Mercadier and A. Coulombe)) Lab Cardio Molec & Cell, URA CNRS 1159, Hôpital M. Lannelongue, F-92350 Le Plessis Robinson, FRANCE.

Although in the DOCA-salt model of cardiac hypertrophy (Hyp), the increase in amplitude and duration of the rat ventricular action potential plateau can be largely attributed to a decrease of the Ca-independent transient outward current (*Pflügers Arch*, 1994, 427:47-55), the possible involvement of the voltage-gated L-type calcium (I_{CaL}) current remained to be assessed. Here we measured I_{CaL} in ventricular myocytes from both sham and left nephrectomized rats treated with deoxycorticosterone acetate (DOCA) + saline. The figure shows I/V-relationships for I_{CaL} in sham and Hyp both in control conditions (C) and in the presence of 10^{-6} M isoproterenol and $2x10^{-5}$ M forskolin (iso + forsk). In C, I_{CaL} (at 0 mV) was significantly larger in Hyp (-2.28 ± 0.61 nA, SD, n=20) than in sham (-1.38 ± 0.33 nA, n=23), whereas I_{CaL} density was not (-9.37 ± 2.52 *vs* -8.81 ± 2.12 pA/pF). In contrast in iso+forsk, I_{CaL} density was significantly lower in Hyp (-15.31 ± 2.71 pA/pF, n=5) than in sham (-21.24 ± 4.50, n=5) (P<0.05).

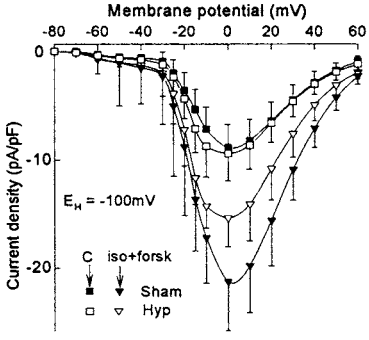

M-Pos476

FOUR MODES OF LATE NA CHANNEL CURRENT IN ISOLATED GUINEA-PIG VENTRICULAR MYOCYTES.
((Liu, Y-M., Li, C-Z., Wang, H-W., and Jin, Z-J.)) Department of Physiology, Shanghai Second Medical University, Shanghai 2000025, P.R.China (Spon. by Ira S. Cohen)

We employed the patch clamp technique to record single Na channel openings following 600 msec. step depolarizations from a hyperpolarized holding potential (-120 mV). Four modes of late Na channel currents were observed. They are: (1) isolated brief openings, (2) scattered openings, (3) long openings, and (4) bursts. Applications of 1 µM tetrodotoxin (TTX) eliminated all four modes of late openings, as well as the early openings which occur immediately upon depolarization. In mode 4, the bursts showed voltage dependent characteristics, and were terminated immediately upon repolarization. Bursts appeared about 1 in every 1000 depolarizations. The frequency of bursting could be increased by applying two or three smaller depolarizing steps instead of one large one. The burst frequency was about 1 in every 1000 depolarizations for each of the smaller individual steps, and the open time was longer. These results suggest that late openings of Na channels could contribute to sustaining the action potential plateau. Further, the openings might present an appropriate target for antiarrhythmic drugs.

Supported by National Scientific Grant #39270280, P.R.China

M-Pos477

AUTOCOID ROLE OF EXTRACELLULAR ATP ON THE DURATION OF THE ACTION POTENTIAL IN CULTURED RAT NEONATE VENTRICULAR MYOCYTES.
((Y.-F. Xiao and H. F. Cantiello)) Renal Unit, Mass. Gen. Hosp. East, and Dept. of Medicine, Harvard Med. Sch., Charlestown, Massachusetts.

Studies from our laboratory recently established that the cardiac isoform of the cystic fibrosis transmembrane conductance regulator (cCFTR) enables the cAMP-induced, electrodiffusional movement of ATP which may be thus responsible for the autocoid release of ATP and modulate ATP-sensitive (P_2) purinergic receptors in the heart. In the present study the effect of extracellular ATP was assessed on the action potential of cultured rat neonate ventricular myocytes. The average action potential duration (APD) at 75% repolarization in single myocytes was 323 ± 51 msec (n=10 cells) as assessed by the whole-cell current-clamp technique in the absence of intracellular ATP. Addition of 8-Br-cAMP (100 nM) caused a 17% increase of the APD (54 ± 20 msec, n=5). Stimulation of the cAMP pathway by either isoproterenol or forskolin, had a similar effect on APD. Addition of β-γ-methylene ATP (100 nM), a non-hydrolyzable ATP analog, in contrast, reduced APD by 63 ± 21 msec (n=4). The cAMP-dependent increase in APD was blocked by extracellular ATP (0.1-100 µM) in spontaneously beating cells. The same effect of both cAMP and ATP on APD was also observed in electrically-stimulated ventricular myocytes. In the presence of intracellular ATP (5 mM), addition of 8-Br-cAMP induced an oscillation in APD. Higher intracellular concentration of ATP (50 mM) induced spontaneous oscillation in APD. Both spontaneous and cAMP-induced oscillations in APD were blocked by addition of ATP (0.1 to 100 µM). The data are consistent with the hypothesis that the autocoid, and cCFTR-mediated, release of ATP from cardiac myocytes regulates APD and thus beating frequency, by a feed-back mechanism involving P_2 purinergic receptors in the heart.

M-Pos478

OVERDRIVE EXCITATION IN THE SINO-ATRIAL NODE IN THE PRESENCE OF HIGH $[K]_o$.
((Y. Choy, E.M. Kim and M. Vassalle)) SUNY, HSC at Brooklyn, NY 11203. (Spon. P. Gootman)

The aim was to study the characteristics and the mechanism of drive-induced spontaneous rhythm ("Overdrive excitation") in the SA node quiescent in high $[K]_o$ (8-14 mM). Overdrive excitation ("OVE") shows the following characteristics: it may be induced by drive in quiescent preparations; a shorter drive may induce only oscillations near the threshold (Th-V_{os}) for the upstroke of the action potential (AP); spontaneous beats may begin during a slow drive; after drive, Th-V_{os} initiate spontaneous APs, and also may follow them; the induced rhythm is fastest immediately after the drive; longer and faster drives induce longer and faster spontaneous rhythms; however, very long and fast drives may not excite; induced spontaneous APs are slow responses followed by diastolic depolarization (DD), but it is the Th-V_{os} (not DD) that excites; OVE may begin several seconds after the end of drive; when the induced rhythm subsides, Th-V_{os} miss the threshold and gradually decay; drive may temporarily accelerate a spontaneous SA node; OVE is not due to sympathetic nerve stimulation, since when the stimuli fail to induce APs there is no OVE. As for the mechanism, drive could induce a spontaneous rhythm because it increases $[Ca]_i$ and therefore DD size, bringing about Th-V_{os} and spontaneous activity. Thus, barium (0.05 mM) induces OVE through a decrease in resting potential and larger Th-V_{os}, high $[Ca]_o$ quickly induces spontaneous activity through Th-V_{os}; and low $[Ca]_o$ stops it. TTX also eliminates OVE, even in $[Ca]_o$ = 8.1 mM. Thus, the K-depolarized SA node is more dependent on Ca, possibly because I_{Na} is partially inactivated, but a Na component seems also important. In high $[K]_o$, OVE is induced through Th-V_{os} in the absence of Ca overload. (Supported by NIH grant HL 27038).

M-Pos479

MECHANOSENSITIVE FIBROBLASTS IN THE MAMMALIAN HEART: A POSSIBLE SUBSTRATE OF POSTISCHAEMIC ARRHYTHMIAS.
((Peter Kohl and Denis Noble)) University of Oxford, OX1 3PT, UK.

Fibroblasts in the amphibian and mammalian heart have been reported to be mechanosensitive. These fibroblasts react on stretch of the cardiac tissue with a reduction in membrane resistance and depolarization. Research on cell cultures of neonatal rat heart (*Wistar*) and on intact isolated rat hearts (*Rattus norwegicus*) confirmed that mechanosensitive fibroblasts may be coupled to adjacent cardiomyocytes both capacitively and electrotonically. Provided that the coupling conductance is sufficient, it is possible to record cardiomyocytelike potentials inside the fibroblast. The findings of these electrophysiological studies were implemented into the OXSOFT HEART V4.2 model of cardiac cells. In this study, possible consequences of such an electrical coupling on the activity of cardiomyocytes were examined. The computations proved that the electrical activity of cardiomyocytes is extremely stable under physiological circumstances. Under the conditions, however, of increased rates of connection to adjacent fibroblasts, plausible during excessive growth of fibroblasts, cardiomyocytes become progressively unstable with time, displaying a tendency to spontaneous late afterdepolarizations. The same can be observed under isolated sodium-overloading of cardiomyocytes. In both circumstances, a very short (0.075 s) diastolic depolarization of the fibroblasts, modelling diastolic stretch of the ventricular wall during atrial systole, is capable of triggering premature action potentials in the adjacent cardiomyocyte. The changes in cardiomyocyte parameters modelled may be observed in the ischaemic and postischaemic myocardium. We suppose that, under these circumstances, cardiac mechanosensitive fibroblasts may have an arrhythmogenic influence of on the heart.
Supported by the BHF and the Boehringer-Ingelheim Foundation.

M-Pos480

Two Populations of Myocytes Isolated From the Rabbit AV Node.
((A. A. Munk, J. Zhao, R. Adjemian and A. Shrier)) Department of Physiology, McGill University, Montreal, Quebec, Canada H3G 1Y6.

Single cells were enzymatically isolated from the atrioventicular node (AVN) of the rabbit. AVN cells were usually found to be either rod-shaped or ovoid. The ovoid cells were found to have smaller cell dimensions [21.6±0.8 um x 14.9 ± 0.6 um (n=41)] than the rod-shaped cells [65.6±4.2 um x 10.9±0.4 um (n=39)]. The ovoid cells were also found to have a significantly lower average membrane capacitance [29.0±1.6 pF (n=27)] than the rod-shaped AVN cells [40.7 ± 6.1 pF (n=8)]. Although the input impedence of the ovoid AVN cells [903±126 MΩ (n=27)] was found to be lower than that observed in rod-shaped AVN cells [1200 ± 227 MΩ (n=8)] this difference was not significant. Ovoid cells yielded action potentials reminiscent of N or NH-like cells and rod-shaped cells yielded action potentials resembling recordings from AN-like cells. When the quasi-steady state I-V relations were compared for the two cell types a significant difference was observed at potentials negative to -90 mV and greater than +20 mV. The two classes of AVN cells could also be distinguished by their different ionic-current profiles. In ovoid cells (n=80) I_{Na} was present in 30% of cells examined, I_{to} in 42%, both I_{Na} and I_{to} in 24%. I_f was found to activate at potentials positive to -100 mV in 95% of these cells. In rod-shaped cells (n=16) I_{Na} was present in all cells, I_{to} in 93%, both I_{Na} and I_{to} in 93%. I_f was observed in only 12% of these cells. $I_{Ca\text{-}L}$ was observed in all cells studied (n=96). Two classes of ovoid cells could also be distinguished due to the fact that in some ovoid cells I_f was found to activate at potentials between -50 mV and -70 mV from a holding potential of -50 mV, where as in others I_f activated at potentials negative to -70 mV.
Supported by HSF of Canada and MRC of Canada.

M-Pos481

A CHARACTERIZATION OF IONIC CURRENTS IN CULTURED HUMAN ATRIAL CELLS.
((J. Feng, G.R Li, B. Fermini, S. Nattel)), Montreal Heart Institute, Montreal, Quebec, HIT IC8. (Spon. by R. Lemieux)

The ability to culture cells allows for studies of gene expression and regulatory factors controlling ionic function. To assess the feasibility of culturing human cells and associated changes in ionic currents, cells isolated from atrial specimens obtained during bypass surgery were maintained in primary culture at 37°C in a humidified, 5% CO_2-enriched atmosphere. Within 24 hours, they assumed a spherical shape which they maintained for up to 7 days. The patch-clamp technique was used to study the current density (CD) of the ultra-rapid delayed rectifier (I_{Kur}), the transient outward current (I_{to}) and sodium current (I_{Na}) in fresh (FC) and cultured (CC) cells. Results: After 1 day of culture, cells rounded and capacitance decreased from 66±3 pF to 23± 2 pF ($p<.001$). The CD of I_{to} decreased from 10.9±0.7 (FC) to 5.9±0.9 pA/pF ($p<.01$) after 1 day of culture. In contrast, I_{Kur} CD increased from 5.1±0.4 to 15.2±0.8 pA/pF ($p<.001$) within 1 day. CD of I_{Na} was not changed in CC. Cell culture did not alter the kinetics or voltage dependence of I_{Na} or I_{Kur}, but slowed recovery and inactivation of I_{to} by about 2-fold ($p<.01$ for each), while shifting V½ of inactivation (-33±1 mV FC, -58±1 mV 1 day CC, $p<.01$). I_{Kur} sensitivity to 4AP remained constant over time (IC_{50} 46-50 μM FC and CC through day 5). All changes in CC occurred within 24 hr, and no changes in cell properties were observed between 1 and 5 days in culture. Conclusions: 1) Various ionic currents are well-maintained in cultured human atrial myocytes; 2) CD of I_{Kur} increases in culture, but 4AP sensitivity is constant; 3) CD of I_{to} decreases, along with a hyperpolarization of inactivation and slowing in recovery. Cultured myocytes may be very valuable for studies of the molecular biology, physiology, and pharmacology of ionic currents in human atrium.

M-Pos482

SINGLE OUTWARDLY-RECTIFYING CHLORIDE CHANNELS IN CELL-ATTACHED PATCHES FROM RABBIT ATRIAL MYOCYTES.
((D. Duan, S. Nattel)) Montreal Heart Institute, Montreal, Quebec, H1T 1C8.

While currents through single outwardly-rectifying chloride channels (ORCC) have been observed in cell-free patches from many tissues, it has been more difficult to record them in cell-attached mode. We previously reported the properties of ORCC in inside-out patches from rabbit atrial myocytes. The present experiments were designed to determine whether similar channels could be recorded in the cell-attached configuration, under basal conditions and in the presence of cell swelling. Cell-attached patches were obtained with pipettes (2-5 MΩ) containing (mM): N´-methyl-D-glucamine chloride (NMDGCl) or Tris 108, HEPES 5, glucose 5.5 (pH 7.4, adjusted to 290 mOsm/kg H_2O by adding mannitol). The hypotonic bath solution contained (mM): NaCl 100, $BaCl_2$ 2, $MgCl_2$ 0.8, $CaCl_2$ 1, $CdCl_2$ 0.2, 4-aminopyridine 2, TEA chloride 10, NaH_2PO_4 0.33, HEPES 10, glucose 5.5 (pH 7.4, 220 mOsm/kg H_2O). For isotonic bath solution the osmolarity was adjusted to 290 mOsm/kg H_2O with mannitol. Under isotonic conditions, single outwardly-rectifying channels were found in 10/198 (5%) patches. Currents reversed at 20±2 mV positive to resting potential (RP, estimated reversal potential -40 mV). Slope conductance averaged 46±0.4 pS from 20 to 140 mV positive to RP. Ensemble-average currents showed outward rectification and no time dependence. These properties were very similar to those of ORCC in inside-out patches. Under hypotonic conditions, cell swelling was seen, and single channels were observed in 32/178 (18%) patches. The kinetics and the form of the I-V relationship of single channel current during cell swelling were similar to those under isotonic conditions. Conclusion: In cell-attached mode, single channel currents similar to ORCC in isolated patches are present in rabbit atrium, and are seen more frequently during cell swelling. These observations support a possible physiologic role for ORCC in the heart.

M-Pos483

$MG^{2+}{}_i$ AND $CA^{2+}{}_i$ MODULATE DRUG BLOCK, BUT NOT RECTIFICATION, OF I_{Kr}.
((Tao Yang and Dan M. Roden)). Vanderbilt University, Nashville, TN

Magnesium and other divalent cations play an important role in determining the inward rectification of some K^+ channels. We have previously reported that the rapidly-activating cardiac delayed rectifier (I_{Kr}) is the only time-dependent outward current elicited from the holding potential of -40 mV in mouse atrial tumor (AT-1) cells. In this and other cardiac preparations, I_{Kr} displays prominent inward rectification and is blocked by antiarrhythmic drugs such as quinidine and dofetilide. In this study, we have further examined the effects of $Mg^{2+}{}_i$ and $Ca^{2+}{}_i$ on inward rectification and drug block of I_{Kr} in AT-1 cells, using whole-cell voltage clamp (22-23°C). Pipette free Mg^{2+} was varied from 0 to 1 mM, and pipette free Ca^{2+} was adjusted using the method of Fabiato and Fabiato. $Mg^{2+}{}_i$ and $Ca^{2+}{}_i$ did not affect I_{Kr} rectification (Figure). However, decreasing $Mg^{2+}{}_i$ or elevating $Ca^{2+}{}_i$ increased the drug concentrations required to block I_{Kr} tails by 50% after 1 sec steps to +20 mV (±SE, n=6-8 each):

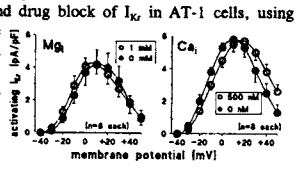

	$Mg^{2+}{}_i$=0 mM	$Mg^{2+}{}_i$=1 mM	$Ca^{2+}{}_i$=500 nM	$Ca^{2+}{}_i$=0 nM
Dofetilide	60±8 nM	12±2 nM	92±7 nM	13±2 nM
Quinidine	2.2±0.2 μM	0.9±0.2 μM	3.7±1.0 μM	1.4±0.1 μM

The finding that I_{Kr} inward rectification is unaffected by changes in $Mg^{2+}{}_i$ or $Ca^{2+}{}_i$ suggests that inward rectification is an intrinsic property of this channel protein. The modulating effects of $Mg^{2+}{}_i$ and $Ca^{2+}{}_i$ on drug block may help explain variability in the clinical actions of these drugs, particularly in the presence of cardiac diseases.

M-Pos484

TTX-SENSITIVE INWARD NA CURRENT IN SINOATRIAL NODE CELLS ISOLATED FROM NEWBORN RABBIT.
((M. Baruscotti, D. DiFrancesco and R.B. Robinson)) Columbia Univ., New York, NY and University of Milan.

The action potential in the adult rabbit sinoatrial node (SAN) has a slow upstroke that is predominantly Ca-dependent and is relatively insensitive to the Na-channel blocker tetrodotoxin (TTX). We asked whether cells isolated from SAN of newborn (2-9 days) rabbits would show similar characteristics. Single cells were prepared by standard enzymatic digestion and studied at room temperature using whole cell patch clamp in a HEPES buffered Ca-free solution containing 50 mM Na (to reduce current magnitude). All cells studied were spontaneously beating in external solution containing physiologic levels of Na and Ca. Initial studies on adult SAN cells confirmed the relative absence of a Na-dependent rapid inward current. Stepping from -80 mV to 0 mV in 7 cells which all exhibited the pacemaker current i_f, only one cell exhibited any significant inward current. In contrast, of 16 i_f-containing cells from newborn SAN, all showed a measurable rapid inward current (peak density in 13 of these cells which were stepped to 0 mV was 96±21 pA/pF). In 7 of these cells, 3 μM TTX was tested and achieved at least 90% block in each case. Three cells also were tested with 2 mM Mn, which achieved less than 5% block in all cells. The voltage dependence of inactivation was determined in 5 cells, and the mean value for the midpoint of the h_∞ curve was -64.4 mV. In addition, 3 μM TTX was able to slow spontaneous rate by 85±8% in 3 spontaneously beating isolated cells studied in current clamp mode. Thus, a TTX-sensitive current may contribute significantly to the action potential in the young SAN, and this influence is reduced with development.

M-Pos485

CHARACTERIZATION OF AZIMILIDE EFFECTS ON ION CURRENTS OF THE REPOLARIZATION PHASE. ((Zhi-Hao Zhang, Mohamed Boutjdir, Robert Brooks*, Long Chen and Nabil El-Sherif)) Cardiology Division, SUNY, Health Science Center, VAMC at Brooklyn, N.Y, 11209 and *Procter & Gamble Pharmaceuticals, Norwich, NY, 13815. (Spon. by M. Boutjdir).

Azimilide (AZ) is a new class III antiarrhythmic agent reported to preferentially block the slow component of the delayed rectifier K current (I_{KS}). Whole-cell patch clamp technique was used to systematically study the effect of AZ on I_{KS} and I_{Kr} (fast component of I_K) in guinea pig ventricular myocytes and L-type Ca (I_{Ca}), fast and slow transient outward K (I_{to} and I_{toS}), and inward rectifier K currents (I_{K1}), in rat ventricular cells. The results show that AZ (100μM) slightly reduced peak I_{to} (n=10) and I_{toS} (n=5) at 40mV and had no significant effect on I_{K1} at voltages from -110 to 0mV (n=5). However, AZ blocked the peak of I_{Ca} at voltages from -30 to 50mV without significantly changing the steady state inactivation of I_{Ca} (n=5). Dose-response curve of AZ concentrations from 1 to 100μM on I_{Ca} resulted in an EC_{50} of 43.6μM. AZ effect on I_{Ca} was partially reversed upon washout. AZ (0.025 to 10μM) inhibited I_{Kr} (induced by 250ms-pulse, EC_{50}= 0.38μM) and I_{KS} (induced by 3s-pulse, EC_{50}=0.97μM). AZ 1μM reduced I_{Kr} tail by 65.9±6.4% (n=5) and I_{KS} tail by 42.8±6.2% (n=6) at 40mV and dramatically scaled down the current density-voltage relation of I_{Kr} and I_{KS}. AZ had no effect on the steady state activation of I_{Kr} and I_{KS}. The degree of AZ inhibition of each current is listed below:

Channels	I_{to}	I_{toS}	I_{Ca}	I_{KS}	I_{Kr}	I_{K1}
EC_{50} (μM)	>100	>100	43.6	1.0	0.4	>>100
Degree of Inhibition	↓	↓	↓↓	↓↓↓	↓↓↓↓	=

Conclusions: AZ prolongation of QT-interval and action potential duration is due to the block of both I_{KS} and I_{Kr} but not I_{to}. AZ block of I_{Ca} in addition to I_K could reduce the occurrence of Ca-induced EAD_S and EAD-dependent *torsade de pointes*.

M-Pos486

EFFECTS OF INTRACELLULAR ACIDOSIS ON Na^+ BACKGROUND CURRENT. ((S.R. Park, J.H. Shin, E.K. Kim, E.J. Park and C.K. Suh)) Department of Physiology, Inha University College of Medicine, Inchon KOREA 402-751.

Reperfusion injury describes the impairment of contraction observed in myocardium that has been reperfused after brief periods of ischemia via cardioplegia or local ischemic injury. One of the hypotheses explaining the cause of reperfusion injury is calcium paradox. The mechanism of calcium paradox might involve a rapid influx of Ca^{2+} by Na^+-Ca^{2+} exchange during the reperfusion. By that reason the accumulation of Na^+ in myocytes during ischemic cardiac arrest is postulated to be one of the main causes of calcium paradox. The factors of increasing intracellular Na^+ activity include Na^+ current, Na^+-H^+ exchange current, Na^+-Ca^{2+} exchange and Na^+ leak current. In this study, we measured Na^+ background current in guinea pig ventricular myocytes with whole cell clamp method and studied the effects of intracellular acidosis on this Na^+ background current with following results. 1) TTX didn't affect Na^+ background current. 2) 2 μM O-(N,N-hexamethylene)-amiloride (HMA) decreased Na^+ background current at negative membrane potential. 3) The addition of Cl^- channel blocker (DNDS) did not affect the Na^+ background current. 4) The intracellular acidification by HMA and nigericin reduced both the inward and outward components of the current, but the reversal potential did not change. These results suggest that the Na^+ background current play a role in increasing the intracellular Na^+ activity during cardioplegia and intracellular acidosis decrease the Na^+ background current during sustained depolarization.

M-Pos487

SCALING AND ORDERING OF NEONATAL HEART RATE VARIABILITY. ((Ali A. Aghili, Rizwan-uddin, M. Pamela Griffin, J. Randall Moorman)) Schools of Medicine and Engineering, University of Virginia, Charlottesville, VA 22908.

Heart rate variability (HRV) is reduced during acute and chronic illness. One way of understanding the mechanism of this change is to study the *interbeat increments (ibi)*, the difference from one RR interval to the next. Two possible explanations for reduced HRV are (1) the *ibi* are smaller, or (2) the *ibi* are the same, but are ordered differently (Peng *et al.*, Phys. Rev. Lett., 70:1343). We have analyzed the increase in neonatal HRV that accompanies recovery from severe illness in a large clinical data set from nine newborn infants during episodes of severe cardiorespiratory failure and from the same infants 5 to15 days later, after they had recovered. The data were low-pass filtered (0.005 Hz) before *ibi* were calculated. We found that the mean *ibi* rose about 2.5 to 3-fold after recovery from illness, suggesting that scaling accounted for some or all of the rise in HRV. To assess order of the filtered RR signal $B_L(n)$, we used a mean fluctuation function $F(n)= \langle |B_L(n'+n) - B_L(n')| \rangle$. We found the slope of the log-log plot of F(n) to be about 0.5 for both ill and recovered data. Runs counting of the *ibi*, another measure of order, was also similar for both data sets. In contrast, another measure of order, the slope β of a log-log plot of the power spectrum of the *ibi* was 0.55 during illness and 1 after recovery. Using numerical simulations of random and deterministic data, we found that this change in β could be explained by a 10% change in *ibi* order. We conclude that the HRV of sick and recovered newborn infants, in contrast to HRV of adults with and without heart disease (Peng *et al.*), differs much more in the amplitude of the interbeat increments and much less in their ordering.

M-Pos488

EFFECT OF ANTIARRHYTHMIC DRUGS ON REENTRANT ARRHYTHMIAS MODEL STUDY. ((Teresa Ree Chay)) University of Pittsburgh, Pittsburgh Pennsylvania 15260.

We have studied the effect of channel blockers on cardiac reentrant rhythms by means of a bifurcation analysis approach as well as a simulation approach. The model we used for this study is a cardiac cell model of ventricular myocardium arranged in a ring. The channel blockers are modelled by varying the maximal conductances of sodium, calcium, and delayed rectifying potassium channels. Antiarrhythmic action is measured by four means: (i) an increase in the critical wave length (CWL), (ii) a decrease in the cycle length (CL), (iii) an increase in the action potential duration (APD), and (iv) the narrowing of the vulnerable window width (WW). Our two-parameter bifurcation analysis revealed the following interesting results: (i) Both sodium and calcium channel blockers decrease the CWL, the former much more effectively than the latter. The potassium channel blockers, on the other hand, increase this length considerably. (ii) As to the APD, both sodium and potassium channel blockers increase APD, but the former only slightly and the latter significantly. The calcium channel blockers on the other hand decrease APD drastically. (iii) As to the CL, both sodium and calcium channels increase CL, whereas the opposite effect was found for the potassium channel blockers. Our numerical experiments reveal that (i) the sodium channel blockers can increase WW, (ii) the calcium channel blockers have little effect on WW, and (iii) the potassium channel blockers can decrease WW. Our results thus explain why those drugs that block the sodium channels have the greatest proarrhythmic effect (i) by slowing the conduction much more than lengthening the APD and (ii) by shortening the CWL. Our result also explains why the potassium channel drugs are most effective in controlling reentry in the ventricular tissues, i.e., they can shorten the WW and lengthen both APD and CWL without altering the conduction velocity.

M-Pos489

Azimilide Dihydrochloride (NE-10064) Prolongs the QTc Interval in Rabbits, a Species Lacking Ventricular Slow K+ Current (I_{Ks})
Anne P. Drexler, Anne E. Maynard, Robert R. Brooks, Carlos Oliva and David R. Kostreva, Procter & Gamble Pharmaceuticals, Norwich, NY

Azimilide dihydrochloride (NE-10064), a new class III antiarrhythmic that protects against ventricular tachycardia and sudden death, has been reported to block both the rapid (I_{Kr}) and slow (I_{Ks}) repolarizing currents in guinea pig myocytes, a species in which "isolation" of I_{Kr} from I_{Ks} is difficult. To clarify azimilide's mechanism profile, we examined it's effects in rabbits, a species known to possess only I_{Kr} as a repolarizing current in the ventricle. Rabbits were anesthetized with alpha-chloralose and ventilated. Arterial blood gases were maintained within physiological limits. Arterial blood pressure was monitored along with a lead II electrocardiogram. QTc interval, which increased maximally to as much as 66% over baseline during infusion of azimilide, was measured 20 minutes after initiation of dosing. Cumulative iv doses of 3, 5.2, 6, and 10 mg/kg of azimilide increased the QTc interval 10 ± 3 (n=3), 20 ± 3 (n=5), 21 ± 3 (n=2), and 32 ± 4 (n=4) percent from baseline, respectively. The dose required to produce a 20% increase in QTc interval was 5.2 mg/kg. Blood pressure was not altered significantly with azimilide. These results indicate that the observed class III action of azimilide in the rabbit may be due to the blockade of I_{Kr} channels.

M-Pos490

BIDISOMIDE PROLONGS ACTION POTENTIAL DURATION IN ISOLATED CANINE ATRIA IN THE PRESENCE OF ISOPROTERENOL AT HIGH STIMULATION FREQUENCIES ((Cynthia L. Martin[1], Maria Palomo[2], Kevin Chinn[1], Ellen McMahon[2])) Searle, [1]Skokie, IL 60077 and [2]St Louis, MO 63167

Bidisomide, a new antiarrhythmic agent in Phase III clinical trials, has been shown to prolong canine atrial effective refractory period (ERP) in vivo and action potential duration (APD) and ERP in isolated canine atria. In order to estimate the effectiveness of bidisomide with elevated sympathetic tone, action potentials were recorded in the presence of the ß-adrenergic agonist isoproterenol (iso) before or after equilibration with bidisomide. Intracellular action potentials were recorded from isolated canine atria at stimulation frequencies of 1-5 Hz. Addition of 1 μM iso caused a 12-28 ms shortening of APD, while 100 nM iso did not affect APD. Bidisomide (30 μM) in the continued presence of 1 μM iso reversed the shortening of APD, while in the presence of 100 nM iso the prolongation was frequency dependent (3 ms at 1 Hz, 19 ms at 5 Hz). In the converse experiment, tissues were equilibrated with 30 μM bidisomide and then challenged with 1 μM or 100 nM iso in the continued presence of bidisomide. Bidisomide increased APD and ERP 20-25 ms. Addition of iso decreased APD and ERP at 1 and 2 Hz, but not at 3.3 or 5 Hz. Bidisomide did not exhibit any functional ß-blocking activity in an assay of isoproterenol-induced positive chronotropy in isolated guinea pig atrium. These data support bidisomide's unique and desirable antiarrhythmic profile in which prolongation of APD and ERP is maintained at high stimulation frequencies and in the presence of ß-adrenergic stimulation.

M-Pos491

IS THE CARDIAC SIGMA-BINDING SITE A POTASSIUM CHANNEL ?
((J. Hinson, C. Liu and P. Cervoni)) Medical Research Division, American Cyanamid Company, Pearl River, NY 10965

Sigma receptor ligands have been reported to modify K channels in the brain. (Neuropharmacol.28(1989)661). Recent evidence suggests that the heart also contains sigma binding sites with characteristics of the sigma-2 receptor subtype. (Eur.J. Pharmacol. 209(1991)245). Because Class III anti-arrhythmic drugs have been shown to interact with sigma-2 binding sites in the brain (Eur. J. Pharmacol,241 (1993) 111), we investigated the possibility that sigma ligands can block cardiac K currents and alter the action potential waveform. Cardiac transmembrane action potentials were recorded from guinea-pig papillary muscles. Whole cell recordings were performed on enzymatically-dissociated guinea-pig ventricular myocytes. At 10uM, R(+)-3-(hydroxyphenyl)-N-propylpiperidine (PPP) prolonged the action potential duration (APD90) by 18%. A similar result was obtained with haloperidol which prolonged APD90 by 16%. To obtain some structure-activity information, the effects of the metabolites of haloperidol were evaluated. Only 'reduced haloperidol' (Metabolite II) prolonged APD90 (23%). R(-)-N-(3-Phenyl-1-propyl)-1-phenyl-2-aminopropane hydrochloride (PPAP), a potent and selective sigma ligand with little affinity for PCP or dopaminergic sites caused a marked prolongation of the terminal phase of the AP waveform (30%). By contrast, sigma-1 ligands mostly shortened APD90: (+)Pentazocine (-16%), Carbetapentane (-16.7%), (+)SKF-10047 (no effect). Surprisingly, 1,3-di(2-tolyl)-guanidine(DTG) which is more selective for sigma-2 than sigma-1, shortened the APD90 (15%). Using the whole-cell patch clamp technique, we found that PPAP, PPP, and Haloperidol block IK1 currents, although PPP also blocked IK. These preliminary findings seem to suggest that sigma ligands are able to alter the cardiac action potential by modulating cardiac ion channels. It remains to be firmly established the structural relationship between the sigma binding sites and the cardiac calcium and potassium channels.

M-Pos492

MODULATION OF I_{CA} BY INTRACELLULAR SODIUM IN GUINEA-PIG VENTRICULAR MYOCYTES. ((M.J. Main and M.B. Cannell)) Department of Pharmacology and Clinical Pharmacology, St. George's Hospital Medical School, London SW17 0RE, England.

It has been reported that substitution of extracellular Na^+ by impermeant cations such as TEA^+ increases the amplitude of the cardiac calcium current (I_{Ca}) (Balke & Wier, 1992). This effect is thought to be secondary to a decrease in intracellular sodium concentration ($[Na^+]_i$), however, the range of $[Na^+]_i$ over which modulation of I_{Ca} takes place is unclear. We have manipulated $[Na^+]_i$ by blocking the Na-pump and using the Na ionophore monensin, in order to examine the relationship between $[Na]_i$ and I_{Ca}.
Isolated myocytes were voltage clamped using patch electrodes containing an NMG - based, Na^+-free pipette solution. Effects of Ca^{2+} on I_{Ca} were eliminated by including 10mM EGTA in the pipette solution and by equimolar substitution of extracellular Ca^{2+} by Ba^{2+}. For experiments involving modulation of Na-pump activity, 5.4mM RbCl replaced KCl in the otherwise standard extracellular recording solution. Barium currents through the calcium channel ($I_{(CaBa)}$) were activated at 10s intervals by applying depolarising voltage ramps from a holding potential of -40mV. Inhibition of the Na-pump, by removal of extracellular Rb^+, led to a rapid reduction (72 +/- 6%, n=4) in $I_{Ca(Ba)}$ amplitude which was fully reversible. As no Na^+ was added to the pipette it seems likely that modulation of I_{Ca} occurs over a low range of $[Na]_i$. This hypothesis was examined in a second series of experiments using the Na^+ ionophore monensin. Increasing extracellular $[Na^+]$ from zero to 4mM in the presence of 50μM monensin led to a decrease in $I_{Ca(Ba)}$ which was similar to that seen during sodium pump block. These data suggest that, under our experimental conditions, very small increases in $[Na^+]_i$ can produce profound effects on calcium channel conductance.

Balke, C.W. & Wier, W.G. (1992). *Proc. Natl. Acad. Sci. USA* **89**, 4417-4421.

M-Pos493

EFFECTS OF CHOLINERGIC AND ADRENERGIC AGONISTS ON INTERNAL RESISTANCE OF SHEEP PURKINJE FIBERS.
((P. Daleau & J. Délèze)) Quebec Heart Institute, Laval Hospital, G1V 4G5; Dept. Pharmacology, Fac. Medicine, Laval University, Ste-Foy, PQ, Canada and Dept. Physiologie Cellulaire, Université de Poitiers, 86022, France.

The presence of low resistance pathways between cardiac cells is an important determinant of action potential propagation and may form the basis for the synchronization of pacemaker activity in the whole sinus node. Although α- and β-adrenoceptors and muscarinic receptors are present throughout the heart, there is still little information available concerning the direct action of cholinergic and adrenergic systems on cardiac cell coupling. The purpose of this study was to determine whether cholinergic and adrenergic agonists modulate internal resistance (r_i) of cardiac fibers. Changes in r_i of cardiac Purkinje fibers were determined using subthreshold current clamp pulses to the side compartments of a single mannitol gap (Circ. 86(4):I-753, 1992). A 20% reduction (n=4) in the initial gap resistance was observed within one minute after application of carbamyl β-methyl choline 10^{-5}M in the central compartment. This reduction of r_i tapered off within 5 min although an acetylcholine esterase inhibitor, eserine 3.5×10^{-6}M, was present. On the other hand, application of norepinephrine 5×10^{-6} (n=4) but not 2×10^{-7}M increased r_i 45$\pm$6% (mean$\pm$SD) in 30 min. This effect could not be reproduced in the presence of the β-agonist isoproterenol 10^{-5}M suggesting that α-adrenoceptors were involved in drug action. Thus, these experiments show that sympathetic and parasympathetic systems may alter cardiac electrical conduction and pacemaker activity by modulating cell-to-cell coupling.

M-Pos494

AFTERCONTRACTIONS AND ABNORMAL MEMBRANE POTENTIALS INDUCED BY β-ADRENOCEPTOR STIMULATION IN HUMAN AND GUINEA-PIG CARDIOMYOCYTES. ((D. Tweedie, P.O'Gara, K.T. MacLeod, and S.E. Harding)) Dept. Cardiac Medicine, National Heart & Lung Institute, Dovehouse Street, London SW3 6LY, UK.

β-adrenoceptor stimulation has been shown to produce aftercontractions (ACs) in cardiac myocytes. We used enzymatically isolated cardiac myocytes from guinea-pig or failing human ventricle to examine the effects of isoprenaline on contraction and membrane potential. In both human (0.2Hz) and guinea-pig (0.5Hz) myocytes, exposure to isoprenaline (1-3nM) caused the formation of ACs. These tended to occur during a prolonged action potential in human and either during (4/12 events) or after (8/12 events) the action potential in guinea-pig. When not occurring within the action potential, the ACs were associated with small changes in membrane potential, (from -95.3$\pm$1.0 mV to -90.3$\pm$2.0 mV, 6 cells, P=0.039, mean $\pm$ S.E.M) and the time-to-peak voltage change was 311$\pm$50 ms (6 cells). Changes in membrane potential preceded changes in cell length by 74$\pm$26 ms (6 cells, P=0.030). The effect of isoprenaline was mimicked by forskolin, and the cAMP analogues dibutyryl cAMP and CPT-cAMP, suggesting a cAMP-dependent mechanism. Lemakalim (10-50μM) abolished or reduced cAMP-dependent ACs in both human (n=5) and guinea-pig (n=11) myocytes, while reducing action potential duration. We conclude that cAMP-dependent ACs are more likely to cause, rather than result from, spontaneous membrane depolarisations, but can be modified by manipulation of action potential duration.

M-Pos495

THE EFFECT OF RYANODINE ON CARDIAC CALCIUM CURRENT AND CALCIUM CHANNEL GATING CURRENT. ((A. LACAMPAGNE[1], C. CAPUTO[2] and J. ARGIBAY[1])) [1]*Laboratoire des Cellules Cardiaques et vasculaires, CNRS EP021, Faculté des Sciences, 37200 Tours, FRANCE,* [2]*Centro de Biophysica y Biochemica, IVIC, Caracas 1020A, VENEZUELA.*

In cardiac muscle, no mechanical interaction between DHPreceptor (DHPr) and Ryanodine receptor (RYr) is expected to occur. This determines the difference in E-C coupling between the two type of muscle. Recently, it has been shown that in skeletal muscle 100 µM Ryanodine, blocks the repriming of intramembrane charge movement (ICM), following a prolonged depolarization state (Gonzales A. and Caputo C. 1994, Biophys. J., 66, A86). We decided then to test 100 µM Ryanodine (5 min application) on isolated guinea-pig cardiac cells.
At this concentration, Ryanodine slowed down the inactivation time course of I_{CaL}, as already described by others and explained by the lack of calcium release by the sarcoplasmic reticulum. Furthermore, Ryanodine induced a 10 mV hyperpolarizing shift in the voltage dependent properties of I_{CaL}. ICM associated with calcium channels were measured after inactivation of sodium channels using a 100 ms prepulse at -50 mV. In those conditions, Ryanodine slightly decreased ICM by about 10 % and induced a small shift, about 5 mV towards the negative potentials, as observed on I_{Ca} experiments. The steady-state repriming of gating current was measured by a test depolarization for at least 30 sec after a 2 min prepulse at 0 mV. We found that Ryanodine did not interfere with the repriming of ICM in cardiocytes. This is the most important result since it excludes the possibility that in skeletal muscle, the inhibition of the repriming was due to a direct effect of Ryanodine on DHPr. These results and those obtained on skeletal muscle provide, by in vivo experiments, further evidence of the postulated differences between the architecture of the E-C coupling system in both tissues. Finally it confirms the hypothesis that there is a retrograde interaction between the RYr and the voltage sensor (DHPr) in skeletal muscle.

M-Pos496

Degradation of Troponin I in Ischemic/Reperfused Myocardium: Molecular Basis of Myocardial Stunning? ((Wei Dong Gao, Dan Atar, Yongge Liu, Anne M. Murphy and Eduardo Marban)) Department of Medicine, The Johns Hopkins University, Baltimore, MD 21205

Recent studies have shown that myocardial stunning reflects decreased Ca^{2+} responsiveness of the myofilaments. Here, we studied whether the decreased Ca^{2+} responsiveness is due to cytosolic factors or to changes in the myofilaments themselves. Isolated rat hearts were retrogradely perfused at 37 °C for either 50 min. (control), or for 10 min. followed by 20 min. of global ischemia and 20 min. reperfusion (stunned). $[Mg^{2+}]_i$, measured in trabeculae from the right ventricles using Mg-fura-2 salt, did not change (control: 0.95±0.29 mM vs stunned: 0.90±0.20 mM, p>0.05). Maximal Ca^{2+}-activated force (F_{max}) was compared before and after skinning in the same rat trabeculae at the same diastolic sarcomere length (2.2-2.3 µm). $[Ca^{2+}]_i$ was determined using fura-2 salt and steady-state activation was achieved by stimulating the muscle at 10 Hz after 10-20 min application of ryanodine (5 µM). The muscles were then skinned with Triton X 100 (1%) for 15-25 min and subsequently activated with solutions containing 25 µM $[Ca^{2+}]$. F_{max} was the same before and after skinning in each muscle, despite a significant decrease of F_{max} in stunned trabeculae. In separate experiments, control and stunned hearts were freeze-clamped, homogenized, and processed for Western blotting. Troponin I immunoblots revealed a band at ~31 kD in both samples and an additional band (~26kD) only in the stunned sample. Western blots for other contractile proteins showed no differences in the expression pattern. These results suggest that contractile dysfunction in stunning may be related to degradation of troponin I.

M-Pos497

A_1 ADENOSINE RECEPTORS MEDIATE PROTECTIVE EFFECTS OF ADENOSINE DURING ISCHEMIA AND REPERFUSION IN VENTRICULAR MYOCYTES.

((J.M. Cordeiro, G.R. Ferrier and S.E. Howlett)) Dept. of Pharmacology, Dalhousie University, Halifax, Canada. (Spon. by M.E.M. Kelly)

The effects of adenosine (ADN) and selective and non-selective ADN antagonists on cardiac electrical and contractile activity were determined during ischemia and reperfusion in guinea pig myocytes. Electrical activity was recorded with conventional and voltage clamp techniques at 37°C. Contractions were monitored with a video edge detector. Myocytes were exposed to simulated ischemia for 20 min in the presence of ADN (50μM), and were reperfused with normal Tyrode's solution. ADN had no electrical or contractile effects under control conditions. However, action potential abbreviation during ischemia was greater in the presence of ADN, and recovery was delayed. In ischemia, contractions were abolished and I_{Ca} declined equally in the absence and presence of ADN. ADN pretreatment abolished contractile overshoot and reduced the incidence of the arrhythmogenic transient inward current from 78% to 37.5%. Both the non-selective adenosine receptor antagonist 8-phenyltheophylline (8-PT, 10μM) and the A_1 selective antagonist cyclopentyltheophylline (CPT, 5μM) reversed the effects of ADN on electrical and mechanical activity. Thus, exogenous ADN in ischemia altered recovery of electrical and mechanical activity and attenuated signs of Ca^{2+} overload upon reperfusion. These effects were reversed by both 8-PT and CPT which suggests that the protective effects of ADN are mediated by A_1 receptors.

M-Pos498

A MODEL OF THE METABOLIC OSCILLATOR DRIVING OSCILLATIONS IN $I_{K,ATP}$ AND E-C COUPLING IN VENTRICULAR MYOCYTES

((B. O'Rourke, D. Romashko, B. Ramza, E. Marban)) Johns Hopkins University, Baltimore, MD 21205

We have recently described a metabolic oscillator induced by substrate deprivation in guinea-pig cardiomyocytes (Science 265:962,1994). Oscillations in metabolism, measurable as cyclical changes in the NAD redox state, induce oscillations in ATP-sensitive K^+ currents ($I_{K,ATP}$) and in the amplitude Ca^{2+} transients. Based on these findings, we have developed a model to describe the mechanism of oscillation. The model consists of five differential equations describing the rates of change of glucose (GLC), fructose 1,6-diphosphate (FDP), glyceraldehyde 3-phosphate (GAP), ADP, and NAD^+. Glycolytic reactions from glucose inflow to pyruvate outflow (V_{in},V_1,V_2,V_3) take place in the cytosolic compartment. Pyruvate oxidation occurs in the mitochondria and drives mitochondrial NAD^+ reduction (nV_3). Mitochondria influence the glycolytic pathway via the adenine nucleotide and NAD pools. Oscillations arise as a consequence of the non-linear allosteric activation of the phosphofructokinase (PFK) reaction (V_1) by ADP (positive feedback loop) and the phase shift in ATP production (negative feedback loop) in the lower part of glycolysis (V_3). Oxidative phosphorylation by the mitochondria (V_{ox}) is controlled by the intracellular concentration of ADP. Several features of the experimental findings are reproduced in the model, e.g., oscillation is strictly dependent on the mean intracellular glucose concentration, a wide input range (V_{in}) supports oscillations, and steady-state behavior is observed at very low or very high glucose inputs. Additionally, bursts of PFK activity produce transient increases in ADP (which would correspond to $I_{K,ATP}$ activation in the cell) in phase with the oxidation of NADH. The model will be useful as a guide for probing the mechanism of control of metabolic oscillation and its dynamic coupling to ion channel activity in the heart.

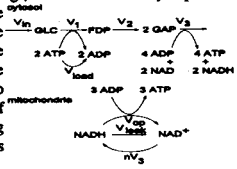

M-Pos499

CHANGES IN MEMBRANE IONIC CURRENTS IN THE HYPERTROPHIED RIGHT VENTRICLE OF RATS WITH MONOCROTALINE-INDUCED PULMONARY HYPERTENSION.

((J.K. Lee, H. Honjo, T. Anno, K. Kamiya, I. Kodama, J. Toyama)) Res. Inst. of Environ. Med., Nagoya University, Nagoya, Japan 464 (Spon. by T. Anno)

Changes in transmembrane action potential and ionic currents in association with hypertrophy were investigated in single ventricular cells isolated from rats with monocrotaline (MC)-induced pulmonary hypertension. Tissue weight of the right ventricle (RV) from 3 weeks rat after subcutaneous MC (60 mg/kg) injection was increased by 55% compared with untreated control (C) rats. Action potential duration (APD) of RV cells from MC rats was significantly greater than that from C rats, whereas there was no significant difference in APD of cells from the left ventricles (LV) of the two groups. The density of 4-AP sensitive transient outward current (I_{to}) in RV cells of MC rats was significantly less than that of C rats (17.0 ± 2.4 pA/pF in MC vs 29.0 ± 3.0 pA/pF in C at +50 mV, $p < 0.01$, $n = 10$). The voltage-dependence of I_{to} activation and inactivation was unaffected by the MC treatment. There was no significant difference in the density of I_{to} in LV cells from MC and C rats. RV cells from MC and C rats showed no significant difference in the density of inward rectifying potassium current (I_{K1}; -8.6 ± 2.4 pA/pF in MC vs -11.4 ± 3.2 pA/pF in C at -100 mV, N.S., $n = 7$) and that of calcium current (I_{Ca}; -23.0 ± 4.2 pA/pF in MC vs -25.4 ± 5.9 pA/pF in C at -10 mV, N.S., $n = 8$). These findings suggest that the increase in APD in the hypertrophied ventricle with pressure-overload is the result of a decrease in the density of I_{to}.

M-Pos500

MODULATION OF K^+ CURRENTS BY ANTIHISTAMINES IN RAT VENTRICULAR MYOCYTES.

((I. Ducic, R. F. Neville and M. Morad)) Department of Surgery and Pharmacology, Georgetown University School of Medicine, Washington, D.C. 20007. (Sponsored by W. C. Barker).

Antihistamines have been reported to prolong Q-T interval leading to arrhythmogenesis. The effect of antihistamines on potassium currents was studied in isolated, whole-cell clamped rat ventricular myocytes dialyzed with high concentration of Ca^{2+} buffers. Transient K^+ current in rat heart expresses both transient (I_{to}) and maintained (pedestal, I_{ped}) component. I_{to} was activated from holding potential of -90 mV to +60 mV. I_{ped} was activated using 100 ms conditioning pulses from -90 mV to -10 mV to activate and inactivate I_{to}, followed by test pulses to potentials ranging from -10 mV to +80 mV. At 2.5 μM I_{to} and I_{ped} were suppressed by 50%, 70% with terfenadine, 30%, 20% with diphenylhydramine, and 20%, 30% with loratadine, respectively. At higher concentrations (25 μM) loratadine also enhanced inactivation time constant of I_{to} (τ) from 40 ms to 12 ms and suppressed its peak by 35%. Terfenadine at 25 μM almost abolished I_{to} (75%) and increased its rate of inactivation from 90 ms to 30 ms. Diphenylhydramine (25 μM) was far less effective than terfenadine, but not significantly different from loratadine. DMSO used to dissolve antihistamines produced no significant effect on I_{to} and I_{ped}. The inwardly rectifying K^+ current (IK_1) was also suppressed by antihistamines at higher concentrations. The data suggest that terfenadine is much more efficacious blocker of I_{to} and I_{ped} than loratadine or diphenylhydramine, and their primary locus of action appears to be on the I_{ped} and to a lesser extent on I_{to}, most probably by interacting with open state of channel. Supported by NIH HL 116152.

[Ca^{2+}] IN CALCIUM STORES

M-Pos501

MEASUREMENT OF INTRAVESICULAR (IVES) Ca^{2+} AND pH IN SINGLE SMOOTH MUSCLE CELLS USING SPECTRAL IMAGING

(R.M. Lynch, L. Laughrey and R. Martinez-Zaguilan) Dept. Physiol., Univ. Arizona, Tucson 85724

Release of Ca^{2+} from intracellular stores plays an important role in many physiological processes. To understand how IVES Ca^{2+} is regulated, a general approach has been to load cells with acetoxymethyl ester forms of Ca^{2+} sensitive fluoroprobes, and reveal IVES by permeabilization which releases cytosolic dye. However, the identity of the loaded vesicles has not been established. Further, Ca^{2+} indicators are pH sensitive, making correction for H^+ binding important, since IVES exhibit dynamic pH responses. We used a spectral imaging microscope to simultaneously monitor signal from both pH and Ca^{2+} probes loaded into IVES compartments. Using this approach responses from individual vesicles were monitored. Many, but not all, vesicles-containing dyes were identified as endosomes/lysosomes by co-labeling with endocytosed dextrans. Antibodies to SERCA2 and calreticulin were used to identify Ca^{2+} compartments. Previous work indicated that Ca^{2+}-ATPase can be activated by initiation of glycolysis (Hardin et al., J.Gen.Physiol., 99:21, 1992; Martinez et al., J.Cell. Physiol., 161:129, 1994). In the present work, addition of glucose generally elicited cytosolic acidification, decreased cytosolic Ca^{2+} and increased IVES Ca^{2+}. However, heterogeneous responses between individual IVES were observed. Increases in IVES Ca^{2+} in response to glucose were observed with both high (Calcium Green) and low (Mag-Fura) affinity Ca^{2+} probes. These findings indicate that glucose metabolism can specifically modulate cell Ca^{2+} by stimulating Ca^{2+} sequestration in intracellular vesicles.

M-Pos502

RECORDING OF FREE CALCIUM AND MAGNESIUM IN INTRACELLULAR STORES IN PATCH CLAMPED SMOOTH MUSCLE CELLS.

((B. Mlinar and F.S. Fay)) Biological Imaging Group, Department of Physiology, UMMC, Worcester, MA 01605 (Spon. by R.W. Craig)

In order to directly monitor free ion concentration in intracellular compartments a new method has been developed. Freshly dissociated gastric smooth muscle cells from the toad, *Bufo marinus* were loaded with the acetoxymethyl ester of Ca^{2+} and Mg^{2+} ratiometric fluorescent indicator mag-fura-2. Upon establishing whole-cell voltage clamp configuration cytoplasmic dye was washed out through the patch pipette, leaving the dye entrapped in intracellular compartments. Incubation of cells in Ca^{2+} free solutions depleted luminal Ca^{2+} and enabled photometric measurement of free luminal Mg^{2+}. The level of free luminal Ca^{2+} was directly proportional to the cytoplasmic Ca^{2+} level, set to 100-400 nM by BAPTA. In conditions preventing CICR, application of 0.1-20 mM caffeine caused a drop in the signal due to luminal Ca^{2+} by >90 % in 10 sec., demonstrating that the dye signal originates almost exclusively from stores with RyR. In the same experimental setup carbachol and acetylcholine caused a much smaller drop in the signal. This may reflect differences in the efficiency of these two stimuli on the same stores or the fact that not all stores have IP_3R. These possibilities are currently being explored.

M-Pos503

RELEASE OF Ca^{2+} FROM SMOOTH MUSCLE SR BY THAPSIGARGIN AND Br-A23187. ((M.E. Kargacin and G.J. Kargacin)) Dept. of Med. Physiology, Univ. of Calgary, Calgary, Alberta, Canada.

We showed previously that Ca^{2+} uptake and release by the sarcoplasmic reticulum (SR) of saponin-permeabilized isolated smooth muscle cells can be monitored with fura-2. Uptake was ATP dependent and was inhibited by thapsigargin, a specific inhibitor of the SR Ca^{2+}-ATPase. Furthermore, addition of thapsigargin at high concentrations, after ATP-dependent uptake occurred, caused a rapid release of stored Ca^{2+}. We have compared the SR Ca^{2+} release induced by thapsigargin with that induced by the Ca^{2+} ionophore Br-A23187. Thapsigargin released 88 $\pm$ 9% of the Ca^{2+} taken up in the presence of ATP; whereas Br-A23187 released 175 $\pm$ 32%. Thus, Br-A23187 released Ca^{2+} from an additional pool that was not effected by thapsigargin. The time constant for Ca^{2+} release in the presence of thapsigargin (55 $\pm$ 4 s) was less than that measured in the presence of the ionophore (160 $\pm$ 19 s). The lower rate of release seen with Br-A23187 may have been due to the fact that SR Ca^{2+} uptake continued in its presence, whereas, in the presence of thapsigargin, uptake was inhibited. The Ca^{2+} release induced by thapsigargin was not inhibited by ryanodine (~1 mM) indicating that release did not occur through the SR ryanodine receptor. Our results indicate the Ca^{2+} release induced by thapsigargin was more specific than that induced by the ionophore; however, the mechanism of this release remains unknown. (supported by MRC (Canada) and AHFMR.)

M-Pos504

MONITORING CALCIUM CHANGES IN INTRACELLULAR STORES IN SINGLE SMOOTH MUSCLE CELLS. ((J.M. Steenbergen and F.S. Fay)) Biomed. Imaging Group. U. Mass. Med. Center, Worcester MA 01605.

A technique was developed for studying how Ca^{2+} was regulated in the intracellular stores in isolated smooth muscle cells. Cells were enzymatically dissociated from the stomach of the toad Bufo marinus, loaded with the low affinity fluorescent Ca^{2+} indicator mag-fura-2 am (1 μM, 2 hr.) and incubated with alpha-toxin (100 U/ml, 30 min.), to allow control of the ionic composition of the cytoplasm and to release dye from the cytoplasm. After skinning the cells were stored in a buffer containing 100 nM Ca^{2+}, 3 mM MgATP and 1 mM Na_3GTP. The three-dimensional distribution of mag-fura-2 was assessed by using digital imaging microscopy. The analysis showed that the dye was distributed beneath the cell membrane in a punctuate manner, similar to that of sarcoplasmic reticulum (SR) markers, and was almost absent from the cytoplasm. Calcium ratios were measured with a high-time resolution microfluorimeter. At rest the Ca^{2+} ratio was 1.68 $\pm$ 0.26 and decreased to 0.91 $\pm$ 0.08 (mean $\pm$ SEM, n = 6) upon caffeine (20 mM) application, which activates the ryanodine receptor of the SR. The decrease in the Ca^{2+} ratio due to caffeine consisted of a rapid followed by a slower decline, and could be fit by a double exponential curve. The refilling of the caffeine sensitive stores was completed in about 2 min. in the presence of 100 nM Ca^{2+}. These data indicate that this technique is a valuable tool for studying the intracellular Ca^{2+} stores sensitive to caffeine in single smooth muscle cells. Use of this technique to study the effect of putative modulators on the SR function will be demonstrated. Supported by HL 14523 and HL 47530.

INOSITOL TRISPHOSPHATE

M-Pos505

TWO INOSITOL 1,4,5-TRISPHOSPHATE BINDING SITES IN RAT BASOPHILIC LEUKEMIA CELLS: RELATIONSHIP BETWEEN RECEPTOR OCCUPANCY AND CALCIUM RELEASE ((J. Watras, I. Moraru, L.A. Kindman*)) Univ. of Connecticut, Farmington, CT 06030; *Duke University Medical Center, Durham, NC 27710

Ligand binding studies indicate the presence of both high affinity (K_D=0.9 nM) and low affinity (K_D=47 nM) $InsP_3$ binding sites in RBL microsomes. Both sites are selective for $InsP_3$ over $InsP_4$. The relative abundance of the two $InsP_3$ binding sites is Ca^{2+} -dependent, as an increase in Ca^{2+} from 0.1 μM to 0.5 μM resulted in the apparent conversion of some low affinity sites into high affinity sites. Ca^{2+} (0.5 μM) also increased the K_D of the low affinity $InsP_3$ binding site. Given the presence of both high and low affinity $InsP_3$ binding sites, two simple mathematical models describing both the kinetics of calcium release and quantal calcium release from RBL cells were developed. Each model assumes that the two types of $InsP_3$ receptors interact randomly to form five different calcium channels (2 homotetramers, and 3 heterotetramers), with a distribution reflective of the relative abundance of the two binding sites. In the first model, binding of 3 or 4 molecules of $InsP_3$ is needed to open the channel. The second model requires $InsP_3$ binding to 2 or 3 low affinity sites to open the channel. Given the Ca^{2+} dependence of the conversion between low affinity and high affinity $InsP_3$ binding sites, the latter model predicts the desensitization of some of the channels following elevation of cytosolic Ca^{2+}. Neither model requires cooperativity, consistent with the lack of cooperativity in the $InsP_3$ binding assays.

M-Pos506

KINETIC ANALYSIS OF THE EFFECT OF INOSITOL 1,4,5-TRISPHOSPHATE ON SR Ca^{2+} IN CULTURED SMOOTH MUSCLE CELLS. ((T. Sugiyama and W.F. Goldman)) Dept. Physiol., Univ. Maryland Med. Sch. and GRECC, Baltimore V.A.M.C., Baltimore, MD 21201

The time- and concentration-dependent effects of inositol 1,4,5-trisphosphate ($InsP_3$) on intra-sarcoplasmic reticulum (SR) free Ca^{2+} concentration ($[Ca^{2+}]_{SR}$) were studied in saponin-permeabilized A7r5 cells. At 0.1 μM, $InsP_3$ elicited slow monoexponential declines in $[Ca^{2+}]_{SR}$ ($k_{0.1}$ = 0.44 x 10^{-3} sec^{-1}). Higher $[InsP_3]$ evoked changes in $[Ca^{2+}]_{SR}$ that were best fit as the sum of two exponentials. Rates for the early fast release component (k_{fast}) were $[InsP_3]$-dependent and ranged from 8.8 to 60.6 x 10^{-3} sec^{-1}, while rates for the late slow component (k_{slow}) were unchanged from $k_{0.1}$. The continuous decline in $[Ca^{2+}]_{SR}$ in the presence of $InsP_3$ made multiple, independent, SR Ca^{2+} pools unlikely. Instead, the data were consistent with a two-state model for $InsP_3$-receptor channels ($InsP_3$-R): a high-conductance, low-affinity state that was converted by allosteric or other means, as function of SR Ca^{2+} content and/or time to a low-conductance, high-affinity form that was already saturated at $[InsP_3]$ = 0.1 μM. By applying measurements of SR membrane permeability to this model, it was found that apparent $InsP_3$ binding affinity, cooperativity and, consequently, $InsP_3$-R activity were all highly dependent on $[Ca^{2+}]_{SR}$ when $InsP_3$-R were in the high-conductance state. As $[Ca^{2+}]_{SR}$ was decreased from 100 to 60 μM, the apparent K_d for $InsP_3$ binding decreased from 5.2 to 3.2 μM, while the Hill coefficient increased from 1.6 to 4.9. These data indicate that the quantal nature of $InsP_3$-induced SR Ca^{2+} release is partly intrinsic to the $InsP_3$-R itself and partly a product of the kinetics of intracellular Ca^{2+} homeostasis.

M-Pos507

SINGLE-CHANNEL IP_3 RECEPTOR CURRENTS REVEALED BY PATCH CLAMP OF ISOLATED *XENOPUS* OOCYTE NUCLEI ((D. D. Mak and J. K. Foskett)) Division of Cell Biology, Hospital for Sick Children, Toronto, Ont., M5G 1X8, Canada. (Spon. by M. Silverman)

Patch clamp of the outer nuclear membrane of isolated *Xenopus* oocyte nucleus was used to measure the single channel properties of the inositol 1,4,5-trisphosphate (IP_3) receptor (IP_3R). The observed channel was activated by IP_3, inhibited by heparin and Ca^{2+}-selective, with ion permeabilities $P_{Ca}:P_K:P_{Cl}$ = 8:1:0.05. In symmetric KCl buffer, the channel was ohmic (113 pS in 140 mM KCl) at low channel currents but rectified at higher positive currents. The nuclear IP_3R normally exhibited three conductance substates: a main substate occuring >90% of channel open time, a double substate with twice the main substate conductance, and a third substate with half the main substate conductance which was observed rarely. Channel open probability fluctuated over time and among nuclei. Mean open channel duration of the main and double substates were ~5 and 1 ms, respectively. Occasionally, the IP_3R entered a flickering mode in which the channel switched rapidly between 2 substates with conductances 0.26 and 0.76 that of the normal main substate and mean durations substantially shorter than 1 ms. Relative open probabilities of the 2 substates in the flicker mode was voltage-dependent with an equivalent gating charge of 1.1e moving across the full transmembrane voltage. Many channels exhibited periods of closure lasting seconds and most inactivated permanently within 5 min of IP_3 stimulation. These results provide the first characterization of the single channel properties of the IP_3R in its native membrane environment and demonstrate that patch clamp electrophysiology of intact nuclei can be used to directly record currents through the IP_3R.

M-Pos508

THE ROLE OF Ca-DEPENDENT INACTIVATION IN QUANTAL Ca RELEASE FROM SARCOPLASMIC RETICULUM. László G. Mészáros and Robin Socci, Department of Physiology and Endocrinology, Medical College of Georgia, Augusta, GA 30912.

The activation of the IP3- and ryanodine-sensitive Ca^{2+} channels by subsaturating concentrations of agonists is transient. The mechanism of this phenomenon (termed as quantal Ca^{2+} release or adaptation) is unknown.

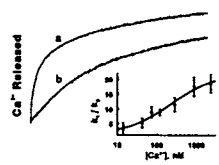

Indicating channel inactivation, Ca^{2+} release from isolated sarcoplasmic reticulum vesicles is biphasic in micromolar extravesicular Ca^{2+} (curve a), i.e. time course is best fitted to a biexponential with k_1 and k_2 rate constants. At reduced extravesicular $[Ca^{2+}]$ (EGTA addition prior to release-induction), the biphasic character became less pronounced (curve b), as shown by the decrease in k_1/k_2 ratios. Ca-dependent inactivation, that presumably stems from slow binding of Ca^{2+} to high-affinity (K_d=210 nM) inactivating Ca-site(s) on the channel, is proposed to account for the transient kinetics. Channel adaptation or quantal release is observed only at subsaturating ligand concentrations. Therefore, Ca-dependent inactivation only occurs, if not all ligand binding sites (less than 4/per channel unit) are occupied.

M-Pos509

Fcγ RECEPTOR-MEDIATED $[Ca^{2+}]_i$ FLUX IS SENSITIVE TO INHIBITION OF PI 3-KINASE. ((F.Y.S.Chuang*†, Z.Shen†, J.Eisinger*, M.Sassaroli* and J.Unkeless†)) *Dept of Physiology and Biophysics, †Dept of Biochemistry, Mount Sinai School of Medicine, New York, NY 10029.

In the course of investigating signal transduction by neutrophil IgG Fc receptors (FcγR), we have discovered that wortmannin -- a fungal metabolite that strongly inhibits phosphatidylinositol (PI) 3-kinase -- also effectively inhibits, in a dose-dependent manner, the rise in $[Ca^{2+}]_i$ normally observed upon FcγR crosslinking. Spectrofluorometric data obtained using the calcium indicator indo-1 demonstrate that wortmannin inhibits the transient rise in $[Ca^{2+}]_i$ in neutrophils induced by the specific crosslinking of either the transmembrane isoform of FcγR (CD32) or the glycosylphosphatidylinositol (GPI) anchored isoform (CD16), with an estimated K_I of 2.0 nM and 2.6 nM, respectively. However, the $[Ca^{2+}]_i$ flux in human neutrophils stimulated by the chemotactic peptide, fMet-Leu-Phe (fMLP), is not affected by wortmannin. The mechanism by which wortmannin inhibits $[Ca^{2+}]_i$ flux is unclear, since the calcium released upon stimulation by FcγR ligation comes almost entirely from intracellular stores, presumably triggered by inositol 1,4,5-trisphosphate ($InsP_3$). Assay of mouse macrophage cell lines transfected with human FcγRIIA shows that wortmannin (10 nM) inhibits the release of $InsP_3$, upon FcγR crosslinking. To further characterize the receptor-mediated signaling pathway, we are also using fluorescence ratiometric imaging of individual fura-2 loaded cells to demonstrate that intracellular calcium flux correlates with specific morphological changes associated with phagocytosis.

MEMBRANE FUSION: EXOCYTOSIS AND ENDOCYTOSIS

M-Pos510

STATISTICAL ANALYSIS OF TRISKELION STRUCTURAL FEATURES: ESTIMATION OF ARM RIGIDITIES. ((Albert J. Jin and Ralph Nossal)), Physical Sciences Laboratory, DCRT, National Institutes of Health, Bethesda, MD 20892.

Clathrin triskelions are supramolecular protein complexes whose structural and energetic properties ultimately determine many aspects of *receptor-mediated endocytosis* in functioning cells. Previously, topological constraints were found to set limiting conditions on coated-pit invagination and coated-vesicle generation (Jin and Nossal, 1993). To extract more detailed properties of individual triskelions, we have developed a quantitative analytical scheme, which systematically examines the distributions of, and correlations between, a series of triskelion shape parameters, and have applied it to a set of electron micrographs supplied by Kocsis *et al.* (1991). Results support an energetic model for triskelions having elastic-like deformation properties. Numerical estimate of the bending modulus of the triskelion arms indicates a near uniform persistence length of about 35 nm, which suggests that the clathrin coat is more rigid than the plasma membrane component of coated pits and coated vesicles.

[1] Jin., A.J. and Nossal, R., 1993, *Biophys. J.*, **65**:1523-1537.
[2] Kocsis, E., Trus, B. L., Bisher, M. E., and Steven, A. C., 1991. *J. Struct. Biol.*, **107**:6-14.

M-Pos511

ENDOCYTOSIS AND EXOCYTOSIS PROVIDE PATHWAYS FOR CALCIUM FLUXES ACROSS THE MEMBRANES OF HYDROZOAN EMBRYOS. ((E. B. Ridgway, and G. Freeman)) VCU/MCV Dept. of Physiol., Richmond, VA. 23298, and Dept. Zool. UT, Austin, TX 78712

Beginning at the 2-cell stage, KCl-depolarization of the embryos of the hydrozoan *Phialidium gregarium* leads to substantial calcium influx as measured by ^{45}Ca. Once calcium is loaded the rate of calcium efflux into ASW (normally in the range of 0.001-0.003/min) is dramatically increased by KCl depolarization to rates with peak values in excess of 0.9/min. This KCl-induced calcium efflux is blocked by nifedipine, implying calcium channel participation. The fraction of calcium lost in such an event typically exceeds 60% of the loaded calcium, suggesting that this efflux is due, at least in part, to release of compartmentalized calcium via exocytosis. We tested this idea in several ways. First, ^3H-inulin can be loaded via KCl-depolarization (suggesting a KCl-induced endocytosis) and subsequent KCl depolarization causes an inulin efflux analogous to that seen for calcium. Second we have visualized (using confocal microscopy) the time course and extent of KCl-induced fluorescein influx in these embryos. Third, NH_4Cl at pH 8.0 which causes a marked rise in intracellular calcium without depolarization causes a calcium influx comparable to that induced by KCl. But nifedipine does not block NH_4Cl-induced calcium efflux, implying that the rise in intracellular calcium alone is sufficient for efflux. Supported by NSF grant DCB-9207470, and IBN 9307441.

M-Pos512

PURIFICATION AND PROTEIN COMPOSITION OF TRITON-INSOLUBLE PLASMALEMMAL CAVEOLAR COMPLEXES FROM CARDIAC MYOCYTES OF MAMMALIAN HEART MUSCLE ((D.D. Doyle, J. Upshaw-Earley, and E. Page)) Department of Medicine, University of Chicago, Chicago, IL 60637

In mammalian myocardial cells, the nonclathrin-coated plasmalemmal vesicles called caveolae contain atrial natriuretic peptide (Circ. Res. 74. Nov.'94), take up extracellular proteins in a stretch-dependent manner (Circ. Res. 71:159,1992), reversibly close and swell in saline made hypertonic with 150 mM sucrose (Circ. Res. 73:135, 1993), and are associated with a cytosolic surface Ca-ATPase (Fujimoto, J. Cell Biol. 120:1147, 1993). To study the proteins associated with physiological roles of cardiac myocyte caveolae, we have used flotation in sucrose density gradients to isolate Triton X-100-insoluble caveolae-enriched membrane complexes from primary cultures of adult rat atrial myocytes (PCAM). We also isolated such complexes from highly enriched sarcolemmal membranes prepared from sheep ventricle (Doyle and Winter, J. Biol. Chem. 264:3811, 1989) which contain mg. amounts of caveolar membrane from both myocardial and nonmyocardial cells. The SDS PAGE profile of PCAM caveolar proteins served to identify cardiac myocyte-specific caveolar protein bands in SDS gels of sheep ventricle. Western immunoblots using a polyclonal antibody against caveolin yielded conspicuous 24 kD bands for PCAM and sheep ventricle. PCAM caveolar complexes extracted with phosphoinositol specific-phospholipase C digestion and Triton X-114 phase separation yielded proteins presumed to be glycosylphosphatidylinositol-linked intracaveolar proteins. Supported by USPHS HL -10513, 20592 and 44004.

M-Pos513

SYNAPTIC VESICLE TURNOVER IN MAMMALIAN INNER HAIR CELLS. ((L.C.Anson and J.F.Ashmore)) Dept. of Physiology, School of Medical Sciences, University of Bristol, Bristol BS8 1TD, UK.

We have previously demonstrated that isolated guinea-pig inner hair cells (IHCs), which form synapses with primary afferent auditory neurones, release an excitatory amino acid (probably glutamate) upon cell depolarisation (*J. Physiol.* **480.P**, 105P). IHCs recorded in the whole-cell patch clamp configuration, using solutions chosen to inhibit outward K^+ currents, exhibit a small (40-50 pA) sustained inward current which is maximal at -20mV. This is a likely candidate for an inward Ca^{2+} current. Cell capacitance measurements were carried out under amphotericin B perforated patch recording conditions. Depolarisations to potentials at which the Ca^{2+} current is activated (-10mV) resulted in an increase in cell capacitance of up to 250fF. The capacitance increase decayed back to baseline with a time constant of 6s at room temperature. We hypothesise that this represents the fusion of synaptic vesicles with the plasma membrane and subsequent retrieval. The retrieval of exocytosed membrane could also be demonstrated by the labelling of IHCs with FM1-43 upon addition of high K^+ (outer hair cells did not take up the dye). Such intracellular labelling is believed to represent the recycling of synaptic membrane into intracellular compartments. These results indicate that cochlear IHCs can be used as a system to study mammalian presynaptic function. Supported by the MRC.

M-Pos514

PH- AND CA^{2+}-DEPENDENT INTERACTION OF SECRETORY VESICLE MATRIX PROTEINS AND CHROMOGRANIN B WITH CHROMOGRANIN A ((Seung Hyun Yoo)) NIDCD, NIH, Bethesda, MD 20892

Chromogranin A and several other secretory vesicle matrix proteins have recently been shown to bind to the vesicle membrane at the intravesicular pH of 5.5 and to be released from them at a near physiological pH of 7.5. The pH-dependent interaction of chromogranin A as well as several other matrix proteins with the vesicle membrane has been manifested regardless of the presence or absence of Ca^{2+} and has been proposed to be an essental step in vesicle biogenesis. Nevertheless, it is not clear how other intravesicular matrix proteins that may not interact with the vesicle membrane find their way into the secretory vesicle.

Therefore, in the present study, the potential interaction of chromogranin A with other intravesicular matrix proteins was studied, and chromogranin A was shown to interact with several other intravesicular matrix proteins, including chromogranin B. The interaction between chromogranin A and other matrix proteins was dependent not only on the intravesicular pH of 5.5, but also on the presence of Ca^{2+}. Unlike the interaction between chromogranin A or other matrix proteins with the vesicle membrane, the interaction between chromogranin A and other matrix proteins was predominantly influenced by the presence of Ca^{2+}, suggesting an important role of Ca^{2+} in the interaction. These results further support the essential roles of chromogranins A and B in vesicle biogenesis.

M-Pos515

PULSED-LASER IMAGING REVEALS THE MECHANISM OF CURRENT RECTIFICATION AND AMPLIFICATION AT THE INTERFACE WITH A SECRETORY GRANULE GEL. P.E. Marszalek*, V.S. Markin#, T. Tanaka♣, H. Kawaguchi♣ and J.M. Fernandez* ♦ Mayo Clinic, #Univ. of Texas Southwestern Med. Ctr, ♣ Massachusetts Inst. of Technol, ♠ Keio Univ., Japan.

The gel matrix of secretory granules, when placed at the tip of a glass pipette, was shown to possess the properties of a diode. The matrix conducted 100 fold larger current at negative potentials compared to positive potentials, and amplified the current by up to six fold over that measured for the pipette alone. We have discovered, that these electrical properties result from focusing an electric field at the gel-electrolyte interface inducing a large, voltage-dependent, accumulation/depletion of ion carriers. By solving the Nernst- Planck electro-diffusion equation we were able to accurately predict the magnitude of the accumulation/depletion of ions at this interface and explain the observed current/voltage characteristics. We confirmed this mechanism by pulsed-laser-imaging of the changes in the concentration of the anionic probe fluorescein [100 μM added to the pipette solution] at the gel-electrolyte interface. We observed that within 4 ms of applying a -9V across the gel, a saturating increase in the fluorescence [>3-fold] accumulated at the gel-electrolyte interface where the electric field was focused. Simultaneously, a large current flowed through the gel. Upon reversal of the voltage to +5V we observed that the previously accumulated ions migrated toward the anode at an approx. speed of 500 μm/s, followed by depletion of fluorescein ions at the interface. These events occurred in parallel with the decay of the measured ionic current. Through the use of synthetic hydrogel microspheres [3-5μm] we found that rectification and amplification are general properties of gel-electrolyte interfaces where the polarity of the rectification is dependent on the sign of the immobilized charge. Rectification was not observed in neutral gels. We speculate that similar mechanisms operate at the interface between narrow pores and hydrogels such as those found in exocytotic fusion.

M-Pos516

NONLINEAR OPTIMIZATION APPLIED TO DUAL FREQUENCY ESTIMATION OF MEMBRANE CAPACITANCE, RESISTANCE, AND ACCESS RESISTANCE. ((D. Barnett and S. Misler)) Washington Univ. Med. Ctr., St. Louis, MO 63110.

Estimation of cell membrane capacitance (C_m) provides evidence of exocytosis and endocytosis from single cells. Techniques based on single frequency sinusoidal stimulation normally provide adequate results when certain underlying assumptions, such as high and/or stationary membrane resistance (R_m), are valid. When these conditions are not met, or if an accurate measure of R_m is sought, then alternative methods are required. Recent approaches based on two frequency stimulation are derived from non-unique algebraic solutions to the problem of estimating the three elemental cell electrical parameters (C_m, R_m, and access resistance R_a) from four measurements. We have optimized the dual frequency approach by applying a nonlinear weighted least squares (nwls) solution to the overdetermined nonlinear system. The nwls solution takes the maximum likelihood estimates of the admittance parameters and produces asymptotically normal estimates of cell parameters. The variance of the capacitance and resistance estimates is a function of both the input parameters, *i.e.*, stimulus frequencies and magnitudes, and the cell's electrical parameters. Simulation and model-circuit results illustrate the trade off between noise, time response, and overall voltage excursion when choosing input parameters. Sample experiments demonstrate the validity of this approach and provide insight into practical implementation issues and limitations of dual frequency solutions. Support: NIH(DK37380)

M-Pos517

INFLUENCE OF CONDUCTANCE CHANGES ON PATCH CLAMP CAPACITANCE MEASUREMENTS USING A LOCK-IN AMPLIFIER AND LIMITATIONS OF THE PHASE TRACKING TECHNIQUE. ((K. Debus, J. Hartmann, G. Kilic and Manfred Lindau)) MPI f. med. Forschung, D-69120 Heidelberg, Germany.

To measure small changes in membrane capacitance associated with exocytosis, generally a sine wave command voltage with about 800 Hz frequency is applied and the resulting current is fed into a two-phase lock-in amplifier. To detect very small changes, the phase is usually set to a value where changes in capacitance and conductance are each detected in only one channel of the lock-in [Neher & Marty (1982) *PNAS* 79:6712]. This method assumes that changes in membrane conductance or membrane capacitance are small. We characterized the influence of large voltage-dependent conductance changes on capacitance measurements done with this method by numerical computer simulations, error formulas, and experimental tests. At correct phase setting the artefacts in the capacitance measurement due to large conductance changes are very small, and reflect mainly second order phenomena. In a 6 pF cell with 5 MΩ access resistance, activation of a linear 10 nS slope conductance generates only an apparent 13 fF change in the capacitance trace. However, a phase error (Δφ) of a few degrees leads to significant projections proportional to sin(Δφ). The phase tracking method, where a resistor is switched into the connection between bath electrode and ground to simulate a pure change of access resistance, determines a phase which may be shifted away from the correct phase by several degrees. Even when phase tracking is performed during periods of low membrane conductance, a phase error is introduced by the second order change in the capacitance trace, and by the fast capacitance between the pipette and the bath solution. We provide practical values setting the range where possible artefacts are below defined limits.

M-Pos518

REGULATION OF EXOCYTOSIS AND Cl^- CONDUCTANCE IN HT29-Cl.16E AND HT29-Cl.19A CELLS ((X.W. Guo, R. Harvey, C. Laboisse and U. Hopfer)) Dept. of Physiology and Biophysics, CWRU, Cleveland, OH 44106 and INSERM U239, Faculte de Medecine, X. Bichat, Paris, France

Cl.16E and Cl.19A are subclones of the human colonic epithelial cell line HT29. Cl.16E secretes mucin granules and electrolytes, while Cl.19A only secretes electrolytes. To obtain information about the temporal correlation of Cl^- secretion and fusion of the granules to plasma membrane, the phase tracking method was applied to measure the Cl^- conductance and capacitance simultaneously. During the experiments, the membrane potential was held at -25 mV and a 1.2 kHz, 40 mV sine wave used to separate the capacitative and conductive currents. Measurement were made on subconfluent cells on glass coverslips. 200 μM extracellular ATP transiently raised Cl^- conductance and cell capacitance in both cell lines. The peak Cl^- conductances increased from 1.3±0.5 nS to 18 ±.5 nS and 1.2±0.5 nS to 24±2 nS for Cl.16E and Cl.19A cells, respectively. The life time of the currents for both cell line was about 40 sec. The cell capacitances were 22±1 pF and 18±1 pF in Cl.16E and Cl.19A, respectively. Interestingly, a big difference was found between the two cell lines with stimulation of extracellular ATP. The capacitance increase was 17% in Cl.16E, but only 1% in Cl.19A. The greater capacitance change with ATP in Cl.16E is consistent with the presence of mucin granules in this cell line which are discharged by stimulation. The life time of the capacitance increases in both cell lines was only about 20 sec which indicated a fast exocytosis followed by endocytosis. Supported by NIH (DK-39658) and the Cystic Fibrosis Foundation.

M-Pos519

SELECTIVE ELECTROCHEMICAL MEASUREMENT OF HISTAMINE AND SEROTONIN RELEASE FROM SINGLE RAT PERITONEAL MAST CELLS ((K. Pihel and R.M. Wightman)) Department of Chemistry, University of North Carolina, Chapel Hill, NC 27599.

Background-subtracted fast scan cyclic voltammetry is an electrochemical technique that allows both quantitative and qualitative identification of electroactive chemical species. While this technique has been used for many years to measure neurotransmitter release in the rat brain, it has only recently been used to measure release of substances from individual biological cells. Measurements at cells are accomplished by placing a microelectrode immediately adjacent to a single cell and then stimulating the cell to release with a secretagogue. This measurement technique is fast enough to quantitate and identify chemical species released from individual vesicles within a cell. Rat peritoneal mast cells are known to store and release histamine and serotonin. Because serotonin oxidizes at a relatively low potential and histamine at a very high potential at carbon fiber microelectrodes, these two species have easily distinguishable cyclic voltammograms. With this technique it can clearly be seen that histamine and serotonin are released simultaneously from mast cells, indicating that they are stored within the same vesicles inside of these cells.

M-Pos520

ABSENCE OF FUSION READY GRANULES IN MAST CELLS AND CHROMAFFIN CELLS. ((A.F. Oberhauser, I.M. Robinson and J.M. Fernandez)) Mayo Clinic, Dept. of Physiol. & Biophys., Rochester, MN 55905.

We measured the exocytotic response induced by a rapid step increase in the concentration of Ca^{2+} or GTPγS (achieved by flash photolysis of caged compounds) in mast cells and chromaffin cells. We measured secretion by following both cell membrane capacitance and amperometry. When Ca^{2+} was used to trigger secretion, we observed an immediate increase in capacitance, however, the first amperometric spike was observed after a long delay. The time integral of the amperometry over the secretory response was sigmoidal and lagged the capacitance trace by 5.1±3.5 s in mast cells and 1.3±0.6 s in chromaffin cells. In contrast, in response to a GTPγS stimulus, we found that the integral of the amperometry followed the same sigmoidal time course as the capacitance. These results suggest that the capacitance increase, when triggered by a large Ca^{2+} step, reports events that do not result in the exocytotic release of oxidizable substances. Capacitance monitors the combined effects of, i) the fusion of different types of vesicles; ii) endocytosis; iii) changes in the electrical equivalent circuit of the cell, whereas, amperometry follows only the release of oxidizable secretory products. Thus the integral of the amperometric recording is a true reflection of the time course of an exocytotic response. The lag observed in the amperometric signal in response to the first step increase in Ca^{2+} or GTPγS suggests the absence of fusion ready granules. We propose that this long lag phase represents a priming step required before fusion of such granules can occur.

M-Pos521

FUSION-PORE DYNAMICS DURING VESICLE FUSION IN CHROMAFFIN CELLS. ((Z. Zhou[1], S. Misler[1] and R.H. Chow[2]) [1]Washington Univ. Med. Ctr., St. Louis, MO 63110. [2]MPI for Experimental Medicine, D-37075 Göttingen, Germany.

Chromaffin cells secrete catecholamines by exocytosis of dense-core vesicles. Single exocytotic events can be detected electrochemically (i.e. amperometrically) in real time as current spikes. 70% of spikes are preceded by a small "foot", which has been interpreted as a pre-fusion signal (Chow et al., 1992, Nature: 356:60). Using improved polyethylene-coated carbon fiber electrodes (pCFEs), we find that 20-50% of amperometric foot signals have rapid fluctuations, far exceeding the baseline noise, which we interpret as flickering of the vesicle fusion pore. Interestingly, there are also many low-amplitude fast-flickering signals lacking a subsequent spike. The rapid rise times suggest that there are fusion events arising near the pCFE, not distant events that have been diffusionally filtered. These may be "stand-alone" foot signals, reflecting transient vesicle fusions that do not lead to complete collapse of the vesicle into the plasma membrane. Selecting events with risetimes of less than 1ms, the average flicker frequency (F_f) and flicker number (N_f) depended on intracellular Ca^{2+} concentration ($[Ca^{2+}]_i$). At $[Ca^{2+}]_i \leq$ 50 μM, F_f = 120 Hz and N_f = 1.8, while at $[Ca]_i \gg$ 50 μM, F_f = 220 Hz and N_f = 2.5. Thus, Ca^{2+} may continue to affect the fusion apparatus after initial pore formation has occurred.

M-Pos522

STIMULUS-SECRETION COUPLING PATTERNS IN DIALYZED CHROMAFFIN CELLS: EFFECTS OF CA BUFFERS ((E.P. Seward and M.C. Nowycky)) Anat &Neurobiol., Med.Coll.Penn. Philadel., PA 19129.

Ca secretion coupling in bovine chromaffin cells was studied with capacitance (C_m) recording technique. Cells were stimulated every 2-3 min with trains of short (6-20 msec) depolarizing pulses. In dialyzed cells, the first stimulus train usually evoked a secretory pattern as in Fig. a, with the biggest C_m jump at the first depolarization (Cm1, *). With 0.1 mM BAPTA in the pipette, the mean Cm1 / 10^6 Ca ions was 4.1 ± 0.8 fF and the rate of exocytosis was 4700 ± 800 fF/sec (n=15). Elevation of $[BAPTA]_i$ to 0.3 mM had no significant effect on the response to the first train (n=26). This pattern of release disappeared quickly in dialyzed cells, and subsequent stimuli elicited a pattern in which C_m jumps begin late in the train after a "threshold" amount of Ca entry (Fig. b). At 0.1 mM $[BAPTA]_i$, C_m jumps began after the entry of 96 ±10x10^6 Ca ions and proceeded on further Ca entry at 1.8±0.2 fF / 10^6 Ca ions (n=6). At 0.3 mM $[BAPTA]_i$, both Ca threshold and dependence increased ~2.4 fold (n=6). Chromaffin cells exhibit both a rapid coupling mechanism that is insensitive to low concentrations of Ca buffers and washes out rapidly, and a second secretory pattern that has a characteristic "threshold," is strongly modulated by Ca buffers, and is maintained in whole cell recordings.

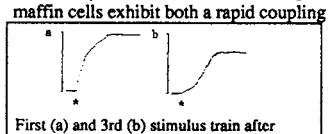

First (a) and 3rd (b) stimulus train after break-in, 0.1 mM BAPTA.

M-Pos523

MULTIPLE FUSION PROTEIN (MFP) MODEL FOR THE CALCIUM DEPENDENCE OF THE RATE AND EXTENT OF EXOCYTOSIS: A PLAUSIBLE STOCHASTIC MODEL. ((Steven S. Vogel, Paul S. Blank, & Joshua Zimmerberg)) LTPB, NICHD, NIH Bethesda, MD 20892

In sea urchin eggs the cellular machinery which mediates calcium triggered exocytosis, the 'fusion machine' (FM), resides on the exocytotic granules, and has two states 'inactive' and 'active' whose transition is regulated by calcium. Additional data suggests that each granule has more than one FM. To better understand the microscopic calcium dependence of exocytosis, we have modeled the macroscopic consequences of having more than one FM per granule. We have developed a model which describes the dependence of exocytosis on the average number of active FMs per granule. If calcium regulates the average number of activated FMs in a population, as in a Hill relationship for example, the MFP model can explain both the calcium dependence of rate and extent of fusion observed in biological systems.

Let t = time in seconds, p = the probability per second per active FM that a fusion event between a granule and the plasma membrane will occur, and $\langle n \rangle$ = the average number of 'active' FMs per granule in the population of granules. Then $S(t,\langle n \rangle,p)$ is the survival curve for a population of granules awaiting to fuse with the plasma membrane:

$$S(t,\langle n \rangle,p) = e^{\langle n \rangle((1-p)^t - 1)}$$

The extent of fusion, $E(\langle n \rangle)$ is $1-S(t \to \infty, \langle n \rangle, p)$;

$$E(\langle n \rangle) = 1-e^{-\langle n \rangle}$$

and the rate of fusion, $R(t, \langle n \rangle, p)$, is the derivative of $1-S(t,\langle n \rangle,p)$. The maximal rate of fusion is:

$$R(t \to 0, \langle n \rangle, p) = -\langle n \rangle \ln (1-p)$$

M-Pos524

MULTIPLE POOLS OF DOCKED VESICLES: LIFE AFTER ATP HYDROLYSIS IN PITUITARY MELANTROPHS. (T.D. Parsons, H. Horstmann & W. Almers) MPI Heidelberg FRG (Spon: W. Almers)

Tracking cell surface area with capacitance (Cm) measurements, and cytosolic Ca with fura-2 or furaptra, we studied the role of Mg-ATP in Ca-triggered exocytosis. Ca was raised to 2-3 μM by dialysis through patch pipettes. With 2 mM Mg-ATP, Cm rose quickly at first and continued to increase more slowly for >8 min by >5 pF. When ATP was omitted or replaced with an analog, Cm increased by 2.8 ± 0.8 pF (no ATP) or 1.7 ± 0.4 pF (AMP-PNP) in 3 - 6 min and then stopped. Hence, sustained exocytosis requires the hydrolysis of ATP. Next, we dialyzed cytosolic Mg out of the cell ([Mg] < 100 nM), in the presence or absence of hydrolysis-resistant ATP analogs, and raised Ca by flash photolysis of DMnitrophen. This triggers an exocytic burst, and a pH-sensitive slower phase. Amplitudes of the exocytic burst (in pF) were: ATP, 0.5 ± 0.1; ATPγS, 0.6 ± 0.1; AMP-PNP, 0.4 ± 0.1. After 5 s, Cm (in pF) had increased by: ATP, 2.3 ± 0.2; ATPγS, 3.1 ± 0.2, AMP-PNP, 2.3 ± 0.3. Evidently, 2 - 3 pF of vesicle membrane are exocytosed independently of ATP-hydrolysis and in distinct kinetic phases. Morphometry of ultra-thin sections revealed an average of 1900/cell of dense-core, β-endorphin-immunoreactive vesicles touching the plasma membrane. With a 237 nm diameter, their combined surface area is 340 μm^2, or 3.4 pF. There are apparently enough docked vesicles to account for ATP-independent exocytosis. However, only a small fraction of the docked vesicles are capable of rapid exocytosis. We propose that the last ATP-driven reaction of the exocytic pathway occurs

M-Pos525

PHOTOACTIVATION OF *NITROPHENYL-EGTA* TRIGGERS RAPID EXOCYTOSIS IN PITUITARY MELANOTROPHS. ((T.D. Parsons, G.C.R. Ellis-Davies, J. Kaplan and W. Almers)) MPI, Heidelberg FRG and OHSU, Portland, Oregon 97201.

The photolysis of the photolabile calcium chelator, nitrophenyl-EGTA (NPE), which selectively binds Ca over Mg, was compared with that of dimethoxyphenyl-nitrophen (DMN) in triggering rapid Ca-dependent exocytosis. Whole cell patch clamping was used to monitor changes in cell membrane capacitance, and to load Ca indicator dye and caged Ca into melanotrophs prior to flash photolysis. A transient increase in intracellular Ca ([Ca]i ≥ 1 μM) observed immediately after patchbreak with the Ca indicator, Fura-2, was recorded from cells dialyzed with DMN *(n=5)*. These loading transients reflect the release of Ca by DMN while binding intracellular Mg. No such transients were seen with NPE *(n=3)*, consistent with the lack of Mg binding to this chelator. Following flash photolysis of DMN and NPE, [Ca]i increased, triggering both a rapid exocytic burst and a slower phase of exocytosis. The photolysis of NPE resulted in a smaller increase in [Ca]i (NPE: 38.4 ± 2.5 μM *(n=3)* vs DMN: 69.2 ± 10.4 μM *(n=11)*) and a slower exocytic burst (rate constant, NPE: 9.5 ± 0.9 /s *(n=6)* vs DMN: 14.9 ± 1.0 /s *(n=19)*). The rate constants for the slow component of exocytosis were comparable (NPE: 0.7 ± 0.1 /s *(n=3)* vs DMN: 0.7 ± 0.1 /s *(n=18)*). However, the amplitude of the slow component observed in NPE loaded cells was larger (NPE: 2.3 ± 0.3 pF *(n=3)* vs DMN: 1.6 ± 0.2 pF *(n=18)*). NPE promises to be a useful and interesting tool for the time-resolved study of Ca-

M-Pos526

THE MECHANISM OF MEMBRANE AGGREGATION BY ANNEXIN I. ((M. de la Fuente)), Dept. Physiol. Biophys., Fac. Med., U. of Chile, Santiago, Chile (Spons. by M.T. Núñez)

The goal of this study was to learn if annexin I mediates membrane aggregation by binding two opposed membrane surfaces simultaneously. Starting from the fact that membrane-bound annexin I does not exchange with other membranes, we attempted to determine if a population of phosphatidylserine (PS) liposomes containing bound annexin I could coaggregate with another population of liposomes devoided of protein. Resonance energy transfer and turbidity experiments showed fast coaggregation between both populations, indicating that the protein indeed mediates membrane aggregation in a bivalent fashion. The rate was similar to that observed when all liposomes contained protein. PS-bound annexin I (but not soluble protein) also could bind phosphatidylcholine liposomes, as estimated from turbidity experiments. The rate of coaggregation was not stimulated by Ca ions. These results suggest that secondary binding of the membrane-bound annexin I to lipids (as opposed to Ca^{2+}-dependent primary binding of the soluble protein) does not involve the Ca^{2+} sites domain thought to participate in the binding of the soluble protein to phospholipids.
Supported by Fondecyt 1930988, DTI B3388.

M-Pos527

STUDIES ON THE MECHANISM OF ANNEXIN V BINDING TO PHOSPHOLIPIDS AND VESICLE AGGREGATION BY ANNEXIN I. ((Paul Meers* and Tanya Mealy)) Boston University School of Medicine, Boston, MA 02118; *current address: The Liposome Company, 1 Research Way, Princeton, NJ 08540-6619 (Spon. P. Meers)

The annexins are a group of Ca^{2+}-dependent phospholipid binding proteins. Some of the annexins, such as annexin I, are capable of mediating Ca^{2+}-dependent vesicle aggregation, suggesting a role in intracellular membrane fusion. In the data presented, binding characteristics of annexin V and aggregation characteristics of annexin I are investigated. It is shown by fluorescence spectroscopy that annexin V undergoes a Ca^{2+}-dependent conformational change that moves its unique tryptophan residue from a solvent inaccessible position to an accessible one where it is utilized to contact phospholipid membranes. By accounting for local surface concentrations of Ca^{2+} and monitoring annexin V binding to membranes and micelles via tryptophan fluorescence, it is shown that that the binding can be separated into two major components, a nonspecific electrostatic interaction with negatively charged surfaces and specific binding utilizing approximately four phospholipid binding sites. In the presence of sufficient negative surface charge, various long phospholipid acyl chains and any headgroup other than inositol are almost equally sufficient for binding to the annexin sites, while the phosphate group and at least a short *sn*-2 acyl chain are required binding determinants. Therefore, annexin V may be ideally suited to utilize most of the phospholipids in negatively charged biological membranes. Annexin I-mediated aggregation of phospholipid vesicles was also studied. Chelator-irreversible, protease-reversible aggregation of vesicles crosslinked with photoactivated phospholipids suggests that monomers of annexin I can contact more than one membrane. Lack of annexin I crosslinking by amine-reactive bifunctional reagents suggests that annexin I self-association may not occur during vesicle aggregation. Therefore multiple mononomers may mediate vesicle aggregation. Experiments involving coaggregation of two vesicle populations of different composition suggest that the "second" binding site of annexin I does not involve a nonspecific hydrophobic interaction.

M-Pos528

CALCIUM-INDUCED LIPID MIXING RATES BETWEEN PHOSPHATIDYLSERINE VESICLES ARE IDENTICAL FOR THE INNER AND OUTER MEMBRANE MONOLAYERS. ((Anne Walter)) Biology Department, St. Olaf College, Northfield, MN 55057.

Calcium-induced fusion between phosphatidylserine (PS) large unilamellar vesicles (LUV) is a model system for testing the energetics of and feasible pathways for the lipid components during membrane fusion. Testing the current fusion models requires being able to separate the behavior of the outer monolayers, that are responsible for the initial contact between the vesicles, and the inner monolayers that must finally join together for a true fusion event to take place. Neither the rate nor the efficiency of these two processes must be identical. In this study, the reducing agent dithionite was added to LUV containing the fluorescent probes NBD-PE and Rho-PE: NBD can be reduced by dithionite to a nonfluorescent molecule. The NBD-PE fluorescence intensity was decreased to 50% of the original value without affecting the remaining energy transfer efficiency. These data are consistent with only the outer monolayer NBD-PE being chemically reduced. The dithionite was removed by washing the vesicles and resuspending them in fresh buffer. Ca^{+2}-induced lipid mixing rates were identical for the control and dithionite treated samples indicating that both the rate and extent of mixing were identical for both the inner and outer monolayers at the level of resolution present, e.g., 20 msec. Moreover, no flip-flop from one monolayer to the other was detected during the fusion process. Thus, in this system, any model for the fusion intermediate must explain tight coupling between mixing of each monolayer with little of no exchange of lipid between the two monolayers. (NRL contract # N00014-94-K2000)

M-Pos529

THE EFFECT OF PHOSPHOLIPASE D AND PHOSPHATIDIC ACID ON EXOCYTOTIC MEMBRANE FUSION IN VITRO. ((K.W. Gasser and A.M. Stahl)) Dept. Biology, Northern Illinois Univ., DeKalb, IL (Spon. by G. Kresheck)

Exocytotic fusion was reconstituted in vitro using zymogen granules and plasma membrane isolated from the rat pancreas. Phosphatidic acid (PA) has previously been shown to accumulate in membranes during stimulus-secretion coupling and the present results show that PA can alter fusion efficiency. Fusion was measured by lipid mixing (R18 quenching) and by the dissolution of the granule core (decrease OD_{540}). The control fusion rate exhibited a half-time of 8.2±3.2 min when the membranes were incubated in a solution of 150 mM KCl, pH 7.0, 37°C. Incubation with dilauroyl (C12:0) PA did not alter the fusion rate; however, the rate decreased when both membranes were incubated with 0.1 ug/ml (dioleoyl, C18:1) PA, with a half-time of 24.7±6.5 min. Similarly, when both membranes were incubated with PL-D, the half-time increased to 14.9±4.6 min. Significantly, when the plasma membrane alone was preincubated with PL-D or PA, the fusion rate increased, (half-time 4.2±3.1 min). The results suggest that PA could regulate fusion efficiency during stimulus-secretion coupling through modification of the apical plasma membrane.

M-Pos530

EFFECTS OF LIPID COMPOSITION AND pH ON THE FUSION OF STRATUM CORNEUM LIPID LARGE UNILAMELLAR VESICLES **((Rita M. Hatfield*+ and Leslie W-M Fung*)) *Dept. of Chemistry, Loyola University of Chicago, Chicago, IL 60626; +Helene Curtis Industries, Inc., Chicago, IL 60639.**

The stratum corneum is the uppermost layer of mammalian skin and functions as a barrier between skin and the external environment. The lipids in the stratum corneum have been shown to form lamellar sheets *in vivo*. However, the molecular arrangement and properties of the lipids in the lamellar sheets are not well understood but are thought to be critical to the integrity of the barrier function. The lipid composition of the stratum corneum is relatively complex, comprised predominantly of ceramides, cholesterol, various fatty acids and cholesterol sulfate. These lipids have been shown to form stable vesicles at basic pH. We prepared large unilamellar vesicles (LUVs) of precise lipid composition at pH 9 by extrusion methods, using commercially-available lipids. These LUVs were used to study lipid thermal properties, fatty acid derivative partitioning in lipid and aqueous phases, and vesicle stabilities at different pH values. We found that LUVs at pH 6 had limited stability, as determined by quasi-elastic light scattering measurements. Studies at pH 6 have functional significance since the surface pH of the stratum corneum is acidic. We have now monitored the fusion of these LUVs by both leakage and mixing of aqueous contents using fluorescence assays at pH 9 and pH 6. The effects of lipid composition on the rate of LUV fusion were also studied. (Supported by Helene Curtis Ind. and Loyola University of Chicago.)

M-Pos531

HEMIFUSION OF LIPOSOMES WITH PLANAR LIPID MEMBRANES ((A.N.Chanturiya, L.V.Chernomordik and J.Zimmerberg)) LTPB/NICHD/NIH Bethesda, MD 20892.

Liposomes formed with fluorescent lipid at a self-quenched concentration were added to planar lipid membranes (BLM). Both decane-based (Mueller-type) and "solvent free" BLMs were used. Liposomes adherent to BLM were observed as bright circular spots that moved when the solution was stirred, but did not leave the plane of the membrane. In the presence of calcium ions, fast redistribution of dye (flashes of light) was observed around individual liposomes due to dye dequenching which indicates fusion of the liposomal membrane with the BLM. This effect was observed for both types of BLM. The frequency of flashes was dependent on the lipid composition of liposomes: increasing the phosphatydyl-ethanolamine content increased the frequency of flashes. Lysophospha-tidylcholine, added to the same compartment as liposomes, at concentrations of 100 μM and above, completely but reversibly inhibited liposome/BLM fusion. Surprisingly, when liposomes were formed with porin channels, a marker commonly used for monitoring membrane merger, these flashes were not accomplained by channel incorporation and were observed even in the absence of an osmotic gradient, a normal requirement for membrane fusion in vesicle/BLM systems. We interpret these findings as hemifusion, *i.e.* fusion of contacting monolayers of liposome and planar membrane.

M-Pos532

LIPID-SENSITIVE AND TRIGGER-INDEPENDENT STAGE OF CELL-CELL FUSION MEDIATED BY VIRAL PROTEINS

((Leonid V. Chernomordik, Eugenia A. Leikina & Joshua Zimmerberg)) LTPB, NICHD, NIH, Bethesda, MD 20892

We studied the effects of membrane lipid composition on low pH-triggered membrane fusion mediated by the specialized envelope proteins of influenza virus (hemagglutinin) and baculovirus (gp64). To test the possibility that biological fusion is controlled by specific alteration of the membrane monolayers' propensity to bend, lipids known to induce opposite intrinsic curvatures were added to membranes. Addition of lysolipids (promoting a micellar positive curvature) and cis-unsaturated fatty acids (promote an inverted hexagonal negative curvature), respectively, reversibly inhibited and promoted pH-independent processes of membrane merger following low pH-induced changes in fusion protein conformation. The lower the surface density of 'activated' fusion proteins in membranes, the stronger was the dependence on the lipid composition. For the experimental system of hemagglutinin-expressing cells (HAb2) fusing with human erythrocytes, application of lysophosphatidylcholine to only one of two membranes (either HAb2 or erythrocyte) was sufficient to inhibit fusion. These results are consistent with a mechanism of membrane fusion involving the formation of highly bent (net negative curvature) local and transient lipidic connections between fusing membranes - 'stalks'.

M-Pos533

FUSION AND INACTIVATION KINETICS OF INFLUENZA VIRUS.

((T. Shangguan, D. R. Alford.and J. Bentz)) Dept. of Bioscience and Biotechnology, Drexel University, Philadelphia, PA 19104.

We have studied the fusion of A/PR/8/34 influenza virus with ganglioside (GD1a) bearing liposomes using the CPT/DABS lipid mixing assay. A prebinding step was introduced to achieve fusion rate limiting conditions, with only a single round of fusion being monitored. Upon acidification, a lag time was observed prior to fusion induced lipid mixing. The lag time is temperature dependent, lasting less than 2 seconds at 37°C and about 1 min at 21°C. This prefusion process can be stopped by neutralization and then restored from the stop point by re-acidification, suggesting it is an irreversible process. Unlike previously reports using influenza X31 strain, shifting virus-liposomes to pH7.4/37°C after 50 seconds incubation at pH4.9/21°C did not result in neutral pH fusion. However, re-acidification of this virus-liposome mixture at 37°C revealed a much faster fusion kinetics than that observed with normal 37°C fusion. This suggests that there are accumulations of prefusion intermediates during the lag time, although the the fusion step itself is still pH-dependent. The kinetics of inactivation has been found to be highly correlated with the kinetics of fusion. This inactivation process is currently being investigated by cryo-electron microscopy. In addition, leakage of liposome content was observed during fusion. The kinetics of leakage appeared to be similar to the kinetics of the lipid mixing, suggesting that fusion is a leaky process. Supported in part by research grant GM-31506 (JB)

M-Pos534

A SLIGHT ASYMMETRY IN THE TRANSBILAYER DISTRIBUTION OF LYSOPHOSPHATIDYLCHOLINE ALTERS THE SURFACE PROPERTIES AND PEG-MEDIATED FUSION OF DPPC LARGE UNILAMELLAR VESICLES.

((Hua Wu & Barry R. Lentz)) Dept. of Biochemistry & Biophysics; Univ. of North Carolina School of Medicine; Chapel Hill, NC 27599-7260.

Large, unilamellar vesicles (LUV) composed of dipalmitoylphosphatidylcholine (DPPC) were made asymmetric in L-α-lysopalmitoylphosphatidylcholine (LPC) either by adding a small amount (total mol fraction = 0.003) of LPC to their outer leaflets (LUV-LPC_{out}) or by extracting a small amount from outer leaflets which already contain 0.0015 mol fraction LPC (LUV-LPC_{in}). The slow rate of the transbilayer redistribution of LPC allowed the asymmetric vesicles to be characterized with regard to both their physical properties and their ability to fuse in the presence of poly(ethylene glycol) (PEG). Treatment with bovine serum albumin extracted only a fraction of total LPC. The ratio of LPC available to that unavailable to BSA extraction was 6 for LUV-LPC_{out} and 0.3 for LUV-LPC_{in}. These asymmetries could not be enhanced significantly by increasing the vesicle LPC content. Measurements of the mixing and leakage of vesicle contents showed that LUV-LPC_{in} fused in the presence of 15% (w/w) PEG without loss of contents but that LUV-LPC_{out} did not fuse in the presence of up to 35% PEG. Quasi-elastic light scattering revealed that LUV-LPC_{in} aggregated at 25°C except when swollen by an osmotic gradient while LUV-LPC_{out} were much less likely to aggregate. Trapped volume determinations suggested that neither type of vesicle was perfectly spherical in shape, but no correlation was found between fusogenicity and vesicle shape. Measurements of the fluorescence properties of TMA-DPH and of C_6-NBD-PC suggested that the interface region of the outer leaflet of LUV-LPC_{in} was slightly less ordered and less well packed than that of LUV-LPC_{out}. This slight perturbation of the external vesicle surface correlated with the ability of juxtaposed vesicle bilayers to fuse. *Supported by USPHS grant GM32707.*

M-Pos535

PEG-MEDIATED FUSION OF HIGHLY CURVED MEMBRANOUS VESICLES: COMPARISON OF FUSION ASSAYS AND LIPID SPECIES

((B.R. Lentz & W.F. Talbot)) Dept. of Biochemistry & Biophysics, Univ. of North Carolina, Chapel Hill, NC 27599-7260.

The poly(ethyleneglycol) (PEG) induced fusion of sonicated, unilamellar vesicles (SUV) and large,unilamellar vesicles (LUV) composed of dipalmitoylphosphatidyl-choline (DPPC), palmitoyl-oleoyl-phosphatidylcholine (POPC), and hen egg yolk phosphatidylcholine (egg PC) was compared using two assays for the mixing and leakage of internal vesicle contents. In the first, which has previously been described by this laboratory (Parente & Lentz [1986] Biochemistry, 6678), disodium 8-aminonaphthalene-1,3,6-trisulfonate (ANTS) fluorescence is quenched by coencapsulated N,N'-p-xylylenebis(pyridinium bromide) (DPX). For this assay, interference by the fluorescence of impurities in PEG demands that PEG content be reduced by sample dilution before measurements are taken. In the second assay (Viguera *et al.* [1993] Biochemistry, 3708), the fluorescence of Tb^{3+} is enhanced by complexation with dipicolinic acid (DPA). This assay can be performed in concentrated PEG solutions. The two assays gave identical fusion profiles for egg PC SUV's treated with increasing concentrations of PEG, thereby confirming the validity of both assays as used to follow PEG-mediated fusion. In addition, this result demonstrates that fusion occurs in the dehydrated state in the presence of PEG. Finally, comparison of results obtained with different lipid species suggests that increasing levels of acyl chain unsaturation in phosphatidylcholines used to prepare highly curved membranes stabilizes these membranes to rupture and encourages fusion at lower PEG concentrations. *Supported by USPHS grant GM32707.*

M-Pos536

PEG MEDIATED ELECTROFUSION OF MAMMALIAN CELLS.

((S.W. Hui, Lin-Hong Li# and N.G.Stoicheva*)) Department of Biophysics, Roswell Park Cancer Institute, Buffalo, NY, 14263. +on leave from Biomedical Engineering Department, Hunan medical University, Changsha, China. *on leave from Central Laboratory of Biophysics, Bulgarian Academy of Sciences, Sofia 1113, Bulgaria.

Polyethylene glycol (PEG) and electrofusion were applied together in a simple and highly efficient cell fusion method. PEG (8000 MW) was used to bring human erythrocytes or CHO cells into contact, and a single 4 kV/cm pulse was applied to cell aggregates. The fusion yield (FY) is PEG-concentration-dependent. A maximum FY (40-50%) was found at about 10% PEG (MW 8000). Higher PEG concentrations (>10%) suppressed FY due to colloid osmotic shrinkage. Diluting cells suspended in higher concentrations of PEG to these optimal concentrations after the pulse application regained the optimal FY. From the swelling behavior, we propose two types of electropores: the pre-fusion sites connecting cell pairs, and electropores on each individual cells connecting intracellular and extracellular space. The latter type is responsible for the colloidal osmotic swelling and shrinking of cells which, together with simple osmotic swelling, is responsible for expanding the pre-fusion sites into fusion lumens. Resealing of electropores resulted in reducing FY. Other polymers and PEG of other molecular weights are not as effective in forming cell aggregates, and their FYs are low. Apparently, PEG plays two opposite roles in this fusion method, one is to promote pre-pulse and post-pulse cell-cell contact, protecting pre-fusion sites, the other suppresses FY by colloid osmotic shrinkage of cells after pulsing, especially when high PEG concentration is used. 10% PEG 8000 represents the optimal combination of these properties.

M-Pos537

SUPPORT FOR THE HYPOTHESIS THAT THE ANTI-VIRAL PEPTIDE CARBOBENZOXY-D-PHENYLALANYL-L-PHENYLALANYLGLYCINE (ZPPG) STABILIZES PLANAR MEMBRANE STRUCTURES

((T. Zhu, M. Caffrey)) Chemistry Dept., The Ohio State University, Columbus, OH 43210.

Membrane fusion requires adjacent membranes to approach one another closely, to expel intervening water and to form transient, highly curved interfaces. The invasion of cells by membrane - bounded or enveloped viruses, which presumably involves membrane fusion at some point in the process, is inhibited by the anti-viral peptide ZPPG. The mechanism of inhibition is not known but hypotheses invoking planar membrane stabilization have been proposed. Our x-ray diffraction measurements on ZPPG in combination with dioleoylphosphatidylethanolamine (DOPE) (ZPPG:DOPE, 1:25 mole/mole) as a function of temperature and hydration provides support for this hypothesis. The evidence includes a stabilization of the lamellar liquid crystal phase at reduced hydration levels by at least 10 °C and an enhanced water carrying capacity of and a larger fully hydrated lattice parameter for the inverted hexagonal phase in the presence of ZPPG. Together, these data provide direct support for the hypothesis that the anti-viral peptide acts by stabilizing a more planar lipid/water interface at the expense of regions of high curvature.

Supported by NIH DK 45295.

M-Pos538

AN AMPHIPATHIC α-HELICAL PEPTIDE DIMER DESIGNED FOR MEMBRANE FUSION. ((A. Sen, R. Balakrishnan, H. Iijima, A.L. Kazim, R. Parthasarathy and S.W. Hui)) Roswell Park Cancer Institute, Buffalo, NY 14263.

Amphipathic peptides which destabilize lipid bilayers can cause fusion between opposing biological membranes. It occurred to us that a higher efficiency of fusion may be realized by a disulfide linked dimer with suitable relative orientation of the helical axes in the two halves, so as to insert into and destabilize adjacent membranes. Based on analysis of known viral fusion peptides, Brasseur and co-workers(Biochim. Biophys. Acta 1029:267(1990)) have proposed that for an amphipathic α-helical peptide to be capable of inducing membrane fusion, the peptide has to have a gradient in its hydrophobic moment both along and around the helix axis. Such gradients in the hydrophobic moment of an α-helical peptide will cause the peptide to insert obliquely into and disrupting the lipid bilayer. We have designed a 14 residue peptide, Ac-GGDRAAibEGAibAKAibLL-NH_2, to form an amphipathic α-helix. The peptide was synthesized on an ABI model 431A peptide synthesizer using suitably protected fmoc amino acids. Following synthesis, the peptide was purified using preparative reversed phase HPLC and examined using amino acid analysis, peptide sequencing and FAB mass spectrometry. We first examined the helix propensity of the 14-mer. CD measurements of the peptide showed that there was 24% and 51% α-helix in aqueous buffer (5mM HEPES, pH7) and in trifluroethanol respectively. The peptide was also found to bind to and destabilize erythrocyte membranes. Since the 14-mer formed a helix and destabilized the membrane, we added a Cys residue at the N-terminus of the peptide. By air-oxidation we have prepared a disulfide linked dimer of this peptide. The structure and fusion activities of the monomer and of the dimer are currently under investigation.

A TALE OF TWO MOTORS: MYOSIN AND KINESIN

Tu-AM-SymI-1

THE STRUCTURE OF THE NUCLEOTIDE BINDING SITE IN MYOSIN SUBFRAGMENT-1. ((I.Rayment)) Univ. of Wisconsin.

Tu-AM-SymI-2

MUTATIONAL ANALYSIS OF MYOSIN. ((H.L Sweeney)) Univ. of Pennsylvania Sch. of Med.

Tu-AM-SymI-3

X-RAY DIFFRACTION STUDIES ON NCD AND KINESIN MOTOR DOMAINS. ((R. FLETTERICK)) Univ. of California, San Francisco.

Tu-AM-SymI-4

THE BEST OF TIMES AND THE WORST OF TIMES: FROM MEASUREMENT TO MECHANISM IN KINESIN MOTORS. ((S. BLOCK.)) Princeton Univ.